FACULTAD DE CIENCIAS BIOLÓGICAS
Departamento de Biología Celular-ERI BioTECMED

Doctorado en Biomedicina y Biotecnología

Role of TET3 in the epigenetic regulation of neural stemness maintenance

Raquel Montalbán Loro

Directora de la Tesis Doctoral

Sacramento Rodríguez Ferrón

Valencia, diciembre de 2017

Dña. Sacramento Rodríguez Ferrón, investigadora “Post Ramón y Cajal” del Departamento de Biología Celular, Biología Funcional y Antropología Física y de la ERI-BioTECMED de la Facultad de Ciencias Biológicas de la Universidad de Valencia

INFORMA QUE:

Doña Raquel Montalbán Loro, licenciada en Biología y Bioquímica por la Universidad de Valencia, ha realizado bajo su dirección el trabajo titulado "*Role of TET3 in the epigenetic regulation of neural stemness maintenance*", y que hallándose concluida, autoriza su presentación, a fin de que pueda ser juzgado por el Tribunal correspondiente para la obtención del grado de Doctor por la Universitat de València.

Y para que conste, en cumplimiento de la legislación, firma el presente informe en Burjassot, a 01 de diciembre del 2017.

Dra. Sacramento Rodríguez Ferrón

Este trabajo de Tesis Doctoral ha sido posible gracias a una beca predoctoral del Programa de Formación de Personal Investigador (FPI) adscrita al proyecto "*Epigenetic regulation of stemness maintenance*" Plan Nacional de I+D+I MINECO, SAF2012-40107 (20132015). La investigación ha sido financiada por los siguientes proyectos de investigación:

- "*Papel de la impronta genómica y su regulación epigenética en células madre neurales: relación con la formación de tumores*". Plan Nacional de I+D+I MINECO, Ministerio de Economía y Competitividad, SAF2016-78845-R (2016-2019). IP: Sacramento Rodríguez Ferrón.

- "*Regulación epigenética de la adquisición del estado pluripotente en células madre neurales*", Fundación BBVA a Investigadores, Innovadores y Creadores Culturales (2014-2015). IP: Sacramento Rodríguez Ferrón.

- "Regulación epigenética del mantenimiento del estado de célula madre". Consellería de Educació, Cultura y esports (Generalitat Valenciana). Ayudas complementarias a proyectos de I+D. Ref: ACOMP/2014/258. 2014. IP: Sacramento Rodríguez Ferrón.

- "*Epigenetic regulation of stemness maintenance*" Plan Nacional de I+D+I MINECO, Ministerio de Economía y Competitividad, SAF2012-40107 (20132015). IP: Sacramento Rodríguez Ferrón.

A mis padres,

Ángeles y Felipe

A mi hermano,

Héctor

A mis abuelos,

A Jesús

Al finalizar este trabajo no quiero dejar pasar la oportunidad de agradecer a todos los que durante estos años lo han hecho posible, porque esto es fruto de un gran trabajo en equipo y porque sin ellos no hubiese sido posible.

En primer lugar, te lo agradezco a ti, Sacri. Me diste la oportunidad de recorrer este camino y me has acompañado de la mano. Tu cariño y paciencia han hecho que nunca desfalleciera, que nunca tirase la toalla, me has mostrado como con cada piedra en el camino podíamos construir un éxito más grande. Me has enseñado lo que es la ciencia, me has contagiado tu tesón y tu amor por esto, me has formado como científica y como persona, en fin, mucho más que una directora, una amiga. Por eso, y por mucho más, este trabajo también es tuyo. Gracias infinitas.

El lugar no podría haber sido mejor, por las personas que me he encontrado en él, mis "neuromoles". A ti especialmente Isabel, gracias, me has acogido en tu laboratorio como a una más transmitiéndome tu pasión por la ciencia, has sido un referente en este mundo tan loco (desde las primeras clases en la Universidad en las que despertaste mi curiosidad por esto) y por estar ahí con todo tu apoyo en lo que hemos necesitado. A Martina y Paco, por vuestra sabiduría y experiencia, por darnos aliento. A mis compañeros. A Salomé, Ana Pérez y José Manuel, por sus consejos y su motivación infinita. A Miquel, Pau, Pere, Sara y Laura, por vuestra sonrisa y bondad, por el aire fresco que le dais al laboratorio. A mi CFN, Bea, Germán y Ana Domingo (nunca olvidaré nuestras batallas en UK), mis confidentes, mis amigos, me habéis acompañado en lo personal y en lo profesional, lo que he vivido junto a vosotros queda grabado para siempre. Para Anna Lozano tengo un lugar especial, mi agradecimiento a ti es infinito, por todo lo que me has dado sin esperar nada a cambio, por tu perseverancia y por tu apoyo siempre. Formamos un equipo y este éxito también es tuyo. A los "tecnomoles", María José, Fabrice, Elba y Cristina, vuestro trabajo y apoyo han sido y son fundamentales en todo esto. No me olvido de los que ya no están, especialmente de María, Alex y Adela, por haber compartido conmigo tantos y tantos momentos. A todos vosotros, ¡GRACIAS!

Este trabajo me ha permitido vivir una de las experiencias más gratificantes de mi vida en la Universidad de Cambridge. Por eso quiero agradecer también a la gente del laboratorio de la Prof. Anne Ferguson-Smith por haberme acogido como a una más. En especial a Anne y Mitsu, por enseñarme otra visión de la ciencia y por dejarme aprender tanto a vuestro lado. También a Lizzie, por tu apoyo en lo personal y en lo profesional y por formar parte de este precioso proyecto. Thanks!

También, mi agradecimiento al SCSIE de la Universidad de Valencia (citometría, producción animal, cultivos y genómica) por sus contribuciones a los resultados de esta tesis y por su accesibilidad siempre.

Gracias a mi pequeña "familia" valenciana, a mis amigos, en especial a Ana, Yuste, Bárbara, Rubén, David, Antonella, Yol y Javi (sin olvidarme de Paula, Carolina y Mauro). Os conocí cuando más os necesitaba y habéis sido mi motor. No me olvido de mis amigos de la infancia, en especial de Estela, aunque hace tiempo que os dejé "allí" siempre habéis estado aquí y os he sentido cerca. Gracias.

A mi familia, a mis padres Felipe y Ángeles, porque hacer que os sintáis orgullosos de mí es mi mayor recompensa. A ti, mamá, por tu amor, tu apoyo y por transmitirme tu capacidad de esfuerzo. Papá, me contagiaste desde pequeña tu amor por saber y te has esforzado por hacer que siempre alcanzase mis metas. También a mi hermano, Héctor, mi mitad, por todo lo que me das siempre. Me habéis ayudado a ser la persona que soy. Aunque lejos, siempre hemos estado cerca y eso me ha ayudado a no desfallecer. No me olvido de mis abuelos, los que están y la que se fue, porque formaréis siempre parte de mí. Este logro también es vuestro. También a Isabel y Alfonso, porque habéis sido unos padres para mí y, a Raúl y Paloma por haberme regalado la mayor de las alegrías, Gonzalo.

Quiero acabar contigo, Jesús, mi amor, mi pilar, mi compañero de viaje. No habría palabras suficientes para agradecerte todo lo que me das. Nada de esto hubiese sido posible sin ti, me apoyaste desde el principio y has sido mi soporte hasta el final. Tu ánimo y sonrisa siempre han llegado cuando más lo necesitaba. Sabemos que formamos un gran equipo y por eso, esta tesis es tan tuya como mía. Te quiero.

"Es preciso sacudir enérgicamente el bosque de las neuronas cerebrales adormecidas; es menester hacerlas vibrar con la emoción de lo nuevo e infundirles nobles y elevadas inquietudes"

SANTIAGO RAMON Y CAJAL, 1916

Index

Index

Abbreviation list

5caC	5-carboxylcytosine
5fC	5-formylcytosine
5hmC	5-hydroxymethylcytosine
5mC	5-methylcytosine
aNSC	activated neural stem cell
ASC	adult stem cell
BBB	blood brain barrier
BER	base-excision repair
BMP	bone morphogenetic protein
BrdU	5-Bromo-2´-deoxyuridine
BSA	bovine serum albumin
CC	corpus callosum
CNS	central nervous system
CP	choroid plexus
CSC	cancer stem cell
CSF	cerebrospinal fluid
DAB	3-3´diaminobenzidine
DAPI	4',6-Diamidine-2'-phenylindole dihydrochloride
DIV	days *in vitro*
DCX	doublecortin
DG	dentate gyrus
DLK1	delta-like homologue 1
DMEM	Dulbecco´s modified eagle medium
DMR	differentially methylated region
DNA	deoxyribonucleic acid
DNMT	DNA methyltransferase
EB	embryoid body
EBSS	Earle´s Balanced Salt solution
ECM	extracellular matrix
EDTA	Ethylendiaminoetetraacetic acid
EGF	epidermal grow factor
EGFR	epidermal grow factor receptor
EGTA	Ethylene glycol-bis (2-aminoethylether)
EpiSC	epiblast stem cell
ESC	embryonic stem cell
FACS	fluorescent activated cell sorting
FBS	foetal bovine serum
FGF	fibroblast grow factor
GFAP	glia fibrillary acidic protein
GFP	green fluorescent protein
GL	glomerular cell layer
GR	granular cell layer
GSC	germ line stem cell
GSK3	glycogen synthase kinase 3
H	histone
HAT	histone acetyltransferase
HDAC	histone deacetylases
HM	hormone mix
hMeDIP	immunoprecipitation of DNA hydroxymethylation
HMT	histone methyltransferases
HSC	hematopoietic stem cell
i.p.	intraperitoneal
ICC	immunocytochemistry
ICM	inner cell mass
ICR	imprinting control region
IGF2	insulin growth factor 2
IHC	immunohistochemistry
iPSC	induced pluripotent stem cell
JMJD3	Jumonji domain-containing protein 3
kDA	kilo Dalton
LIF	leukaemia inhibitor factor
LRC	label retaining cell
MBD	methyl-binding domain protein
MeDIP	immunoprecipitation of DNA methylation
MEK	mitogen-activated protein kinase kinase
MSC	multipotent stem cell
NPC	neural progenitor cell
NSA	neurospheres assay
NSC	neural stem cell
OB	olfactory bulb
OSKM	*oct4*, *sox2*, *klf4* and *c-myc* factors
P	postnatal
PBS	phosphate buffer saline
PBS-T	phosphate buffer saline tween 20

PCR	polymerase chain reaction
PEDF	pigmented epithelium-derived factor
PFA	paraformaldehyde
PGC	primordial germ cell
PSA-NCAM	polysialylated neural-cell-adhesion molecule
PWS/AS	Prader-willi/Angelman syndrome
qNSC	quiescent neural stem cell
RGC	radial glial cell
RMS	rostral migratory stream
RNA	ribonucleic acid
ROS	reactive oxygen species
RT	room temperature
RT-PCR	quantitative real-type PCR
SC	stem cell
SSC	somatic stem cell
SDS	sodium dodecyl sulphate
SDS-PAGE	polyacrylamide gel electrophoresis
SGZ	subgranular zone
shRNA	short hairpin RNA
SmN	survival motor neurons protein
Snrpn	small Nuclear ribonucleoprotein polypeptide N
SOX	sex determining region Y-box
SVZ	subventricular zone
T/E	trypsin/EDTA
TAP	transit-amplifying progenitor
TBR2	T-box gene-2
TDG	thymidine DNA glycosylase
TET	ten-eleven translocation protein
TSS	transcription start site
TTS	transcription termination site
TUJ1	βIII-tubulin
TX	triton X-100
VZ	ventricular zone
WM	whole-mount
WT	wild-type

Introduction

1. Stem cells: units of development and regeneration

Stem cells (SC) are unspecialized cells with the ability to self-renew and capable of differentiating into one or more specialized cell types and play a crucial role in organogenesis, homeostasis and tissue repair (Potten and Loeffler 1990). Self-renewal is the process by which stem cells divide symmetrically or asymmetrically to generate new stem cells with similar developmental potential to the cell of origin maintaining the undifferentiated state (Morrison and Kimble 2006, He et al., 2009). However, the differentiation process involves changes in the cell phenotype that are largely due to highly controlled modifications in gene expression finalizing with the acquisition of a concretely cell identity.

According to their differentiation potential, stem cells are categorized either as totipotent, pluripotent and multipotent (**Fig. 1**). Totipotent cells are located in the zygote and are able to give rise to all the embryonic and extra-embryonic cell types. However, pluripotent cells are located in the inner cell mass (ICM) of the blastocyst and can generate the three germ layers (mesoderm, ectoderm and endoderm). These cells are also known as Embryonic Stem Cells (ESCs) (Chambers and Smith 2004). From here and along the embryonic development, pluripotent cells start a process of increasing commitment losing their pluripotency and generating all the variety of differentiated tissue-specific cell types including germ-line stem cells (GSCs) for reproduction and somatic stem cells (SSCs) for organogenesis. Although diversified, GSCs and SSCs retain the feature of self-renewal and both are progressively restricted in development giving rise to discrete populations of multipotent SCs (MSCs) that remain during the adult lifespan to ensure tissue renewal and a certain degree of tissue regeneration and repair (Weissman 2000, Fuchs et al., 2004). Stem cells can be also categorized based on their origin: physiological stem cells that are present at different stages of life such as ESCs and adult SCs (ASCs), engineered stem cells known as induced pluripotent stem cells (iPSCs) (Takahashi and Yamanaka 2006) (**Fig. 1**), and cancer stem cells (CSC), present in tumors, that also have some stem cells attributes (Alvarez et al., 2012).

All these properties convert SCs in fundamental candidates for regenerative medicine and tissue repair. The regenerative potential of these cells and their progenitors can be exploited therapeutically by transplantation to replenish the stem cell pool, by endogenous manipulation to stimulate the repair activity of already presented cells or through *in vitro* modelling of disease (Wagers 2012).

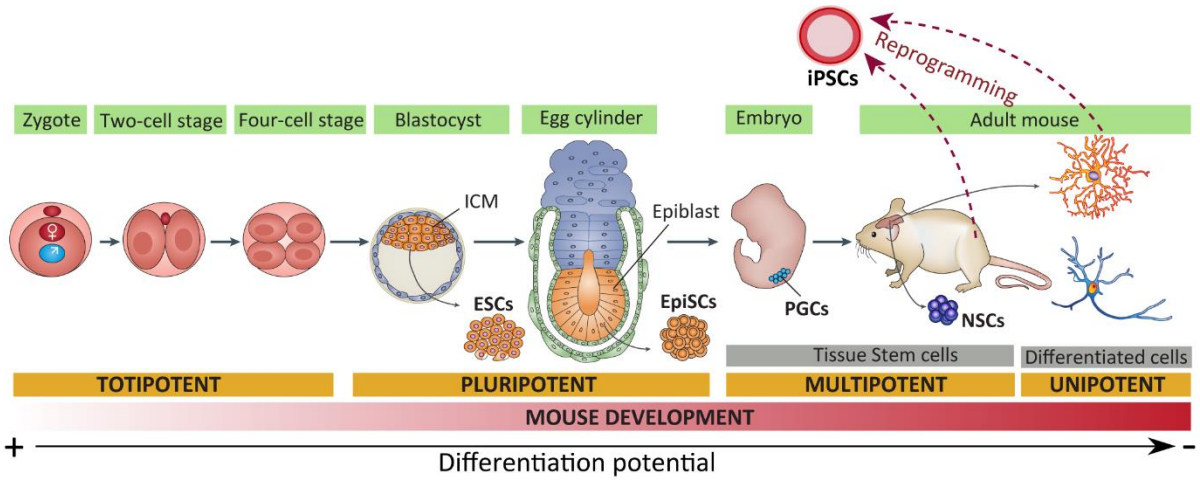

Figure 1. Stem cells (SCs) and their differentiation potential during mouse development. Schematic representing types of stem cells according to their differentiation potential. The zygote and both two- and four-cells stages contain totipotent stem cells that give rise to the blastocyst in which pluripotent embryonic stem cells (ESCs) form the inner cell mass (ICM) that can be isolated and expanded *in vitro*. After the implantation, the egg cylinder is formed containing epiblast stem cells (EpiSCs) that can be also propagated *in vitro*. Both ESCs and EpiSCs are pluripotent stem cells that can generate cells from the three germ layers, mesoderm, ectoderm and endoderm. Pluripotent stem cells differentiate to generate foetal or adult multipotent SCs which are cells capable to generate lineage-specific cells. For example neural stem cells (NSCs) give rise to committed unipotent progenitors that form terminally differentiated cells in the brain. These more differentiated cells can be reprogrammed *in vitro* into induced pluripotent stem cells (iPSCs). Modified from Hirai *et al* 2011 and Wu and Zhang, 2017.

1.1 Embryonic stem cells and derivation of pluripotent stem cells

The first pluripotent cell lines to be established were embryonic carcinoma cell lines, derived from the undifferentiated compartment of murine germ cell tumours, also called teratocarcinome (Finch and Ephrussi 1967). These cells could be expanded continuously in culture and could also be differentiated into cells of all three embryonic germ layers (Kleinsmith and Pierce 1964). Several years after, in 1981, Evans and Martin firstly derived ESC from the inner cell mass in the mouse blastocyst showing their differentiation capability (Evans and Kaufman 1981). Although these pluripotent cells are relatively short-lived in the embryo *in vivo*, they can be propagated infinitely in culture in an undifferentiated state (**Fig. 1**) (Smith et al., 1988, Vila-Cejudo et al., 2017) an their pluripotency can be assessed by their capability to generate embryoid bodies (EBs) *in vitro* and teratomas *in vivo* (Hopfl et al., 2004, Prokhorova et al., 2009). Their full potency is revealed by blastocyst injection. This yields chimeric mice with extensive contribution from the injected ESC progeny to all tissues, including functional colonization of the germline (Nichols and Smith 2009).

Epiblast stem cells or EpiSCs, are also pluripotent stem cells and are generated from post-implantation embryonic epiblast stages (**Fig. 1**) (Brons et al., 2007, Tesar et al., 2007). The epiblast is derived from the inner cell mass and gives rise to the three primary germ layers (ectoderm, definitive

endoderm and mesoderm) and to the extraembryonic mesoderm. Importantly, *in vitro* derived EpiSCs, can generate teratocarcinomas but do not contribute effectively to blastocyst chimeras. Moreover, EpiSCs express *Oct4* but have reduced or no expression of *Rex1*, *Nanog* and several other transcription factors expressed in ESCs. Compared with ESCs they show higher expression of factors present in the post-implantation epiblast, such as FGF5 and Brachyury (Brons et al., 2007, Tesar et al., 2007). For these reasons, they are often termed as "*naïve*" (for ESCs) and "*primed*" (for EpiSCs) pluripotent stem cells to highlight their early and late phases of development (Nichols and Smith 2009).

Pluripotent stem cells need specific conditions to maintain their pluripotency *in vitro,* for instance cell-cell contacts and trophic factors that inhibit cell differentiation. The leukaemia inhibitory factor (LIF) was recognized as a critical factor for robust self-renewal and pluripotency of mESCs (mouse ESCs) (Smith et al., 1988, Williams et al., 1988, Hirai et al., 2011) and since then LIF-supplemented culture medium became a global standard for the culture of ESC. LIF is a member of the unterleukine-6 (IL-6) cytokine family that is able to activate several pathways implicated in pluripotency identity (Hirai et al., 2011). However, LIF signalling is not enough for mESCs maintenance as it has been shown that in serum-free culture medium is not able to maintained ESCs pluripotent state and finally differentiate into neural precursors (Ying et al., 2003). Thus, in optimal conditions, both LIF and serum act antagonizing the differentiation and maintaining the self-renewal capacity of mESCs in culture. EpiSCs cultures do not survive efficiently as isolated single cells and do not respond to ESC culture conditions, but instead are dependent on FGF2 and activin. However, if cultured to high density on feeder cells in the presence of LIF and serum, such EpiSCs may spontaneously generate ESCs at low frequency (Hayashi and Surani 2009, Bernemann et al., 2011).

Notably, mouse EpiSCs closely resemble human ESCs in several aspects including colony morphology and cytokine requirements as none of them are maintained in the pluripotent state by LIF (Pera and Tam 2010). These evidences suggest that hESCs are more closely related to a later stage of development.

1.2 Induced pluripotent stem cells and cell reprogramming

In the late 19th century, August Weismann postulated a genetic theory in which he described that because of inheritance is only mediated by germ cells, unnecessary genetic code must be deleted or inactivated in somatic cells that are committed to a specific state, and that this was an irreversible process (Weismann et al., 1893). Consequently, in the mid-20th century, Conrad Waddington developed a model that represented normal embryonic development in which a cell, reimagined as a ball, rolling downhill to its final differentiated state (Waddington 1957) where the destiny of lineage-committed cells was permanent (**Fig. 2a**).

Although fate commitment cannot normally be reversible *in vivo* during development, several experiments showed the possibility of direct fate conversion. Firstly, John Gurdon from the University of Cambridge, established that fate commitment was reversible by the transference of somatic cell into enucleated oocytes in *Xenopus* giving rise to swimming tadpoles (Gurdon 1962). More recently, reprogramming of somatic cells, such as fibroblast, into pluripotent cells has become possible (Takahashi and Yamanaka 2006). Finally, transdifferentiating of one cell type directly to another, such as conversion of a fibroblast directly into a neuron, suggested that pluripotent o totipotent state may not even be necessary (Vierbuchen et al., 2010). Therefore, in recent years, the Waddington diagram has been repurposed to illustrate how cellular identity changes in the context of reprogramming (**Fig. 2b**).

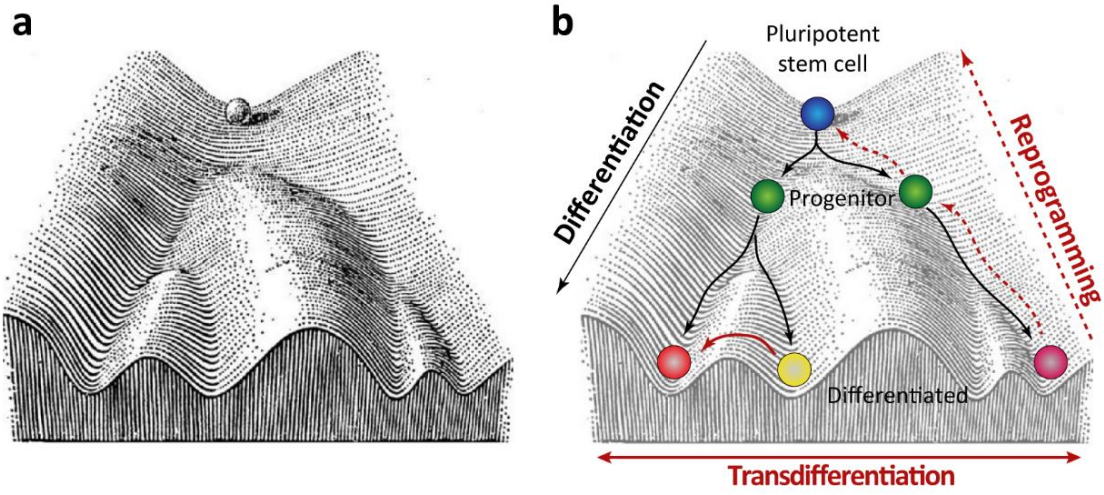

Figure 2. Waddington diagram and its current reinterpretation. (a) Original Waddington model where a developmentally immature cell, represented as a ball at the top rolls downhills, and is diverged right or left to acquire a differentiated status. **(b)** Current reinterpretation of the Waddington diagram showing the reversible processes to differentiation, such as reprogramming or transdifferentiation. Adapted and modified from Waddington, 1957.

In 2006, Takahashi and Yamanaka identified genes expressed in ESCs that would be sufficient to induce the formation of induced pluripotent stem cells (iPSCs). An initial list of 24 candidates was compiled from existing data and they were cloned into retroviral expression factors. iPSCs were then generated even though they showed aberrant expression of key pluripotency genes (Takahashi and Yamanaka 2006). Finally, the ectopic expression of basal reprogramming factors *Oct4*, *Klf4*, *Sox2* and *c-myc* ("*Yamanaka factors*") in human fibroblasts led to their reprogramming into iPSCs (Takahashi and Yamanaka 2006). The generation of these iPSCs came out as breakthrough as it gave a way of generating pluripotent stem cells from somatic cells without having any requirement of ESCs which have associated ethical concerns. Since then, researchers have reported generating iPSCs *in vitro* from

different somatic tissues both humans and mice (Yu et al., 2007, Aasen et al., 2008, Park et al., 2008a, Park et al., 2008b) and even in mice *in vivo* (Abad et al., 2013).

Induced pluripotent stem cells are an incomparable model to study early development of mammals and a promising tool in future cell therapy for human diseases due to their capability for unlimited self-renewal and differentiation of adult cell types. However, the most commonly way to generate iPSCs involve the use of retrovirus or lentivirus as a vectors to introduce ectopic transcription factors that randomly integrate in the host genome (Takahashi and Yamanaka 2006, Sridharan et al., 2009, Stadtfeld and Hochedlinger 2010). To achieve a reliable reprogramming, ectopic factors must to be silenced, but this process is often incomplete resulting in a partially reprogram cell lines that continue to depend on the exogenous factors and lack the expression of some endogenous genes (Takahashi and Yamanaka 2006, Sridharan et al., 2009, Stadtfeld and Hochedlinger 2010). Consequently, retroviruses possess some properties that make iPSCs improper for cell therapy. Firstly, the copy number of the exogenous retroviral DNA that is integrated into a genome may vary and retrovirus can introduce promoter elements and polyadenylation signals as well as they can also interpose coding sequences affecting transcription. On the other hand, the high probability that the ectopic gene expression will resume, makes impossible to apply these retrovirus-induced iPSCs.

Another problem to take into account for the use of iPSCs is that the expression of *Oct4*, *Sox2*, *Klf4* and *c-myc* is related to the development of multiple tumours (Ben-Porath et al., 2008). In particular, overexpression of *Oct4* causes murine epithelial cell dysplasia (Hochedlinger et al., 2005), aberrant expression of *Sox2* causes squamous-cell carcinomas (Boumahdi et al., 2014), some breast tumours are characterized by elevated expression of *Klf4* (Lee et al., 2015), and the improper expression of *c-myc* is observed in a high percentage of human tumours (Kuttler and Mai 2006). Therefore, now strategies are being developed to avoid the above-mentioned problems such as the minimization of the number of genes required for reprogramming (Kim et al., 2009a), the search for inducible systems allowing the elimination of the exogenous DNA from the host cell genome after reprogramming (Abad et al., 2013) or the development of protocols to reprogram somatic cells using recombinant proteins (Feng et al., 2009). Although generation of iPSCs from somatic cells have a promising future, the safety issues related to gene reprogramming and the uncontrolled proliferation and/or differentiation *in vivo* must be solved.

However, iPSCs are already a powerful tool to modelling diseases *in vitro* due to patient-specific iPSCs can be obtained and differentiated into different cell types with the same genetic background as the donor patient, providing the opportunity to study their pathogenesis (Sanchez-Danes et al., 2012, Lu and Zhao 2013, Calatayud et al., 2017). This use of iPSCs to model a disease also remains challenging,

owing to the difficulties involved in differentiated them into an organ and the complexity of pathogenesis.

1.3 Adult stem cells: reservoir of multipotent cell precursors

Adult stem cells (ASCs) are tissue-resident cells with the ability to divide, self-renew and generate functional differentiated cells that replace lost cells throughout the organism´s lifetime and represent the essential component for the maintenance of tissue homeostasis and repair in multicellular organism (Biteau et al., 2011) (**Fig. 1**). The presence of ASCs was first described in tissues with high proliferation rates, such as the hematopoietic system (Till and Mc 1961). Since then, stem cells have been found in almost all adult tissues including the nervous system (Li and Xie 2005).

In homeostatic conditions, ASCs divide to produce new SCs and non-renewing, rapidly cycling cells or transit amplifying progenitors (TAP), cells that proliferate for a discrete number of cycles to eventually differentiate into functional cells specific of their particular tissue. However, ASC and progenitor cell populations show remarkable diversity in their proliferative behaviour reflecting the different regenerative requirements of individual tissues. Between them, we can find continuously cycling cells, such as intestinal or hematopoietic stem cells (HSC), or cells whose proliferative activity can be strongly induced by injury, including muscle satellite cells, and stem cells with alternative quiescent and proliferative periods, such as hair follicle SCs (Biteau et al., 2011).

ASCs reside on specific well-organized neighbourhoods termed "*niches*". This term was originally proposed by R. Schofield in 1978 to describe the physiologically limited microenvironment that supports stem cells, after the observation that, HSCs properties differed depending on the location they were isolated from: the spleen or the bone marrow (Schofield 1978). Stem cell niches have been identified and characterized in many tissues, including the germline, bone marrow, digestive, skeletal muscle, mammary gland and nervous system (Zhang et al., 2003, Barker et al., 2007, Kuang et al., 2007, Blanpain and Fuchs 2009, Goodell et al., 2015, Lim and Alvarez-Buylla 2016). Current studies have begun to elucidate the critical components of the niches including surrounding cells such as the vasculature, molecules and physical parameters such as stress, oxygen tension and temperature (Wagers 2012). Particularly, cell-cell interaction within the niche provides structural support, regulates adhesive interaction and produces signals that can control stem cell function. Signalling molecules such as Sonic hedgehog (shh), Wnt, bone morphogenetic proteins (BMPs), fibroblast growth factors (FGFs) and Notch (Tumbar et al., 2004, Ramirez-Castillejo et al., 2006, Soen et al., 2006), as well as adhesion molecules such as integrins or cadherins (Lapidot and Kollet 2002, Arai et al., 2004), can also play an important role in the self-renewal and differentiation regulation of ASCs (see (Wagers 2012) for a review). Moreover, the interaction with the extracellular matrix (ECM) produces mechanical signals

which allow stem cells to respond to external physical force and is also a reservoir of regulatory molecules (Gilbert et al., 2010). Therefore, the signals provided by these cellular and acellular components of the niche affect SC fate decisions, including choices between quiescence or proliferation, self-renewal or differentiation, migration or retention, and cell death or survival being essential for the tissue homeostasis regulation.

2. Neural stem cells and adult neurogenesis

Neurogenesis is the process of generating new neurons from neural stem cells (NSCs) that have the ability to divide, self-renew and generate functional differentiated cells that replace lost cells throughout the adulthood. NSC are multipotent cells that give rise to astrocytes, oligodendrocytes and neurons upon differentiation (Lim and Alvarez-Buylla 2016). In the embryonic mammalian brain, radial glia cells (RGCs) are the primary precursors of new born neurons (Malatesta et al., 2000, Noctor et al., 2001). These cells reside in the ventricular zone (VZ) but possess long processes penetrating the brain parenchyma and contacting to the pial surface of the brain. At the end of foetal development, the VZ is largely composed by glial cell bodies that remain proliferative with the ability to migrate and serve as progenitors of new neurons. After bird, the remaining RGCs in the VZ differentiate either into ependymal cells, that will line the lateral ventricles, or into glial cells, including adult NSCs that retain many of the RGCs features and populate the neurogenic niches (Tramontin et al., 2003, Xu et al., 2015). Thus, adult NSCs express astrocytic markers such as the glial fibrillary acidic protein (GFAP) or the astrocyte-specific glutamate transporter known as excitatory amino acid transporters (GLAST) (Doetsch 2003, Merkle et al., 2004). Moreover, NSCs are relatively quiescent (Morshead et al., 1994) and express the transcription factor Sox2 (SRY-related HMG box 2) and the neural progenitor marker Nestin (Suh et al., 2007).

2.1 The subventricular zone (SVZ) and the olfactory bulb (OB) system

In the adult mammal brain, two main regions continue to generate new neurons: the subgranular zone (SGZ) in the dentate gyrus (DG) of the hippocampus (Gage et al., 1998, Kempermann et al., 2015, Lim and Alvarez-Buylla 2016) and the subventricular zone (SVZ) in the walls of the lateral

ventricles (Doetsch et al., 1997). The SVZ is the most active neurogenic niche and the largest germinal zone in the adult brain.

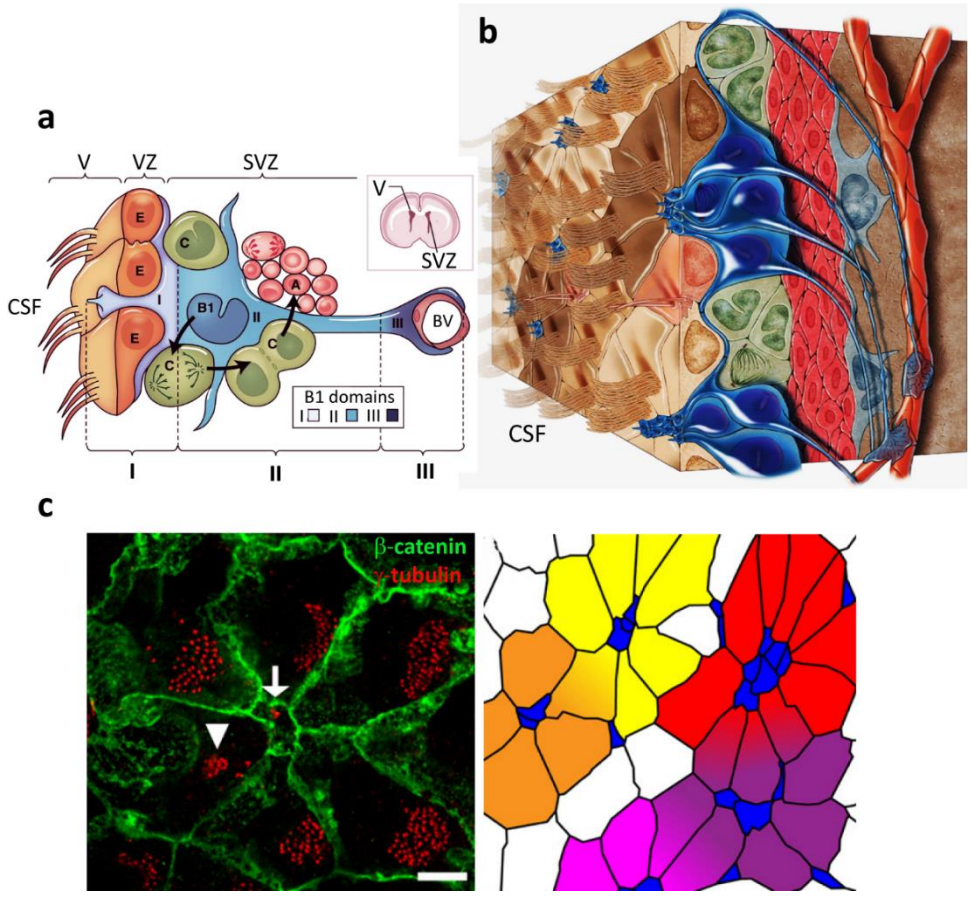

Figure 3. Cellular composition and organization of the SVZ. (a) Coronal section of adult mouse brain showing the SVZ niche (upper panel right). Type B1 cell (blue) is the neural stem cell and presents three domains: domain I contain the apical process contacting the ventricle; domain II contains the cell body of most type B1 cell and are in contact with type C and A cells; domain III contacts with blood vessels (BV). Once activated, type B1 cell divides and produces type C cells (TAP; green). Type C cells give rise to type A migratory neuroblast (red). E represents ependymal cell forming a tight barrier between the SVZ and the ventricle lumen. Adapted from Lim and Buylla, 2016. **(b)** Three-dimensional model of the adult SVZ neurogenic niche illustrating B1 cells (blue), C cells (green), and A cells (red). B1 cells have a long basal process that terminates on blood vessels (orange) and an apical ending at the ventricle surface. Note the pinwheel organization (brown) composed of ependymal cell surrounding B1 apical surfaces. **(c)** Confocal image of the surface of the lateral wall of the ventricle stained for γ-tubulin (red) and β-catenin (green) showing the pinwheel structure of E cells. A B1 apical surface is indicated in the centre of the pinwheel (arrow) and E apical surface (arrowhead) on the periphery. Color-coded tracing of the pinwheels is also included**.** Scale bar in c: 5 µm. Adapted from Mirzadeh *et al*. 2008.

Two types of stem cells coexist in the SVZ lining the ventricles. Type B1 cells that have light cytoplasm, relatively disperse chromatin and show null replication activity. Type B1 NSCs present a radial glia-like morphology, with an apical primary cilium in direct contact with the CSF and a basal process reaching the basal lamina and the vasculature structures (Tavazoie et al., 2008) (**Fig. 3a,b**). The walls of the lateral ventricles show a typical organization where the small apical process of type B1

cells are surrounded by a rosette of epithelial ependymal cells forming structures known as pinwheels (Mirzadeh et al., 2008) (**Fig.3**). Type B2 cells with darker cytoplasm and clamped chromatin are closer to blood vessels and replicate de DNA content incorporating traceable nucleoside analogues. (Doetsch et al., 1997). Once activated, the slowly dividing NSCs give rise to fast cycling cells called transit-amplifying progenitors (TAP or type C cells). Mash1-positive type C cells generate chains of polysialylated-neural cell adhesion molecule (PSA-NCAM) and doublecortin (DCX) positive neuroblasts (type A cells) that migrate along the rostral migratory stream (RMS) (**Fig. 4a,c**). These neuroblasts reach the core of the OB, where they detach from the RMS and migrate radially into the granular and glomerular layers contributing to OB function and the neural plasticity of olfactory information processing (Zhao et al., 2008, Ming and Song 2011) (**Fig. 4b,d**).

In addition of being a neurogenic region, the SVZ can serve as a source of oligodendrocytes although generated in much lower numbers than neuroblasts. Thereby, Olig2-positive transient amplifying cells give rise to oligodendroblast that migrate to the corpus callosum (CC) and striatum where they differentiate into myelinating and nonmyelinating oligodendrocytes (Menn et al., 2006).

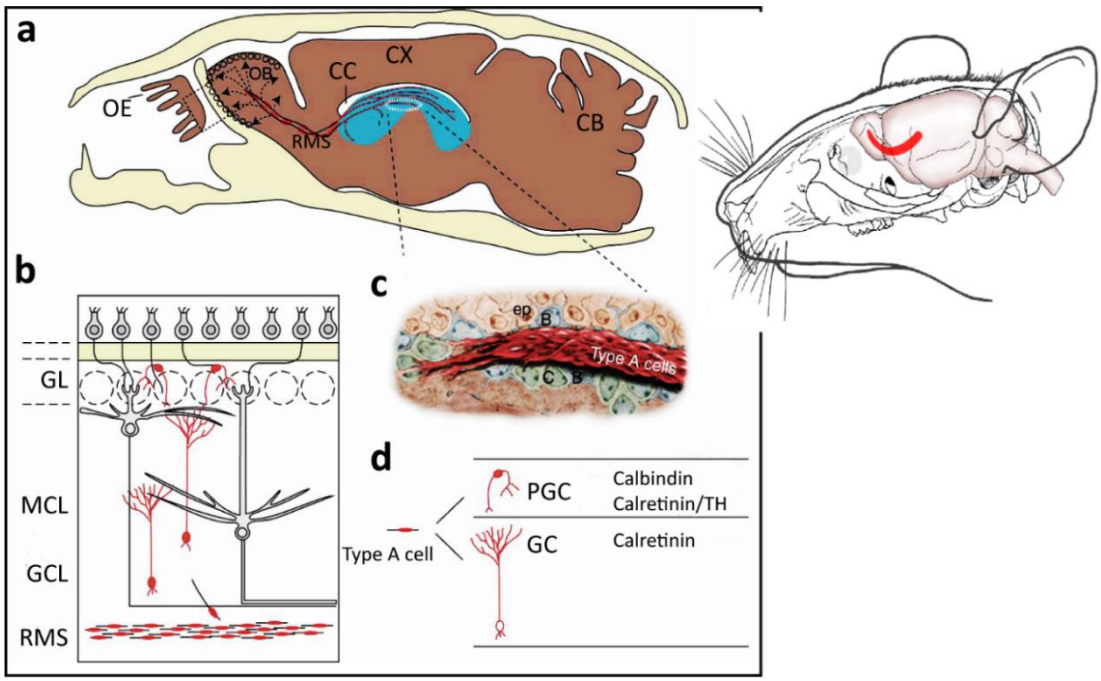

Figure 4. Overview of adult mouse olfactory bulb (OB) neurogenesis from the subventricular zone (SVZ). (a) Sagittal section through mouse head. Neuroblasts (type A cells) born in the SVZ of the lateral ventricle (blue) migrate through a network of paths (red) into the rostral migratory stream (RMS), which enters the OB. Cells then leave the RMS (arrows, dashed lines) and migrate radially into the OB. Boxed area is shown enlarged in b. **(b)** Neuronal layers of OB. Migratory cells depart the RMS and differentiate into granule cells (GC) or periglomerular cells (PGC), which reside in the granule cell layer (GCL) and glomerular layer (GL), respectively (type A cells and differentiated interneurons are red). **(c)** Chains of migratory type A cells. These chains are surrounded by glial cells (type B cells, blue) and are associated with clusters of transit-amplifying cells (type C cells, green). **(d)** Diversity of OB interneurons. Type A cells differentiate into either PGCs or GCs, which can be distinguished by morphology and markers. CC, Corpus callosum; CX, cortex; CB, cerebellum; OE, olfactory epithelium; MCL, mitral cell layer; ep, ependymal cell; TH, tyrosine hydroxylase. Adapted from Lim and Buylla, 2016.

The SVZ constitutes a complex microenvironment in which proliferation and self-renewal of NSCs are strongly regulated by multiple extracellular factors such as EGF, BMP or pigment epithelium derived factor (PEDF) (Ramirez-Castillejo et al., 2006, Faigle and Song 2013, Porlan et al., 2013) (**Fig. 5**). This extrinsic signalling is possible due to the special cytoarchitecture of the niche allowing NSCs to be in direct contact with the CSF produced by the choroid plexus in the ventricles, with the vasculature and with other cells from the niche like astrocytes or microglia (Silva-Vargas et al., 2013) (**Fig. 5**). For instance, CP-secreted interleukin-1β regulates the expression of vascular cell adhesion molecule 1 (VCAM1) that promotes anchoring to the neural stem cell niche (Kokovay et al., 2012) as well as the insulin growth factor 2 (IGF2) and the neurotrophin 3 (NT3), also secreted by CP contributes to NSCs maintenance in SVZ (Delgado et al., 2014, Ferron et al., 2015).

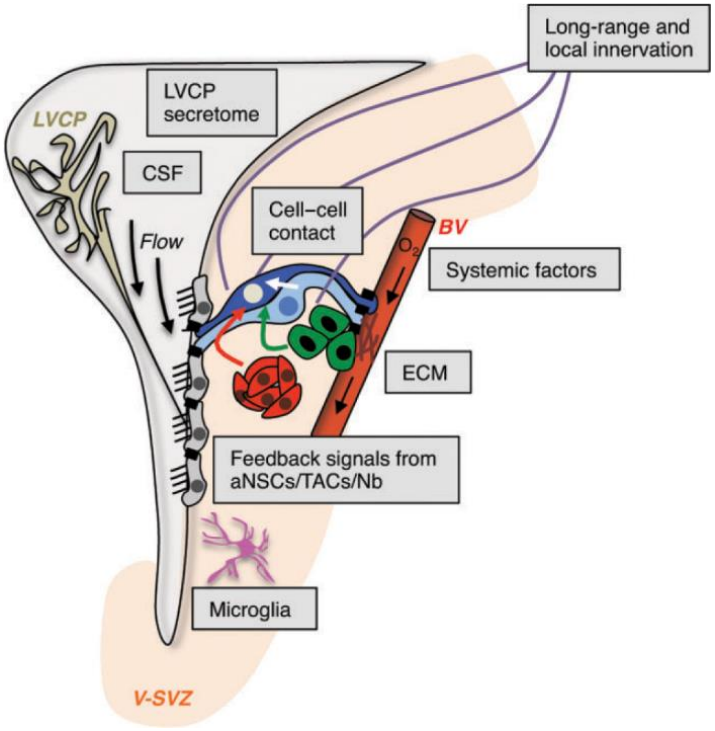

Figure 5. Extrinsic factors regulate SVZ adult neurogenesis. SVZ niche is exposed to several sources of extrinsic factors that regulate NSCs behaviour, including blood vessels and the lateral ventricle choroid plexus (LVCP). Moreover, NSCs contact with other cells as well as with the extracellular matrix (ECM). Adapted from Chaker *et al.* 2016.

The close association of SVZ stem cells with blood vessels suggest that they may receive important signals from the vasculature that have a relatively permissive blood-brain barrier (BBB) due to the lack of astrocyte endfeet (Tavazoie et al., 2008) (**Fig. 5**). In this way, NSCs can receive distant produced factors including hormones, metabolites and cytokines.

Moreover, cell contact between adult NSCs and ependymal cells promote quiescence, highlighting the importance of anchorage for NSCs (Porlan et al., 2014). Additionally, NSCs receive external signals by cell-cell contacts with other niche cells, such as microglia or ependymal cells influencing stem cell activation and quiescence (Ribeiro Xavier et al., 2015). The interaction between

NSCs and their progeny is also important, so that NSCs receive signals that promote dormancy controlling stem cell depletion (Chaker et al., 2016) (**Fig. 5**).

2.2 Identifying the NSC population in the adult SVZ

So far, there is no single marker that unequivocally identifies each pool of NSCs. However, several different strategies have been used to successfully identify NSCs populations. *In vivo*, actively dividing SVZ stem cells are eliminated by antimitotic treatment. In contrast, slowly dividing cells survive treatment with antimitotic drugs and are able to regenerate the SVZ afterwards (Doetsch et al., 1999). More recently, it has been shown that a proportion of GFAP/GLAST-positive astrocytes that also expressed the ependymal growth factor receptor (EGFR) are sensitive to antimitotic drugs whereas EGFR- NSCs survive the treatments and retain the ability to restore the production of newborn neurons (Pastrana et al., 2009, Codega et al., 2014). Thus, it is well stablished the co-existence of both quiescent (qNSCs) and active (aNSCs) NSCs that participate in tissue homeostasis (Llorens-Bobadilla and Martin-Villalba 2017) (**Fig. 6**).

Using transgenic animals, lineage-tracing strategies, immunohistochemical assays and strategies based in fluorescent activated cell sorting (FACS) we know that both aNSCs and qNSCs express GFAP, GLAST, CD133 (Prominin 1), CD9, LeX, Bmi1, Plexin B2 and Hes5 whereas they do not express the terminally differentiated astrocyte marker S100β and the immature neuroblast adhesion molecule CD24 (Codega et al., 2014, Chaker et al., 2016). Interestingly, EGFR and Nestin expression are specifically expressed in aNSCs thus they are also used to differentiate both states (Codega et al., 2014, Chaker et al., 2016) (**Fig. 6**).

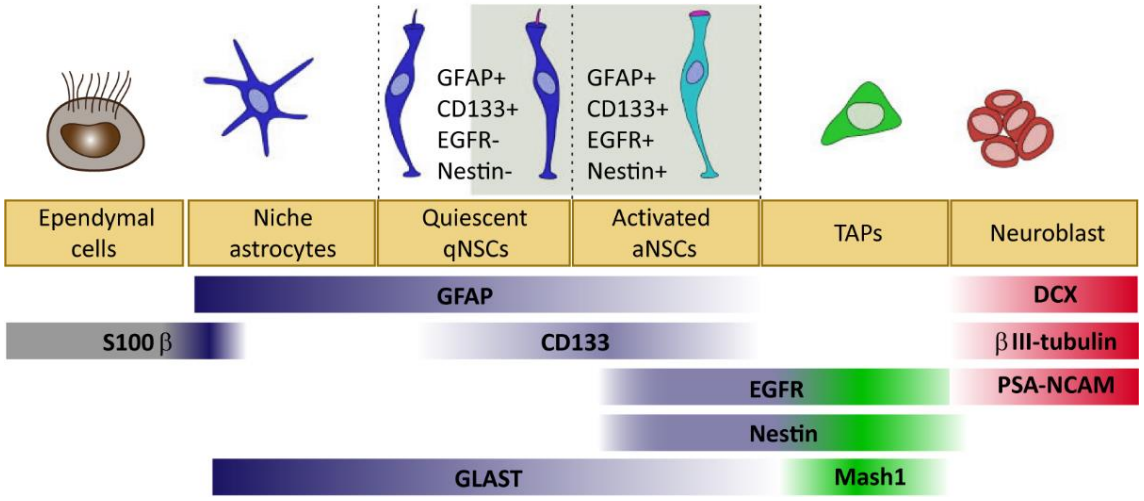

Figure 6. Markers for the identification of the SVZ cells. The combination of several markers allows the identification of the different populations within the adult SVZ. Quiescent (qNSCs) and activated (aNSCs) neural stem cells share some expression markers, but qNSCs are Nestin negative while aNSCs express EGFR. TAPs and neuroblasts can be identified by the expression of Mash1 and DCX, respectively. Adapted from Codega *et al*. 2014**.**

Recently, the isolation and transcriptome analysis of NSCs in different activation states has allowed a better characterization of the qNSCs and aNSCs (Codega et al., 2014, Chaker et al., 2016). For example, aNSCs transcriptome revealed higher expression of genes related to cell cycle and DNA repair whereas qNSCs showed enrichment in genes of cell adhesion, transmembrane transporters and extracellular-matrix-response showing their interaction with the environment (Codega et al., 2014). In addition, taking advantage of the novel single-cell RNAseq analysis, it has been described a more detailed sequence of molecular changes that take place between qNSCs, aNSC, TAPs and neuroblasts also revealing the existence of different quiescent and activate states (Llorens-Bobadilla et al., 2015).

2.3 NSCs *in vitro* and the neurosphere assay.

Stem cells from diverse tissues are typically cultured *in vitro* under conditions that promote their selective expansion. These cultures are widely used, as theoretically both self-renewal and differentiation can be evaluated at the single-cell level. Given the absence of unique and decisive markers to identify the neural stem cell population *in vivo,* the analysis of NSCs has been widely based on the *ex vivo* behaviour of cells isolated from the neurogenic niches. The *in vitro* NSCs culture was initially described by Reynolds and Weiss who dissected striatal parenchyma including the periventricular area encompassing the SVZ from young adult mice, dissociated the tissue to single cells and plated them in non-adherent conditions in serum-free medium in the presence of epidermal growth factor (EGF). Under these culture conditions, a small population of cells began to divide forming floating spheres of proliferating cells, called primary "*neurospheres*" (Reynolds and Weiss 1992). In these neurospheres, the majority of cells expressed Nestin and new secondary neurospheres were obtained after the mechanical dissociation and culture again in the presence of EGF. Additionally, when plated on adherent substrate, they differentiated into both neurons and glial cells providing the firs evidence that multipotent stem cells were present in the adult mammalian brain (Reynolds and Weiss 1992). Since these early experiments, the neurosphere assay has evolved into a powerful tool that enables the study of NSCs proliferation, self-renewal and differentiation potential under highly controlled environmental conditions (Ferron et al., 2007, Belenguer et al., 2016).

Individual cells dissected from either the postnatal SVZ or SGZ can proliferate in medium containing EGF and basic fibroblast growth factor (FGF2) to produce these multipotent clonal aggregates. The frequency of long-lived NSCs dissociated from the SVZ/SGZ is often estimated as the number of cells capable of generating the primary neurospheres that include cells able to generate new aggregates upon clonal passage (self-renewal) and that can be expanded for limited periods of time. Additionally, neurospheres can be induced to differentiate in culture to generate the three major

cell types of the central nervous system (CNS), βIII-tubulin+ neurons, GFAP+ astrocytes and O4+ oligodendrocytes (Ferron et al., 2007, Belenguer et al., 2016).

Despite the evident advantages of the neurospheres cultures, they have some limitations. The most important is the heterogeneous composition of neurospheres as NSCs coexist with their progeny (different types of more committed progenitors and even differentiated cells). Moreover, NSCs produce cell progeny *in vitro* and some of the highly proliferative committed progenitors appear also capable of forming neurospheres, but only for a few passages (Reynolds and Rietze 2005). Furthermore, the strong mitogenic stimulation of culture conditions promotes the selective expansion of aNSCs while qNSC rarely form neurospheres (Pastrana et al., 2011, Mich et al., 2014). Therefore, the neurosphere cultures in the current culture conditions better reflects the potential of aNSCs and TAPs. Recently, FACS has made possible the isolation of NSCs and their progeny from the adult SVZ using different combination of markers (Pastrana et al., 2009, Codega et al., 2014, Daynac et al., 2015, Llorens-Bobadilla et al., 2015) and have started to shed light on gene regulatory networks and cell identity in adult SVZ. Especially, the discrimination between aNSCs and qNSCs enable studies of their properties and dynamics in the adult brain (Daynac et al., 2015). Concretely, the identification of markers that allow the isolation of qNSCs will allow their sphere-forming capacity to be directly tested.

Furthermore, experimental variability has been introduced into sphere-forming assay including, cell density and medium composition favouring differences and sometimes conflicting results between different groups because it is sometimes difficult to merge findings from different laboratories to gain a more complete understanding of a particular process (Jensen and Parmar 2006). Importantly, there are established some critical steps that are crucial in the performance of the neurosphere cultures (Pastrana et al., 2011). Cell density is one of the most important parameters because it has a critical impact on clonality (Ferron et al., 2007). Thus, it is important for the community to standardize the culture method so that different assays can be compared. Therefore, there is still controversy about the real functional relationship between neurosphere-forming cells and the stem cell population *in vivo* and the neurosphere assay cannot be used alone to define the *in vivo* stem cells. Nevertheless, this system represents a tractable model to investigate the contribution of signalling pathways, expression, and/or epigenetic mechanism to cell-fate specification with potential applicability to neural stem cells for restorative neurogenesis in disease or trauma.

2.4 Reprogramming of NSCs into iPSCs.

Reprogramming of somatic cells is a valuable tool to understand the mechanisms associated to pluripotency as well as the characteristics of the cell-of-origin, and further opens up the possibility of generating patient-specific pluripotent stem cells. NSCs are multipotent stem cells that endogenously

express *Sox2*, *c-myc* and *Klf-4* which may function in maintaining the stemness and multipotency of NSCs (Kim et al., 2009b). Moreover, *Sox2* was suggested to maintain cellular pluripotency by regulating *Oct4* expression (Masui et al., 2007). In contrast, *Oct4* is not expressed in NSCs being a key regulator of mouse embryogenesis (Pesce et al., 1998).

Different combinations of reprogramming factors have been attempted to reprogram postnatal NSCs into iPSCs (Eminli et al., 2008, Kim et al., 2008). Specifically, three different combinations were also capable of generating iPSCs: *Oct4*, *Klf4* and *c-myc* (OKM); *Oct4*, *Klf4* and *Sox2* (OKS); and *Oct4*, *c-myc* and *Sox2* (OMS), with similar efficiency and comparable expression profiles than ESCs. The ability of two-factor combination to induce iPSCs was also assessed. In this case, only two combinations were successful to reprogram NSCs into full pluripotent iPSCs: *Oct4* and *Klf4* (OK) and *Oct4* and *c-myc* (OM). However, two-factor reprogramming showed less efficiency than the use of four-factors (0.11% and 3.6%, respectively) (Kim et al., 2008). It has been reported that *c-myc* exhibit an oncogenic effect and increases telomerase activity, responsible of immortalization of NSCs (Miura et al., 2001), so that iPSCs generation without the *c-myc* retrovirus represents a significant finding (Kim et al., 2008). More recently, it has been described that iPSCs can be generated without the oncogenic factors *c-myc* and *Klf4* being exogenous expression of *Oct4* sufficient to generate iPSCs from postnatal NSCs, albeit with ten-fold lower efficiency than two factor approach (Kim et al., 2009b). This result demonstrates the crucial role of *Oct4* in the process of reprogramming and supports the hypothesis that NSCs represent an intermediate state between differentiated and pluripotent cells.

The induction of pluripotency is an extraordinary phenomenon that is currently poorly understood and inefficient (Hirai et al., 2011). Usually, reprogrammed cells do not gain some essential properties of induced pluripotency, such as *Nanog* expression, however it has been described that the use of defined culture conditions, combining the dual inhibition (2i) of mitogen-activated protein kinase signalling (MEK) and glycogen synthase kinase-3 (GSK-3) with LIF, promotes the rapidly upregulation of pluripotency-associated genes such as *Nanog*, *Oct4* and *Rex1* at a similar levels to ESCs as well as the silencing of retroviral transgenes (Silva et al., 2008, Ying et al., 2008). Therefore, 2i/LIF condition consolidates the reprogramming process where non-completely reprogrammed cells (pre-iPSCs) undergo a transcriptional and epigenetic resetting that rapidly culminates in a full pluripotent status (Silva et al., 2008).

3. Epigenetic regulation of adult neurogenic niches

Epigenetic is defined as the study of heritable alterations in genome function that do not involve changes in the DNA sequence itself (Jaenisch and Bird 2003, Bird 2007). These epigenetic marks can modulate gene expression either by directly altering the chromatin structure or by creating binding

sites for chromatin and transcription regulatory subunits. It is becoming apparent that epigenetic modifications to developmental genes, are very important cell-intrinsic programs that can interact with transcription factors and environmental cues to co-ordinately activate and repress arrays of genes at specific steps during development (Hsieh and Gage 2004, Surani et al., 2007).

Two general classes of epigenetic regulation can be defined: covalent modifications to DNA and post-translational covalent modifications to the histones (H) around which the DNA is bound, influencing whether DNA is accessible or not for gene transcription (Strahl and Allis 2000, Kouzarides 2007). Moreover, the three-dimensional structure and arrangement of chromatin within the nucleus are both regulated and contribute to the establishment and maintenance of epigenetic states (Bird 2007, Montalban-Loro et al., 2015). These different classes of epigenetic regulators are intimately related, resulting in multiple layers of control allowing cells to maintain their identity over time (Jaenisch and Bird 2003, Bird 2007, Montalban-Loro et al., 2015). Dysregulation of these mechanisms leads to new cellular phenotypes by causing altered gene expression without a change in genotype. In the neurogenic niches, epigenetics regulators and their associated transcription factors play an important role in the control and maintenance of NSCs stemness.

3.1 DNA methylation and neurogenesis

DNA methylation involves the addition of a methyl group to the fifth carbon in the cytosine pyrimidine ring. Traditionally, studies of DNA methylation have focused on regions that contain a high frequency of CG dinucleotides, known as "*CpG islands*" (Bird 1986) (**Fig. 7a,b**). Most mammalian CpG dinucleotides are methylated which often have regulatory functions and tend to be found in the promoter and first exon regions of genes where it promotes a closed chromatin structure and aids to the prevention of expression (Schilling and Rehli 2007). Thus, transcription depends in part on the CpG density of the promoter.

There are two types of methylation reactions both mediated by DNA methyltransferases (DNMTs) (**Fig. 7a,b**). One is *de novo* methylation catalysed by DNMT3a and DNMT3b, important for normal embryogenesis and development and responsible for the establishment of new methylation patterns. The other type is maintenance methylation mediated by DNMT1 that effectively maintains CpG methylation upon DNA replication and provides the heritable "*memory*" of the methylation state of the parent cell (Montalban-Loro et al., 2015). A mutation in any of the three major *Dnmt* genes in mice leads to severe developmental abnormalities and embryonic, or early postnatal, lethality. *Dnmt1* is highly express in the embryonic and adult CNS in both proliferating neural progenitors and differentiated neurons where it maintains DNA methylation (Goto et al., 1994, Feng et al., 2010). In support of this, mice deficient for *Dnmt1* specifically in neural progenitors at embryonic stages exhibit

deficits in neuronal function and die postnatally, suggesting a requirement for methylation in brain development (Fan et al., 2001). Genome-wide analysis of DNMT3A-binding sites, in embryonic neural progenitors cells (NPCs), have revealed its direct epigenetic regulation of many neurogenic genes whereas depletion of DNMT3B in the neuroepithelium promotes NPC differentiation instead of proliferation (Yao et al., 2016).

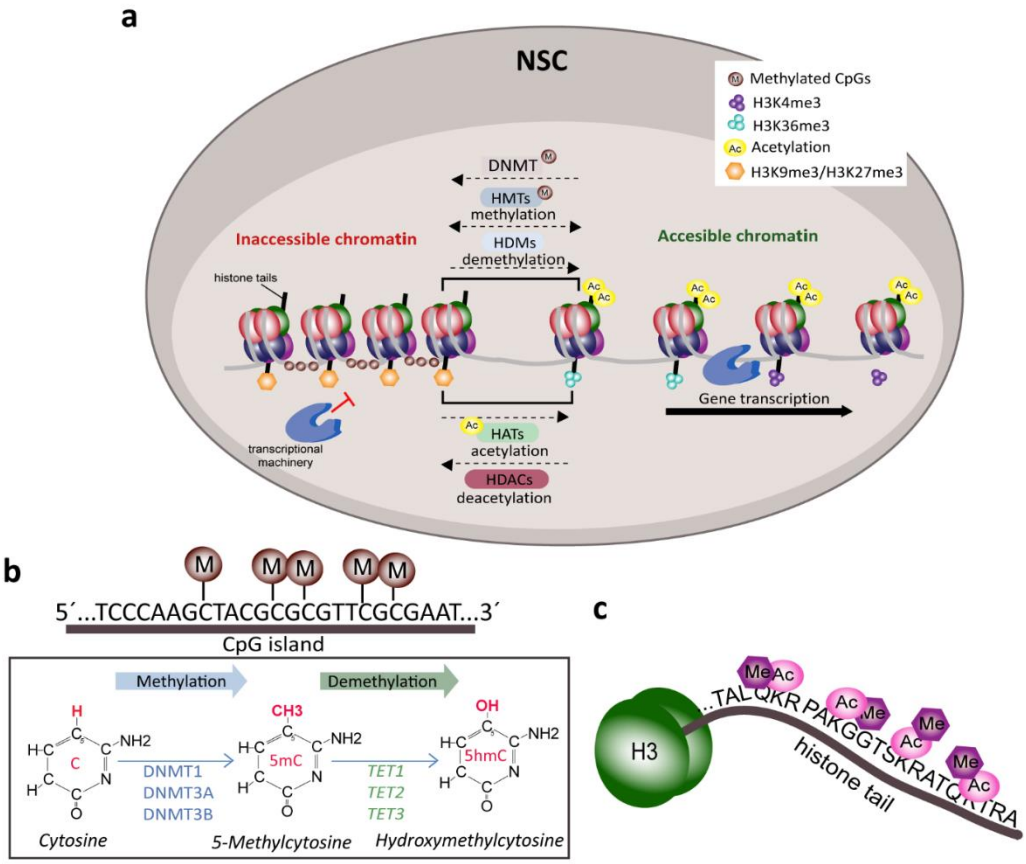

Figure 7. Epigenetic regulation of gene expression. (a) Schematic of DNA methylation and histone modifications in neural stem cells (NSCs). DNA is compressed through interactions with histones and methyl groups (M) are added to cytosine-guanine (CpGs) dinucleotides in regulatory regions. Methylation reactions are mediated by DNA methyltransferases (DNMTs). Histone methylation reactions are catalyzed by histone methyltransferases (HMTs) and the reverse process is mediated by histone demethylases (HDMs). $H3K9me^3$ and $H3K27me^3$ inhibit transcription while $H3K4me^3$ and $H3K36me^3$ activate transcription. Histone acetylation is mediated by histone acetyltransferases (HATs) that leads to chromatin decondensation (accessible chromatin) and transcription activation. Histone deacetylases (HDACs) catalyze the reverse process inducing inactivation of transcription (inaccessible chromatin). **(b)** Schematic of DNA methylation at the cytosine-guanine dinucleotides in gene regulatory regions. DNMTs transfer methyl groups (M) to the fifth position of the pyrimidine ring. This is a reversible process mediated by the ten-eleven translocation (TET) family of enzymes TET1, TET2 and TET3 dioxygenases that catalyze the conversion of the modified genomic base 5-methylcytosine (5mC) into 5-hydroxymethylcytosine (5hmC) playing a key role in active DNA demethylation. **(c)** Schematic of the histone tail showing multiple sites for epigenetic modifications as acetylation (Ac) or methylation (Me). All these modifications provide a unique epigenetic signature that governs either active or closed chromatin structure. Adapted from Montalbán-Loro *et el* 2015.

DNA methylation marks repress gene expression either by attracting DNA methyl-binding domain proteins (MBDs) such as methyl-CpG binding protein 2 (MeCP2) which recruit repressors and

chromatin remodelling molecules to generate an inactive chromatin environment or by directly inhibiting transcription factor binding (Bird 2002, Yao et al., 2016). MBD proteins have been implicated in neurogenesis. For example, MBD1 occupies and protects the methylation of the promoter for basic FGF2, which encodes a growth factor essential for neural development. Indeed, mice deficient in MBD1 show decreased neurogenesis and hippocampus-related behaviours defects (Li et al., 2008). *Mecp2*-knockout mice exhibit pronounced deficit in neural maturation, altered expression of presynaptic proteins and reduced dendritic spine density in the DG of the hippocampus (Smrt et al., 2007). Additionally, many transcription factors exhibit specific binding to methylated or unmethylated DNA motifs and some of them, such as recombining binding protein (RBPJ) and Fez family zinc finger protein 2 (FEZF2), have been implicated in the regulation of neurogenesis (Faigle and Song 2013).

3.2 DNA hydroxymethylation and TET enzymes

DNA methylation marks are reversible through both passive replication-dependent demethylation and active demethylation which involve the recently characterized 5-hydroxymethylcytosine (5hmC), 5-formylcytosine (5fC) and 5-carboxylcytosine (5caC) intermediates (Wu and Zhang 2017), which are produced by the oxidation of 5-methylcytosine (5mC), a reaction catalyzed by the ten-eleven translocation (TET) family of enzymes (Tahiliani et al., 2009, Ito et al., 2011) (**Fig. 7b**). TET proteins are capable of converting 5mC to 5hmC in the presence of ATP and further transform 5hmC to 5fC and 5caC (He et al., 2011). Both derivatives can be successively excised by thymidine DNA glycosylase (TDG) and replaced by an unmodified cytosine through the base-excision repair (BER) pathway to complete the active DNA demethylation process (Wu and Zhang 2017) (**Fig. 8a**). In mammals, three members of the TET family have been identified: TET1, TET2 and TET3 (Ito et al., 2010) (**Fig. 7b**).

TET proteins are iron(II)/α-ketoglutarate (Fe(II)/α-KG)-dependent dioxygenases. The core catalytic domain at the carboxyl terminus is comprised of a double-stranded β-helix (DSBH) domain and a cysteine-rich domain (Pastor et al., 2013). However, the three TET proteins differ in terms of domain architecture and tissue specificity (**Fig. 8b**). Full-length TET1 (TET1FL) and TET3 (TET3FL) isoforms have a CXXC domain at their amino terminus that binds CpG dinucleotides. Interestingly, mouse TET1 isoform lacking the CXXC domain (TET1s) has a reduced global chromatin binding compared with TET1FL (Zhang et al., 2016). TET3 exists as three major isoforms, including two without the CXXC domain, TET3s and TET3o (Jin et al., 2016) (**Fig. 8b**). TET3o is specifically expressed in oocytes, whereas TET3s and TET3FL are upregulated during neuronal differentiation. Unlike TET1, TET3s and TET3o display stronger demethylation activity than TET3FL (Jin et al., 2016).

TET-mediated active DNA demethylation might be different depending on the biological context (Wu and Zhang 2017). 5hmC is relatively abundant in mouse ESCs, the early embryo and in adult brain (Ito et al., 2010, Iqbal et al., 2011). Immediately after fertilization mouse zygotes undergo a rapidly epigenetic reprogramming including DNA demethylation of both paternal and maternal genomes. Recent evidences indicate that on the paternal genome this occurs by TET3 mediated conversion of 5mC to 5hmC, whereas the demethylation of the maternal genome mainly occurs through passive dilution (Gu et al., 2011). In addition, it has been proposed that TET enzymes in the blastocyst and ESC are involved in pluripotency by maintaining the hypomethylated state of key regulator regions (Ito et al., 2010, Koh et al., 2011). For individual tissues, the levels of 5hmC, 5fC and 5caC are not obviously correlated. For example, although 5hmC is more abundant in the mouse brain cortex than in ESCs, the levels of 5fC and 5caC are reverse suggesting that different steps of demethylation cycle are differentially regulated in different tissues (see (Wu and Zhang 2017) for a revision).

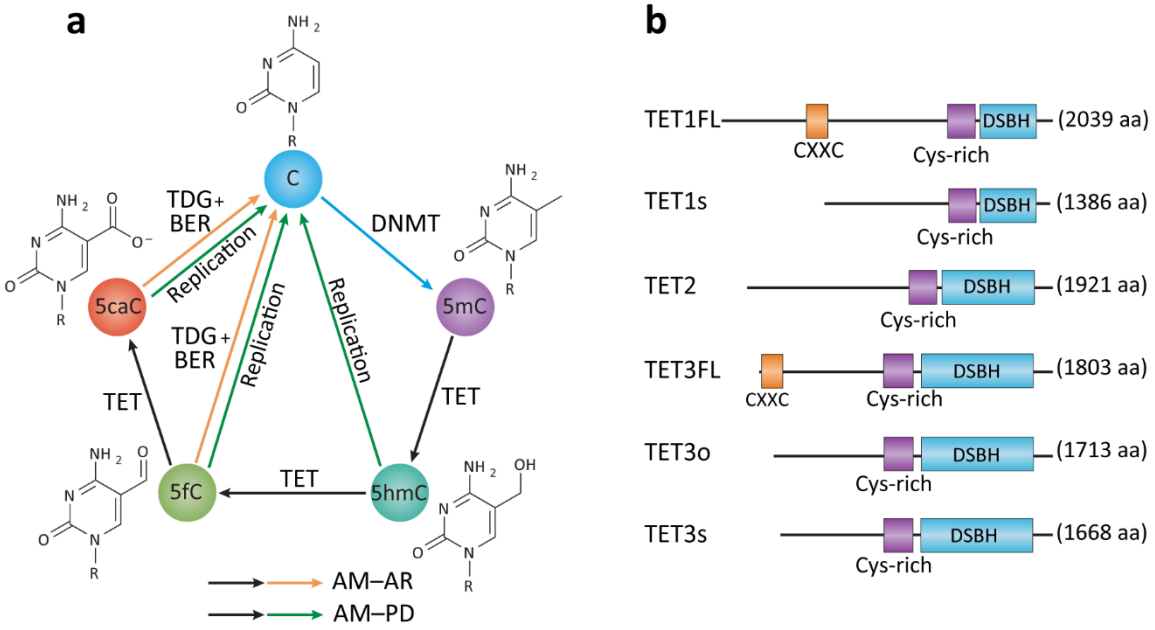

Figure 8. TET-mediated DNA demethylation. (a) DNA methylation cycle. TET can convert 5mC to 5-hydroxymethylcytosine (5hmC), 5-formylcytosine (5fC) and 5-carboxylcytosine (5caC). Finally, thymine DNA glycosylase (TDG) coupled with base excision repair (BER) return to the unmodified state (active modification-active removal; AM-AR). Modified cytosines can also be modified by replication-dependent dilution (active modification-passive dilution; AM-PD). **(b)** Structure of TET proteins. Cysteine-rich and double-stranded β-helix (DSBH) domains at the carboxyl terminus confer catalytic activity. Both full-length isoforms (TET1FL and TET3FL) have a CXXC DNA binding domain at the amino terminus. Adapted from Wu and Zhang, 2017.

In the brain, DNA methylation is both spatially and temporally dynamic and has been proposed to play and integral role in the coordination of neural development (Munzel et al., 2010, Szulwach et al., 2011). For instance, neuronal commitment requires de-repression and re-activation of neuronal genes associated with increase DNA methylation (Sikorska et al., 2008). The suppression of astrogliogenesis during neuronal specification is also associated with changes in DNA methylation

(Lunyak et al., 2002, Ballas et al., 2005). In the embryonic mouse brain, 5hmC levels increase during neuronal differentiation and this is not associated with substantial DNA demethylation. Indeed, functional perturbation of *Tet2* and *Tet3* leads to defects in neuronal differentiation suggesting that formation of 5hmC promotes brain development (Hahn et al., 2013). Moreover, neural progenitors can be induced efficiently from *Tet3* knockout ESCs, but undergo apoptosis rapidly, and terminal differentiation of neurons is greatly reduced, suggesting that *Tet3* is critical in neural progenitors cell maintenance and terminal differentiation of neurons (Li et al., 2015). DNA methylation also plays an important role in neurogenesis by regulating the proliferation and survival of neural progenitors as well as dendritic growth of newborn neurons in both embryonic and adult brains (Fan et al., 2001, Hutnick et al., 2009, Wu et al., 2010). It has been demonstrated that TET1 contributes to the regulation of neural progenitor cell proliferation as mice lacking *Tet1* exhibit impaired hippocampal neurogenesis as a consequence of the hypermethylation and downregulation of genes involved in progenitor proliferation (Zhang et al., 2013b). However, the full role and importance of hydroxymethylation and TET oxidases in neurogenesis remains to be elucidated.

Despite the well described catalytic activity of TET proteins, recently the preferential binding of TET proteins at 5mC-free promoter and their interaction capability with various proteins suggest their probably function independent of its catalytic activity (Wu and Zhang 2017). This is supported by the demonstration that catalytic dead TET mutants are able to rescue the phenotype of TET3 knockout (Xu et al., 2012, Kaas et al., 2013, Montagner et al., 2017). For example, TET3 catalytic dead mutants in *Xenopus laevis*, can partially rescue the developmental defects caused by TET3 knockdown (Xu et al., 2012). Moreover, in mouse hippocampus, overexpression of TET1 or a catalytically inactive mutant resulted in the upregulation of several neuronal memory-associated genes (Kaas et al., 2013). In the majority of these scenarios, the catalytic-activity-dependent and –independent functions probably coordinate to reinforce the functional outcome.

3.3 Histone modifications in the brain

DNA is packaged into a highly ordered chromatin structure in eukaryotes by wrapping around an octamer a histone proteins (H) that include H2A-H2B dimers and H3-H4 tetramer to form the nucleosome (Luger and Richmond 1998, Olins and Olins 2003). The interaction between histones and DNA is mediated by an N-terminal tail of histone proteins available for post-translational modifications that control the chromatin structure (Luger and Richmond 1998, Montalban-Loro et al., 2015) (**Fig. 7a,c**). These covalent modifications in the histone tails alter the interaction between adjacent nucleosomes and/or between histones and the DNA, changing the three-dimensional chromatin structure. Modification in the body of histones have also been shown to alter chromatin structure

influencing gene expression (Tropberger and Schneider 2013). Histone modifications are divided into repressive and active marks accordingly to how they correlate with levels of transcriptional activity and it is well stablished that histone methylation and acetylation, the main histone modifications, have fundamental roles in neurogenesis.

Histone acetylation is catalyzed by histone acetyltransferases (HATs) being a reversible process. Histone acetylation of lysine residues of histones enhances the recruitment and activation of the transcriptional machinery and is generally associated with areas of active gene transcription (Tessarz and Kouzarides 2014). However, histone deacetylases (HDACs) remove acetyl groups promoting the condensation of chromatin (Marmorstein and Trievel 2009) (**Fig. 7a**). It is well established that histone acetylation have fundamental roles in neurogenesis. HDAC1 is expressed by GFAP-positive cells within the SVZ whereas HDAC2 is found in migrating neuroblast and in TAP cells. Deletion of HDAC2 in the SVZ results in a defective neurogenesis to the OB and neurospheres treated with HDAC inhibitors promotes neuronal differentiation suggesting a role for this enzyme in neuronal fate determination (Siebzehnrubl et al., 2007, Jawerka et al., 2010, Foti et al., 2013). Furthermore, oligodendrocyte fate commitment is accompanied by a decrease in histone deacetylation at transcriptional repressors of oligodendrocytic differentiation such as *Sox2* (Lyssiotis et al., 2007).

Histone methylation is the other main histone modification and is associated with both active and silent chromatin being catalysed by histone methyltransferases (HMTs) (**Fig. 7a**). Trimethylation of lysine (K) 27 and lysine 9 of histone H3 (H3K27me^3 and H3K9me^3) tend to associate with regions of inactive gene transcription, whereas H3K4, H3K36 and H3K79 methylations are associated with active transcription (Li et al., 2007). Histone demethylases (HDMs) also have a key role in regulating neural development. Enhances expression of *Jumonji domain-containing protein 3* (JMJD3), which belongs to H3K27me^3 demethylases promotes demethylation of several neuronal genes, including *Dcx*, which induces neuronal differentiation (Park et al., 2014). H3K9me^3 is enriched in the adult murine SVZ and it has been recently shown that its repression in undifferentiated cells is engaged in the maintenance of cell type integrity in this neurogenic niche (Foret et al., 2014).

Taken together, these results demonstrate that proper histone modifications dynamics need to be tightly regulated to ensure the precise control of gene expression during neurogenesis in the mammalian CNS although these modifications are not the focus of this thesis.

3.4 Epigenetic changes during reprogramming

Cell reprogramming involves changes in the transcriptome and chromatin state of the reprogrammed cells to that of a pluripotent stem cell (Montalban-Loro et al., 2015). Evidence is

emerging that epigenetic priming events early in the process may be critical for pluripotency induction later (Papp and Plath 2013) (**Fig. 9**).

iPSCs have lower levels of methylation than somatic cells, suggesting that demethylation is an important chromatin feature to achieve pluripotency (Lee et al., 2014). During reprogramming, it is stipulated that reprogramming factors interfere with methylation by binding to specific promoters or enhancer regions leading to demethylation and activation of the pluripotency genes (Hochedlinger and Jaenisch 2015). Recent studies in NSCs have shown the importance of methylation level in the context of reprogramming. It is then probable that NSC chromatin is dynamically remodelled and that modification of DNA methylation are essential for reprogramming to a pluripotent state. DNA demethylation of pluripotency genes seems to be crucial for faithful reprogramming and both active and passive mechanism of demethylation have been implicated in iPSC reprogramming (Apostolou and Hochedlinger 2013). For instance, downregulation of DNMT1 in reprogramming facilitates the iPSCs generation consistent with the role of passive demethylation (Kohli and Zhang 2013).

TET enzymes, responsible of active demethylation, have been described to have a role on the reprogramming process. TET2 induces hydroxymethylation of key pluripotent genes such as *Nanog* for a subsequent transcriptional activation (Doege et al., 2012). Interestingly, proteomic and genomic analyses revealed that TET1 and TET2 directly interact with NANOG and co-occupy many pluripotent targets activating genes such as *Oct4* or *Esrrb* (Estrogen-related receptor beta). In support of such mechanism, TET2 depletion completely ablated reprogramming of fibroblast whereas TET1 overexpression enhances pluripotency acquisition (Pastor et al., 2013). However, reprogramming is often incomplete and leaves epigenetic marks including DNA methylation, chromatin modifications and transcriptional regulation known as "*epigenetic memory*" (Kim et al., 2011, Tobin and Kim 2012). Thus, reprogrammed iPSCs often present the limitation of not being fully reprogrammed thus keeping epigenetic traces of the tissue of origin. Future generation of iPSCs without epigenetic memory is an important challenge in the field to ensure that differentiation decisions are not affected by events from the past (Lee et al., 2014).

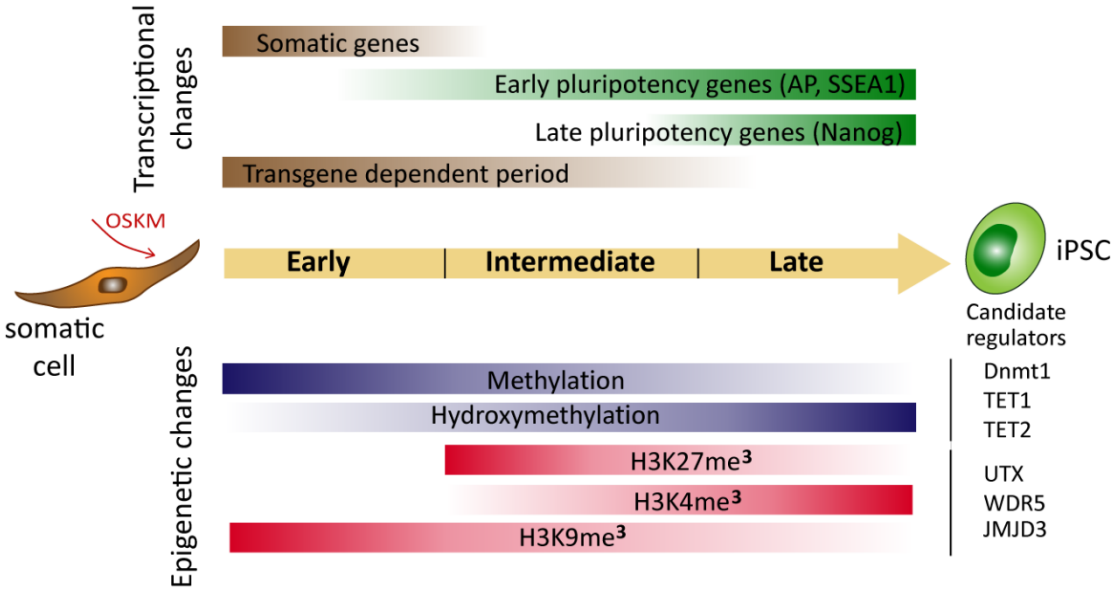

Figure 9. Dynamics of key molecular events during reprogramming. Summary of the main transcriptional and epigenetic changes (coloured bars) occurring during reprogramming of fibroblast into iPSCs, and examples of candidate regulators described. Modified from Apostolou and Hochedlinger, 2013.

3.5 Genomic imprinting and regulation of adult neurogenesis

During mammalian development, the vast majority of genes are expressed or repressed from both alleles. However, there are a small number of genes, termed "*imprinted genes*" that are expressed monoallelically from either the maternally or the paternally inherited chromosomes (**Fig. 10a,b**). Approximately 150 imprinted genes have been described in mammals (complete list in *http://www.mousebook.org/mousebook-catalogs/imprinting-resource*) and are generally organized in clusters, although examples of singleton imprinted genes do exist (da Rocha and Ferguson-Smith 2004, Ferguson-Smith 2011, Barlow and Bartolomei 2014) (**Fig. 11)**. An imprinting cluster is usually under the control of a DNA element, called the imprinting control region (ICR) that consists of differentially DNA methylated regions (DMRs) on the two parental chromosomes (**Fig. 10a,b**). Thus, ICRs can be divided into those which are methylated on the paternally inherited copy and those with maternally inherited methylation. Importantly, deletion of an ICR results in loss of imprinting of multiple genes in the cluster (Ferguson-Smith 2011, Barlow and Bartolomei 2014) (**Fig. 10b**).

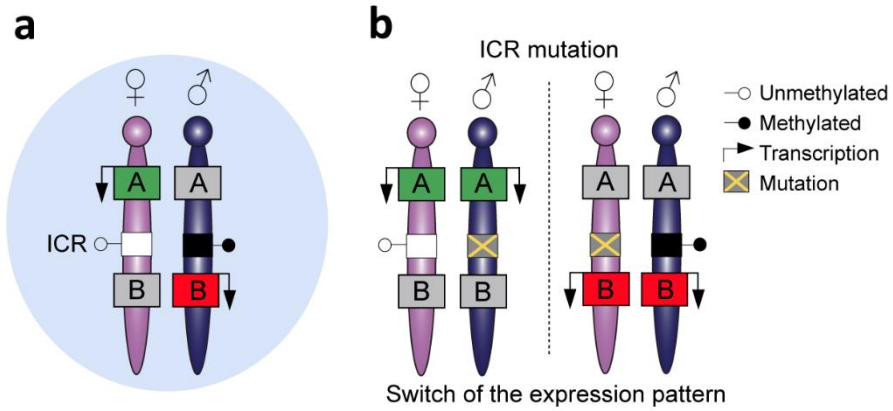

Figure 10. Imprinted genes are under control of the imprinting control region (ICR). (a) Mammalian somatic cells contain a maternally inherited chromosome (pink) and a paternally inherited chromosome (blue). Imprinted genes are located in clusters and can be expressed from the maternally inherited chromosome and repressed in the paternally inherited chromosome (Green box A), or expressed from the paternally inherited chromosomes and repressed from the maternally inherited chromosome (Red box B). Imprinting in the cluster is regulated by a DNA element, called imprinting control region (ICR) that has differentially methylated regions (DMRs) on the two parental chromosomes. **(b)** Mutations in the ICR can modify imprinting affecting several genes in the cluster resulting in a switch in the expression patterns with the paternally inherited chromosome acquiring an epigenotype typical on the maternal one or *vice versa*. Adapted from da Rocha and Ferguson-Smith, 2004.

It is well stablished that parental specific marks are assigned in the germline (Edwards and Ferguson-Smith 2007). At this time, both genomes are in distinct compartments and the modifications can be performed according to the sex of the transmitting gametes. During embryogenesis, the primordial germ cells (PGCs), which give rise to the gametes, have the methylation patterns that are characteristic of somatic cells. However, in the genital ridges, the imprints are erased during gamete formation to allow re-establishment of new parental specific marks (**Fig. 12**). After demethylation and differentiation of the PGCs, methylation is established at the ICRs in an allele-specific manner depending on whether the developing gamete is in the male or female germline. This occurs by *de novo* methylation process catalysed by DNMT3a methyltransferase (**Fig. 12**). DNMT3L is a regulatory co-factor of DNMT3a and is also required (Lozano-Ureña et al., 2017). After fertilization, a rapid an extensive reprogramming of the parentally inherited genomes occurs, and most DNA methylation is lost (Smallwood and Kelsey 2012). However, the parental-specific imprints must be maintained during this period and a memory of parental origin is propagated into daughter cells during somatic cell divisions (**Fig. 12**). Critical factors such as the Kruppel-like zinc finger protein ZFP57, protect imprints during the post-fertilisation period (Takahashi et al., 2015). Somatic heritability is conferred by the DNMT1 that recognizes newly replicated hemi-methylated DNA and places methylation on the newly replicated strand (Goll and Bestor 2005). Moreover, it has been reported the implication of TET proteins in removal of DNA methylation imprints (Liu et al., 2015).

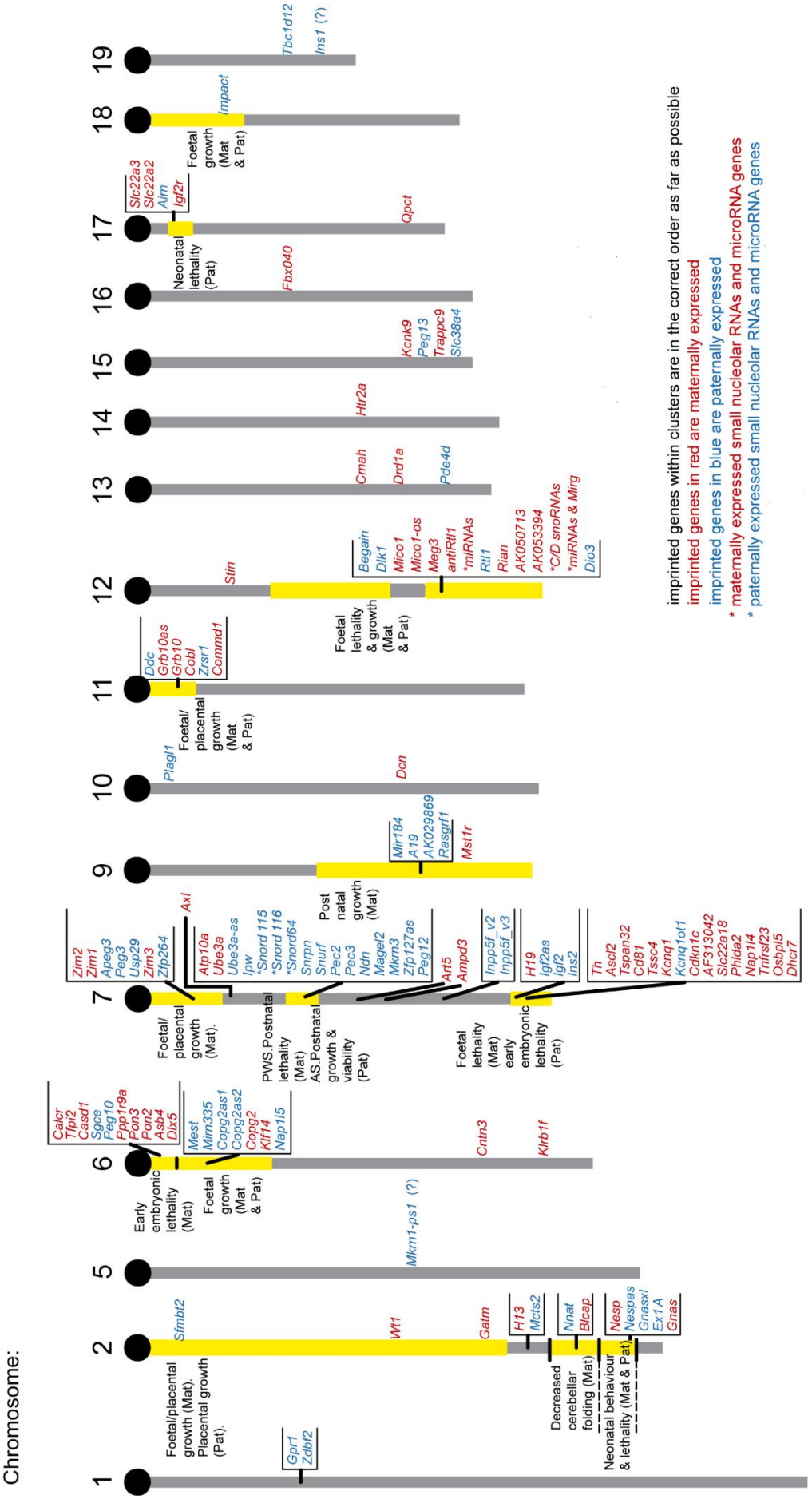

Figure 11. Imprinted genes are located in clusters. Map of mouse imprinted genes, regions and phenotypes. Imprinted genes are distributed through the genome, preferentially organized in clusters (boxes). Vertical grey lines represent mouse chromosomes. Imprinted genes within the clusters are in the correct order as far as possible. Maternally expressed genes are represented in red while paternally expressed genes are indicated in blue. Yellow boxes represent regions with abnormal imprinting phenotypes (source: http://www.mousebook.org/all-chromosomes-imprinting-chromosome-map).

Maternal germline DMRs are found at gene promoters, whereas paternal germline DMRs are found in intergenic regions (Edwards and Ferguson-Smith 2007). There are also somatic or secondary DMRs that acquire their DMR status after fertilization. Mapping experiments and germline DMR deletion experiments in mice demonstrated that the primary ICRs are essential to establish monoallelic expression and that the secondary somatic DMRs play important roles in imprinting maintenance. (Sutcliffe et al., 1994, Thorvaldsen et al., 1998, Williamson et al., 2006).

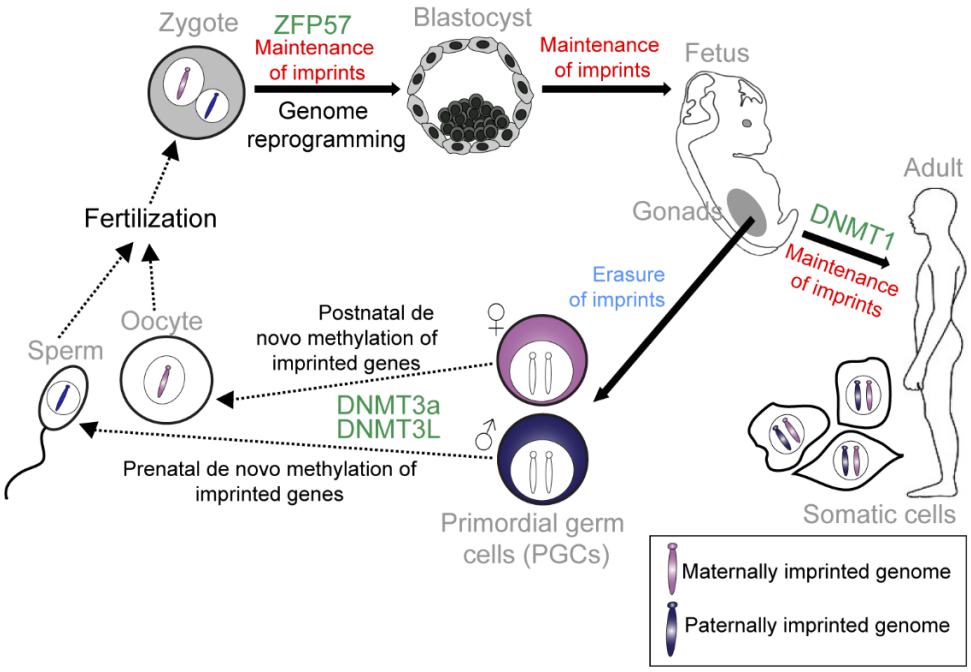

Figure 12. Establishment and maintenance of imprints during development. DNA methylation is erased in primordial germ cells (PGCs) in the genital ridge; however, imprints are maintained in somatic cells throughout the lifetime of the organism. Imprints are acquired in a sex-specific manner in the germline: maternally and paternally DNA methylated ICRs gain DNA methylation in oocytes and sperm, respectively for transmission to the next generation. Following fertilization, the parental-specific imprints are maintained in the developing organism despite genome-wide reprogramming elsewhere. ZFP57 protects imprints during the post-fertilization epigenetic reprogramming period. DNMT3a and DNMT3L catalyse de novo methylation process and DNMT1 participates in the maintenance of imprints in somatic tissues.

Imprinted genes are expressed widely and highly during prenatal stages and predominantly downregulated after birth. They are involved in multiple developmental processes. After birth, imprinted genes modulate postnatal neurological and metabolic functions but their monoallelic expression makes these *loci* very vulnerable since mutation or loss of imprinting of the expressed allele can compromise expression and lead to severe developmental defects (Cleaton et al., 2014). The majority of imprinted genes are expressed in the placenta and brain (Coan et al., 2005, Wilkinson et al., 2007) and disruption of imprinting can result in a number of human congenital imprinting syndromes including Prader-Willi (PWS) and Angelman syndromes (AS), characterized by neurological and behavioural impairments and learning difficulties (Hirasawa and Feil 2010). Disruption of

imprinting can also predispose to tumour formation and loss of imprinting at several genes has been observed in human cancers making aberrations of imprinting a potentially valuable tool for both diagnosis and treatment (Jelinic and Shaw 2007).

Recent evidences suggests that the genomic imprinting process can be selectively lost or "*switched off*" in particular cell types or at specific developmental time points to activate an allele that is usually repressed (Ferron et al., 2011, Ferron et al., 2015). These heritable changes have an impact on stem cell plasticity and are likely to be essential for normal development and tissue regeneration (Kar et al., 2014). For instance, in the SVZ, the paternally expressed gene *Delta-like homologue 1* (*Dlk1*), an atypical Notch ligand, plays an important dual function in postnatal neurogenesis. *Dlk1* that is canonically imprinted in the brain shows a selective absence of imprinting in these cell types. Biallelic expression of *Dlk1* is required for the stem cell maintenance in the SVZ and final neurogenesis (Ferron et al., 2011). *Insulin-like growth factor 2* (*Igf2*) canonically expressed from the paternally-inherited allele, is biallelically expressed in the choroid plexus and secreted to the CSF to regulate NSCs proliferation (Ferron et al., 2015). During cortical neurogenesis, radial-glia highly expressed the paternally expressed zinc finger protein *Zac1*. Elevated *in vivo* levels of ZAC1 promote cell cycle exit, disrupt neurogenesis and also induced the expression of other imprinted genes such as the maternally expressed cyclin-dependent kinase inhibitor *Cdkn1c*, known to promote NSCs cell cycle arrest and differentiation (Rraklli et al., 2016).

Genomic Imprinting has also been lightly studied in the reprogramming process. An initial report showed that several imprinted genes (*H19*, *Peg1*, *Peg3* and *Snrpn*) maintained their allele-specific DNA methylation after reprogramming of fibroblast (Wernig et al., 2007). Interestingly, maintenance of the state of imprinting is also evident in iPSCs generated from AS and PWS patient fibroblast (Chamberlain et al., 2010). Thus, it appears that imprints present in the somatic cell of origin are retained in iPSCs even though more analysis is needed to define how imprinting is regulated during the reprogramming process. Particularly, in NSCs, it has been described that *Oct4* seems sufficient to repress genes responsible for NSCs molecular identity and to activate the pluripotency genes, suggesting that epigenetic of NSCs renders them easier to reprogram (Kim et al., 2009b). However, the particular epigenetic mechanisms involved in the regulation of NSCs and during their acquisition of a pluripotent state are poorly understood.

This thesis leads to the understanding of some of the basic epigenetic regulators in adult NSCs under physiological conditions, and identifies new epigenetic mechanisms that are modulated during the reprogramming of NSCs into iPSCs. We show that the dioxygenase TET3 inhibits the acquisition of a pluripotent state in NSCs and describe a crucial role for TET3 exerting its function in the maintenance

of the neural stem cell (NSC) pool in the adult SVZ niche through a mechanism that is independent of its catalytic function.

Objectives

The discovery of neural stem cells (NSCs) in the adult nervous system implies the potential for endogenous repair and exogenous cell-based therapeutics, therefore the determination of positive and negative regulators that work to provide and optimal number of NSCs and their specific cell types is crucial for their future use in cell therapy. The epigenetic changes involved in neural stem cells maintenance remains to be elucidated thus the main objective of this work is the identification of the epigenetic signature (including genomic imprinting) that might control NSCs function in physiological conditions.

The specific objectives proposed in this Thesis are:

1. Cell reprogramming of adult NSCs into a pluripotent state with a minimum number of exogenous factors.

2. Identification of the epigenetic changes occurring in adult NSCs during the acquisition of a pluripotent state focusing on the regulation of genomic imprinting and DNA methylation.

3. Study of the role of the DNA dioxygenase TET3 in the regulation of NSCs maintenance and neurogenesis in the adult SVZ niche.

Material and Methods

1. Experimental animals

1.1 Mice handling

Mice used were housed under 12 hours light/darkness conditions, with a constant temperature between 20 and 22 ºC and with a free accessible diet of pellets and water (*ad libitum*). Experimental procedures were performed in accordance with Spanish RD 53/2013 guidelines following the protocols approved by the ethical committee and under the supervision of the responsible of *Servicio de Producción Animal del Campus de Burjassot* from the Universitat de València. Litters were weaned with 21 days old.

When performance of highly invasive techniques was inevitable, mice were deeply anesthetized by intraperitoneal (i.p.) injection of a mixture of medetomidine (0.5-1 mg *per* kilogram of body weight) and ketamine (50-75 mg *per* kilogram of body weight) diluted in saline solution (0.9% NaCl).

1.2 Mice strains

All experiments were done using 2-4 months-old adult mice. The following mouse strains were used along this thesis:

- C57BL/6 (*Mus musculus domesticus)*: wild-type strain used as a source of biological samples for the different *in vivo* and *in vitro* experiments. These mice were also used to generate heterozygous and hybrids animals.

- CAST/EiJ (*Mus musculus castaneus)*: wild-derived mice used to generate hybrids animals through reciprocal crosses with C57BL6 strain.

- *Tet3*$^{loxP/loxP}$: mice carrying *LoxP* sites flanking the *Tet3* gene were kindly provided by Dr. Wolf Reik (Babraham Institute, Cambridge). To generate these mice C57BL/6 ES cells were targeted with a vector containing *LoxP* sites around exon 5 of the *Tet3* gene (Santos et al., 2013). This region contains residues required for chelation of Fe(II) and is upstream of exons containing other key catalytic residues of *Tet3* (Tahiliani et al., 2009). Thus, expression of *Cre-recombinase* results in the excision of this region and a frame-shift from exon 6 that affects all downstream exons until a premature stop codon in exon 7. Mice were maintained on a C57Bl6 background.

- B6.Cg-Tg(Gfap-cre)73.12Mvs/J (*GFAPcre*): mice obtained from Jackson laboratory. *GFAPcre* mice were generated using a 15-kb promoter cassette containing the full sequence of the mouse *Gfap* gene (Garcia et al., 2004) directing expression of a *Cre-recombinase*. This cassette (clone 445) contains all introns, promoter regulatory elements, exons and 2 kb of 3´and 2.5 kb of 5´flanking DNA of the *Gfap*

gene. The *Gfap* expression is prevented by the removal of a small fragment of the first exon (Johnson et al., 1995). *GFAPcre* line was maintained in heterozygosis. When these transgenic mice are bred with mice containing a *LoxP*-flanked sequence, Cre-mediated recombination is expected to result in deletion of the floxed sequences in the *Cre-recombinase* expressing tissues of the offspring. Cre-recombinase activity was observed in essentially all adult neural stem cells, thus this strain was used to generate *Tet3* conditional mutant mice in the GFAP+ cells in the SVZ (see *TET3-GFAPcre* strain). Importantly, donating investigator (Michael V. Sofroniew, University of California) reports that this strain show *Cre-recombinase* expression in the male germline (Zhang et al., 2013a), and suggests breeding *GFAPcre* females with floxed males for Cre-Lox experiments.

- *TET3-GFAPcre*: To generate the specific deletion of *Tet3* in GFAP positive cells within the SVZ, heterozygous *GFAPcre* transgenic females were bred with $Tet3^{loxP/loxP}$ males. Mice were maintained on a C57Bl6 background. All experiments were performed in F3 offspring mice.

- B6;129S-$Gt(ROSA)26Sor^{tm1Sor}$/J (*Rosa26-LacZ*): mice obtained from Jackson laboratory. Heterozygous mice for the $Gtrosa26^{tm1Sor}$ targeted mutation were crossed with *GFAPcre* transgenic mice to test the tissue/cellular expression pattern of the *cre-recombinase*. *Cre-recombinase* expression results in the removal of a *LoxP*-flanked DNA segment that prevents expression of a *LacZ* gene. Consequently, β-galactosidase was present in cells/tissues where *cre*-recombinase was expressed. The *Rosa26-LacZ* strain was particularly useful for this purpose as the *Rosa26* promoter led to generalized expression of *LacZ* in the adult.

- *NU/J*: mice obtained from Jackson Laboratory. Homozygous mice for the nude spontaneous mutation (*Foxn1nu*, formerly *Hfh11nu*) have abnormal hair growth and defective development of the thymus epithelium. Nude mice are also athymic, lack T cells and suffer from a lack of cell-mediated immunity. Homozygous immunosuppressed mice were used for the teratome formation assay (see page 52.

1.3 Genotyping

The genotype of the different strains was determined by the end-point Polymerase Chain Reaction (PCR) using genomic DNA extracted from a small ear or tail tissue fragment using the commercial Thermo Scientific™ Phire™Animal Tissue Direct PCR kit (Thermo Fisher, cat. no. F140WH), in accordance with the manufacture´s protocol. The presence of mutant or wild-type alleles was determined using 2 µl of gDNA to perform a PCR using GoTaq® G2 Flexi DNA Polymerase (Promega, cat. no. M7801). The specific conditions for each PCR are detailed in **Table 1.** The size of each PCR product was resolved through electrophoresis in 2-3 % agarose gel prepared in TAE buffer (40 mM Tris-

HCl pH 7.6, 20 mM acetic acid and 1 mM EDTA) with 1x Real Safe (Real©, Cat. no. RBMSafe). A commercial loading dye was used (Thermo fisher, cat. no. F-350). Finally, gels were photographed with UV light in a Kodak transiluminator.

Table 1. Genotyping primers and PCR conditions. 64TD58 indicates a touch-down, a PCR protocol where annealing temperature (Tª) starts at 64 degrees during 30 sec and reduces 0.5 degree each cycle during the first 11 cycles. After that, 24 cycles were performed at 58 degrees. DEL indicates delectioned allele**.**

Gene	Primer sequence (5´-3´)	Amplicon	Allele	T (ºC)	Cycles
Tet3	Tet3-F TACCTCTGCCTCTGGAGTGCTAA Tet3-R2 GTCAGGAAAGTCACATGGTTGTTG	320 bp	WT	60	39
	Tet3-F TACCTCTGCCTCTGGAGTGCTAA Tet3-R2 GTCAGGAAAGTCACATGGTTGTTG	400 bp	LoxP		
	Tet3-F TACCTCTGCCTCTGGAGTGCTAA Tet3-R1 ATGGCTACTCACAACCCAGTGAC	237 bp	DEL		
GFAPcre	oIMR7338 CTAGGCCACAGAATTGAAAGATCT oIMR7339 GTAGGTGGAAATTCTAGCATCATCC	300 bp	WT	60	39
	oIMR1084 GCGGTCTGGCAGTAAAAACTATC oIMR1085 GTGAAACAGCATTGCTGTCACTT	100 bp	CRE		
Rosa26-LacZ	OIMR39 ATCCTCTGCATGGTCAGGTC OIMR40 CGTGGCCTGATTCATTCC	200 bp	WT	64TD58	11+24
	OIMR15 CAAATGTTGCTTGTCTGGTG OIMR16 GTCAGTCGAGTGCACAGTTT	300 bp	LACZ		

2. Study of the SVZ cytoarquitecture

2.1 BrdU administration

5-Bromo-2´-deoxyuridine (BrdU) is a structural thymidine nucleotide analogue which is incorporated into de DNA of cells in S phase of the cell cycle at the administration moment. Three weeks before killing, two-month-old mice were injected with BrdU (Sigma Cat. no. B5002) at 50 mg/kg of body weight. In the SVZ, fast-proliferating transit-amplifying progenitors and migrating neuroblasts dilute out the BrdU, which is only retained in slowly proliferating NSCs (label-retaining cells, LRCs) and OB newborn neurons that ceased to divide and terminally differentiated soon after the injection (Ferron et al., 2007). In order to analyse the largest number of labelled cells, BrdU was injected every 2 hours for 12 consecutive hours (seven injections in total) and mice were sacrificed by transcardial perfusion 28 days later. BrdU was prepared freshly every time in saline buffer (0.9% NaCl). The solution was sonicated in an ultrasound water bath (Transsonic 310/H, Elma®) for a few minutes immediately

before injection. We detected LRCs using a specific antibody against BrdU in histological slices (see Immunohistochemistry section).

2.2 Histological techniques

Mice usedfor *in vivo* experiments were deeply anaesthetized as indicated above. In order to maintain brain and tissue structures, mice were transcardially perfused first with 27.5 ml of saline buffer (0.9% NaCl) in order to remove blood cells, followed by 4% paraformaldehyde (PFA) in 0.1 M Phosphate Buffer Saline pH 7,4 (PBS) at a flow rate of 5.5 ml/min. After that, brains were extracted and post-fixed by immersion in 4% PFA during 1 hour and washed 1 additional hour with PBS. Finally, brains were serial coronal sectioned at 40 µm of thickness using a vibratome (Leica® VT1000S) and kept in PBS-0.05% sodium azide at 4º until the analysis.

For SVZ whole-mounts, mice were sacrificed by cervical dislocation and the lateral ventricles were carefully dissected out. The resulting whole-mounts were fixed and permeabilized in 4% PFA with 0.5% Triton™ X-100 (TX) in PBS for 8-12 hours. Next day, tissue was rinsed three times in 0.5% Tx-100 PBS before the immunohistochemical analysis.

2.3 Immunohistochemistry (IHC)

Immunohistochemical techniques used in this thesis include immunofluorescence and peroxidase detection techniques. Primary antibodies used are in **Table 1 Annex I**. Specifically, for the detection of BrdU, 5hmC and 5mC, slices were initially treated with 2N HCl at 37ºC during 20 min to allow denaturation of DNA. After that, pH was neutralized washing the slices with 0.1M sodium borate (pH 8.5) for 10 min followed by some washes with PBS. When peroxidase was used as primary antibody, endogenous peroxidase was inhibited using a 3% hydrogen peroxide solution (Panreac) for 30 min at RT. To prevent non-specific antibody binding, the tissue was incubated in blocking buffer (0.2% Tx-100, 1% glycine and 10% FBS in 0.1 M PBS) for 1 hour at a RT before using specific antibodies. Slices were then incubated overnight at 4ºC with primary antibody diluted in the same blocking buffer. The day after, slices were washed and incubated with secondary antibodies conjugated with different fluorophores (**Table 2 Annex I**) for 1 h at a room temperature in the dark. After several washes, nuclei were counterstained with 5 µg/ml of DAPI (4',6-Diamidine-2'-phenylindole dihydrochloride; Sigma) for 5 min and mounted with a specific mounting solution for fluorescent preparations (FluorSave™, Millipore, cat. no.345789).

For peroxidase detection, samples were incubated with specific biotinylated secondary antibodies (**Table 2 Annex I**) followed by avidin-biotin-peroxidase complex (ABC) using the Vectastain® commercial Kit (Vector Laboratories, cat. no. PK4000). After several washes in PBS, slices were

incubated with 0.02% of DAB (3-3´diaminobencidine, Sigma, cat. No. D7304) and 0.01% H_2O_2 in 0.1M PBS until the signal appeared. For β-galactosidase staining, perfused brain slices were rinsed in Tissue Rinse solution A (2 mM $MgCl_2$, 5 mM EGTA and 0.1 M PO_4, pH 7.4) for 30 min at a room temperature and rinsed then with Tissue Rinse Solution B (2 mM $MgCl_2$, 0.01% sodium deoxycholate (Sigma, cat. no. D6750), 0.02% Nonidet P-40 (Sigma, cat. no. 21-32775AJ) and 0.1 M PO_4 pH 7.4) for 30 min. Sections were incubated in Tissue Stain Base Solution (0.1 M PO_4 pH 7.4, 2 mM $MgCl_2$, 0.01% sodium deoxycholate, 0.02% Nonidet P-40, 5 mM $K_3Fe(CN)_6$, 5 mM $K_4Fe(CN)_6$ and 1 mg/ml X-Gal) at 37ºC overnight. Slices were washed several times with PBS, dehydrated with increasing concentration of alcohols, clarified with citrosol and mounted with Eukitt (Panreac®).

Due to its thickness, SVZ whole-mounts were washed three times in PBS containing 2% Tx-100 for 15 min each and blocked for 2 hours in blocking buffer with 2% of Tx-100. Primary antibody incubation was done during 48 hours at 4ºC prepared in the same blocking buffer.

2.4 SVZ cell populations counting

For the analysis of the different populations within the adult SVZ, 2-8 immunostained slices for each animal were visualized and photographed in an Olympus FluoView FV10i confocal laser scanning microscope (Olympus, Japan) equipped with 405, 458, 488 and 633 nm lasers. Images were processed using FV10-ASW 2.1 viewer software (Olympus, Japan). When more than one fluorophores were analysed in the same sample, they were excited separately to avoid interferences. Cell populations were manually counted in captured images and data was obtained as a percentage of positive cells relative to a specific population or to the total number of DAPI cells. Merged images were done with Adobe Photoshop CS5. BrdU-LRCs in the SVZ, OB and *corpus callosum* were manually counted in a fluorescent microscope (Nikon Eclipse Ni) in 10-12 slices applying the Cavalieri estimator (C=N x S x TH) which takes into account the number of counted cells per section (N), the total number of slices obtained (S) and section thickness.

3. Adult Neural Stem Cells (NSCs) culture

The isolation and culture of NSCs have been previously described by our laboratory (Ferron et al., 2007, Belenguer et al., 2016). The protocol is detailed below.

3.1 SVZ dissection and tissue dissociation.

Two-month old mice were sacrificed by cervical dislocation. The brains were removed and collected in a plate with cooled and sterile PBS (Biowest, cat. no. X0515). Brain dissections were made under a dissection microscope with a pair of scalpels. The cerebellum and olfactory bulbs were first

removed and both hemispheres separated for fine dissection. SVZ area was delimited removing the surrounding tissue and ventricle wall was finely cut, separating the SVZ from the rest of the brain tissue (**Fig. 13**). After that, both SVZs from each mice were diced together and enzymatically digested with a previously activated (20 min at 37ºC) solution of papain (12U/mouse; Worthington Biochemical Corporation, cat. no. LS003120) containing 0.2 mg/ml L-cysteine hydrochloride (Sigma, cat. no. C8277) and 0.2 mg/ml EDTA (Sigma, cat. no. E6511) in EBSS (Earle´s Balanced Salt Solution, Gibco™, cat. no. 24010-043). After 30 min of incubation at 37ºC, tissue was washed in control medium (**Table 2**) and carefully disaggregated using a fire polished glass pipette. Once the cellular suspension was obtained, cells were plated in complete medium (**Table 3**). Cells obtained from two SVZs were distributed in 8 wells of a p48-well plate and incubated at 37ºC and 5% CO_2 atmosphere. After 7 days of incubation, differentiated cells died and some isolated cells (NSCs and some progenitors) proliferate to form clonal aggregates called primary "*neurospheres*".

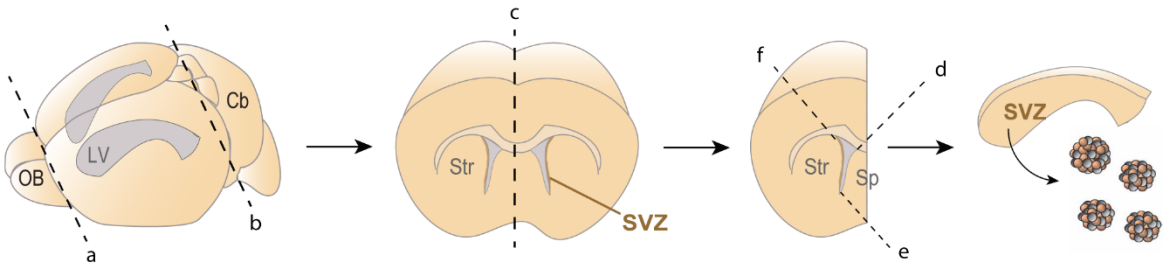

Figure 13. Schematic of the SVZ dissection protocol. Initially, olfactory bulbs (OB) and cerebellum (Cb) were removed (a-b) to obtain a 4-5 mm thick slice containing the lateral ventricles (LV). Then, both hemispheres were separated (c) for fine dissection. After that, to isolate the SVZ: cuts to separate the ventricular zone from the septum (Sp) (d,e) and cuts to exclude the striatum (str) were performed (f). Finally, the SVZ block was finely cut under the surface of the ventricle wall, separating the SVZ from the subjacent striatal parenchyma. Black dashed lines indicate cut zones.

After neurospheres acquired the right size (150-200 μm), the number of primary neurospheres was manually counted on an inverted microscope (Nikon eclipse TE2000-S). The total number of neurospheres was considered as an estimation of the number of forming neurospheres cells in the SVZ tissue. The cultures were then subcultured (passaged; see 3.2).

3.2 Subculture and expansion of adult NSCs

NSCs subculture is one of the most critical steps in the establishment of the NSCs cultures. Only few cells from a neurosphere are able to generate new spheres and this capacity depends on age, strain, etc. Once primary neurospheres were obtained from the tissue, they were expanded by dissociating and seeding individually under the same culture conditions.

To proceed, neurospheres were centrifuged in a 15 ml conical tube at 100-130 g during 5 min. Pelleted spheres were treated with 200 µl of Accutase® solution (Sigma, cat. no. A6964) for 10 min at RT. After this incubation, 800 µl of control medium were added and spheres were mechanically dissociated by pipetting 10-15 times using a p1000 micropipette. Dissociated cells were washed with control medium and centrifuged again at 200 g for 10 min. Single cells pellet was resuspended in complete medium and the cell concentration was estimated using the automatic ADAM cell counter system (NanoEnTek®).

For culture expansion, a relative high density of viable cells (10.000 cells/cm^2) were seeded in complete medium and incubated at 37ºC with a 5% CO_2 humidified atmosphere. After 5-7 days, secondary neurospheres were big enough to be processed for a new passage**.** To determine the cellular growth rate of the cultures, the number of cells generated after each passage was quantified and accumulative growth curve was represented in a graph considering the number of cells generated after several passages.

3.3 The neurosphere formation assay (NSA).

Neural stem cells have the capability to proliferate and self-renew and these capacities can be evaluated *in vitro*. The NSA assay was utilized to accurately quantify *bona fide* stem cell frequency based on neurosphere numbers (Pastrana et al., 2011) (**Fig. 14**). After obtaining a single cell suspension solution, cells were plated at low density (5 cel/µl; 1000 cells *per* well of a p96-well plate in a total volume of 200 µl of complete medium). In order to minimize possible pipetting bias, an intermediate dilution of 50 cell/µl was prepared. Cells were incubated at 37ºC in a 5% CO_2 humidified incubator. Five days after, the neurospheres formed were manually counted on an inverter microscope under phase contrast optics.

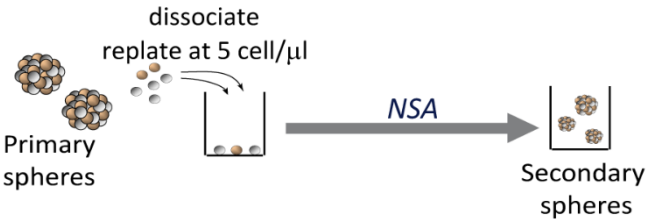

Figure 14. The neurospheres assay (NSA). Schematic of the neurospheres assay. Primary neurospheres were dissociated and replated at low density (5 cells/µl). Spheres were allowed to develop for 5 days and counted.

For diameter assessment, at least 200 neurospheres were photographed with a camera coupled in an inverted microscope (Nikon DXM1200F) and their diameters were measured using the free ImageJ software (NHI).

3.4 Determination of the proliferation capacity in NSCs

3.4.1 Determination of the BrdU incorporation rate

To determine the BrdU incorporation rate in neurosphere cultures, single cells were attached to glass coverslips pre-treaded with Matrigel® (Corning®, cat. No. 354230; diluted 1:100 in control medium for 24h) and incubated at 37ºC for a variable period of time depending on the experiment. After that, cells were treated for 5 min with 2 µM BrdU diluted in the culture medium and cells were fixed for 20 min with 4% pre-warmed PFA in PBS. After several washes, BrdU incorporation was analysed by immunocytochemistry (see Immunocytochemistry section).

3.4.2 Cell cycle analysis

Single cells were grown in complete medium at 10.000 cell/cm^2 and incubated at 37ºC in a 5% CO_2 humidified incubator. Two days after, neurospheres were pelleted and treated with Accutase® during 10 min to obtain a single cells suspension that were stained with the BD Cycletest™ Plus DNA Kit (BD FACs, cat. no. 340242) in accordance with the manufacture´s protocol. Finally, the percentages of cells in the different cell cycle phases were determined in a FACSVerse (BD) flow cytometer and analysed with FlowJo® software.

3.5 Differentiation assay and reactivation of NSCs

NSCs are multipotent cells that are able to differentiate into the three neural lineage cells: astrocytes, oligodendrocytes and neurons. Although NSCs have the ability to proliferate in the presence of EGF and FGF, once EGF is removed and an adherent matrix is provided, NSCs initiate the differentiation program. To induce bulk differentiation, secondary neurospheres were dissociated, washed with control medium to remove mitogens contamination, and 80.000 cell/cm^2 were plated on Matrigel® coated coverslips (for ICC) or plates (for RNA extraction) with Differentiation medium I (control medium supplemented with 10 ng/ml of bFGF) to promote cell survival at the beginning of the differentiation. After 2 days in culture, medium was replaced by Differentiation medium II (control medium supplemented with 2% FBS) that allows maturation of astrocytes and neuronal differentiation. Differentiating cells were incubated five more days. Glass coverslips for immunocytochemistry, were coated with Matrigel® diluted 1:100 in control medium and incubated at 37ºC in a 5% CO_2 humidified incubator for 24h. Coverslips with differentiated cultures were next washed twice with sterile dH_2O and processed for ICC (see immunocytochemistry section).

For reactivation experiments, 7-days differentiated cells (as indicated above) were detached by treating the cultures with Trypsin-EDTA (T/E) (Gibco, cat. no. 25200-056) for 10 mins. Cells were

mechanically dissociated to get a single cell suspension and were washed with PBS several times to remove FBS contamination. These cells were then resuspended in complete medium and re-plated at a low density (5 cell/µl) in a 96-well plates. Neurospheres were allowed to grow during 6-7 days and manually counted using an inverted microscope with phase contrast optic. The number of new neurospheres-forming cells was considered as an indication of the neural stem cell number in the cultures.

3.6 Cryopreservation and cellular thawing of NSCs.

Once neurospheres lines were established, they were expanded and cryopreserved for further use. Two-day neurospheres were centrifuged and softly resuspended in fresh complete medium supplemented with 10 % dimethyl sulfoxide (DMSO; Sigma, cat. no. D4540). Cells were transferred to labelled cryotubes and placed at -80ºC for at least 4 hours in a freezing container (CoolCell™, BioCision) designed to permit a slow temperature drop (1ºC/min). For long-time storage, cell cryotubes were transferred to a liquid nitrogen tank (-196 ºC).

To thaw cells, cryotubes were placed in a 37ºC water bath until complete thawing. Cell suspension was transferred to a 15 ml tube and centrifuged for 5 min at 100 g. Cells were resuspended and plated in complete medium.

3.7 Culture media and solutions for NSCs

Table 2. Control medium preparation. DMEM/F12 (Dulbecco´s Modified Eagle Medium / Ham´s F12 Nutrient Mixture).

Reagent	Working concentration	Stock conc.	Provider	Cat. no.
DMEM/F12 (1:1)	1x	1x (4ºC)	Gibco	11320-074
D(+)-Glucose	0.6 %	30% (-20ºC)	Panreac	141341
$NaHCO_3$	0.1 %	7.5% (4ºC)	Biowest	L0680-500
HEPES	5 mM	1M (4ºC)	Boiwest	L0180-100
L-Glutamine	2 mM	200mM (-20ºC)	Gibco	25030-081
Antibiotic/Antimycotic	1x	100x (-20ºC)	Gibco	15240-062
"Hormone mix"	1x	10x (-20ºC)	Homemade (Table 4)	
Heparin sodium salt	0.7 U/ml	350 U/ml (4ºC)	Sigma	H3149
Bovine Serum Albumin (BSA)	4 mg/ml	Powder (4ºC)	Sigma	B4287

Table 3. Complete medium preparation. EGF: Epidermal growth factor); FGF: Fibroblast Growth Factor.

Reagent	Working concentration	Stock conc.	Provider	Cat. no.
Control medium	Described in Table 2			
EGF	20 ng/ml	4 µg/ml (-20ºC)	Gibco	530003-018
bFGF	10 ng/ml	25 µg/ml (-20ºC)	Sigma	F0291

Table 4. Homemade "Hormone mix (HM)" preparation. It is prepared 10x concentrated and kept at -20ºC until use.

Reagent	HM 10x concentration	Stock conc.	Provider	Cat. no.
DMEM/F12 (1:1)	1x	1x (4ºC)	Gibco	11320-074
D(+)-Glucose	0.6 %	30% (-20ºC)	Panreac	141341
NaHCO3	0.1 %	7.5% (4ºC)	Biowest	L0680-500
HEPES	0.5 mM	1M (4ºC)	Biowest	L0180-100
Apo-Transferrin	1 mg/ml	Powder	Sigma	T2252
Bovine Insuline	14.5 µM	145 µM in 0.01N HCL	Sigma	I6634
Putrescine	0.1 mg/ml	1 mg/ml	Sigma	P7505
Progesterone	0.2 µM	2 mM in 95% etOH	Sigma	P6149
Sodium selenite	0.3 µM	3 mM	Sigma	S9133

4. Analysis of proliferating and differentiating NSCs by immunocytochemistry

Four-day proliferating neurospheres were plated on Matrigel® coated coverslips and incubated for 20 min to allow cell attachment followed by a fixation step in 2% PFA at 37ºC for 15 min and washed 3 times with PBS. After that, cells were kept in PBS-0.05% sodium azide at 4º until the analysis. For BrdU, 5hMe and 5mC detection, samples were initially treated with 2N HCl at 37ºC for 20 min to allow denaturation of DNA. PH was then neutralized with 0.1M sodium borate (pH 8.5) for 10 min followed by some washes with PBS. To prevent unspecific binding of antibodies, samples were incubated with blocking buffer (0.2% Tx-100, 10% FBS, 1% glycine in PBS) for 1 hour. Neurospheres were then incubated with primary antibodies (**Table 1 Annex I**) diluted in blocking buffer at 4ºC overnight. The day after, cells were washed in PBS and incubated with secondary antibodies (**Table 2 Annex I**) for 45 min at room temperature.

To analyse the NSCs during the differentiation process, coverslips with differentiated cultures (see section 3.5) were fixed at 2, 3 and 7 DIV. Samples were incubated for 1 hour in blocking buffer (0.2% Tx-100, 1% glycine and 10% FBS in 0.1 M PBS) with the exception of O4 detection (without Tx-100). Cells were incubated with primary antibodies (**Table 1 Annex I**) prepared in the same blocking buffer, at 4ºC overnight. Next day, the samples were washed several times with PBS before the incubation with the secondary antibodies (**Table 2 Annex I**). For O4 detection, primary antibody was incubated in blocking buffer without TX-100. Samples were both incubated with biotinylated secondary antibody for 40 min followed by one hour of incubation with streptavidin coupled with a fluorophore. After secondary antibody, coverslips were washed in PBS and stained with 1 µg/ml of DAPI for 5 min before mounting on microscope slides with Fluorsave™ reagent. The percentage of positive cells both in proliferating or differentiating conditions was determined counting the number

of immuno-positive cells related to the total number of DAPI positive cells in at least 40 fields captured using an Olympus FluoView FV10i confocal laser scanning microscope (Olympus, Japan).

5. Lentiviral shRNA gene silencing

Transient introduction of exogenous DNA for expression of the shRNA molecules can be synthesized exogenously into lentiviral vectors permitting the generation of continuous cell lines in which RNA enforces stable and heritable gene silencing (Paddison et al., 2002).

5.1 Lentivirus production in packing HEK293T cells

Lentivirus containing shRNA plasmids were generated in HEK293T packing cells. 293T cells were transfected with a "*plasmid solution*" containing the three lentivirus packaging plasmids and the specific shRNA (shSCRAMBLE or shSNRPN) (**Table 6**). To proceed, 4-5 x 10^6 of the packing cells HEK293T cells were plated in a 56 cm^2 culture plate. The day after, when 70-80% confluence was observed, the culture medium was changed to fresh HEK296T medium (**Table 5**) to improve transfection efficiency. For transfection, a "*plasmid solution*" containing 10-20 ng of the three lentivirus packaging plasmids and the specific shRNA (shSCRAMBLE or shSNRPN) (**Table 6**) was prepared in a total volume of 360 µl Opti-MEM™ (Gibco). 22 µl of Lipofectamine 2000 (Invitrogen) was also prepared in 360 µl Opti-MEM™. Both solutions were incubated for 5 min at RT and then incubated together for 20 min more. Mixture was added drop by drop to the HEK293T cells and cultures were incubated at 37ºC in a 5% CO_2 humidified incubator. After 14-16 hours, HEK293T culture media was changed by NSCs complete medium to obtain supernatants with lentiviral particles. As the plasmid vectors included the expression of a GFP (Green Fluorescent Protein) reporter, the presence of fluorescence was checked in a fluorescent inverted microscope as a control of the transfection process.

5.2 NSCs transduction

Approximately 30 hours after transfection, when the lentiviral production is maximum, supernatants with lentiviral particles were collected and filtered with a 0.45 µm nitrocellulose filter. At the same time, neurospheres to be transduced were dissociated using Accutase® and 1x10^6 cells were acutely infected with the lentiviral supernatant supplemented with 4 µg/ml of Polybrene (cationic polymer used to increase the efficiency of infection; Sigma, cat. no. H9268). One hour after, 4 ml of complete medium were added and cells were incubated for 4-6 hours. Finally, infected cells were washed and plated in a 25 cm^2 culture flask. Cells were allowed to grow for experiments.

Table 5. HEK293T culture medium. *FBS inactivation was performed by incubation at 65ºC for 10 min.

Reagent	Working conc.	Stock conc.	Provider	Cat. no.
DMEM high glucose	1x	1x (4º)	Biowest	L0101
FBS heat inactivated*	10 %	Pure (-20ºC)	Labclinics	S181B-500
L-glutamine	2 mM	200 mM (-20ºC)	Gibco	25030-081
Penicillin/Streptomycin	1x	100x (-20ºC)	Biowest	L0018-100

Table 6. Plasmids utilized in HEK293T transfection.

Plasmid	ng per transfection	Codified molecule	Use	Reporter	Provider	Cat. no.
pMDLg/pRRE	4.8 ng	Gag, pol, RRE	Lentiviral packaging	None	Addgene	#12251
pRSV.REV	2.5 ng	Rev		None	Addgene	#12253
pMD2G	3.5 ng	Env		None	Addgene	#12259
pLL3.7 shRNA scramble	11.6 ng	shRNA scramble	Expression silencing	GFP	Addgene	#11795
pLKO shRNA SNRPN	11.6 ng	ShRNA SNRPN		GFP	Sigma	TRCN0000109285

6. CRISPR-Cas9-Mediated Gene Manipulation in NSCs

Plasmids to perform CRISPR/Cas9 (*Clustered Regularly Interspaced Short Palindromic Repeats*) assay for *Tet3* were kindly provided by Dr. Myriam Hemberger (Babraham Institute, Cambridge). To generate the specific CRISPR-Cas9 plasmid for gene mutation, Tet3-gRNA was synthesized, annealed, and ligated into the pSpCas9(BB)-2A-GFP (PX458) plasmid (Addgene #48138) using the *BbsI* restriction enzyme. The cloned gRNA sequence was: 5´-CACCGGAAAAGGCCACCAGGTCGT´-3. A PX458 empty plasmid was used as a control.

NSCs were nucleofected with a Nucleofector™ (Amaxa) to introduce the exogenous DNA into the cells. To do so, 3-4 days-grown neurospheres were dissociated using Accutase® to obtain a single cell suspension of NSCs of known cell density. Cells (1.5-2x10^6) were centrifuged for 10 min at 100 g. After centrifugation, 5 µl of a mix containing 5 µg of the different plasmids were directly added to the cell pellet which was then resuspended in 95 µl of Nucleofection Solution from the Mouse Neural Stem Cell Nucleofector™ kit (Lonza, cat. no. VPG-1004) and placed in a Nucleofector™ cuvette (Amaxa). Cells were electroporated in a Nucleofector™ 2b device (Amaxa) using the A-31 specific program. Electroporated cells were gently collected, seeded in a T25 culture flask with pre-warmed complete medium and incubated at 37ºC in a 5% CO_2 humidified incubator. After 48 hours, GFP expressing cells

were isolated by flow cytometry (MoFlo® XDP, Beckman Coulter) and plated at a 10 cell/µl to expand *Tet3* deficient cultures.

7. Reprogramming of NSCs into Induced Pluripotent Stem Cells (iPSC)

The reprogramming protocol used in this thesis was an adaptation from Kim J.B. *et al.* 2009 (Kim et al., 2009c) (**Fig. 15**). To generate iPSCs form adult NSCs with a minimal number of factors and given that NSCs express higher endogenous levels of *Sox2* and *c-Myc* than ESCs, only exogenous *Oct4* together with *Klf4* (2F) were used for reprogramming as previously described (Kim et al., 2008).

7.1 Retrovirus production in Platinum-E (Plate-E) packaging cells and NSCs transduction

Retroviruses are an efficient tool for delivering heritable genes into the genome of dividing cells. The Plat-E cell line (Cell Biolabs, cat. no. RV-101) is a potent retrovirus packaging cell line based on the HEK293T cell line that was generated using packaging constructs with an EF1α promoter to ensure longer stability and high-yield retroviral structure protein expression (Morita et al., 2000).

To produce retroviruses, Plat-E cells were plated with Plat-E medium (**Table 7**) without antibiotics (Blasticidin and Puromycin) and incubated at 37ºC in a 5% CO_2 atmosphere. After 24 hours (aprox 70% confluence), cell culture medium was changed with fresh medium and transfection with viral vectors was carried out (day 1). For that, a plasmid solution was prepared containing 1 ml of Opti-MEM™, 60 µl of 1mg/ml polyethylenimine (PEI, Polysciences, cat. no. 23966) and 20 µg of the retroviral vectors pMXs-Oct4 (#13366, Addgene), pMXs-*Klf4* (#13370, Addgene) and pMXs-Cherry (pMX-2A-CH, designed and kindly provided by Dr. Jose Manuel Torres). After 20 min of incubation, mixture was added drop by drop to the Plat-E cells (one plasmid per dish) for 24 hours (day 2). Plat-E culture medium was then replaced by NSCs complete medium. Transfection efficiency was checked by *cherry* expression in plat-E cells. The day after (day 3), each retrovirus-containing supernatant was collected and filter with a 0.45 µm nitrocellulose filter.

Neurospheres grown for two days were transduced with a mixture of virus-containing supernatant (SN) as follow (volume *per* plate): 3 ml of *Oct4* SN, 3 ml of *Klf4* SN, 1 ml of *cherry* SN and 3 ml of fresh NSCs complete medium. A control of infection was made with a mixture containing 7 ml of *cherry* retrovirus containing medium and 3 ml of fresh complete medium. In order to enhance the efficiency of retroviral infection, retrovirus mixture was supplemented with 4 µg/ml of Polybrene (Sigma). NSCs were then incubated for 14-18 hours at 37ºC in a humidified incubator. Infected NSCs medium was then changed by fresh complete medium (day 4) and neurospheres were allowed to develop.

7.2 Reprogramming of NSCs by retroviral transduction

To promote the reprogramming process, the mouse fibroblast cell line SNL (Cell Biolabs, cat. no. CBA-316) was used as feeder cells during the reprogramming process of infected NSCs. To avoid SNL feeder cells growing, they were mitotically inactivated by treatment with 4 µg/ml of Mitomycin C (Sigma, cat no M4887) for 2-4 hours. Plates were treated with 0.1% of gelatine (Sigma, cat. no. G1890) at 37ºC for at least 20 min and then mitomyzed SNLs were plated at high density ($2.5x10^6$ cell/plate) in gelatine-treated plates (day 7).

Five days after transduction (day 8), neurospheres were dissociated with Accutase® and $1,5x10^5$ of infected NSCs were re-plated on SNL *feeder* cells with reprogramming medium (RM) containing 15% FBS and the cytokine Leukaemia Inhibitory Factor (LIF) (**Table 8**). RM medium was changed every other day until Stage-specific Embryonic Antigen-1 (SSEA-1; also known as CD15) positive colonies appeared (pre-iPSCs), checked by staining with StainAlive SSEA-1 Antibody (DyLight 488) (Stemgent®, cat. no. 09-0067, 1:100 dilution) (**Fig. 15**). At this moment, reprogramming medium was replaced with 2i/LIF medium (**Table 9**) which is based on dual inhibition (2i) of mitogen-activated protein kinase (MAPK) signalling and glycogen synthase kinase-3 (GSK3) combined with LIF. This defined medium allows pre-iPSCs to advance to ground state pluripotency with high efficiency (Silva et al., 2008). 2i/LIF medium was changed every other two day until well-defined iPSCs colonies appeared. For further expansion of iPSCs, individual colonies were isolated and plated on gelatine treated plates with 2i/LIF medium in order to establish and expand clonal lines of iPSCs.

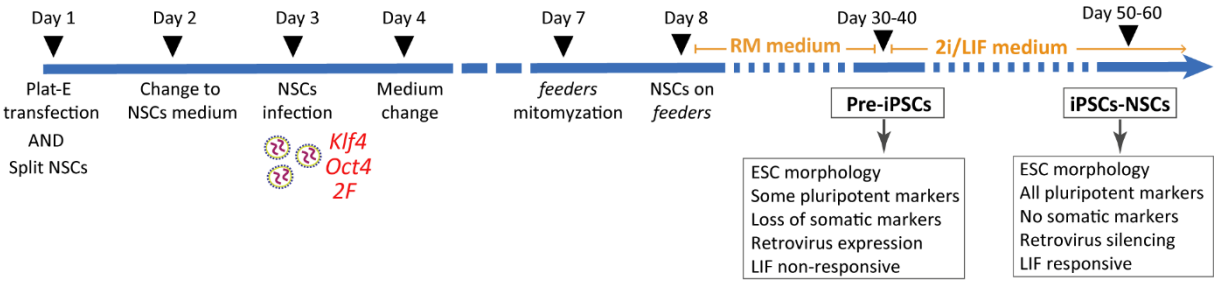

Figure 15. **Schematic representing the NSCs reprogramming protocol.** The protocol started with the plat-E transfection and NSCs passage. After changing the Plat-E medium to NSCs complete medium, NSCs were infected with retrovirus on day 3. Five days after the infection, NSCs were dissociated and plated on mitomyzed *feeders* with RM medium. Medium was changed every other day until pre-iPSCs appeared. At that moment, 2i/LIF medium was used to allow final iPSC development. When well-defined iPSCs colonies appeared, they were picked and re-plated for expansion.

7.3 iPSCs characterization

7.3.1 Alkaline phosphatase (AP) staining

Alkaline phosphatase detection method was used in reprogrammed cells to check the presence of iPSCs after one month in 2i/LIF medium on *feeders*. Cells were fixed with cold methanol for 2 min and washed three times with 0.1M Tris-HCl pH 8.5 buffer. Samples were incubated with the "*staining solution*" which contained 0.1 mg/ml Naftol phosphate (Sigma, cat. no. N4875), 0.5% Dimethylformamide (Sigma, cat. no. D4551) and 0.6 mg/ml Fast Red Salt (Sigma, cat. no. F2256) in 0.1M Tris-HCl pH 8.5. When red precipitate appeared, cells were washed with 0.1M Tris-HCl and distilled water. Finally, the different plates were photographed using a dissection microscope.

7.3.2 Embryoid bodies assay

Embryoid bodies' differentiation assay was performed using the "*hanging drops*" method. iPSCs were treated with Accumax® (Millipore, cat. No. SCR006) and the cell pellet was resuspended in EB differentiation medium (**Table 10**). Cells were counted and a dilution of 30.000 cell/ml was prepared. In a bacterial petri plate (less adherent) several rows of 20 µl drops of the cell suspension (about 5 ml) were plated using a multichannel pipet and the petri plate was incubated upside-down for 3 days at 37ºC in a 5% CO_2 humidified incubator to allow the EBs appearance. After this incubation time, the plate was inverted and 10 ml of EB medium were added. To avoid EBs attachment, a new culture plate was previously treated with 0.4% poly (2-HEMA) solution (Sigma, cat. no. P3932) prepared in Ethanol:Acetone (1:1). After washing poly (2-HEMA), EBs were re-plated with the same culture medium and incubated at 37ºC in a 5% CO_2 humidified incubator for 4 more days. After that, EBs were transferred to a 15 ml conical tube, dropped to the bottom of the tube and culture medium removed. In this point, sample for RNA extraction was collected and the remaining EBs were plated on gelatine-treated plates for 3 more days before analysing them by immunocytochemistry.

7.3.3 Karyotype analysis in iPSCs

To perform the karyotype analysis, cells needed to be 50% confluent. Cell division was inhibited using 0.6 µg/ml of KarioMAX® Colcemid (Gibco, cat. no. 15210-0.40) at 37ºC. After 2 hours, culture medium was removed and 0.85% sodium citrate, previously warmed at 37ºC, was added. A cell Scraper (Biofil®) was used to raise the cells. Cell suspension was transferred to a 15 ml conical tube and incubated at 37ºC for 15 mins. After that, 10 drops of codl Carnoy fixative (Methanol-Acetic acid, 3:1) were added to the suspension and softly mixed using a Pasteur pipette. Samples were washed several times with 5 ml of cold Carnoy solution and, after centrifugation (10 min 300 g), pellets were resuspended in 2 drops of Carnoy fixative. Cells extensions were made in microscope slides following

by fixation by heat. Samples were stained with Leishman´s stain (Sigma, cat. no. L6254) following the manufacture´s guidelines and the number of chromosomes were counted in an upright microscope (Nikon Eclipse Ni).

7.3.4 Immunocytochemical characterization during reprogramming

In order to assess the different cell populations at different stages of the reprogramming process, iPSCs and EBs were analysed by immunocytochemistry. Both of them were previously plated on coverslips coated with 0.1% gelatine (20 min at 37ºC). Two days after, cells were fixed with 4% PFA for 20 min and incubated in blocking buffer (0.2% Tx-100, 1% glycine and 10% FBS in 0.1 M PBS) for 1 hour. Samples were then incubated with primary antibodies (**Table 1 Annex I**) prepared in blocking buffer, at 4ºC overnight. The day after, samples were carefully washed and incubation with secondary antibodies (**Table 2 Annex I**) was performed for 1 hour. After several washes, DAPI (1µg/ml) was used to counterstain nuclei and coverslips with cells were mounted in microscope slides using FluorSave™ reagent.

7.3.5 Teratoma formation assay

To evaluate the capacity of iPSCs to generate teratomas, mouse iPSCs cultures were collected by treatment with Accumax™ (Millipore, cat. No. SCR006). Matrigel supplementation improves the efficiency of tumour formation (Prokhorova et al., 2009) thus iPSCs were washed in PBS and resuspended in PBS supplemented with 30% Matrigel® (Corning®, cat. No. 354230). Cells were kept on ice and drawn into a 1-mL syringe immediately before injection. Approximately 1.5×10^6 cells/200 µL of solution were injected in the dorso-lateral area of the subcutaneous space on both sides of the mice back. Teratomas were allowed to develop for 15-20 days when the size of the teratomas was approximately 1.5-2 cm. Mice were sacrificed by cervical dislocation and teratomas were extracted for analysis.

For teratoma analysis, samples were fixed in 4% PFA overnight at 4ºC with shaking. The day after, samples were embedded in paraffin: dehydration with increasing concentration of alcohols (70%, 96% and 100% ethanol) for 2 hours each, clarification with citrosol (Panreac, cat. no. 253139.1612) for 3 hours and immersion in paraffin (Panreac, cat. no. 256993) at 60ºC overnight. Teratoma samples were serially sectioned into 7 µm sections using a microtome (Leica, cat. no. RM2125). Slices were treated with citrosol for 15 min and with decreasing concentration of alcohols (100%, 96% and 70% ethanol) for 5 min each. After a final incubation in distilled water, samples were stained with haematoxylin and eosin and cell types from the three embryonic layers were identified by optic microscopy.

7.4 Embryonic Stem cells (ESCs) culture

The Embryonic Stem Cells (ESCs) line E14Tg2a (Hooper et al., 1987) was used as a pluripotency positive control in the different experiments. ESCs were cultured on gelatine-treated plates and when confluence was reached, approximately two days after plating, cells were treated with Trypsin/EDTA and re-plated following a dilution of 1:5 in ESC culture medium (**Table 8**).

7.5 Culture media and solutions for reprogramming and iPSCs expansion

Table 7. Plat-E cells and SNL cells culture medium. *Puromycin and blasticidin must to be removed in the transfection experiments and in SNL culture medium.

Reagent	Working conc.	Stock conc.	Provider	Cat. no.
DMEM high glucose	1x	1x (4ºC)	Biowest	L0101
FBS heat inactivated*	10 %	Pure (-20ºC)	Labclinics	S181B-500
L-glutamine	2 mM	200 mM (-20ºC)	Gibco	25030-081
Penicillin/Streptomycin	1x	100x (-20ºC)	Biowest	L0018-100
Puromycin*	1 µg/ml	2 mg/ml (-20ºC)	Sigma	P8833-25MG
Blasticidin*	10 µg/ml	10 mg/ml (-20ºC)	Sigma	8014001976

Table 8. Reprogramming medium and ESC medium. *LIF was obtained from the supernatant of transfected COS7 cells with pCAGGs-LIF plasmid. LIF was tested in ESC before use.

Reagent	Working conc.	Stock conc.	Provider	Cat. no.
GMEM	1x	1x (4ºC)	Sigma	G5154
FBS (ES tested)	15 %	Pure (-20ºC)	Capricorn	FBS-12A
L-glutamine	2 mM	200 mM (-20ºC)	Gibco	25030-081
Sodium Pyruvate	1mM	100 mM (-20ºC)	Gibco	11360070
Non Essential Amino Acids	1x	100x (-20ºC)	Gibco	11140050
Penicilin/Streptomicin	1x	100x (-20ºC)	Biowest	L0018-100
Leukemia inhibitor factor (LIF)	1x	1000x (-20ºC)	Homemade*	
B-mercaptoethanol	0.1 mM	1 M (4ºC)	Sigma	M6250

Table 9. Preparation of 2i culture medium. The medium must to be prepared fresh each time. *LIF was obtained from the supernatant of transfected COS7 cells with pCAGGs-LIF plasmid. LIF was tested in ESC before used.

Reagent	Working Conc.	Stock conc.	Provider	Cat. no.
N2B27 medium	Described below			
Leukaemia inhibitory factor (LIF)	1x	1000x	Homemade*	
iMEK	1 µM	10 mM	Millipore	444968
iGSK3β	3 µM	10 mM	Millipore	361571
Preparation of N2B27 culture medium				
Neurobasal	0.5x	1x (4ºc)	Gibco	21103049
DMEM/F12 (1:1)	0.5x	1x (4ºC)	Gibco	11320-074
$NaHCO_3$	0.1 %	7.5% (4ºC)	Biowest	L0680-500
L-glutamine	2 mM	200 mM (-20ºC)	Gibco	25030-081
Sodium Pyruvate	1mM	100 mM (-20ºC)	Gibco	11360070
Non Essential Amino Acids	1x	100x (-20ºC)	Gibco	11140050
Penicillin/Streptomycin	1x	100x (-20ºC)	Biowest	L0018-100
B27	0.5x	50x (-20ºC)	Gibco	17504044
B-mercaptoethanol	0.1 mM	1 M (4ºC)	Sigma	M6250
"Hormone mix N2"	1x	10x	Homemade (below)	
Preparation of Homemade 10x "hormone mix" N2				
DMEM/F12 (1:1)	1x	1x (4ºC)	Gibco	11320-074
D(+)-Glucose	6 %	30% (-20ºC)	Panreac	141341
NaHCO3	1 %	7.5% (4ºC)	Biowest	L0680-500
HEPES	5 mM	1M (4ºC)	Biowest	L0180-100
Apo-Transferrin	1 mg/ml	Powder (-20ºC)	Sigma	T2252
Bovine Insulin	50 µM	5 mg/ml	Sigma	I6634
Putrescine	16 µg/ml	160 mg/ml	Sigma	P7505
Progesterone	60 ng/ml	0.6 mg/ml	Sigma	P6149
Sodium selenite	0.3 µM	3 mM	Sigma	S9133
Bovine Serum Albumin (BSA)	50 µg/ml	Powder (4ºC)	Sigma	B4287

Table 10. Preparation of EB culture medium.

Reagent	Working conc.	Stock conc.	Provider	Cat. no.
GMEM	1x	X1 (4ºC)	Biowest	L0101
FBS heat inactivated*	10 %	Pure (-20ºC)	Labclinics	S181B-500
L-glutamine	2 mM	200 mM (-20ºC)	Gibco	25030-081
Sodium Pyruvate	1mM	100 mM (-20ºC)	Gibco	11360070
Non Essential Amino Acids	1x	100x (-20ºC)	Gibco	11140050
Penicilin/Streptomicin	1x	100x (-20ºC)	Biowest	L0018-100
B-mercaptoethanol	0.1 mM	1 M (4ºC)	Sigma	M6250

8. Gene expression analysis

8.1 RNA extraction, cDNA synthesis and real-time PCR

RNA samples were obtained using the commercial RNeasy Mini Kit (Qiagen, cat. no. 74104) following the instructions provided by the manufacturer, including a DNase (Qiagen, cat. no. 79254) digestion step. RNAs were quantified using the Qubit® RNA HS Assay kit (Thermo Fisher, cat. no. Q32852) in a Qubit Fluorometer (Thermo Fisher) and kept at -80ºC until used. Briefly, 0.5-1 µg of RNA was retrotranscribed to cDNA using the RevertAid H Minus First Strand cDNA Synthesis Kit (Thermo Fisher, cat. no. K1632) following the manufacture´s guidelines.

Gene expression analysis was assessed by real-time PCR in a Step One Plus real-time PCR device (Applied Biosystem), using 4-10 ng of cDNA and specific TaqMan™ probes (Applied Biosystems) (**Table 3 Annex I**) or SYBR-green primers (**Table 4 Annex I**). For TaqMan™ assays, the reactions were carried out with TaqMan™ Fast Advanced Master Mix (Applied Biosystems, cat. no. 4444557) in 10 µl of final volume. For SYBR green amplification, SYBR® Premix Ex Taq™ (Takara, cat. no. RR420) was used according to the manufacturer instructions with a specific annealing temperature for each pair of primers. A standard curve, made up of dilutions of pooled cDNAs, was used for relative quantification. Expression levels of each gene were calculated relative to *Gapdh* which was used as a housekeeping endogenous control.

8.2 RNA sequencing (RNAseq)

Total RNA was obtained from, at least, $1x10^6$ cells and RNA extraction was done as indicated above. RNAseq methodology was performed by the *Servei Central de Suport a la Investigació Experimental* (SCSIE, Universitat de València). Briefly, RNAseq was based on deep-sequencing technologies and consisted in the conversion of a population of heterogeneous RNA into a library of cDNA fragments with adaptors attached to one or both ends. Then, each molecule was sequenced in a high-throughput manner making use of SOLiD 5500XL sequencer to obtain short sequences. Reading obtained were incorporated to FastQC v0.11.5 software to quantify and to check their quality by Phred value, GC percentage, nucleotides content, readings size and ambiguous base content (N). The number of obtained readings was $4\text{-}9x10^7$.

Analysis of the RNAseq data was performed by EpiDisease S.L. Briefly, readings were aligned with the reference mouse genome, version GRCm38.p5 (Ensembl). Afterwards, the number of readings for each gene was quantified. Mapping and quantification were carried out using Subread package. Less represented genes were removed and genes specific dispersions were estimated. Finally, differential gene expression was analysed using a test based on maximum conditional authenticity with

adjusted quantile and the resulting genes were grouped according to their role in KEGG routes by Enrichment Browser package.

9. Protein immunodetection by western-blot

Neurospheres grown for 4 days were collected by centrifugation. Samples were lysed in cold RIPA buffer (150 mM NaCl, 0.5% sodium deoxycholate, 50 mM Tris-HCl pH 8.0, 1% Tx-100 and 1% SDS) supplemented with Complete® protease inhibitor cocktail (Roche, cat. no. 11836153001) and placed on ice for 30 min. Lysates were centrifuged at 12000 g for 15 min at 4ºC and supernatants were transferred to new Eppendorf tubes and kept at 80ºC until use. Concentration of each sample was previously determined using the Pierce® BCA Protein Assay Kit (Thermo Fisher, cat. no. 23227) following the manufacturer's instructions and BSA as a standard curve. Absorbance at 560 nm was measured in a Victor® 3 Multilabel Plate reader (Perkin Elmer).

30-50 µg per sample were mixed with sample buffer (20% Glycerol, 10% SDS, 10% β-mercaptoethanol, 40 µg/ml Bromo phenol blue and 250 mM Tris-HCl pH 6.8) and boiled at 95ºC for 10 min to denature proteins. Proteins were resolved by sodium dodecyl sulphate polyacrylamide gel electrophoresis (SDS-PAGE) loading them in 6-10% poly-acrylamide gels with running buffer (25 mM Tris-base, 0.2 M glycine and 1% SDS). The Precision Plus Protein™ Dual Color Standards (Bio-Rad, cat. no. 161-0374) was used as a molecular weight marker. Proteins were transferred to polyvinylidene difluoride (PVDF) membranes using the Trans-Blot Turbo Transfer Pack (Bio-Rad, cat. no. 1704157) and the Trans-Blot Turbo transfer device (Bio-Rad).

After electrophoresis, membranes were repeatedly washed in PBS-T buffer (0.1 M PBS pH 7.5, 0.1% Tween®-20 (Sigma, cat. no.P9416)) and incubated 1 hour with shaking in blocking buffer (5% skimmed milk in PBS-T) to minimized unspecific binding. Primary antibodies (**Table 1 Annex I**) were prepared in the same blocking buffer and membranes were incubated overnight at 4ºC with shaking. The day after, membranes were carefully washed with PBS-T and incubated with HRP-labelled secondary antibodies (**Table 2 Annex I**) for 1 hour. After several washes proteins were revealed by a chemiluminiscence reaction with Lightning® Plus-ECL (Perkin Elmer, cat. no. NEL103001EA) and the signal was captured in an Alliance Mini HD9 (UVITEC) image capture system.

10. DNA methylation analysis.

DNA concentration was measured with a Qubit™ 3.0 Fluorometer or using the Quant-iT PicoGreen dsDNA Reagent (Invitrogen) according to the manufacturer's protocols. We performed the pyrosequencing experiments in Anne Ferguson-Smith´ laboratory at the University of Cambridge.

10.1 Enzyme-Linked ImmunoSorbent Assay (ELISA) for the quantitative determination of global DNA 5hmC and 5mC contents.

ELISA was used to determine global levels of 5hmC and 5mC. 100 ng of DNA per sample was denatured at 98ºC during 10 min. DNA solutions were immobilized onto a 96-well plastic plate with Reacti-Bind DNA Coating Solution (Thermo Fisher, cat. no. 17250) and incubated overnight at room temperature. Solutions were removed and plates were washed several times with washing buffer (0.1 M PBS-T containing 0.1% Tween®-20) and blocked with blocking buffer (5% skimmed milk in PBS-T) for 1 hour. Primary antibodies for 5hmC and 5mC (**Table 1 Annex I**) were incubated for 2 hours at RT. After three washes, HRP-conjugated secondary antibodies (**Table 2 Annex I**) were incubated for 1 hour at room temperature. After the last three washes, 60 µl per well of 1-Step Ultra TMB-ELISA Substrate Solution (Thermo Fisher, cat. no. 34028) were added to develop chemiluminiscence signals until the desired colour appeared (at least 30 min). To stop the reaction, 60 µl of 2M Sulfuric acid were added to each well and the absorbance was then measured at 450 nm using the Victor® 3 Multilabel Plate reader (Perkin Elmer). The amounts of 5mC and 5hmC were obtained by comparison to a standard curve of commercial hydroxymethylated and methylated DNA standards (Diagenode, cat. no. C02040010) respectively. The percentage of 5hmC and 5mC was calculated by dividing the amount of hydroxymethylated and methylated DNA by that of total DNA, respectively.

10.2 High-Throughput Sequencing of Immunoprecipitated Methylated DNA (MeDIP-seq)

MeDIP-seq protocol was modified from Taiwo *et. al.* (Taiwo et al., 2012). DNAs from NSCs and iPSCs were extracted using DNeasy Blood and Tissue kit (Qiagen, cat. no. 69504) according to the kit guidelines. The steps prior to the immunoprecipitation were briefly, 3 µg of DNA were sonicated to obtain 150-200 bp fragments and the efficiency was checked by the Bioanalyzer (Agilent). DNA libraries were then prepared using NEBNext® reactives (New England Biolabs) by the *Servei Central de Suport a la Investigació Experimental* (SCSIE, Universitat de València).

The MeDIP was performed in the lab and 1.5 µg of DNA were diluted in 80 µl of TE buffer (10 mM Tris-HCl, 1 mM EDTA, pH 7.5). DNA was denatured for 10 min at 99ºC and immediately cooled on ice for 10 min. After that, 20 µl of 10x IP buffer (100 mM Na-Phosphate pH 7.0, 0.5% TritonX-100) and 100 µl of milk buffer (5% skimmed milk powder, 2M NaCl) were added. 2 µg of 5mC antibody (Diagenode, cat. no. C15200006) were put in the sample and incubated for 2 h at 4ºC with rotation. In parallel, 11 µl *per* sample of Dynabeads® M-280 sheep anti-mouse IgG (Thermo Fisher, cat. no. 11201D) were collected with a magnetic rack and pre-washed with 500 µl PBS-BSA (1 mg/ml BSA in 0.1 M PBS) for 2 hours at 4ºC with rotation. After both incubations, beads were collected with a magnet, resuspended in the original volume with 1x IP buffer (10 mM Na-Phosphate pH 7.0, 0.05% TritonX-100,

1 M NaCl) and added to the DNA samples. DNAs were then incubated overnight at 4ºC with rotation. The day after, beads were collected using the magnet and the supernatant (unbound fraction) was transferred to a new tube. Beads were washed three times with 500 µl of 1x IP buffer for 10 min with rotation. After final wash, bound and unbound fractions were treated with 35 µg of Proteinase K (Roche, cat. no. 03115879001) with 125 µl of digestion buffer (50 mM Tris-HCl pH 8.0, 10 mM EDTA, 0.5% SDS) and incubated at 55ºC for 30 min on a shaking heating block. Finally, samples were purified using MiniElute PCR purification kit (Qiagen, cat. no. 50928004) eluting with 11 µl kit elution buffer.

In order to calculate 5mC enrichment in the bound fraction, real-time PCRs for unmethylated and methylated regions were done from bound and unbound 0.5 µl aliquots. Primers used to evaluate MeDIP efficiency were for methylated regions, Meth-F: 5´-CATGGCCCACAAAGTAATAAAA-3´and Meth-R: 5´-AACGACTTACAACGAGCTCAAA-3. Primers for unmethylated regions were, Unmeth-F: 5´-GGCTAGAACTGACCAGACAGAC-3´ and Unmeth-R: 5´-ATCTGTAGCCAATCCTAGAGCA-3´.

After real-time PCR analysis, calculations for both bound and unbound fractions were performed as described:

- Adjusted Input Ct = Unbound Ct – log [2AEx dilution difference of bound vs. unbound DNA]
- Recovery (%) = $2AE^{(\text{Adjusted Input Ct} - \text{MeDIP Ct})} \times 100$
- Specificity = 1- (unmethylated recovery/methylated recovery)
- Fold enrichment = $\frac{2AE^{(\text{Ct input\_meth} - \text{CtMeDIP\_meth})}}{2AE^{(\text{Ct input\_unmeth} - \text{CtMeDIP\_unmeth})}}$

Enrichment should be of at least 25x (**Fig. 16b**), specificity should be more than 95% and unmethylated recovery should be less than 1%. Alternatively, synthetic *Arabidopsis* methylated sequences (DNA methylation control package, Diagenode, cat. no. C02040012) were added to the samples after the adapter-ligation. The high-throughput sequencing of the samples were done by the *Servei Central de Suport a la Investigació Experimental* (SCSIE) using SOLiD 5500XL technology. Methylation data were analysed by Dr. Elizabeth Radford (University of Cambridge).

10.3 Study of 5mC and 5hmC enrichment at the *Snrpn*-DMR region.

DNA methylation levels were quantified using bisulfite conversion and pyrosequencing (**Fig. 16a**). Treatment of DNA with Bisulfite converts cytosine residues to uracil, but leaves 5-methylcytosine residues unaffected. Therefore, bisulfite-treated DNAs retained only methylated cytosines allowing single-nucleotide resolution information about the methylation status of a segment of DNA. DNA from NSCs and brain tissue was bisulfite converted using EZ DNA Methylation-Gold™ kit (Zymo research,

cat. no. 5005) in accordance with the manufacture´s protocol. Bisulfite-converted DNA was amplified for *Snrpn*-DMR region (chr7: 60,003,561-60,005,296; Mouse GRCm38/mm10). PCR was done with specific primer pair for bisulfite-converted DNA (F: 5´-TTGGTAGTTGTTTTTTGGTAGGAT-3´, R (Biot): 5´-TCCACAAACCCAACTAACCTTC-3´). One of the primers was biotinylated for posterior purification. This PCR was carried out in a total volume of 20 µl, with 2U HotStar Taq polymerase (Qiagen, cat. no.203203), PCR Buffer 10x (Quiagen cat. no. 1018996), 0.2 mM dNTPs and 400 mM of primers. PCR conditions were: 96 ºC for 5 min, followed by 39 cycles of 94 ºC for 30 s, 60ºC for 30 s and 72 ºC for 1 min.

For pyrosequencing (PSQ) analysis, the biotin-labelled PCR primer was used to purify the final PCR product. To do that, PCR product was prior mixed with Streptavidin Sepharose® High Performance Beads (GE Healthcare, cat. No. 17-5113-01) and binding buffer (10 mM Tris-HCl pH 7.6, 2M NaCl, 0.1 mM EDTA and 0.1% Tween®-20). Mixture was incubated on a shaker at least for 5 min. At the same time, 12 µl of pre-mixed sequencing solution containing sequencing primer (0.42 µM, 5´-GTGTAGTTATTGTTTGGGA-3´) and annealing buffer (20 mM Tris-acetate pH 7.6, 2 mM magnesium acetate) were dispensed into the wells of a 96-well PSQ plate. Denaturing and purification of samples were performed by PyroMark® Q96 Vacuum Workstation (Qiagen) doing serial washes with 70% ethanol, 0.2 N NaOH and 10 mM Tris-acetate pH7.6. Samples were then added to the prepared PSQ plate. Pyrosequencing was done in the PiroMark® MD (Qiagen) system using PyroMark® Gold Q96 Reagents (Qiagen, cat. No. 972804).

To evaluate 5hmC content at the *Snrpn*-DMR, a 5-hmC immunoprecipitation (hMeDIP) was done using 5 µg of sonicated DNA at 150-200 bp. DNA was denatured at 98ºC for 10 min and immediately cooled on ice for 10 min. Milk buffer (5% skimmed milk powder, 2M NaCl) and 10x-IP buffer (100 mM Na-Phosphate pH 7.0, 0.5% TritonX-100) were added. DNAs were incubated with 0.5 µl of 5hmC primary antibody (Active Motif, cat. no. 39769) for 2 h. In parallel, specific DNAbeads® Protein G (Thermo Fisher, cat. No. 10003D) were washed with 0.1M PBS containing 1 mg/ml BSA for 2 h. Beads were then collected with a magnet, added to the DNAs and incubated overnight at 4ºC with rotation. The day after, beads were collected using a magnet and the supernatant was kept (Unbound fraction, UB). Beads were washed several times with 1x IP buffer (10 mM Na-Phosphate pH 7.0, 0.05% TritonX-100, 1 M NaCl) and both fractions were treated with 35µg of Proteinase K (Roche) at 55ºC for 30 min. Finally, samples were purified using MiniElute PCR purification kit (Qiagen) following the manufacturer's instructions.

To evaluate the immunoprecipitation efficiency, DNAs were spiked with 0.3 ng of synthetic *Arabidopsis sp.* (Diagenode) hydroxymethylated DNA (Zymo, cat no. D5405) and non-hydroxymethylated DNA (Diagenode, cat. no. C02040012). Efficiency was calculated using specific primers for synthetic DNAs as indicated above (**Fig. 16b**).

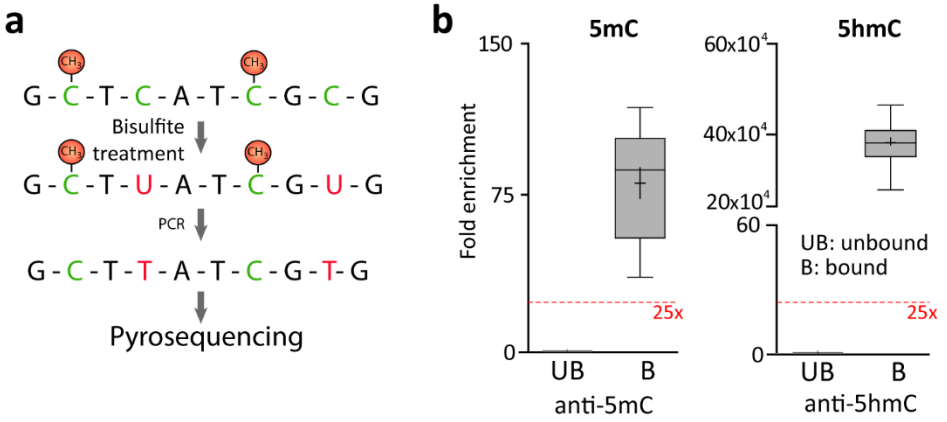

Figure 16. DNA methylation analysis strategies. (a) Schematic of bisulfite conversion. DNA was treated with Sodium Bisulfite and non-modified cytosines were converted to uracil whereas 5mC/5hmC remained as cytosines. Final pyrosequencing was used to quantify the percentage of 5hmC/5mC. (**b)** Calculated fold enrichment after MeDIP (left panel) and hMeDIP (right panel). Controls for the enrichment of 5hmC in genomic DNA spiked with synthetic *Arabidopsis thaliana* DNA containing either 5mC or 5hmC (n=6). Enrichment was always over 25x.

After immunoprecipitation of 5hmC, bound and unbound fractions were analysed by qPCR in order to quantify *Snrpn*-DMR enrichment. *Snrpn*-DMR region is located at chromosome 7, concretely between positions 60,003,561 and 60,005,296 (Mouse GRCm38/mm10). Specific primers were designed including 9 CpG (**Table 4 Annex I**). Real-time PCR was performed in a Step One Plus real-time PCR device (Applied Biosystem), using SYBR Green reactive. A standard curve made up of doubling dilutions of pooled aliquots from unbound fractions was run on each plate, and quantification was performed relative to the standard curve. Fold enrichment was calculated in the same way than for the MeDIP.

11. Imprinting analysis by pyrosequencing

All imprinting assays were based on PCR amplification of cDNA followed by direct sequencing to analyse parental-specific expression of the genes. CRISPR was used to knockdown *Tet3* in NSCs derived from adult F1 mice hybrids offspring from C57BL6/J males and CAST/EiJ females (CxB NSCs), in which a single-nucleotide polymorphisms (SNP) in the *Snrpn* gene was identified between the two subspecies. The sequence of murine *Snrpn* gene was obtained from GenBank (accession number NM013670). The *Snrpn* polymorphism was located at nucleotide 1,270 of exon 10, is a 'C' in BL6 mice

and a 'T' in Cast mice. SNP flanked primers were designed for the studied gene and a PCR was done to amplify the region. The *Snrpn* imprinting assay used the following primers to amplify the SNP containing fragment: *Snrpn*-F, 5´-TAAATCTCAGCCCTTCTCTTCCC-3´ and *Snrpn*-R, 5´-AATGCAGTAAGAGGGGTCAAAAA-3´. PCR was performed at 62ºC of annealing temperature and for 35 cycles. DNA was finally sequenced in a pyrosequencer (PiroMark® MD, Qiagen) using a specific sequencing primer: 5´-CCCTTCTCTTCCCCTA-3´.

12. Chromatin Immunoprecipitation (ChIP)

ChIP was performed essentially as it was previously described (Strogantsev et al., 2015). Five 100 cm dishes with wild-type NSCs isolated from the adult SVZ were cross-linked and chromatin isolated. Chromatin was sheared to an average size of 200-500 bp using a Bioruptor sonicator (Diagenode, UCD-200). After that, chromatin was pre-cleared with 10 µg non-immune rabbit IgG (Santa Cruz, cat. no. sc-2027) and 20 µl of protein G magnetic beads (Dynabeads®, cat. no. 10003D) for 3 h at 4ºC with rotation. 10 µg of TET3 antibody (**Table 1 Annex I**) or rabbit IgG were added and incubated overnight at 4ºC on a rotation wheel. Chromatin was precipitated with 10 µl protein G beads for 3 h at 4ºC. A bit aliquot of chromatin before the immunoprecipitation was used as input material. Beads were then washed followed by crosslink reversal and protein digestion. Finally, DNA was purified using MiniElute PCR purification kit (Qiagen) following the manufacturer´s instructions.

To analyse the TET3 interaction with *Snrpn* promoter, ChIP enriched DNA was analysed by qPCR using SYBR-green primers (**Table 4 Annex 1**). Pull-downs using non-immune rabbit IgG were used to control for non-specific enrichments. The comparative Ct method was used to calculate fold enrichment levels normalizing to input DNA and non-specific IgG.

13. Statistical analysis of the data

All statistical tests were performed using the GraphPad Prism® 5 software (GraphPad software, USA). Significance of differences between experimental groups was assessed using the paired two-tailed Student t-test or one-way ANOVA (*ANalysis Of VAriance*) followed by a Tukey post-hoc test. Relative values (normalized values and percentages) were transformed using arcsen (square root (value/100)) before statistical analysis. P-values (p) lower than 0.05 were considered significant in all cases. All data were expressed as mean ± standard error of the mean (s.e.m.) and the number of independent cultures or animals (n) was specified in each figure. * refers to $p<0.05$, ** to $p<0.01$ and *** to $p<0.001$.

Annex I

Table 1. **List of primary antibodies along the different applications.** ICC: immunocytochemistry, IHC: immunohistochemistry, WB: western-blot and E: ELISA.

Primary antibody	Source	Host	Dilution	Cat. no.	Application
5hmC	Active Motif	Rabbit	1:1000	36769	ICC/IHC/E
5mC	Diagenode	Mouse	1:1000	C15200006	ICC/IHC/E
BrdU	Abcam	Rat	1:500	Ab6326	ICC/IHC
Caspase 3	Cell Signaling	Rabbit	1:300	9661	ICC
DCX	Santa Cruz	Goat	1:300	sc-139186	IHC
GAPDH	Millipore	Mouse	1:5000	MAB374	WB
GFAP	Dako	Rabbit	1:600	Z0334	ICC/IHC
GFAP	Millipore	Chiken	1:600	AB5541	IHC
Ki67	Abcam	Rabbit	1:100	ab15580	ICC
Nanog	Reprocell	Rabbit	1:100	RCAB002PF	ICC
Nanog	Cell signaling	Rabbit	1:100	8822	ICC
Nestin	Hybridoma Bank	Mouse	1:4	rat-401	ICC
O4	Hybridoma Bank	Mouse	1:300	rip	ICC
OCT-4	Santa Cruz	Rabbit	1:200	sc-5279	ICC
PSA-NCAM	AbCys S.A.	Mouse	1:300	ABC0019	ICC
S100β	Dako	Rabbit	1:300	Z0311	ICC/IHC
Smoth Muscle Actin (SMA1)	Abcam	Mouse	1:100	ab18147	ICC
Snrpn	Abcam	Rabbit	1:300	Ab224330	ICC
Sox2	R&D Systems	Goat	1:200	AF2018	ICC/IHC
SSEA1	Santa Cruz	Mouse	1:50	SC-21702	ICC
TET3	Millipore	Rabbit	1:100	ABE290	ICC/IHC/WB/ChIP
TET3	Santa Cruz	Rabbit	1:100	sc-139186	ICC/IHC
α-phetoprotein	R&D	Rabbit	1:100	mab1368	ICC
B-catenin	Cell Signalling	Rabbit	1:300	9587	IHC
βIII-tubuline	Covance	Mouse	1:300	PRB-435P	ICC
Γ-tubulin	Santa Cruz	Goat	1:300	sc-7396	IHC

Table 2. List of secondary antibodies along the different application. ICC: immunocytochemistry, IHC: immunohistochemistry, WB: western-blot and E: ELISA.

Secondary antibody	Source	Dilution	Cat. no.	Application
Alexa Fluor® 488 Donkey Anti-Chicken	Jackson ImmunoResearch	1:600	703-545-155	IHC
Alexa Fluor® 488 Donkey Anti-Goat	Jackson ImmunoResearch	1:600	705-547-003	ICC/IHC
Alexa Fluor® 488 Donkey Anti-Mouse	Molecular Probes	1:600	A-21202	ICC
Alexa Fluor® 488 Donkey Anti-Rabbit	Jackson ImmunoResearch	1:600	711-547-003	ICC/IHC
Alexa Fluor® 647 Donkey Anti-Chicken	Jackson ImmunoResearch	1:600	703-605-155	IHC
Alexa Fluor® 647 Donkey Anti-Rabbit	Jackson ImmunoResearch	1:600	711-607-003	IHC
Cy3-Donkey Anti-Rabbit	Jackson ImmunoResearch	1:800	711-165-152	ICC/IHC
Cy3-Donkey Anti-Mouse	Jackson ImmunoResearch	1:800	715-165-151	ICC/IHC
Cy3-Donkey Anti-Rat	Jackson ImmunoResearch	1:800	712-165-153	ICC/IHC
Cy3-Donkey Anti-goat	Jackson ImmunoResearch	1:600	705-166-147	IHC
Goat Anti-Mouse IgG-HRP	Dako	1:5000 1:2000	P0447	WB E
Goat Anti-Rabbit IgG-HRP	Santa Cruz	1:5000 1:2000	SC-2004	WB E

Table 3. List of TaqMan probes used. *TaqMan probes designed by us.

Gene	TaqMan code (Applied Biosystems)	Gene	TaqMan code (Applied Biosystems)
Cdkn1c	Mm01272135_g1	***Nanog***	Mm02384862_g1
Cer1	Mm00515474_m1	***Nestin***	Mm00450205_m1
Cntn3	Mm00500947_m1	***Oct4***	Mm00658129_gH
Cobl	Mm01187905_m1	***Olig2***	Mm01210556_m1
Dlk1	Mm00494477_m1	***Peg3***	Mm01337379_m1
Dnmt1	Mm01151063_m1	***Phlda2***	Mm00493899_g1
Dnmt3a	Mm00432881_m1	***RETRO Klf4****	FAM-CCCCTTCACCATGGCTG-MGB
Dnmt3b	Mm01240113_m1	***RETRO Oct4****	FAM-CACCTTCCCCATGGCTG-MGB
Foxa2	Mm01976556_s1	***S100β***	Mm00485897_m1
Gapdh	Mm99999915_g1	***Snrpn***	Mm04204818_m1
Gfap	Mm01253033_m1	***Sox2***	Mm03053810_s1
H19	Mm01156721_g1	***Tet1***	Mm01169087_m1
Igf2r	Mm00439576_m1	***Tet2***	Mm00524395_m1
Kdr1	Mm01222421-m1	***Tet3***	Mm00805756_m1
Klf4	Mm00516104_m1	***Tubb3***	Mm00727586_s1
Meg3	Mm03456293_m1	***Zfp42***	Mm01194089

Table 4. List of SYBR-green primers used in real-time PCR.

Gene	Primer sequence (5´-3´)	Temperature (ºC)
Cre-recombinase	F: GCGGTCTGGCAGTAAAAACTATC	60
	R: GTGAAACAGCATTGCTGTCACTT	
Gapdh	F: GAACATCATCCCTGCATCCA	60
	R: CCAGTGAGCTTCCCGTTCA	
Gnas	F: AGAAGGACAAGCAGGTCTACCG	60
	R: GTTAAACCCATTAACATGCAGGA	
Tet3	F: AGACCCTTCTCAGGGGTCAC	60
	R: GTGCAGTTGCTCGTCCTCAG	
Tet3FL	F: TGGAAAACTGTGGGTCTTGTAC	60
	R: GAGCATTTATTTCCACCTCCTTA	
Tet3s	F: GCCGATGCAGTAGTGGAGG	60
	R: CTGCCTTGAATCTCCATGGTAC	
Tet3o	F: CACATGTTCCTCCCATGGTAC	60
	R: CTGCCTTGAATCTCCATGGTAC	
Snrpn-DMR1-1 (R1)	F: GGCAAAAATGTGCGCATGTG	60
	R: GGAGTGATTTGCAACGCAAT	
Snrpn-DMR1-2 (R2)	F: ACTCCTTGGGTGTGTTAGTG	60
	R: CCTCTGGACTCCTGGAAGTC	
Snrpn (R3)	F: TATGGCCGCCTACTTTTGTC	60
	R: AAGTCAGTGCAGCAGGTCCT	
Clcn6	F: CAACTCCTGAGGACCTGACA	66
	R: GCTCAGACACAGCCTCCTCT	

Results

1. Epigenetic landscape of NSCs is significantly changed during their reprogramming into iPSCs.

1.1 Induced Pluripotent Stem Cells generated from adult NSCs are similar to embryonic stem cells.

1.1.1 NSCs from the adult SVZ convert into a pluripotent state only with transduction of *Oct4* and *Klf4*.

Epigenetic reprogramming consists in the transition from one cell type to another, permitted by the loss of particular molecular characteristics of the cell of origin and the acquisition of a new molecular identity without changing the genomic sequence (Krishnakumar and Blelloch 2013). The identification of conditions that would allow specialized adult cells to be genetically reprogrammed to assume a stem cell-like state (Takahashi and Yamanaka 2006) has supposed a powerful new way to "*de-differentiate*" cells whose developmental fates had been previously assumed to be determined. In particular, epigenetic modifications can also occur during reprogramming of NSCs into pluripotent stem cells (Montalban-Loro et al., 2015) and a better understanding of this process will help to elucidate the mechanisms required for stem cell maintenance.

Since the discovery by Takahashi and Yamanaka in 2006 that the introduction of four transcription factors (*Oct4*, *Klf4*, *Sox2*, and *c-myc*) could reprogram mouse embryonic stem cells and adult fibroblast into iPSCs, the field of reprogramming has considerably evolved and several studies have reported the use of sets of these transcription factors in various combinations to reprogram mouse and human somatic cells (Park et al., 2008b, Wernig et al., 2008, Hester et al., 2009). Previous studies also report that mice neurospheres cultures obtained from postnatal day 5 endogenously express *Sox2*, *c-myc* and *Klf4* so that they can be reprogrammed with *Oct4* and *Klf4* factors or only with *Oct4* at a similar efficiency to the reprogramming rate of murine fibroblast with the original four factors (Kim et al., 2008, Kim et al., 2009b).

We first analysed by qPCR and immunocytochemistry the levels of expression of the four transcription factors classically used to induce pluripotency in somatic cells *Sox2*, *Klf4*, *c-myc* and *Oct4* (Takahashi and Yamanaka 2006). NSCs derived from the adult SVZ expressed significant levels of *Sox2*, *Klf4*, and *c-myc* while *Oct4* was not expressed (**Fig. 17**). These data indicated that *Oct4* alone or in combination with another transcription factor such as *Klf4,* could be suficient to induce pluripotency in adult NSCs. This could mean that NSCs might represent a more advanced stage in the reprogramming process.

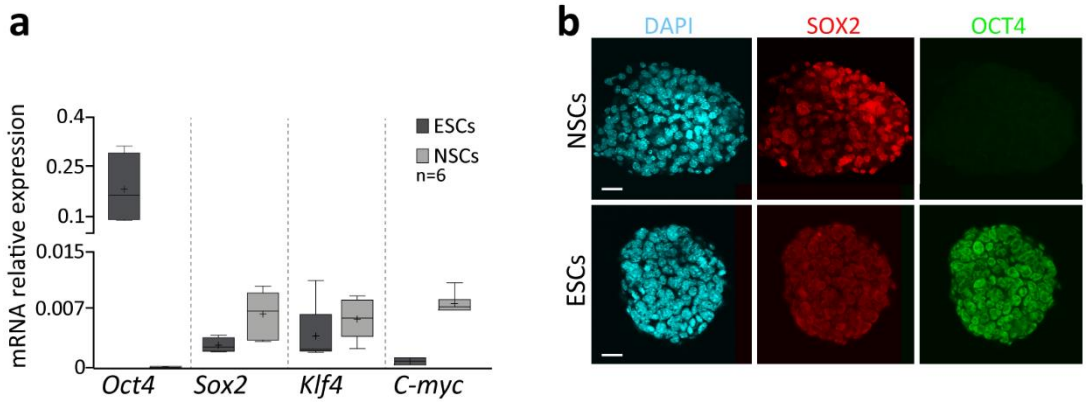

Figure 17. Adult NSCs endogenously express *Sox2*, *Klf4* and *c-myc*. (a) Gene expression levels of the reprogramming factors *Oct4*, *Sox2*, *Klf4* and *c-myc* quantified by qPCR in adult NSCs. ESCs pluripotent cultures were used as a control of expression for the four transcription factors. *Gapdh* expression levels were used to normalize data. **(b)** Immunocytochemistry for SOX2 (red) and OCT4 (green) in NSCs and ESCs cultures. DAPI was used to counterstain nuclei. All error bars show s.e.m. of at least 6 cultures. Scale bars in b: 20 µm.

Due to our particular interest in the study of specific epigenetic marks associated to adult neural stem cells multipotency and that adult NSCs are originally closer to the pluripotency state than somatic cells, we developed a protocol to reprogram adult NSCs from SVZ (**Fig 18a**). This protocol constitutes a simple and attractive system to study epigenetic signatures that define the pre-reprogramming (somatic self-renewing multipotent stem cells) *vs.* the post-reprogramming (induced pluripotent self-renewing stem cells) states in the neural system.

To address this point we used NSCs cultures obtained from the SVZ of 2 months-old wild-type C57Bl6 mice. Based on our previous gene expression studies, adult NSCs would require in principle just the exogenous expression of *Oct4*. Thus, we produced retrovirus for *Oct4 and Klf4* by transfecting Plat-E packing cells with retroviral plasmids. Retrovirus for *Cherry* was also generated to use as a reporter of the exogenous expression of reprogramming factors (**Fig. 18a,b**). After two days of retrovirus production by Plat-E packing cells, supernatants with the virus for *Oct4* and *Cherry* were used to co-transduce adult NSCs (1 Factor condition, 1F). A combination of retrovirus for *Oct4* and *Klf4* (2 Factors condition, 2F) together with *Cherry* was also used to transduced NSCs. *Cherry* expression was checked in transduced NSCs to confirm their infection (**Fig. 18b**). NSCs infected with both *Oct4* and *Klf4* transcription factors were grown on a feeder layer of SNL cells with the cytokine leukaemia inhibitory factor (LIF) and started to form clone-like aggregates 30-40 days after infection (**Fig. 18a,b**), however no clones were formed just with *Oct4* 1F (data nor shown). These aggregates were large, with poorly defined edges and some of them expressed the pluripotency marker stage-specific embryonic antigen 1 (SSEA-1) (**Fig. 18b**). Importantly, retroviral vectors are transcriptionally silent in pluripotent stem cells (Hotta and Ellis 2008), thus we used this feature to determine the pluripotent state of the

clones generated together with the acquisition of pluripotency markers and silencing of neural genes (**Fig. 18c**). We observed that most of the clones formed were still positive for *Cherry*, indicating that despite expressing *SSEA-1* they were only partially reprogrammed. For this reason we named these cells as pre-iPSCs.

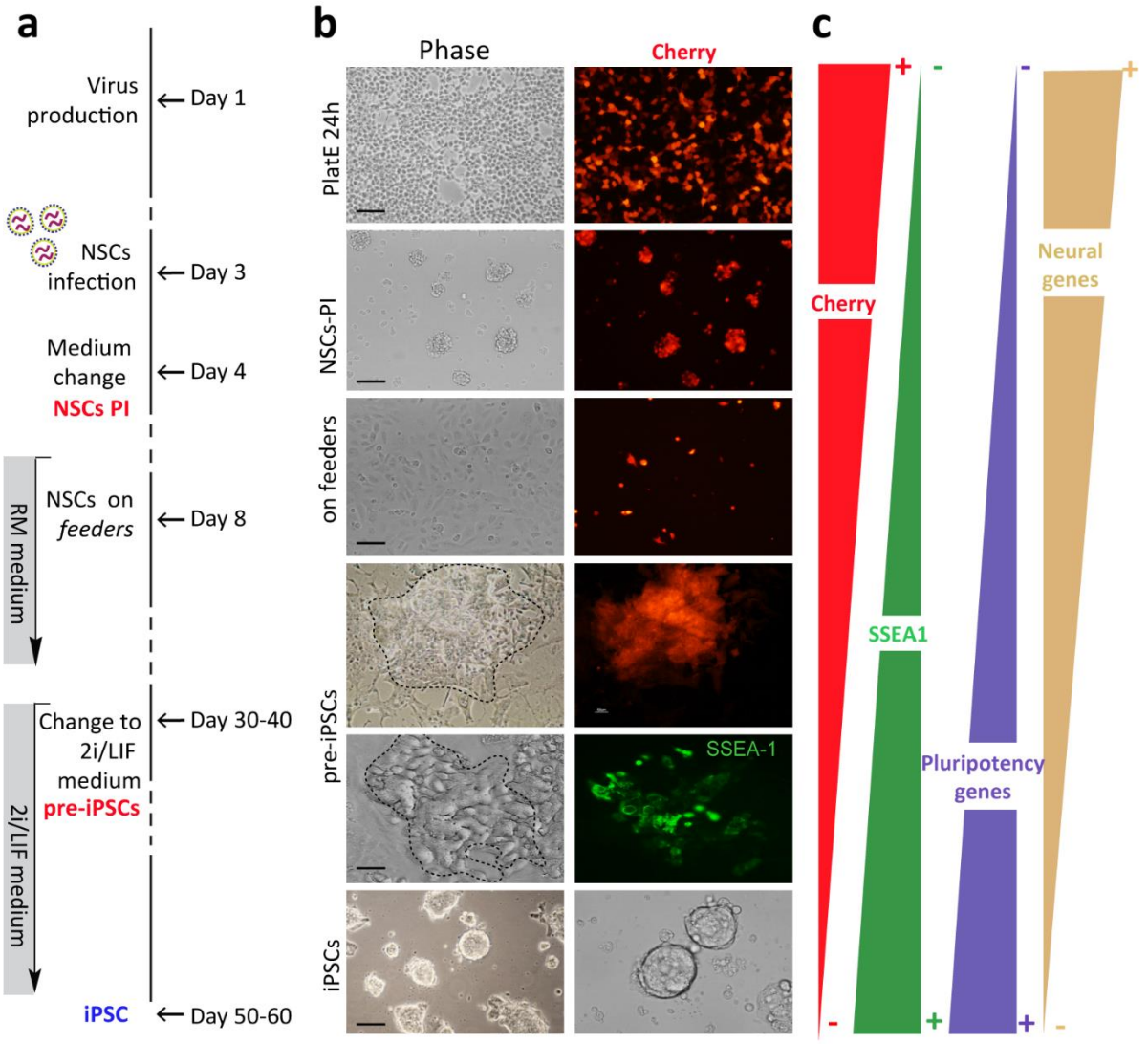

Figure 18. Pre-iPSCs have intermediate characteristics of NSCs and iPSC. (a) Schematic of the reprogramming protocol which started with plat-E transfection to generate viral particles used to infect NSCs 3 days after. Infected NSCs were seeded on *feeders* 5 days after infection. *Cherry* and SSEA-1 positive clone-likes aggregates appeared (pre-iPSCs) after 30-40 days and the culture medium was changed to 2i/LIF medium. iPSCs appeared 50-60 days after infection. **(b)** Phase contrast and immunofluorescent images for *Cherry* in Plat-E, post-infected NSCs (NSCs-PI) and pre-iPSCs. Phase contrast images of pre-iPSCs (left panel) and immunofluorescent image for SSEA-1 (right panel) in pre-iPSCs cells are also shown. Phase contrast images of iPSCs established lines are shown (lower panels). **(c)** Schematic of the regulation of pluripotency and neural genes during the reprogramming process. Retroviral vectors were transcriptionally silent in iPSC. Scale bars in b: 100 µm.

To acquire full reprogramming, and once achieved the pre-iPSCs state, we applied molecularly defined conditions for the derivation and propagation of authentic pluripotent cells (Silva et al., 2008). These conditions were designed to sustain cells in a pluripotent state by neutralizing inductive

differentiation stimuli combining dual inhibition (2i) of mitogen-activated protein kinase signalling (MEKi) and glycogen synthase kinase-3 (GSK3). LIF was also included to maximize clonogenic self-renewal of pluripotent cells in a free-serum culture medium (Williams et al., 1988, Ying et al., 2008) (**Fig. 18a**). Again the retroviral vector silencing served as a beacon marking the fully reprogramming pluripotent state (Hotta and Ellis 2008). After 10-20 days in the new controlled conditions, we obtained ESC-like colonies that did not express *cherry*, suggesting that fully reprogramming was already acquired (**Fig. 18a-c**).

1.1.2 Reprogrammed NSCs lose the expression of neural genes and gain the expression of pluripotency markers.

As we expected, expression studies performed by qPCR corroborated that post-infected NSCs (NSCs PI) expressed high levels of both *Oct4* and *Klf4* retroviral transgenes and that although lower, they were still present in pre-iPSCs (**Fig. 19b**). Moreover, although expression levels of the neural markers *Olig2* and *Nestin* were already downregulated (**Fig. 19c**), pre-iPSCs only showed a slightly increase of endogenous levels of *Oct4* (**Fig. 19d**) whereas the expression of other pluripotency markers such as *Zfp42 (Rex1)* and *Nanog* was undetectable (**Fig. 19d**). Taken together, our results confirmed that pre-iPSCs were in an intermediate state in which critical attributes of true pluripotency, including stable expression of endogenous *Oct4* and *Nanog* were not attained yet.

Complete downregulation of retroviral transgenes, essential for full reprogramming, was corroborated in derived iPSCs compared to the infected NSCs (**Fig. 19b**). This was accompanied with the stable induction of the endogenous pluripotency-related genes *Nanog*, *Zfp42* and *Oct4* (**Fig. 19d**). Consistently with the acquisition of a pluripotent state, the expression of neural-specific genes such as *Olig2* and *Nestin*, was absent in iPSCs (**Fig. 19c**). All these data were confirmed at protein level by immunocytochemistry (**Fig. 19e**). Expression of OCT4 and Cherry was detected in pre-iPSCs (**Fig. 19e**). Moreover, OCT4 and NANOG were expressed whereas no expression of OLIG2 was found (**Fig. 19e**) confirming the acquisition of a full pluripotent state.

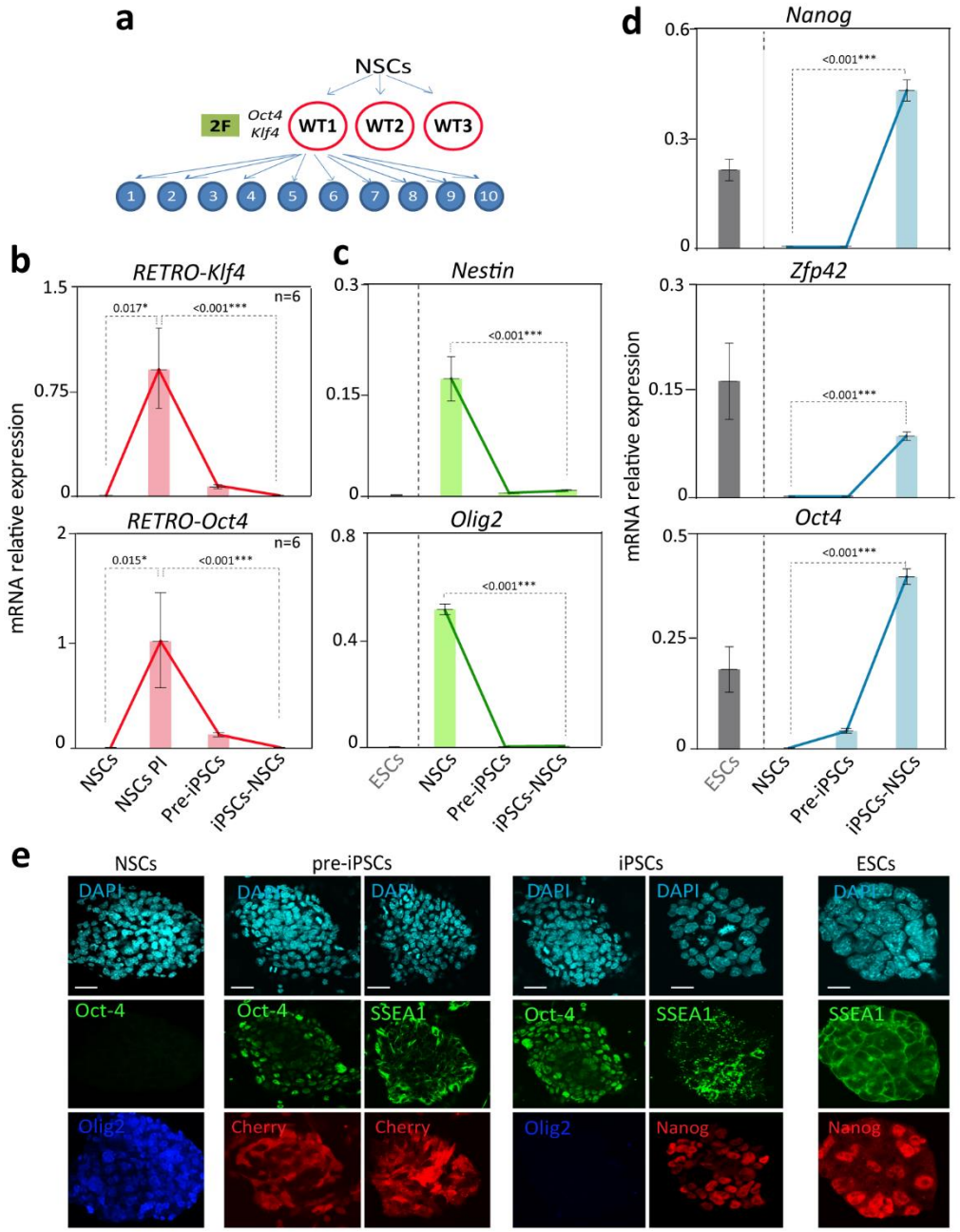

Figure 19. MEK and GSK3 inhibitors (2i) promote reprogramming to full pluripotency in adult NSCs. (a) Schematic representing the protocol of selection of iPSCs clones. NSCs from three different mice were transduced with *Oct4* and *Klf4.* Once iPSCs were generated, ten clones were picked, isolated and expanded for further characterization. **(b)** qPCR for *Klf4* and *Oct4* retroviral expression in NSCs, NSCs PI, pre-iPSCs and iPSCs. NSCs before the infection were used as a negative control. **(c)** qPCR for the neural genes *Olig2* and *Nestin* in the same samples. ESCs were used as a control. **(d)** qPCR for the pluripotent-related genes *Nanog*, *Zfp42* and *Oct4* in NS Cs, pre-iPSCs and iPSCs. ESCs were used as a control. **(e)** Immunocytochemistry images for OCT4 in NSCs, pre-iPSCs and iPSCs (green), OLIG2 in NSCs and iPSCs (blue), SSEA-1 in pre-iPSCs, iPSCs and ESCs (green) and *Nanog* in iPSCs and ESC (red). *Gapdh* was used to normalize expression data. DAPI was used to counterstain nuclei. All error bars show s.e.m. of at least 6 samples. P-values are indicated. Scale bars in f: 20 μm.

1.1.3 Genomic stability was maintained throughout reprogramming of NSCs into iPSCs.

Genetic variations, including aneuploidy or polyploidy, can be introduced into cells during iPSCs generation (Liang and Zhang 2013). Therefore, in order to evaluate the chromosomic dotation of each iPSCs line, we performed a karyotype analysis. As mentioned before, 10 colonies or clones were isolated and expanded from each biological replicate and three of them were selected based on their gene expression profile (high expression of pluripotency genes and low expression of neural and retroviral genes) to assess their genomic stability and pluripotency characteristics. The vast majority of the lines analysed (90%) showed a normal karyotype with around 40 chromosomes per metaphase (**Fig. 20,** purple bars) while a small proportion of iPSCs lines showed abnormalities in the number of chromosomes (10%) including tetraplody (4n) (**Fig. 20,** red bars). Those iPSCs lines that showed chromosomic abnormalities were discarded for further studies.

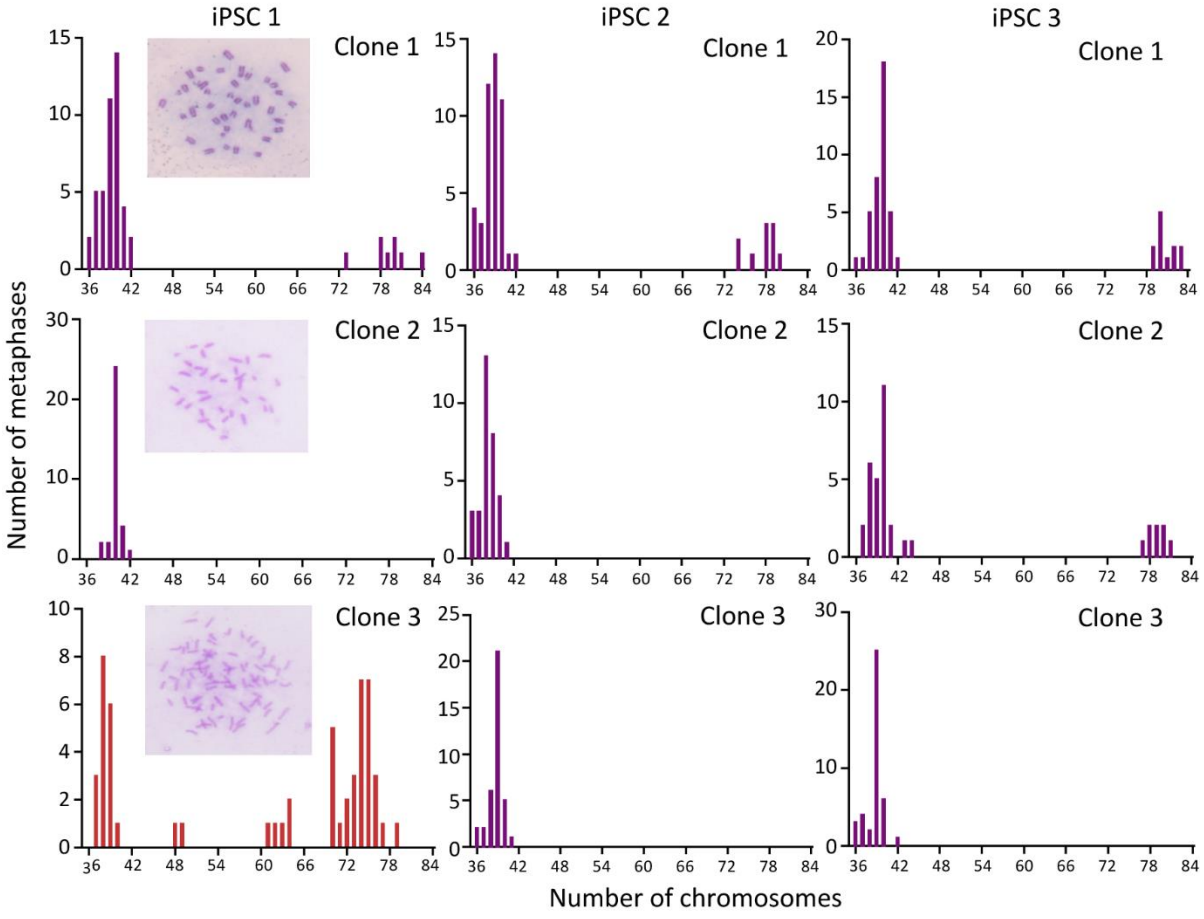

Figure 20. Chromosome number is maintained in iPSCs lines. Number of chromosomes per metaphase in the iPSCs lines. The majority of clones showed normal chromosomic dotation was (purple bars) while one of the analysed clones (iPSCs-1-clone 3) showed chromosomic aberrations (red bars). Examples of phase contrast images for Leishman staining are also included. At least 50 metaphases were counted for each iPSCs line.

1.1.4 iPSCs generated from NSCs can be differentiated *in vitro* and *in vivo* into the three germ layers.

Pluripotent stem cells have the potential to differentiate into any of the three germ layers, endoderm, mesoderm and ectoderm. This potentiality can be verified demonstrating the ability of the iPSCs to form 3D structures known as *embryoid bodies* (EBs) containing cells belonging to the three germ layers (Hopfl et al., 2004). The EB mimics the structure of the developing embryo, thereby providing a means of obtaining any cell lineage (Spelke et al., 2011). EBs can be generated by culturing pluripotent stem cells under conditions that are adverse to pluripotency and proliferation using the "*hanging drops*" method (**Fig. 21a**). This suspends iPSCs on the lid of a dish and EBs form through aggregation at the bottom of the drops (**Fig. 21a**) resulting in reproducibly produced homogeneous EBs.

We performed the analysis by qPCR in EBs of specific markers for the differentiated cell types. We found significant expression for *Kdr1* (mesoderm), *Foxa2* (endoderm) and *Cer1* (ectoderm) demonstrating the presence of cells from the three germ layers in the EBs generated from the iPSCs lines (**Fig. 21b**). Strikingly, these iPSCs have a higher differentiation ability to form ectoderm and endoderm compared to ESCs after differentiation (**Fig. 21b**) suggesting an influence of the somatic origin on the properties of resultant iPSCs, as previously reported (Polo et al., 2010). These results were also confirmed by immunocytochemistry using specific antibodies for SMA1, α-fetoprotein and βIII-tubulin (**Fig. 21c**). All these data verified the pluripotency capacity *in vitro* in iPSCs induced from NSCs.

We next evaluated pluripotency capacity *in vivo* using the teratoma assay. Teratomas are a particular class of non-malignant tumours that originate from pluripotent cells after a process of expansion and disorganized differentiation and they develop in mice from transplanted embryonic stem cells (Przyborski 2005, Prokhorova et al., 2009). Thus, iPSCs were injected in the dorsolateral area into the subcutaneous space of immunocompromised *Nude* mice. After 10 days, teratomas were obvious to the naked eye but they were extracted when reached approximately 2 cm of diameter approximately 20 days after injection (**Fig. 22a**). Animals were then sacrificed and the teratomas were histologically analysed. As expected, the tumoral cytoarchitecture of the teratomas was disorganized and the presence of cells from the three germ layers was confirmed by haematoxylin-eosin staining (**Fig. 22b**).

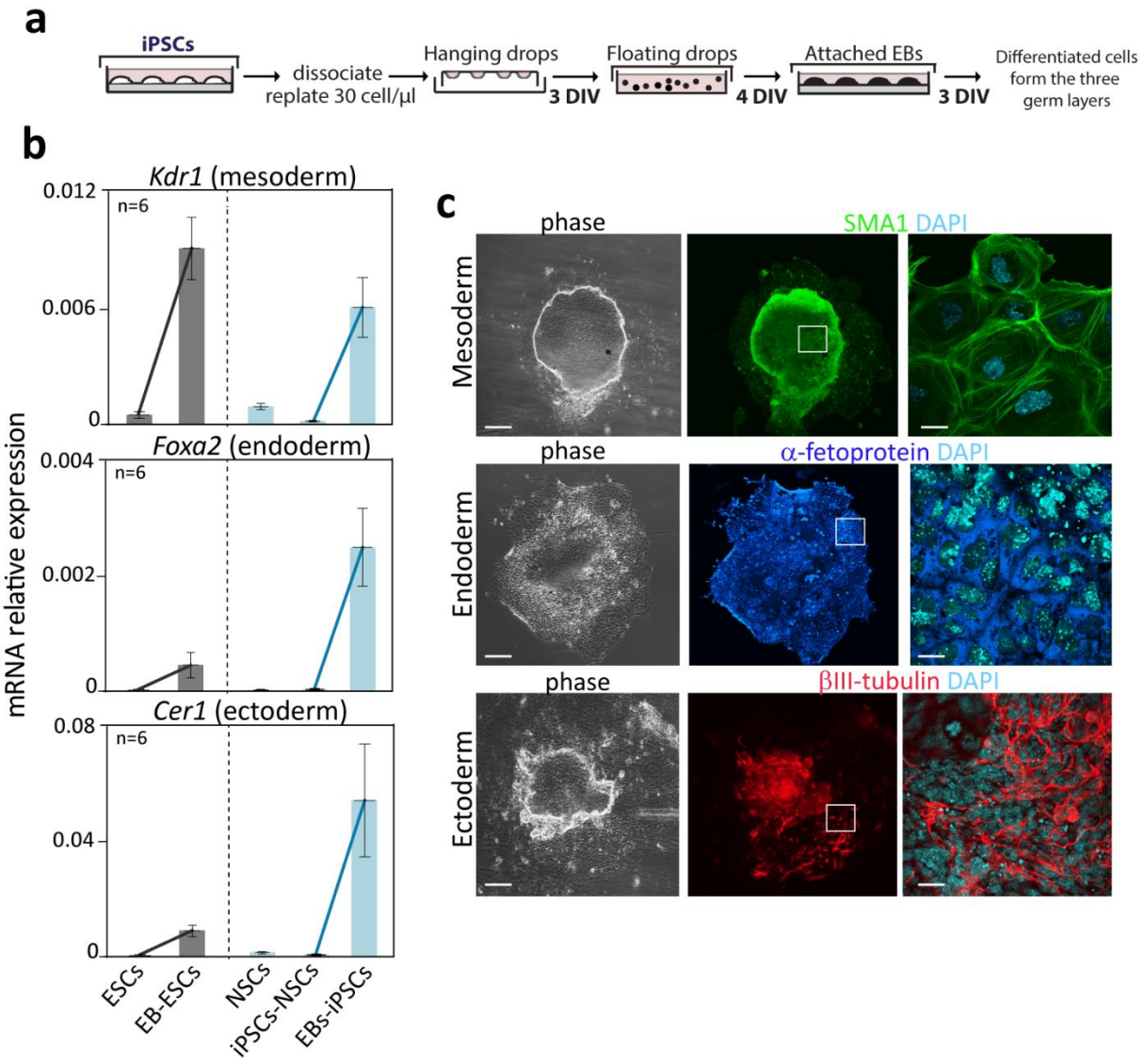

Figure 21. iPSCs are able to differentiate into cells of the three germ layers. (a) Schematic representation of the embryoid bodies (EBs) assay using the "*hanging drops*" method. iPSCs were dissociated and the cell suspension was distributed in drops in a plate that was incubated upside-down for 3 days. Then, the plate was inverted, culture media was added and incipient EBs were incubated for 4 more days. Finally, EBs were seeded in pre-treated plates with gelatine to allow differentiation. After 3 days, samples were analysed by ICC**. (b)** qPCR for *Kdr1* (mesoderm), *Foxa2* (endoderm) and *Cer1* (ectoderm) in NSCs, iPSCs and EBs-iPSC. ESCs and EBs from ESC (EBs-ESC) were used as a control of pluripotency and differentiation respectively. *Gapdh* was used to normalize expression data. **(c)** Immunocytochemistry confocal images for SMA1 (mesoderm; green, upper panels), α-fetoprotein (Endoderm; red, middle panels) and βIII-tubulin (ectoderm; blue, lower panels) in EBs derived from iPSCs. Phase contrast images of the EBs are also included. DAPI was used to counterstain nuclei. Scale bar in c: 100 µm (high magnification images in c: 10 µm).

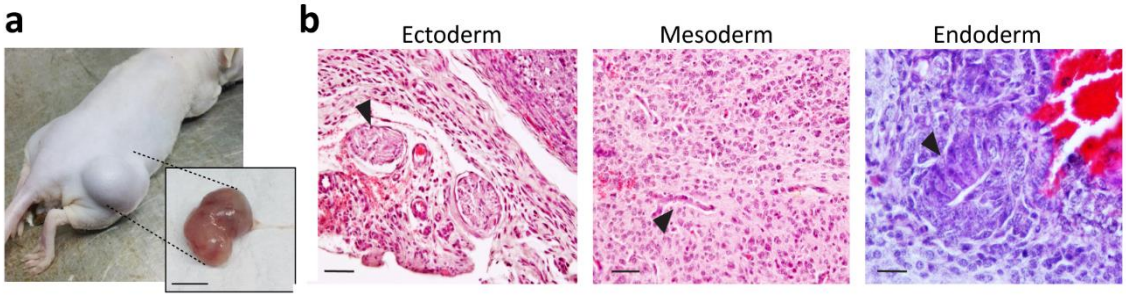

Figure 22. iPSC derived from NSCs give rise to teratomas *in vivo*. (a) Image of a teratoma developed in the dorsolateral area of an immunocompromised *Nude* mouse 4 weeks after the injection. Detailed teratoma image after its extraction is also included. **(b)** Histological analysis of teratomas using haematoxylin-eosin dyes. Epithelial cells derived from ectoderm, muscle fibres derived from mesoderm and columnar epithelium from endoderm are shown and indicated with arrowheads. Scale bar in a: 1 cm; in b, 50 µm.

1.2 Imprinted genes expression change during the generation of iPSCs from adult NSCs.

The majority of imprinted genes are expressed in the brain and recent evidences suggest that genomic imprinting can be selectively lost in particular cell types or at specific developmental time points (Polo et al., 2010, Ferron et al., 2011, Kim et al., 2013, Ferron et al., 2015). These changes have an impact on stem cell plasticity thus regulation of genomic imprinting might be a normal mechanism of modulation gene dosage to control stem cell potential in the brain (Perez et al., 2016). Consequently, the knowledge of imprinting regulation during reprograming of NSCs into iPSCs may give us information about the imprinting regulation in NSCs as well as in iPSCs and may also be employed to dissect the mechanisms of erasure, reacquisition and maintenance of genomic imprinting in mammals.

Therefore we decided to focus on the study of the regulation of gene expression during the reprogramming process by performing an RNAseq analysis in NSCs and derived iPSCs. The principal component analysis (PCA) based on RNAseq data showed a clearly segregation between iPSCs and NSCs populations (**Fig. 23a**). Concretely, iPSCs identified differential expression of a large number of genes compared to NSCs, with 6062 downregulated and 5301 upregulated genes (**Fig. 23b,c**). Notably, the majority of the most differentially expressed genes (FDR<2.5e-68) were upregulated genes in iPSC compared to NSCs (**Fig. 23b**). Consistent with previously shown data (**Fig. 19c,d**), RNAseq confirmed the downregulation of several neural genes such as *Olig2, Nestin* and *Zic1* and the upregulation of essential genes involved in pluripotency such as *Pou5f1* (*Oct4), Zfp42* and *Nanog* (**Fig. 23d**) in iPSCs compared to NSCs cultures.

Based on RNAseq data we performed a "*Gene Set Enrichment Analysis*" (GSEA) which is a computational method that determines whether a defined set of genes shows statistically significant differences between NSCs and derived iPSCs (**Fig. 1 Annex II**). Remarkably, the GSEA method identified

39 sets of genes that showed downregulation in iPSCs and that were involved in important biological functions including focal adhesion, axon guidance and apoptosis (**Fig. 1 Annex II**). Moreover, 97 set of genes were upregulated including cancer and MAPK signalling pathways (**Fig. 1 Annex II**).

We next focused on the analysis of the changes in the expression of imprinted genes in iPSCs. From 152 imprinted genes described, the RNAseq data identified 122 imprinted genes expressed in NSCs and iPSCs (**Fig. 23e**). From these 122 imprinted genes only 71 were analysed based on the number of reads per sample (1 million reads in at least two samples). The RNAseq data identified 47 imprinted genes from the 71 genes analysed (around 40% of all imprinted genes) that were differentially expressed (FDR<0.05) between iPSCs and NSCs (**Fig. 23f,g**). Among them, we obtained changes in both paternally and maternally expressed genes indistinctly (**Fig. 23g**). Taken together, our data indicated that the acquisition of a pluripotent state requires significant changes at transcriptome levels and that regulation of genomic imprinting is crucial in this process.

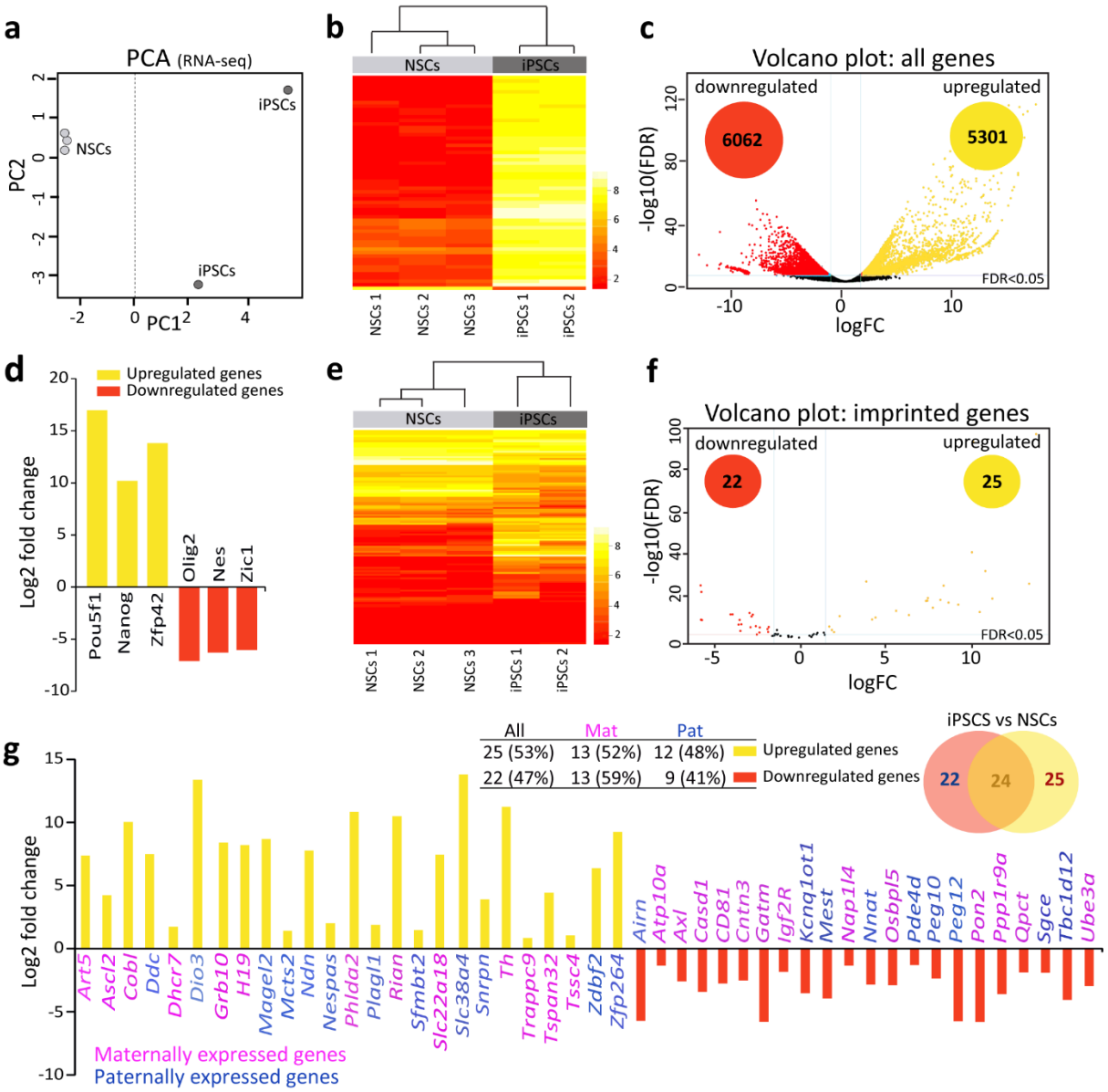

Figure 23. Expression of imprinted genes is importantly regulated during the reprogramming process. (a) Principal component analysis (PCA) from RNAseq of 3 NSCs and 2 iPSCs cultures where samples are represented based on their total expression levels. **(b)** Heatmap representing the 60 most differentially expressed genes between iPSCs and NSCs (FDR<2.5e-68). Genes with higher expression levels are shown in yellow, whereas genes with lower expression levels are shown in red. **(c)** Volcano plot for all genes differentially expressed by RNAseq. Number of downregulated (red) and upregulated (yellow) genes in iPSC compared to NSCs is indicated. **(d)** Fold change of three pluripotency genes (*Pou5f1, Nanog* and *Zfp42*) and three neural genes (*Olig2, Nestin* and *Zic1*) based on RNAseq data. **(e)** Heatmap of the expression of all analysed imprinted genes between iPSCs and NSCs. Non-expressed imprinted genes were discarded from subsequent analysis. **(f)** Volcano plot for differentially expressed imprinted genes in the RNAseq analysis. The number of downregulated (red) and upregulated (yellow) genes in iPSC compared to NSCs is indicated. **(g)** Fold change of expression levels of imprinted genes with differential expression based on RNAseq data. Upregulated genes are indicated in yellow whereas downregulated genes are in red. Maternally and paternally expression is also indicated. Venn diagram representing the number of both upregulated (yellow) and downregulated (red) imprinted is also shown. The intersection indicates the number of unchanged genes.

1.3 Acquisition of pluripotency in NSCs resets DNA methylation patterns.

Previous studies have shown that changes in DNA methylation patterns are essential for successful cell reprogramming, exemplified by the necessity for loss methylation at the promoter of pluripotency genes (Takahashi and Yamanaka 2006, Lee et al., 2014, Hochedlinger and Jaenisch 2015). Moreover, DNA methylation is one of several epigenetic mechanisms that cells use to control gene expression. In order to determine the specific distribution of methylation among genome and specifically within imprinted clusters, we carried out a genome-wide analysis of DNA methylation in iPSCs and NSCs by MeDIPseq. This experimental approach uses a 5-methylcytosine antibody to enrich for DNA fragments containing this modification followed by high throughput sequencing. Sequencing was performed by the *Servei Central de Suport a la Investigació Experimental (SCSIE)* from Universitat de València and the data were analysed by Dr. Elizabeth Radford at the University of Cambridge. Based on changes in methylome from MeDIPseq data obtained, a principal component analysis showed a clear segregation between the NSCs of origin and the generated iPSCs (**Fig. 24a**).

It has been described that iPSCs have lower levels of methylation than somatic cells, suggesting that demethylation is an important chromatin feature to achieve pluripotency (Lee et al., 2014). In agreement with this, the genome-wide analysis demonstrated that 9354 DMRs exhibited reduced methylation levels in iPSCs compared to NSCs, while 893 DMRs had elevated levels of methylation (**Fig. 24b**). Based on the MeDIPseq data, we performed a "*Gene Set Enrichment Analysis*" (GSEA) (**Fig. 24b**). Remarkably, the GSEA method identified 21 sets of genes that showed hypomethylation and that were involved in important biological functions including cell adhesion, cytoskeleton, DNA binding, splice variant, alternative splicing, zinc finger proteins and transcriptional regulation (**Fig. 24b**). Only three sets of genes showed significant hypermethylation levels (**Fig. 24b**). This alteration of the methylome was consistent with a global DNA demethylation needed to acquire a pluripotent state also in NSCs.

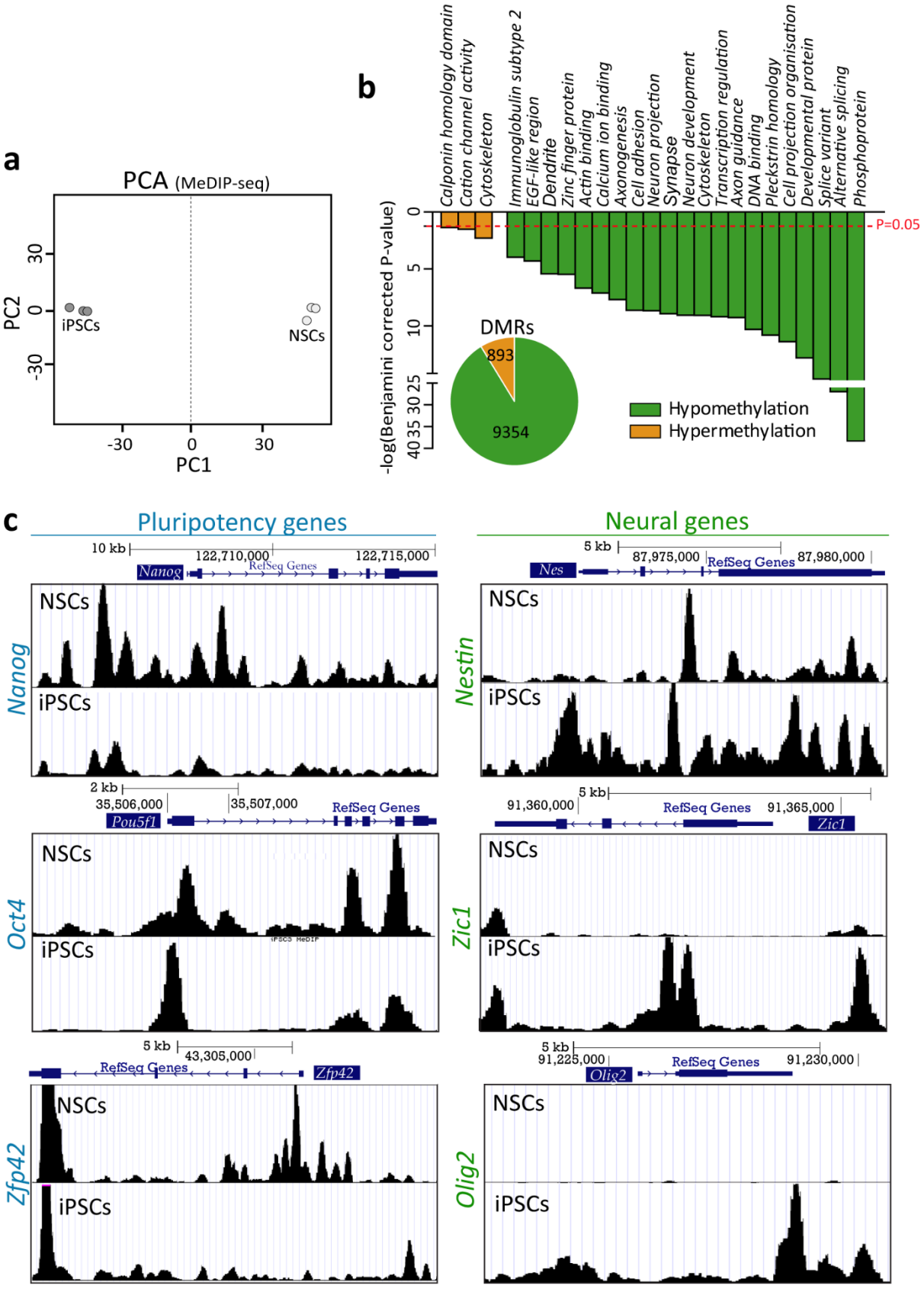
a
PCA (MeDIP-seq)
PC2
PC1
iPSCs
NSCs
b
Calponin homology domain
Cation channel activity
Cytoskeleton
Immunoglobulin subtype 2
EGF-like region
Dendrite
Zinc finger protein
Actin binding
Calcium ion binding
Axonogenesis
Cell adhesion
Neuron projection
Synapse
Neuron development
Cytoskeleton
Transcription regulation
Axon guidance
DNA binding
Pleckstrin homology
Cell projection organisation
Developmental protein
Splice variant
Alternative splicing
Phosphoprotein
P=0.05
-log(Benjamini corrected P-value)
DMRs
893
9354
Hypomethylation
Hypermethylation
c
Pluripotency genes
Neural genes
Nanog
Nestin
Oct4
Zic1
Zfp42
Olig2
NSCs
iPSCs
RefSeq Genes

Figure 24. Methylome is modified during reprogramming of NSCs into iPSCs. (a) Principal component analysis (PCA) from MeDIPseq of 3 iPSCs and 3 NSCs cultures represented based on their global methylation levels. **(b)** *Gene Set Enrichment Analysis* (GSEA) showing statistically significant differences between NSCs and derived iPSCs. Several sets of genes involved in different biological functions showed changes in methylation. Global quantification of the differentially methylated regions (DMRs) found after MeDIPseq in iPSCs compare to NSCs is also shown. **(c)** DNA methylation profile analysis of *Nanog, Oct4* and *Zfp42* (left panels) and *Nestin*, *Zic1* and *Olig2* (right panels) including the predicted promoter regions by MeDIPseq. A schematic representation of each gene from Genome Browser (http://genome.ucsc.edu) is included.

To establish a link between altered DNA methylation pattern and transcriptional activity we determined if changes of expression in pluripotency and neural genes observed in iPSCs, correlated with a gain or loss of the methylation especially at the promoter regions (**Fig. 24c**). Notably, lower methylation correlated with up-regulation of gene expression (**Fig. 24c**). For example, genes such as *Nanog*, *Oct4* and *Zfp42* that were up-regulated in iPSCs (**Fig. 19d** and **Fig**. **23d**) showed low levels of methylation in iPSCs compared to NSCs (**Fig. 24c**). Consistently, a gain of methylation was found at the promoters of downregulated genes such as *Nestin*, *Zic1* and *Olig2* (**Fig. 24c**). These data suggested that the acquisition of a pluripotent state implies a re-establishment of the methylation landscape in the genome to modulate the new gene expression profile.

1.4 Methylation of DMRs at imprinting control regions is modified during reprogramming of NSCs into iPSCs.

As it has been mentioned in the introduction, the majority of imprinted genes are grouped in clusters. An imprinting cluster is usually under the control of a DNA element, called the imprinting control region (ICR) that consists of differentially DNA methylated region (DMR) on the two parental chromosomes (Ferguson-Smith 2011). DNA methylation is the mainstay of establishing imprinting marks on either paternal or maternal alleles (Elhamamsy 2017). The identified DMRs fall into two categories: those that acquire their DMR status in the germline (germline DMR) and those that become differentially methylated after fertilization (somatic DMRs). Somatic DMRs are sometimes tissue-specific and they depend on the presence of a germline DMR (Ferguson-Smith 2011). Deletion of these germline DMRs results in loss of genomic imprinting of multiple genes in the cluster (Sutcliffe et al., 1994, Lin et al., 2003, Williamson et al., 2006) showing that they are crucial ICR that are essential for mono-allelic expression within an imprinted cluster. However, the dynamics of genomic imprinting during the reprograming process remains to be elucidated.

Due to the important effects of DNA methylation at DMRs of imprinted genes in the regulation of gene expression, we focused on the analysis of the methylation profile of different imprinted clusters. From 32 imprinted DMRs analysed, we observed that the methylation profile had been substantially modified in 22 of them (**Fig. 25, Table 1 Annex II**). Interestingly, the vast majority of DMRs

showed lower levels of methylation in iPSC compared to NSCs (**Fig. 25a, Table 1 Annex II**). Only one DMR was hypermethylated in iPSCs (**Table 1 Annex II**). Notably, 86% of the analysed maternal DMRs showed hypomethylation whereas 37% of the paternal DMRs were hypomethylated in iPSCs compared to NSCs (**Fig. 25a**, **Table 1 Annex II).** These results suggested that the alteration of DNA methylation pattern that occurred during the acquisition of a pluripotent state seem to be more frequent in maternally methylated DMRs and thus the control of the gene expression of imprinted genes at these cluster could be altered during this process.

We wanted next to define the relationship between the methylation profile within the imprinted clusters and the expression of imprinted genes in iPSCs. Usually, DNA methylation leads to silencing of gene expression and DNA demethylation leads to activation of gene expression. However, this is not always the case in imprinted genes. Paternally methylated DMRs such as the germline DMRs, IG-DMR (Chr 12) and Igf2-H19 DMR (Chr 7), did not show any change in their methylation status (**Fig. 25b**) and accordingly very few genes within these clusters altered their expression levels after reprogramming (**Fig. 25b; Table 1 Annex II**). Interestingly, H19 was upregulated in iPSC correlating with loss of methylation at the H19 promoter somatic DMR (**Fig. 25c**). Moreover, the *Rasgrf1* imprinted locus showed hypomethylation in iPSCs but this change did not correlate with changes of any of the genes within the cluster, as *Mir184*, *A19*, *AK029869* or *Rasgrf1* were normally expressed (**Table 1 Annex II**).

In contrast, we found that several maternally methylated DMRs, did lose methylation (**Fig. 25d; Table 1 Annex II**). Interestingly, at these loci, both somatic and germline DMRs were hypomethylated in iPSCs and we did not find any DMR regions which gain methylation (**Table 1 Annex II**). Hypomethylation at maternally methylated DMRs correlated with changes in the expression levels of several genes within the clusters. For example genes from the *Kcnq1ct1*, *Snrpn* or *Nespas* imprinted clusters were significantly altered (**Fig. 25d; Table 1 Annex II**) indicating that changes in DNA methylation patterns at imprinted loci during reprogramming result in changes in gene expression. To confirm these data, validation by pyrosequencing of the methylation levels at these DMRs together with the confirmation by qPCR of the changes of imprinted genes in iPSCs compared to NSCs need to be done next.

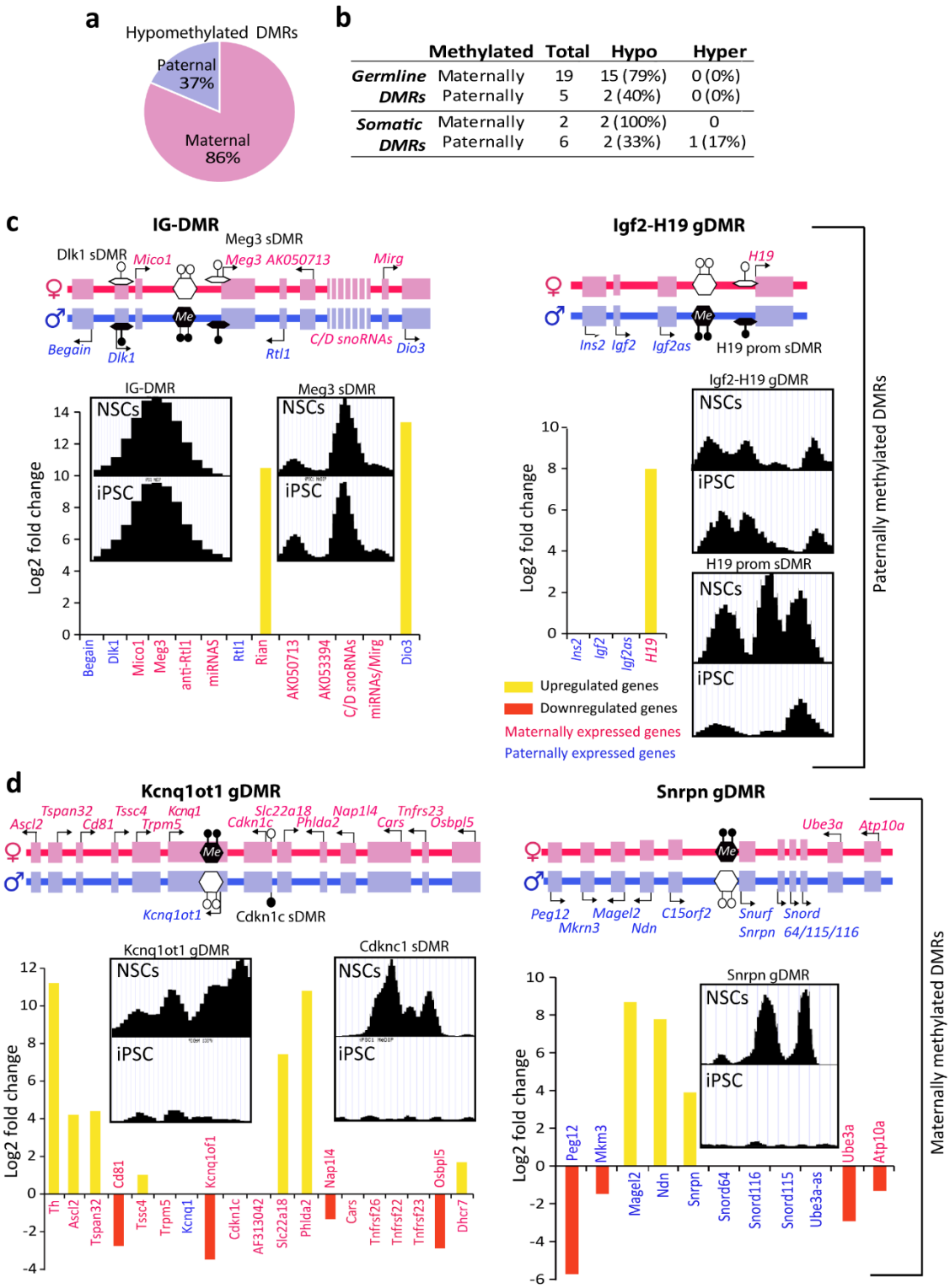

Figure 25. Changes in the expression of imprinted genes correlate with hypomethylation at the maternally methylated DMRs. (a) Percentage of maternally (pink) and paternally (blue) methylated DMRs that show hypomethylation in iPSCs compared to NSCs (FDR<0.05). A table with number and changes of germline and somatic DMRs analysed is shown. **(b)** Schematic of the *Dlk1-Dio3* and the *Igf2-H19* imprinted clusters representing the germline and somatic paternally methylated DMRs (upper panels). Fold change of the expression of the genes within the clusters. Methylation profiles by MeDIP-seq at the DMRs show no changes (lower panels). H19 promoter somatic DMR showed hypomethylation. **(c)** Schematic of the two maternally methylated clusters *Kcnq1ot1* and *Snrpn*. Expression of the genes within the clusters and methylation profiles of the DMRs are shown. Hypomethylation at the DMRs causes alteration of several genes within the clusters. Downregulated genes are indicated in red and upregulated are in yellow. Maternally (pink) and paternally (blue) expressed genes are indicated.

1.5 TET3 prevents reprogramming of NSCs into iPSCs *in vitro*

We have described that DNA methylation is a heritable epigenetic modification that plays a central role in genomic imprinting. Moreover, in mammals, active erasure of 5mC from DNA is catalysed by Ten-Eleven Translocation (TET) family members (TET1, TET2 and TET3) that oxidase 5mC to 5-hydroxymethylcytosine (5hmC), 5-formylcytosine (5-fC) and 5-carboxylcytosine (5-caC) (Wu and Zhang 2017). TET enzymes have been previously implicated in imprinting regulation. For example, TET1 deficiency results in aberrant methylation patterns at imprinted *loci* in primordial germ cells (PGCs) and sperm cells and the progeny exhibit phenotypes associated with abnormal imprinting erasure (Yamaguchi et al., 2013). Nevertheless, it is still unclear how epigenetic machinery recognizes ICRs.

Given the importance of DNA methylation on the regulation of genomic imprinting during reprogramming of adult NSCs, we next studied the expression levels of TET proteins during the reprogramming process as a potential candidate to remove methylation at the maternal methylated DMRs. qPCR data showed low levels of expression of *Tet1* and *Tet2* in NSCs and these were significantly increased in iPSCs (**Fig. 26a**). However *Tet3,* which is the most abundant member of the TET dioxygenase in the adult NSCs, was significantly downregulated during the reprogramming process (**Fig. 26a**) suggesting a relevant role in the multipotent state of NSCs.

In order to clarify the role of TET3 in the maintenance of neural phenotype, we induced *Tet3* deficient NSCs into iPSCs using the 2F protocol described before (**Fig. 18a**). To obtain *Tet3* deficient NSCs, we generated a murine genetic model by crossing male mice carrying *loxP* sites flanking the *Tet3* gene ($Tet3^{loxP/loxP}$) (Santos et al., 2013) with female mice expressing the *Cre-recombinase* under the control of the mouse *Gfap* promoter ($Gfap\text{-}Cre^{+/0}$) (This model is explained in the next chapter). In this assay, deficient *Tet3* NSCs ($Tet3\text{-}Gfap^{cre}$) were compared to control NSCs ($Tet3\text{-}Gfap^{control}$) (**Fig. 26b**). To evaluate the efficiency of the reprogramming process in the absence of *Tet3*, we determined the presence of pluripotent colonies by detecting the presence of alkaline phosphatase positive clones in the cultures. Interestingly, *Tet3* deficient NSCs formed more pluripotent clones compared to controls (**Fig. 26c,d**), indicating that the downregulation of *Tet3* expression was essential for a successful reprograming of adult NSCs into iPSCs. This also suggests that TET3 is not the enzyme that catalyses the demethylation process observed in maternally methylated DMRs during the reprogramming of NSCs into iPSC. Therefore, TET1 and TET2 need to be analysed in this context to determine their role in the demethylation of imprinted DMRs.

However, based on these new results, we propose that TET3 might have an important role in the maintenance of the multipotent identity of adult NSC and we study in the next chapter the function

of this protein in the subventricular neurogenic niche focusing on the role of the enzyme in the maintenance of genomic imprinting in adult NSCs.

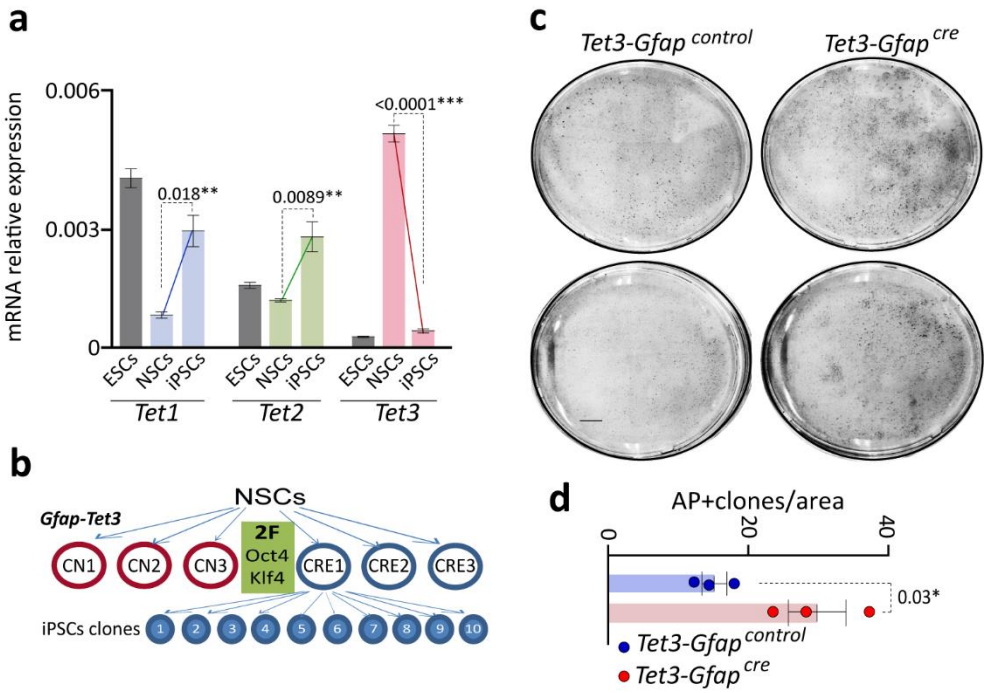

Figure 26. *Tet3* downregulation is essential for the acquisition of a pluripotent state. (a) Quantitative PCR for *Tet1*, *Tet2* and *Tet3* in NSCs and iPSCs. *Tet1* and *Tet2* were upregulated during reprogramming whereas *Tet3,* highly expressed in NSCs, was downregulated in iPSCs compared to NSCs. ESCs were used as a control of expression. *Gapdh* was used to normalize qPCR expression data. **(b)** Schematic of the reprogramming of TET3 deficient NSCs. Three independent cultures of each genotype were used to reprogram NSCs with 2F, *Oct-4* and *Klf4*. When iPSCs clones were big enough, 10 clones of each culture were isolated for expansion. **(c)** Alkaline phosphatase (AP) staining after the reprogramming of *Tet3* deficient NSCs (right panel) and control NSCs (left panel) showing a higher number of positive clones in *Tet3-Gfap*^{cre} iPSCs. **(b)** Number of AP+ clones per area analysed in both genotypes. All error bars show s.e.m. of at least 4 cultures per condition. P-values are indicated (*p-value<0.05, **p-value<0.01 and ***p-value<0.001). Scale bar in c: 1cm

Annex II

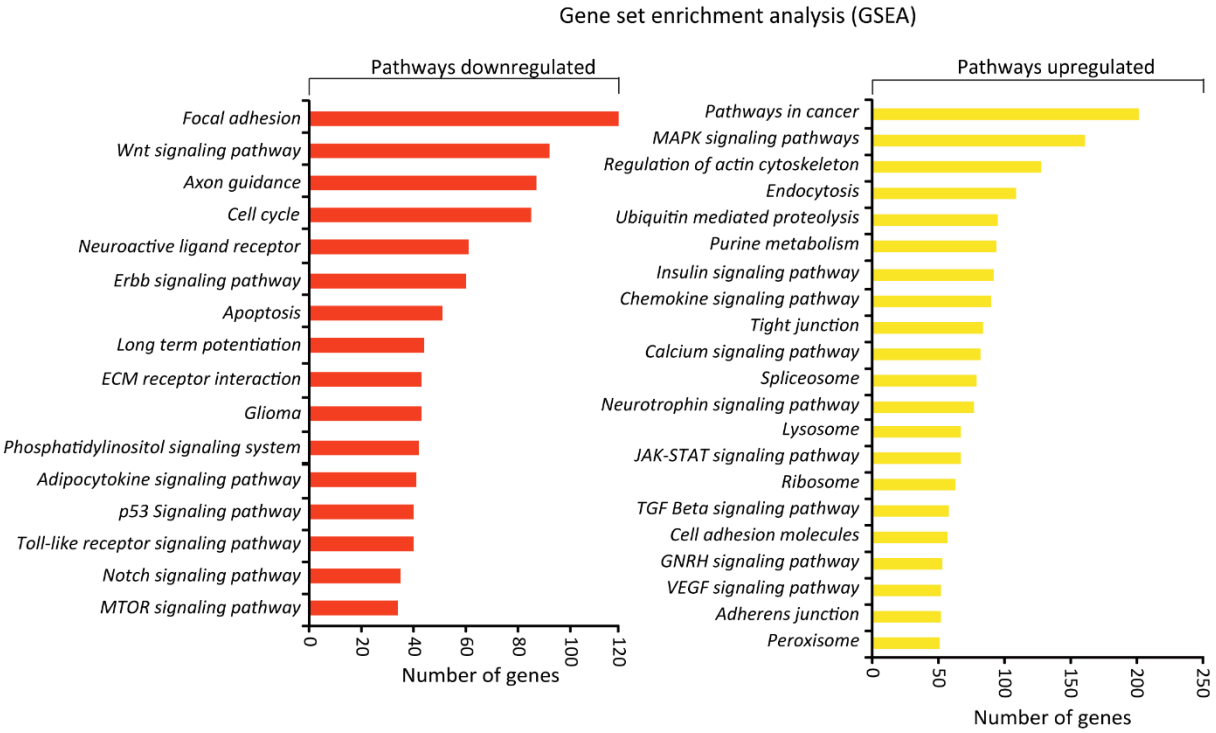

Figure 1 Annex II. *Gene Set Enrichment Analysis* (GSEA) showing the more significant changed metabolic pathways in iPSCs compare to NSCs. Coloured red bars represent the number of downregulated genes in pathways with more than 35 genes differentially expressed. Coloured yellow bars show the number of upregulated genes in pathways with more than 50 differentially expressed genes.

Table 1 Annex II. Changes in maternally and paternally methylated DMRs from MeDIPseq (iPSCs vs NSCs). Maternally and paternally methylated DMRs are indicated. The start and end nucleotide position based on the Genome Reference Consortium Mouse Build 38 (GRCm38/mm10) are also indicated. The methylation status of the DMRs and the number of differentially expressed genes within the cluster are shown.

Imprinted locus		DMR		Chr.	Start	End	Methylation	Differentially expressed genes
Maternally methylated	***Gnas***	*Nespas-Gnas*	*germline*	chr2	174294124	174297817	hypo	1 (5)
		Gnas1A	*germline*	chr2	174327075	174329319	hypo	
	Mcts2	*Mcts2*	*germline*	chr2	152686755	152687275	hypo	1 (2)
	Nnat/Peg5	*Nnat*	*germline*	chr2	157559270	157561662	hypo	1 (2)
	Fkbp6	*Fkbp6 DMR1*	*germline*	chr5	135351732	135351863	unchanged	1 (1)
		Fkbp6 DMR2	*germline*	chr5	135349819	135350194	hypo	
	Peg10	*Peg10*	*germline*	chr6	4745857	4749483	hypo	6 (10)
	Mest/ Nap1l5	*Mest/Peg1*	*germline*	chr6	30734007	30739966	hypo	1 (7)
		Nap1l5	*germline*	chr6	58906696	58907062	hypo	
	Peg3	*Peg3*	*germline*	chr7	6727344	6732689	hypo	1 (7)
	Snrpn	*Snrpn*	*germline*	chr7	60003561	60005296	hypo	7 (13)
	Inpp5f_v2	*Inpp5f_v2*	*germline*	chr7	128688274	128688642	hypo	0 (2)
	Kcnq1ot1/ Lit1	*KvDMR*	*germline*	chr7	143293662	143296905	hypo	11 (19)
		Cdkn1c	*somatic*	chr7	143461406	143461537	hypo	
	Cdh15	Cdh15	*germline*	chr8	122865050	122865261	unchanged	0 (1)
	Plagl1/Zac1	Plagl1/Zac1	*germline*	chr10	13090043	13091998	hypo	1 (1)
	Grb10/ Zrsr1	*Grb10*	*germline*	chr11	12025460	12027097	hypo	4 (6)
		Zrsr1	*germline*	chr11	22971765	22974028	hypo	
	Peg13	*Peg13*	*germline*	chr15	72809482	72810159	unchanged	0 (1)
	Igf2R	*Igf2r DMR2*	*germline*	chr17	12741303	12742867	unchanged	1 (4)
		Igf2r DMR1 promoter	*somatic*	chr17	12769907	12770094	hypo	
	Impact	*Impact*	*germline*	chr18	12971926	12974626	hypo	0 (1)
Paternally methylated	***Gpr1-Zdbf2***	*Gpr1*	*germline*	chr1	63200129	63200349	hypo	1 (2)
		Zdbf2	*germline*	chr1	63264669	63264855	unchanged	
	Igf2-H19	*H19 ICR*	*germline*	chr7	142580083	142582190	unchanged	1 (4)
		H19 promoter	*somatic*	chr7	142578136	142578879	hypo	
		Igf2 DMR0	*somatic*	chr7	142669087	142669626	unchanged	
		Igf2 DMR1	*somatic*	chr7	142665179	142665719	unchanged	
		Igf2 DMR2	*somatic*	chr7	142653809	142654708	hyper	
	Rasgrf1	*Rasgrf1*	*germline*	chr9	89876748	89883626	hypo	0 (4)
	Dlk1-Gtl2	*IG-DMR*	*germline*	chr12	109528206	109528523	unchanged	2 (11)
		Dlk1 DMR	*somatic*	chr12	109459858	109460079	unchanged	
		Gtl2 DMR	*somatic*	chr12	109539232	109543185	unchanged	

2. TET3 plays an important role in the regulation of NSC in the SVZ.

2.1 TET3 is highly abundant in the adult neural stem cell pool

TET dioxygenases are most abundant in the brain and can convert 5mC to 5hmC resulting in the removal of the methylated cytosine in somatic tissues, including the brain (Kriaucionis and Heintz 2009, Jin et al., 2010, Munzel et al., 2010, Szwagierczak et al., 2010, Szulwach et al., 2011).

Since the discovery of TET proteins (Iyer et al., 2009), TET1 and TET2 has been extensively studied. It has been demonstrated that *Tet1* and *Tet2* are widely expressed during embryonic development and in ESC, whereas *Tet3* is less widely expressed (Koh et al., 2011, Hahn et al., 2013). TET3 has been previously implicated in the maintenance of neural progenitors derived from ESCs and in their terminal differentiation into neurons (Li et al., 2015). Nonetheless, the specific role of TET3 in NSCs function and in adult neurogenesis has not been determined. Consistently, qPCR for TET expression patterns showed low mRNA levels of *Tet1* and *Tet2* and high levels of *Tet3* in adult NSCs (**Fig. 27a**). Moreover, in the SVZ tissue, *Tet3* was the most abundant member of the TET dioxygenases being also highly expressed in the NSCs pool in the early postnatal brain (**Fig. 27a**). Interestingly, *Tet3* expression was maintained postnatally in the stem cell pool and in more differentiated cells, whereas *Tet1* and *Tet2*, highly expressed in the ESCs and early in NSCs development, were downregulated in the adult NSCs (**Fig. 27a**).

It has been reported that the mammalian *Tet3* possess three known isoforms generated by alternative splicing (Perera et al., 2015), one containing a CXXC DNA binding domain, refer as *Tet3-full-length* (*Tet3FL*), one lacking a CXXC domain called *Tet3-short* (*Tet3s*) and *Tet3o* which is specific of oocytes and contains an additional N-terminal exon and also lacks the CXXC domain (**Fig. 27b**). It has been also described that *Tet3FL* isoform is the predominant TET3 protein in neurons, is localized precisely at transcription starting sites (TSSs) and shows less catalytic activity than *Tet3s* isoform due to the presence of the CXXC domain (Jin et al., 2016). However, *Tet3s* isoform pattern expression in the brain remained to be elucidated.

To characterize the expression pattern of the *Tet3* isoforms in the adult SVZ and in NSCs, we examined the transcripts of *Tet3FL*, *Tet3s* and *Tet3o* using qPCR with primer pairs spanning the isoform-specific exons at the 5´-end (Jin et al., 2016) (**Fig. 27b**). We observed that the most abundant isoform in the brain and in the SVZ was the *Tet3s*. Interestingly, despite being also the predominant isoform, in NSCs the expression of *Tet3FL* was higher than in brain or SVZ (**Fig. 27c**). In ESCs both isoforms were almost equally expressed (**Fig. 27c**). As expected, *Tet3o* was not expressed in the neurogenic niche or NSCs (data not shown).

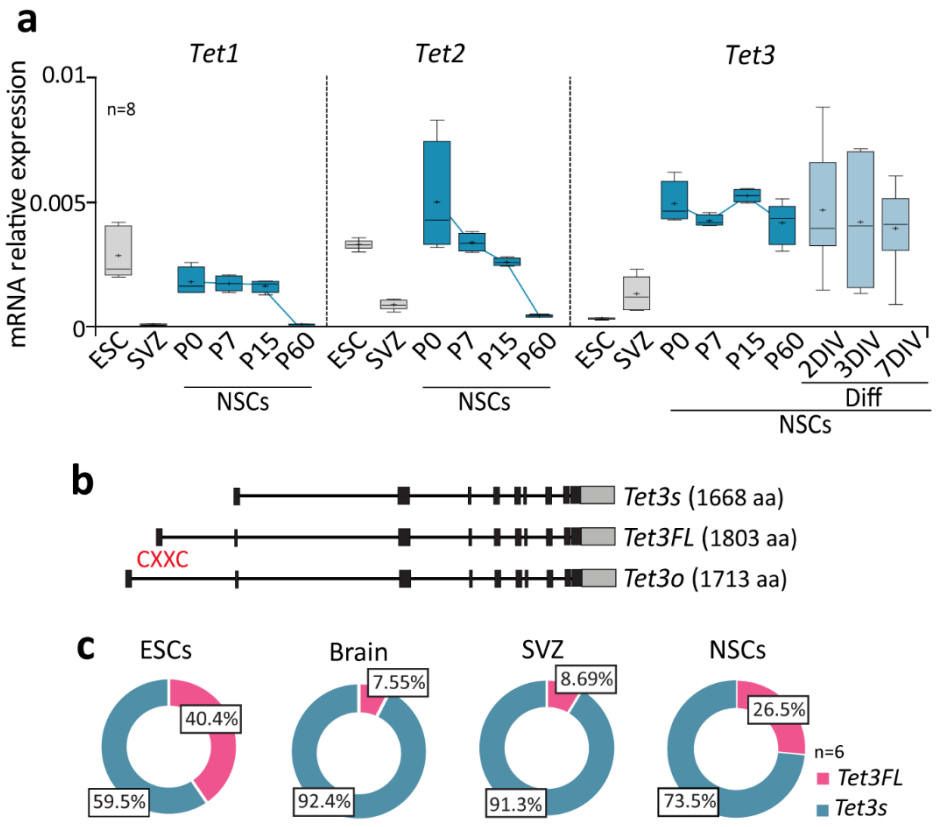

Figure 27. TET3 is the most expressed member of the TET family in the SVZ neurogenic niche. (a) qPCR for *Tet1*, *Tet2* and *Tet3* genes in different cell types and tissues. *Tet1* is not expressed in adult NSCs and *Tet2* downregulates postnatally. *Tet3* is highly expressed in the SVZ and is maintained postnatally in the NSCs population. Dark blue bars represent proliferating NSCs and light blue bars show NSCs after 2, 3 and 7 days growing in differentiation conditions. Significant levels of *Tet3* were also observed during the differentiation process. P: postnatal day. **(b)** Schematic of the three TET3 isoforms of mouse and human. N-terminal domains are different between the isoforms. The conserved CXXC domain is depicted in red. **(c)** Percentage of isoforms expression related to total *Tet3* levels measured by qPCR in ESCs, Brain, SVZ and NSCs. The percentage of *Tet3FL* is increased in NSCs compare to brain and SVZ. *Gapdh* was used to normalize data. All error bars show s.e.m. of at least 6 cultures per genotype or tissue samples.

To determine more specifically the cellular distribution of TET3 in the adult brain, immunostaining of TET3 in combination with the astrocytic marker GFAP, was performed in wild-type adult brains. TET3 protein distribution within the adult SVZ showed nuclear staining for the enzyme in the GFAP positive population located close to the lateral ventricles, whereas no expression of the protein was observed in more committed progenitors cells or DCX positive neuroblasts (**Fig. 28a**). TET3 staining was also observed in mature neurons in the striatal parenchyma. Furthermore, neurospheres cultures isolated from the adult SVZ, showed the presence of TET3 in all SOX2 positive cells in proliferating conditions (**Fig. 28b**). Consistently with mRNA levels, TET3 protein was maintained during 3 and 7 days of differentiation *in vitro* in Nestin positive progenitors and in mature GFAP positive astrocytes respectively (**Fig. 28c**). All these data suggest a relevant role for this dioxygenase in adult NSCs behaviour.

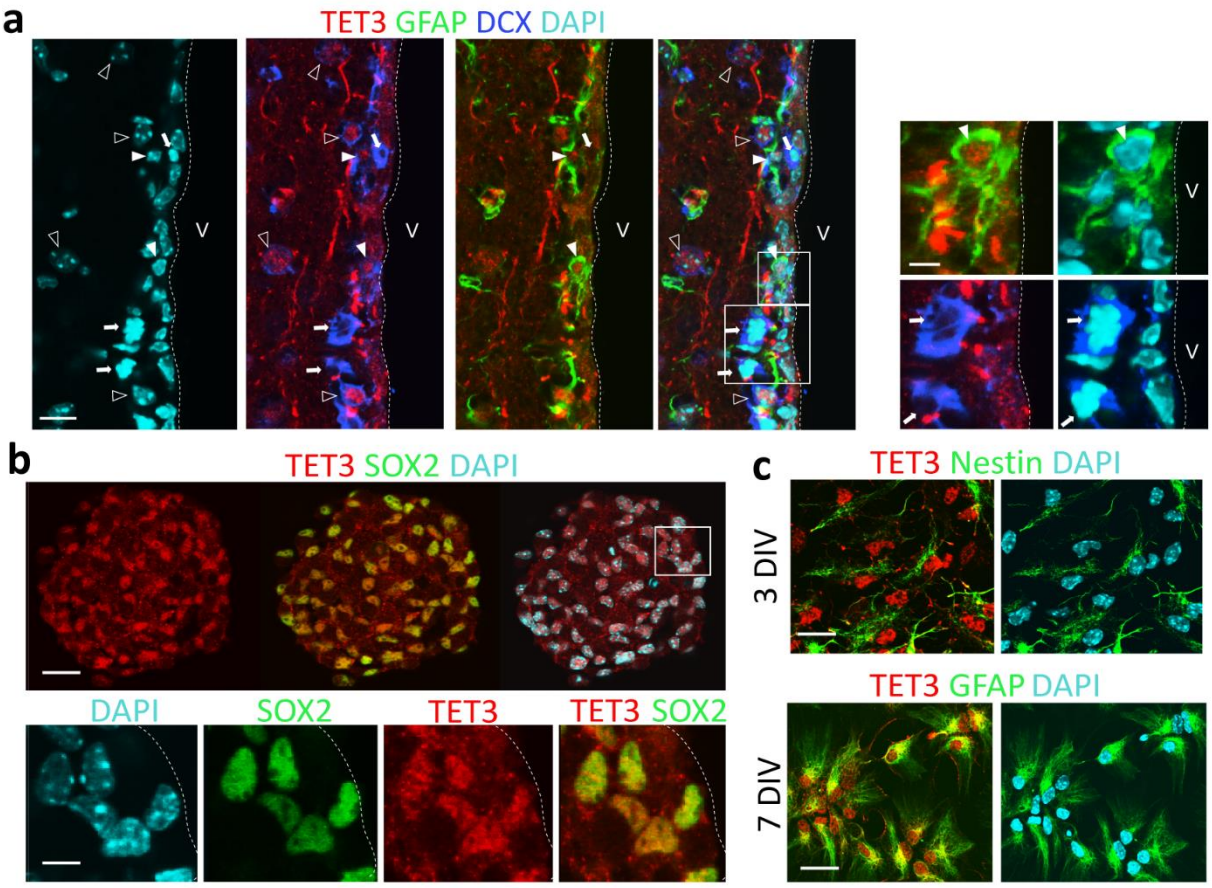

Figure 28. TET3 is highly expressed in adult NSCs *in vivo* and *in vitro*. (a) Immunohistochemistry confocal images for TET3 (red), GFAP (green) and doublecortin (DCX, blue) in the SVZ of adult wild-type mice. Dark arrowheads indicate GFAP+ astrocytes cells. Open arrowheads indicate mature neurons in the striatal parenchyma. Neuroblast are also indicated (arrows). V: lateral ventricle lumen. **(b)** Immunocytochemistry for TET3 (red) and SOX2 (green) in proliferating neurospheres isolated from the adult SVZ. **(c)** Immunocytochemistry for TET3 (red) and Nestin (green) or GFAP (green) in adult NSCs after 3 (upper panels) and 7 (lower panels) days of differentiation. DAPI was used to counterstain DNA. Scale bar in a and b: 20 µm (high magnification images, 7 µm); in c: 15 µm.

2.2 TET3 promotes stemness maintenance in the adult SVZ

2.2.1 Deletion of *Tet3* by a Cre/LoxP system was confirmed in GFAP positive cells

NSCs in the SVZ express astrocytic markers such as the glial fibrillary acidic protein (GFAP) (Doetsch 2003). Thus, in order to evaluate the regulatory function of TET3 in the adult SVZ neurogenic niche we generated a murine genetic model by crossing male mice carrying *loxP* sites flanking the *Tet3* gene ($Tet3^{loxP/loxP}$) (Santos et al., 2013) with female mice expressing the *Cre-recombinase* under the control of the mouse *Gfap* promoter ($Gfap\text{-}Cre^{+/0}$) (Garcia et al., 2004) (**Fig. 29a**). Significant expression of *cre*-recombinase in deficient brains and SVZ-derived NSCs was first confirmed by qPCR (**Fig. 29b**). The expression levels of *Tet3* in the $Tet3^{loxP/loxP}Gfap^{cre/0}$ (referred to as $Tet3\text{-}Gfap^{cre}$) compared to $Tet3^{loxP/loxP}Gfap^{0/0}$ ($Tet3\text{-}Gfap^{control}$) control mice was determined. Whereas it was not found a reduction

of *Tet3* in *Tet3-Gfap*^{cre} whole brain or SVZ tissue, probably because of cell heterogeneity, the elimination of *Tet3* was confirmed selectively in NSCs (**Fig. 29c**). The levels of *Tet3FL* and *Tet3s* were measured by qPCR and the results showed no changes of the TET3 isoforms in brain. However, as expected, both *Tet3FL* and *Tet3s* mRNA levels were downregulated in *Tet3-Gfap*^{cre} (**Fig. 29d**). Downregulation of TET3 protein was also confirmed by immunocytochemistry and western-blot in neurospheres isolated from deficient SVZ (**Fig. 29e,f**). However, no changes in the expression of the other two members of the TET dioxygenases family, *Tet1* and *Tet2* were observed (**Fig. 29g**), demonstrating the specific downregulation of the *Tet3* gene in the GFAP positive NSCs population.

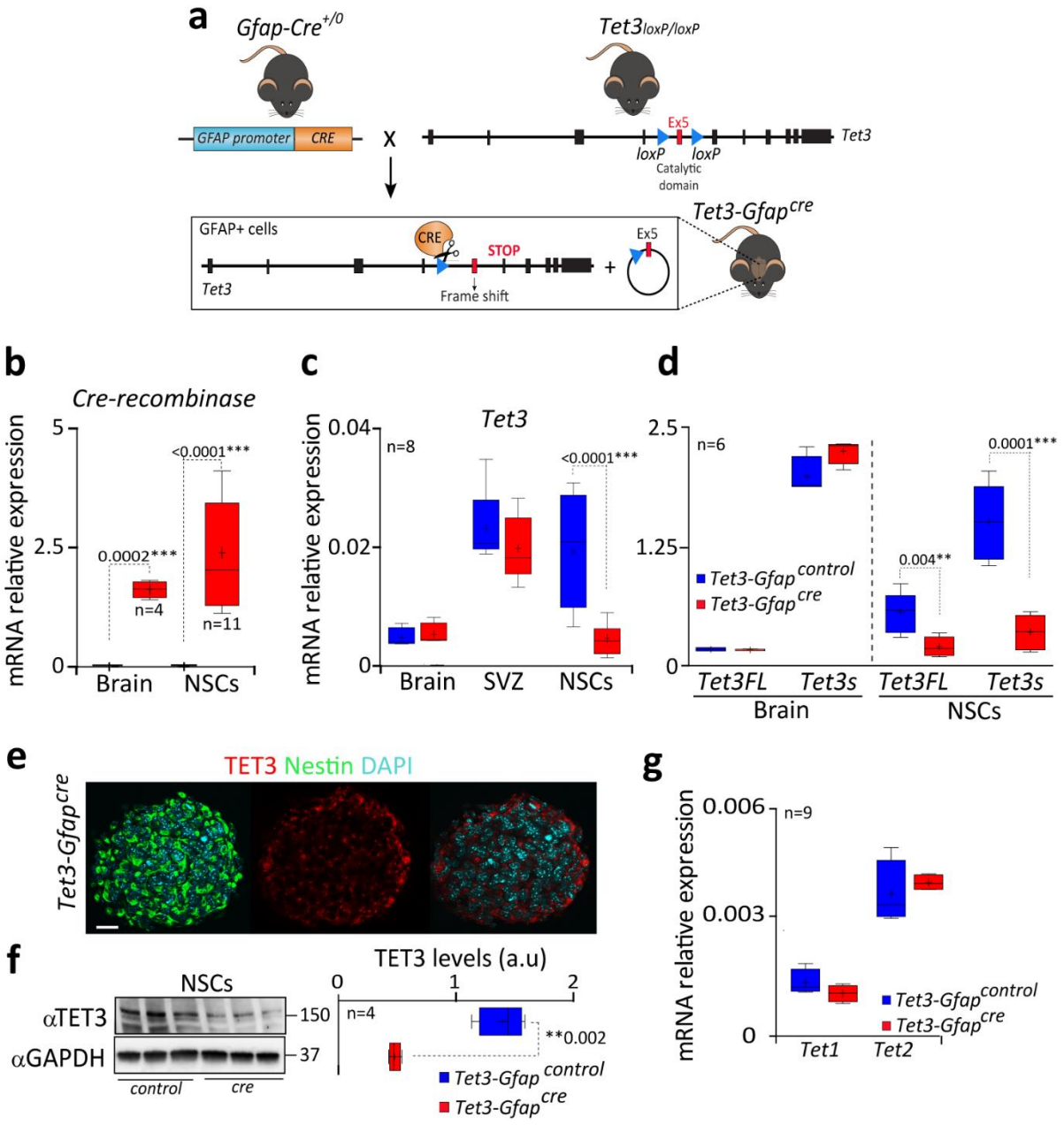

Figure 29. *Tet3* is specifically down-regulated in GFAP+ cells in *Tet3-Gfap^{cre}* mice. (a) Schematic representing the generation of the murine model. Mice expressing *cre-recombinase* under the mouse GFAP promoter (*Gfap-cre$^{+/0}$*) were crossed with mice carrying *LoxP* sites flanking the exon 5 of the *Tet3* gene (*Tet3$^{loxP/loxP}$*) which encodes residues required for chelation of Fe(II) and is upstream of other catalytic residues. Expression of *cre-recombinase* results in excision of this region and a frame-shift from exon 6 affecting all downstream exons until a premature stop codon in exon 7**. (b)** qPCR for *cre-recombinase* in the brain and NSCs of *Tet3-Gfap^{control}* and *Tet3-Gfap^{cre}* mice. **(c)** qPCR for *Tet3* in adult brain, SVZ and NSCs in *Tet3-Gfap^{control}* and *Tet3-Gfap^{cre}* mice. **(d)** qPCR for *Tet3FL* and *Tet3s* isoforms in *Tet3-Gfap^{control}* and *Tet3-Gfap^{cre}* brains and NSCs. **(e)** Immunocytochemistry for TET3 (red) and Nestin (green) in *Tet3-Gfap^{cre}* neurospheres. DAPI was used to counterstain DNA. **(f)** Western-blot for TET3 in *Tet3-Gfap^{control}* and *Tet3-Gfap^{cre}* neurospheres cultures growing in proliferating conditions. **(g)** qPCR for *Tet1* and *Tet2* in *Tet3-Gfap^{control}* and *Tet3-Gfap^{cre}* NSCs. *Gapdh* was used to normalize data. All error bars show s.e.m. of at least 6 cultures per genotype or tissue samples. Scale bar in d: 20 µm. P-values are indicated. **p-value<0.01 and ***p-value<0.001.

To confirm that the floxed allele had effectively recombined in the GFAP population postnatally, *GFAP-cre* mice were crossed to *ROSA26-LacZ* reporter mice that carry *β-galactosidase* expression gene (*LacZ*) under the regulation of the ubiquitous *Rosa26* promoter (resulting animals were referred to as *Gfap-CRE/LacZ*). *Cre-recombinase* expression results in the removal of a *LoxP*-flanked DNA segment that prevents expression of the *LacZ* gene and β-galactosidase activity which can be detected by histochemistry. X-gal was performed in the adult brain of *Gfap-CRE/LacZ* and of their control mice (without the *cre-recombinase* and referred to as *Gfap-CN/LacZ*) (**Fig. 30a,b**). X-gal showed positive staining in the SVZ, rms and olfactory bulbs of the adult *Gfap-CRE/LacZ* brains whereas no staining was observed in their controls (**Fig. 30a**). Moreover, X-gal staining was found to colocalize with GFAP+ cells (**Fig. 30b**), indicating a specific recombination in the GFAP positive stem cell population that is maintained in their progeny.

To determine if deficiency of *Tet3* in the *Gfap* population could cause any developmental defect, we determined body and brain weights in *Tet3-Gfap^{cre}* mice compared to their controls at postnatal days 21 (P21) and 60 (P60). No changes were observed and around 50% of mice from each genotype was obtained from the breeding between *Tet3$^{loxP/loxP}$;Gfap-Cre$^{0/0}$* males and *Tet3$^{loxP/loxP}$;Gfap-Cre$^{+/0}$* females in accordance with Mendelian law (**Fig. 30c-e**) indicating that conditional mutation of *Tet3* in the GFAP population does not cause any general developmental alterations.

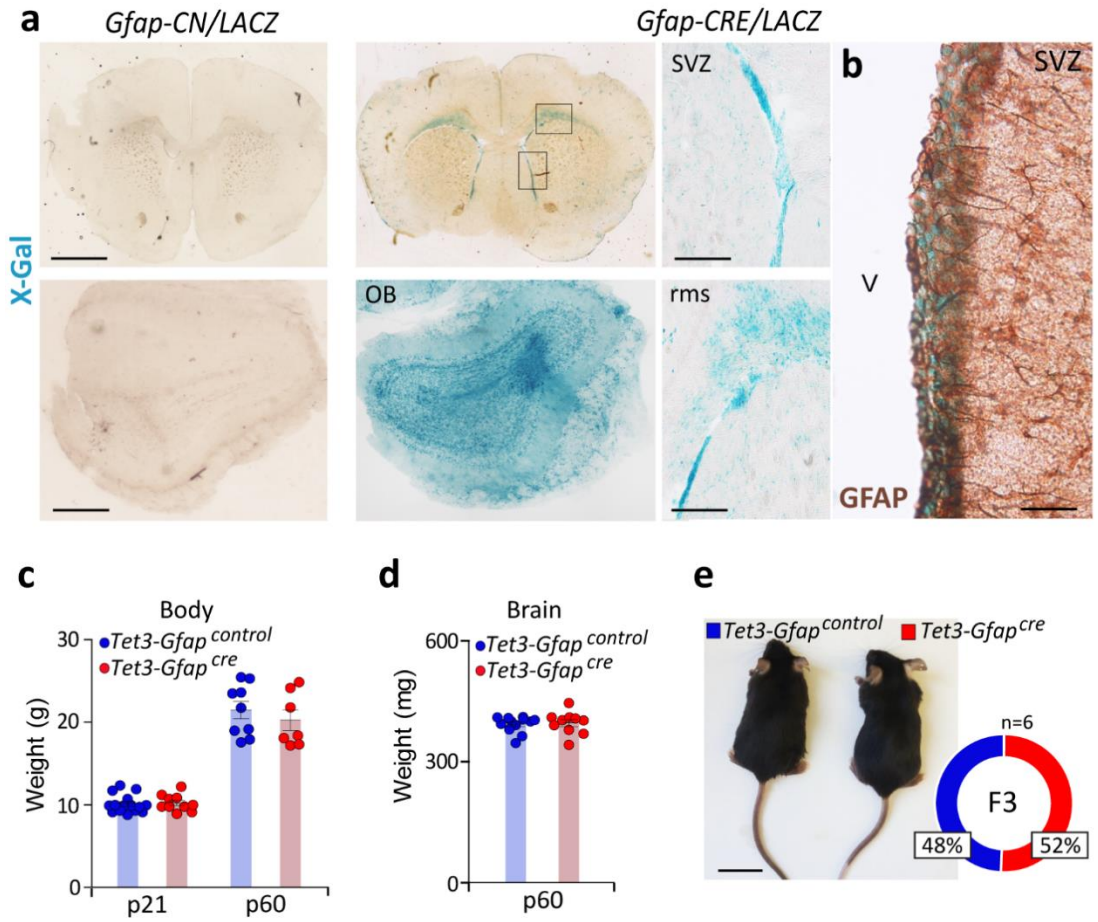

Figure 30. *Cre*-mediated recombination is specific of GFAP stem cells. (a) β-galactosidase staining (blue) in the SVZ, olfactory bulb (OB) and rostral migratory steam (rms) of Gfap-CRE/LacZ mice. Gfap-CN/LacZ mice with no *cre-recombinase* were used as control for the staining. **(b)** β-galactosidase staining (blue) and immunohistochemistry for GFAP in the SVZ of *Gfap-CRE/LacZ* mice. **(c)** Body weights (in grams) in mice from the two genotypes at postnatal day 21 (p21) and 60 (p60). **(d)** Brain weights (in milligrams) in P60 *Tet3-Gfap*^{control} and *Tet3-Gfap*^{cre} mice. **(e)** Images of *Tet3-Gfap*^{control} and *Tet3-Gfap*^{cre} mice. Percentage of mice from each genotype in F3 offsprings is indicated. V: lateral ventricle. Scale bars in a (upper panel): 1000 µm; in a (lower panel and right panels): 500 µm; in b: 20 µm; in e: 2.5 cm. All error bars show s.e.m. of at least 6 samples per genotype. Number of samples used is indicated as coloured dots.

2.2.2 *Tet3* deficiency causes depletion of the adult SVZ neural stem cell pool *in vivo*

SVZ niche populations including NSCs population, show morphological, molecular and functional heterogeneity (Morrens et al., 2012). The identification of NSCs in the adult SVZ has been a challenge since their discovery, given that there were not specific markers that allowed the unequivocally identification of the different populations in this niche (Codega et al., 2014, Chaker et al., 2016). The ability to label dividing cells has been very useful in verifying the existence of adult neurogenesis and in monitoring changes in neurogenesis in different conditions (Ferron et al., 2007, Codega et al., 2014). The use of thymidine analogous like bromodeoxyuridine (BrdU) and its immunocytochemical detection has permitted single or multiple labelling when was combined with different astroglial or stem cell markers and this strategy has been classically used in histological analysis to study NSCs and their

progeny (Ferron et al., 2007, Kuhn et al., 2016). When BrdU is given repeatedly and examined long after administration, remaining labelled cells are candidate stem cells due to their slowly division mode. Indeed, three to four weeks after the analogue administration, the rapidly dividing progenitors C cells and A neuroblasts dilute the nuclear label while it is only retained in slowly proliferating NSCs (LRC) and olfactory bulb newborn neurons that ceased to divide and terminally differentiate soon after the injection (Ferron et al., 2007).

Therefore, to further investigate the role of TET3 in the adult SVZ-NSCs *in vivo*, two-month-old mice were injected with the nucleotide analogue BrdU three weeks before killing (**Fig. 31a**). TET3 deficient mice showed a specific reduction in the proportion of BrdU-LRCs GFAP+ that, in addition, were less proliferative as measured by the cell-cycle antigen Ki67 (**Fig. 31b**), suggesting a role for TET3 in regulating the activated NSCs within the SVZ. Notably, the overall rate of proliferation in *Tet3-Gfap* deficient SVZ was similar to their controls as the percentage of total Ki67+ cells in the intact SVZ of 2-months-old mice was similar in both genotypes (**Fig. 31c,d**). Interestingly, the proportion of terminally differentiated GFAP positive cells was increased in the *Tet3-Gfap*^{cre} SVZ as we found a higher proportion of GFAP+ cells that were also positive for the calcium-binding protein S100β in 2-months-old *Tet3-Gfap*^{cre} mice compared to control mice (**Fig. 31e**). This support the hypothesis that the loss of NSCs in *Tet3-Gfap*^{cre} mice *in vivo* might be due to a premature differentiation of the stem cell population.

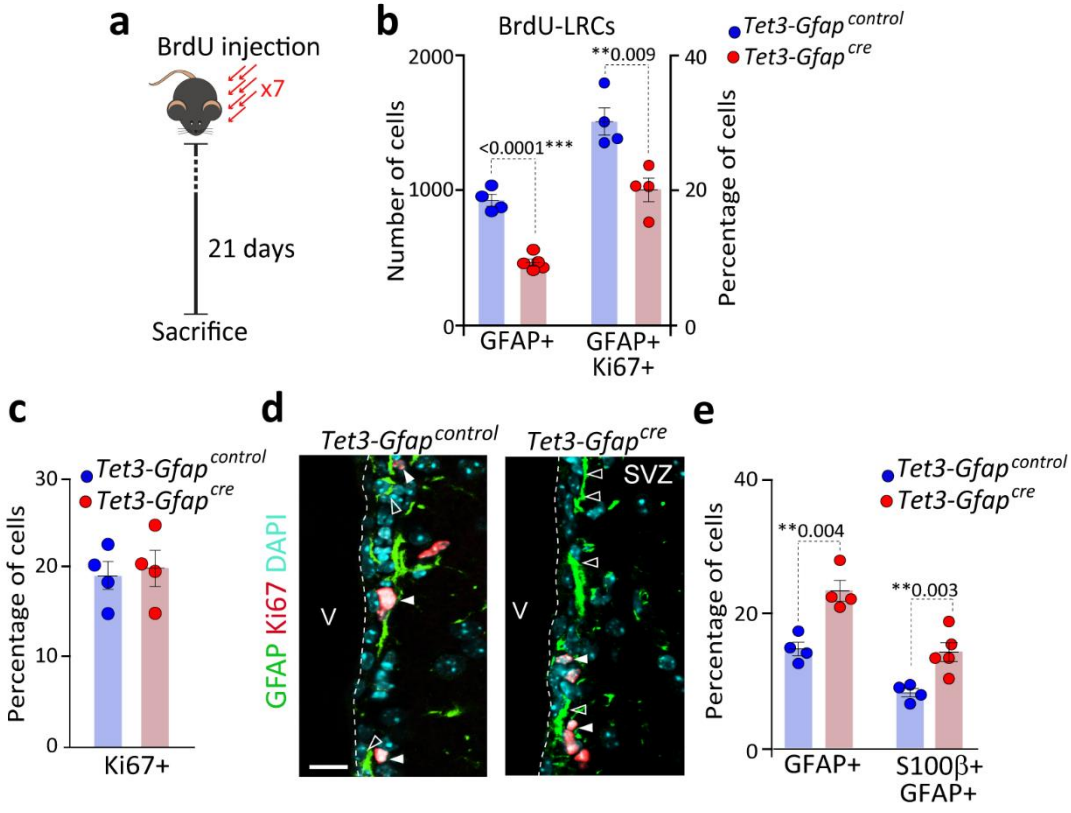

Figure 31. Removal of *Tet3* in the SVZ GFAP+ population causes a depletion of the neural stem cell pool *in vivo*. (a) Schematic drawing of the BdrU injection protocol. **(b)** Number of BrdU-label retaining cells (BdrU-LRCs) that are GFAP+ and GFAP/Ki67+ in the SVZ of *Tet3-Gfap*^{control} and *Tet3-Gfap*^{cre} mice. **(c)** Percentage of total Ki67+ cells in the SVZ of *Tet3-Gfap*^{control} and *Tet3-Gfap*^{cre} mice. **(d)** Immunohistochemistry confocal images for GFAP (green) and Ki67 (red) in SVZ of mice from both genotypes. Open arrowheads indicate GFAP+ cells. Dark arrowheads indicate GFAP+ cells that are also Ki67+. DAPI was used to counterstain nuclei. **(e)** Percentage of GFAP+ and S100β/GFAP+ cells in the SVZ of *Tet3-Gfap*^{control} and *Tet3-Gfap*^{cre} mice. All error bars show s.e.m. of at least 4 cultures per genotype or tissue samples. Number of samples used are indicated as coloured dots. **p-value<0.01 and ***p-value<0.001. Scale bars in d, 20 µm.

Whole-mount or *in toto* staining within the SVZ provides a tridimensional vision of the ventricular surface allowing the study of the pinwheel organization specific to this region (Mirzadeh et al., 2008). Type B1 cells, located in the centre of the pinwheel, are displaced from the ventricular zone by multiciliated ependymal cells but extend a short apical ending to directly contact the ventricle (Mirzadeh et al., 2008, Lim and Alvarez-Buylla 2016). The pinwheel was identified by a triple staining for GFAP (Type B cell), β-catenin (cell membranes) and γ-tubulin (basal cilia). Consistently with previous data, a decrease in the number of type-B1 NSCs γ-tubulin positive apical cells in the pinwheels contacting the lateral ventricles was found at the same time of an increase in the terminally differentiated astrocytes in the *Tet3-Gfap*^{cre} SVZ wall (**Fig. 32a,b**).

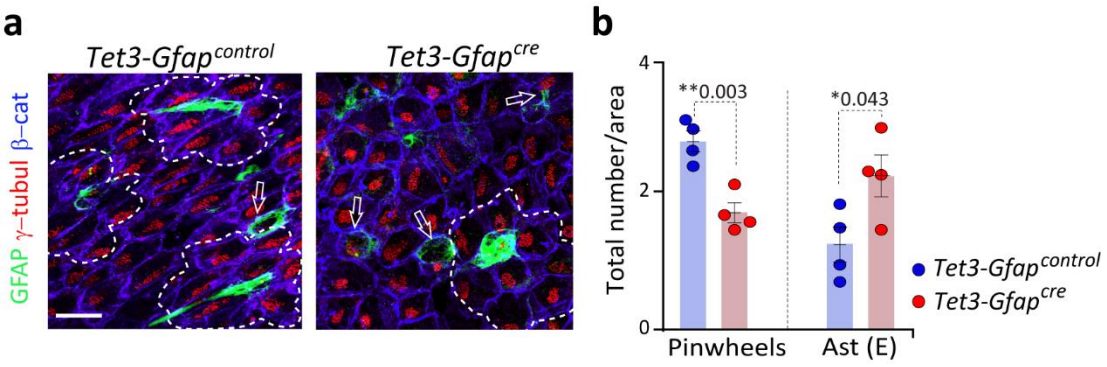

Figure 32. Removal of *Tet3* in the SVZ GFAP+ population causes a depletion of the Type B1-NSCs contacting with the ventricle lumen. (a) Immunohistochemistry images for GFAP (green), γ-tubulin (red) and β-catenin (blue) in whole-mounts of the SVZ from *Tet3-Gfap*^{cre} and *Tet3-Gfap*^{control} mice. Differentiated astrocytes are also indicated (arrows). **(b)** Total number of pinwheels and differentiated astrocytes found in the SVZ of *Tet3-Gfap*^{control} and *Tet3-Gfap*^{cre} mice. All error bars show s.e.m. of at least 4 cultures per genotype or tissue samples. Number of mice used are indicated as coloured dots. *p-value<0.05, **p-value<0.01. Scale bars in a, 10 µm.

In the adult neurogenesis process, stem cell-derived neuroblasts leave the SVZ and migrate rostrally towards the OB, where they ultimately differentiate into inhibitory interneurons (Bjornsson et al., 2015, Bond et al., 2015). As a consequence of the reduced number of NSCs in the *Tet3* deficient SVZ, a decrease in the percentage of the DCX+ and PSA-NCAM+ population was found (**Fig. 33a-c**), resulting in a less densely populated rostral migratory stream in the *Tet3-Gfap*^{cre} mice (**Fig. 33c**).

As we mentioned before, after BrdU administration, olfactory bulb newborn neurons that ceased to divide soon after the injection retain the analogue and can be used to determine the neurogenesis rate to the OB (Ferron et al., 2007). Using immunohistochemistry we quantified the number of BrdU positive cells in the olfactory bulb of *Tet3-Gfap*^{cre} mice compared to their controls. Consistent with a reduced neuroblast population migrating through the rms, we observed a lower number of newborn neurons reaching the OB in *Tet3* deficient mice, visualized by the postmitotic BrdU+ newly formed neurons in the glomerular (GL) and granular (GR) layers of the mutant OB (**Fig. 33d,e**). We also analysed the number of BrdU+ cells reaching the corpus callosum (CC) and observed that in this case oligodendrogenesis was similar in both genotypes (**Fig. 33f**). These data together indicate that TET3 could be essential for the maintenance of the neural stem cell pool in the SVZ of adult mouse brain preventing the differentiation of B cells into non-neurogenic astrocytes *in vivo*. TET3 could then participate in the formation of new neurons through the adult life.

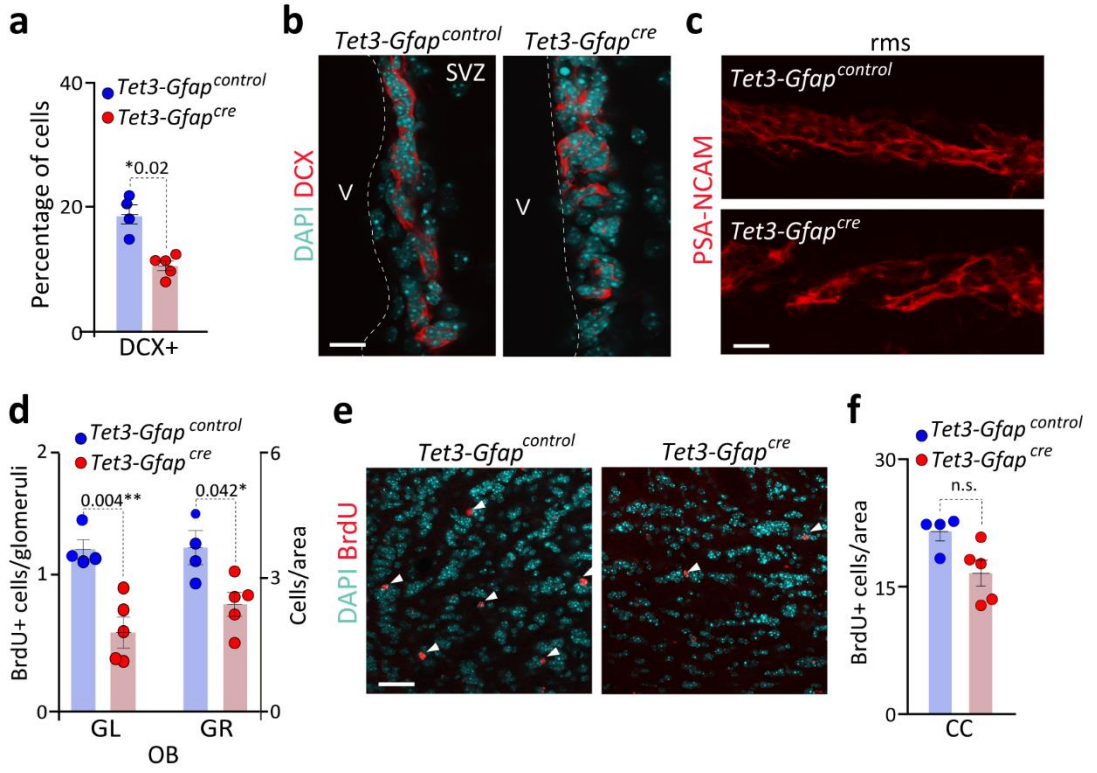

Figure 33. Absence of TET3 causes an impairment of adult neurogenesis. (a) Percentage of total DCX+ cells in the SVZ of *Tet3-Gfap*^{control} and *Tet3-Gfap*^{cre} mice **(b)** Immunohistochemistry for DCX (red) in SVZ of mice from both genotypes. V: lateral ventricle. **(c)** Immunohistochemistry images for PSA-NCAM+ (red) chains of neuroblast in the rms of mice from both genotypes. **(d)** Quantification of the number of newborn neurons incorporating in the granular (GR) and glomerular (GL) layers in the olfactory bulbs (OB) of *Tet3-Gfap*^{control} and *Tet3-Gfap*^{cre} mice. **(e)** Immunohistochemistry images for BrdU (red) in the granular layer in OB of *Tet3-Gfap*^{control} and *Tet3-Gfap*^{cre} mice. Arrowheads indicate BrdU+ cells. **(f)** Quantification of the number of BrdU+ cells in the CC of mice from both genotypes. DAPI was used to counterstain nuclei. All error bars show s.e.m. of at least 4 cultures per genotype or tissue samples. Number of mice used are indicated as coloured dots. *p-value<0.05, **p-value<0.01. Scale bars in b and c: 40 µm.

2.3 TET3 maintains stem cell properties *in vitro*

Under appropriate conditions, dissociated cells obtained from the SVZ, proliferate forming clonal aggregates called "neurospheres" and this *in vitro* assay is considered the demonstration of the presence of stem cells in the SVZ (Reynolds and Rietze 2005, Ferron et al., 2007, Pastrana et al., 2011). In order to address the specific effects of TET3 dioxygenase on the NSC population, neurospheres formation and NSCs differentiation were evaluated in *Tet3-Gfap*^{cre} and *Tet3-Gfap*^{control} cultures.

2.3.1 TET3 is required for self-renewal and expansion of adult NSCs

To investigate the self-renewal capacity of neural progenitors we next set out to study whether the same *in vivo* phenotype could be reproduced *in vitro*. Neurospheres from adult SVZ of *Tet3-Gfap*^{cre} and *Tet3-Gfap*^{control} mice were first derived under controlled culture conditions in which neural progenitors undergo an orderly program of cell proliferation. As we previously showed, significant mRNA expression of *cre-recombinase* was found in *Tet3* deficient neurospheres correlating with a downregulation of *Tet3* expression (**Fig. 29b,c**). As a consequence, NSCs isolated from *Tet3-Gfap*^{cre} adult SVZ yielded fewer primary neurospheres compared to those of *Tet3* controls (**Fig. 34b,c**). To better characterize the self-renewal capability of these cultures, primary neurospheres were individually dissociated into single cells and plated at a clonal density (2.5 cell/µl) (**Fig. 34a**). *Tet3* deficient secondary neurospheres also exhibit a significant reduction on the number of new clones formed at different passages (P6 and P9) (**Fig. 34b,c**).

To determine whether this reduction in the self-renewal capacity in *Tet3* deficient cultures could be due to a proliferation or survival defect, we determined the size of primary and secondary neurospheres at different passages and found no changes in *Tet3* deficient neurosphere diameter in any condition (**Fig. 34d**). In line with this, a cell cycle analysis of *Tet3-Gfap*^{control} and *Tet3-Gfap*^{cre} neurospheres cultures was performed by staining the cells with propidium iodide (PI). Notably, no changes in the proportion of the cell cycle phases were observed in mutant compared to wild-type cultures (**Fig. 34e**). Moreover, the reduction in the number of neurospheres could not be either ascribed to a decreased in cell survival as evidenced by the lack of changes in the proportion of apoptosis in the mutant cultures (relative to total cells: 2.6 ± 0.2% in control cultures and 2.3 ± 0.2% in *Tet3-Gfap*^{cre} cultures). This was confirmed by immunostaining for Caspase 3+ cells in neurospheres cultures from the two genotypes (relative to DAPI+ cells: 3.8 ± 0.5 % in *Tet3-Gfap*^{control} and 4.2 ± 0.3 in *Tet3-Gfap*^{cre}). As a result of the specific defect on self-renewal in *Tet3-Gfap*^{cre} cultures, their bulk growth expansion rate after several passages was also impaired compared to the *Tet3-Gfap control* cells (**Fig. 34f**).

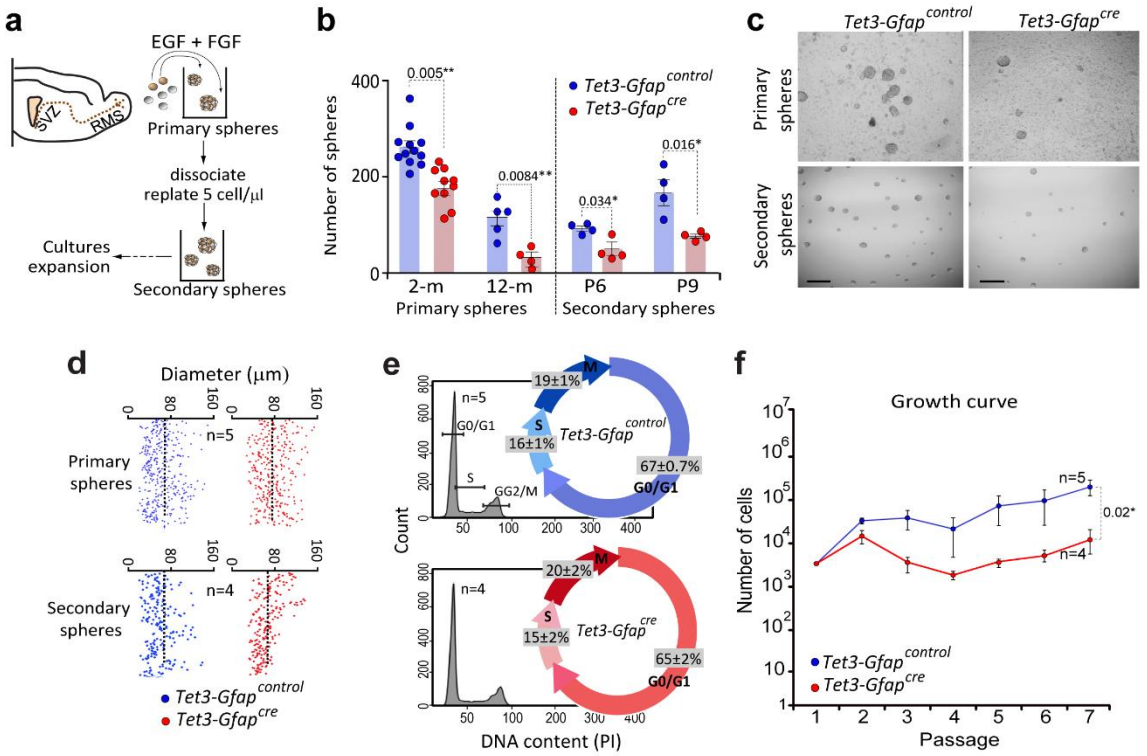

Figure 34. *Tet3* deficiency in GFAP+ NSCs causes a decrease in their self-renewal capacity and expandability. (a) Schematic representing the primary and secondary forming neurospheres assay and the expansion protocol. Neurospheres are cultured in proliferation conditions with the mitogens EGF and FGF. **(b)** Number of primary neurospheres obtained from the SVZ of 2 and 12 months-old *Tet3-Gfap*^{control} and *Tet3-Gfap*^{cre} mice (left panel). Number of secondary spheres formed after passages 6 and 9 for both genotypes (right panel). **(c)** Phase contrast images of primary and secondary spheres from *Tet3-Gfap*^{control} and *Tet3-Gfap*^{cre} mice. **(d)** Diameter of primary and secondary neurospheres formed in *Tet3-Gfap*^{control} and *Tet3-Gfap*^{cre} cultures. Dashed lines indicate the mean diametre. **(e)** Cell cycle analysis in neurospheres cultures from both genotypes after 3 days *in vitro*. Percentages of G0/G1, S and G2/M phases are indicated. **(f)** Growth curve showing the total number of cells formed after 7 passages in *Tet3-Gfap*^{control} and *Tet3-Gfap*^{cre} neurospheres cultures. All error bars show s.e.m. of at least 4 cultures per genotype or tissue samples. Number of mice used are indicated as coloured dots. *p-value<0.05, **p-value<0.01. Scale bars in c, 300 µm.

Neurogenesis occurs throughout adult life in the SVZ of the lateral ventricles, however, during aging, NSCs and their progenitors exhibit reduced proliferation and neuron production (Apple et al., 2017). To further evaluate if the phenotype showed above was maintained in aged TET3 deficient mice, NSCs cultures from the SVZ of 12-months-old *Tet3-Gfap*^{control} and *Tet3-Gfap*^{cre} mice were established and the number of primary spheres determined (**Fig. 34b**). A reduction in the number of primary spheres in ageing TET3 deficient mice compared to the control was observed, demonstrating the essential role of *Tet3* in the stemness maintenance also in the ageing brain. Finally, to discard a possible effect of the presence of the *Cre-recombinase* on the *in vitro* phenotype observed in *Tet3-Gfap*^{cre} NSCs, we isolated neurospheres from the SVZ of *Gfap-Cre* mice used to generate the conditional mutant. As expected, expression of *Cre-recombinase* was confirmed in *Gfap-cre* cultures while no expression was detected in *Gfap-control* NSCs (**Fig. 35a**). In addition, the portion of cells capable of forming primary neurospheres was similar in both genotypes (**Fig. 35b**). Primary neurospheres were dissociated and

plated again for the neurosphere assay and no differences between genotypes were observed in the number of secondary spheres formed (**Fig. 35b**). In conclusion, these results suggest that the expression of *cre-recombinase per se* do not cause phenotypic effects on NSCs *in vitro*.

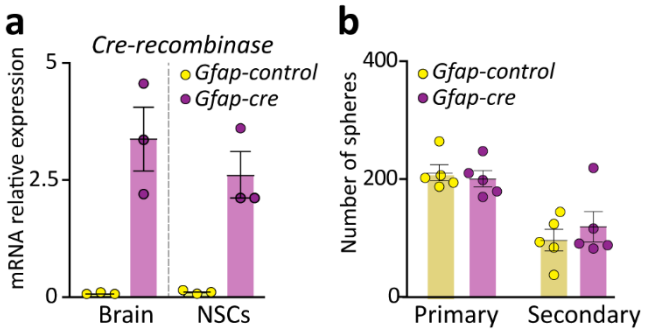

Figure 35. *Cre-recombinase* expression do not produce NSCs alterations *in vitro*. (a) qPCR for *Cre-recombinase* expression in brain and NSCs in *Gfap-control* and *Gfap-cre* mice. **(b)** Number of primary and secondary neurospheres obtained from the SVZ of *Gfap-control* and *Gfap-cre* mice. *Gapdh* was used to normalize data. All error bars show s.e.m. of at least 3 cultures per genotype or tissue samples. Number of samples used are indicated as coloured dots.

2.3.2 TET3 prevents differentiation of non-neurogenic astrocytes

Adult NSCs retain *in vitro* their capacity to give rise to the three cell lineages characteristics of the central nervous system: astrocytes, neurons and oligodendrocytes (Reynolds and Weiss 1992, Belenguer et al., 2016). Because our data suggested that *Tet3* deficiency results in increased astrocytic fate *in vivo*, we next tested whether this enhanced astrocytic differentiation was also accompanied by a reduction in the multipotentiality of stem-like astrocytes *in vitro*. The differentiation of neurospheres cultures derived from 2 months-old wild-type and *Tet3* deficient mice were induced for 7 days (**Fig. 36a**). To do so, disaggregated neurospheres cells were plated on Matrigel and cultured first for 2 days *in vitro* (2DIV) in medium containing FGF2 (proliferative conditions) to allow the expansion of the neural progenitor cell population. Afterwards, FGF2 was removed and the medium was supplemented with 2% FBS (required for astroglial differentiation). Cells were then allowed to fully differentiate for 5 more days (7DIV, full differentiation) into neurons, astrocytes and oligodendrocytes (**Fig. 36a**) as previously described (Gritti et al., 1999, Belenguer et al., 2016). We first observed by qPCR a decrease of the *Nestin* gene together with an increase of the *S100β* gene in 2 DIV *Tet3-Gfap*^{cre} compared to wild-type neurospheres cultures (**Fig. 36b**), whereas no changes in the neuronal *βIII-tubulin* gene (*Tubb3*) were found (**Fig. 36b**). Accordingly to the mRNA expression levels, immunocytochemistry in deficient *Tet3,* after two days of differentiation, revealed a reduced percentage of proliferating BrdU/Nestin+ cells (**Fig. 36c,d**).

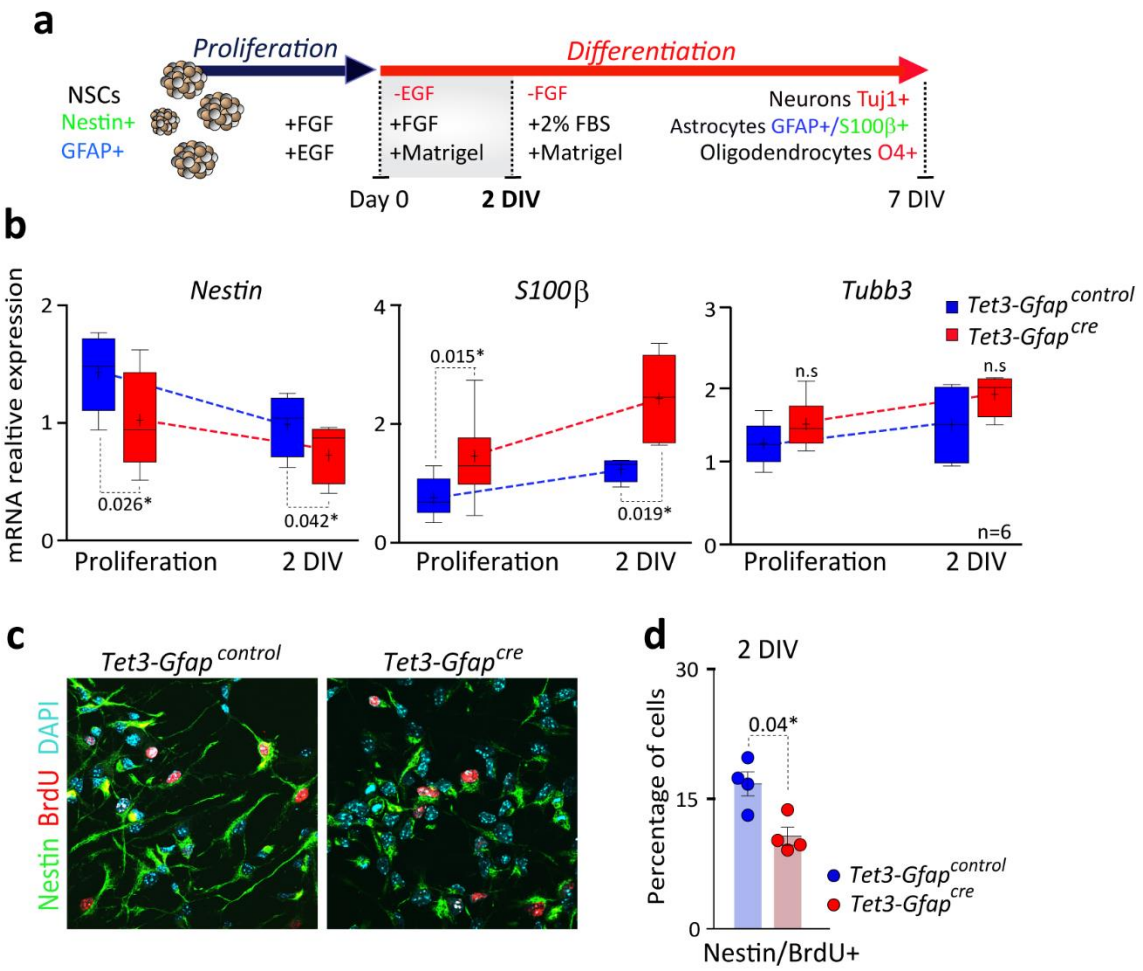

Figure 36. TET3 depletion causes an impairment of NSCs differentiation induction. (a) Schematic representation of the differentiation protocol. To induce NSCs differentiation EGF is removed and cells plated in matrigel to attach the cells. Two days after (2DIV), FGF is removed and 2% FBS added to the growth medium. Five days after (7 DIV) cells are fixed for immunostaining. **(b)** qPCR for the undifferentiation marker *Nestin* (*Nes*), the terminally differentiated marker S100β and the neuronal marker βIII-tubulin (*Tubb3*) in *Tet3-Gfap*^{control} and *Tet3-Gfap*^{cre} NSCs in proliferation conditions and after 2 DIV of differentiation. *Gapdh* was used to normalize data. **(c)** Immunocytochemistry images for Nestin (green) and BrdU (red) in NSCs isolated from *Tet3-Gfap*^{cre} and *Tet3-Gfap*^{control} cultures after 2 DIV of differentiation. **(d)** Percentage of *Tet3-Gfap*^{cre} and *Tet3-Gfap*^{control} cells that are positive for Nestin and incorporate the thymidine analogue BrdU two days growing in differentiation conditions. All error bars show s.e.m. of at least 4 cultures per genotype or tissue samples. Number of samples used are indicated as coloured dots. DAPI was used to counterstain DNA. Scale bar in c: 40 µm. P-values are indicated. *p-value<0.05.

After 7 DIV of differentiation, *Tet3*-deficient cultures were immunostained for the simultaneous detection of the terminally differentiated astrocytic marker S100β, the neuronal marker βIII-tubulin and the oligodendrocyte marker O4 (**Fig. 37a,b**). *Tet3-Gfap*^{cre} cultures contained a higher proportion of cells that were strongly positive for S100β than wild-type cells (**Fig. 37b,c**). Conversely, neuronal and oligodendroglial differentiation was normal in both genotypes, as no differences were found in the percentage of βIII-tubulin or O4 positive cells (**Fig. 37b,c**). S100β protein that is largely absent from neurogenic GFAP+ cells, correlates with loss of neurosphere forming potential (Raponi et al., 2007). Thus, terminal differentiation of normal NSCs to a non-multipotent mature astrocyte unavoidably leads

to a reduction of the stem cell pool in the cultures (Raponi et al., 2007). In order to test whether enhanced astrocytic differentiation in the absence of TET3 is consistently accompanied by a reduction in the capacity of NSCs to form neurospheres, 7-DIV differentiated NSC cultures were detached and replated again in the presence of mitogens and in the absence of adherent conditions (**Fig. 37a,d**). This led to the reactivation of a small portion of cells that still kept the capacity to form neurospheres in non-adherent conditions after 12 days *in vitro* (12 DIV) (**Fig. 37a**). Notably, the number of neurospheres-forming cells in *Tet3-Gfap*^{cre} cultures was significantly reduced, indicating that the *bias* toward the astrocytic fate correlates with a reduction in the stem cell pool in the absence of TET3 (**Fig. 37d**). This suggests that TET3 can directly promote the neurogenic potential of the multipotent stem cell-like astrocytes by preventing their premature differentiation.

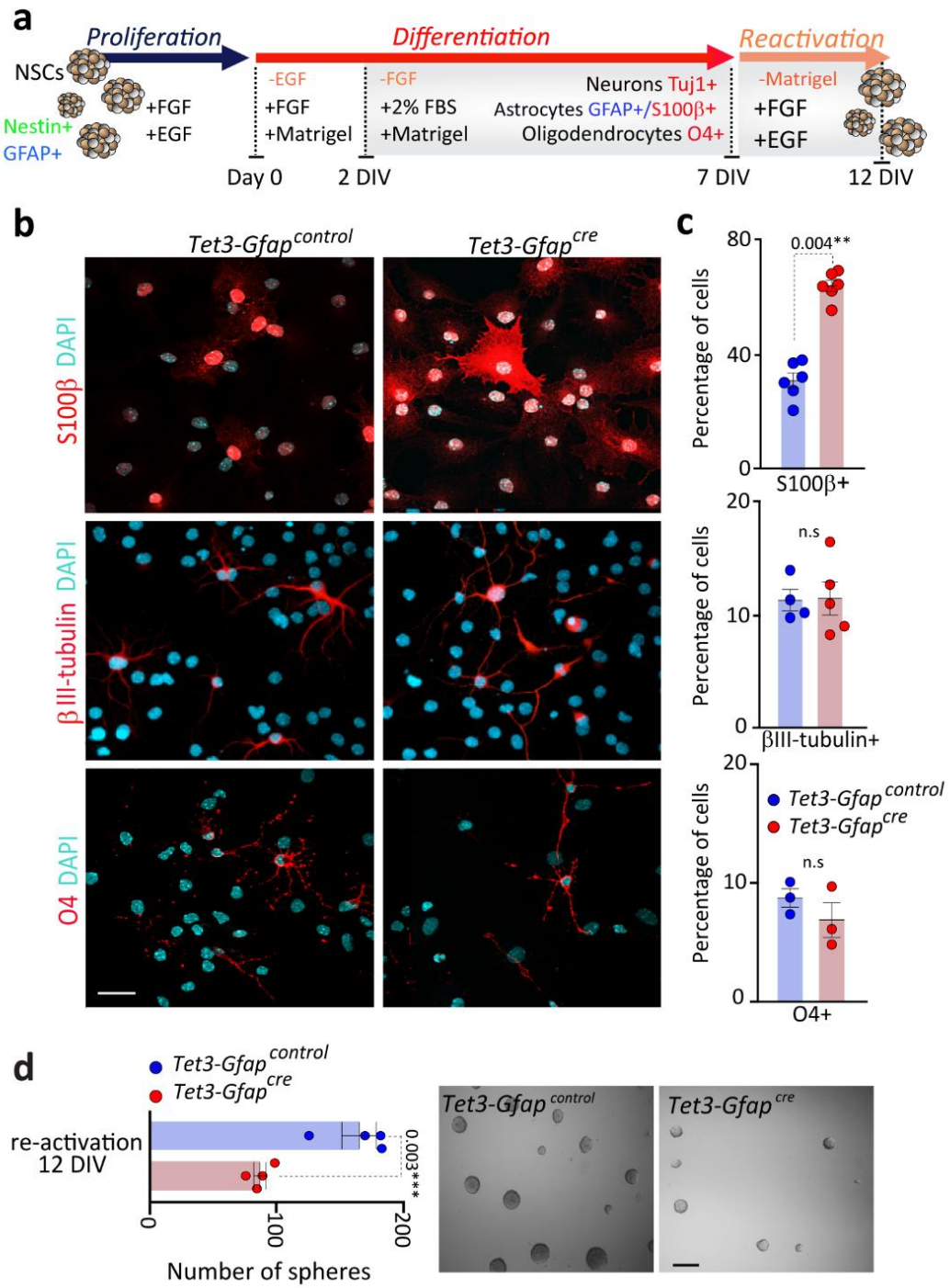

Figure 37. TET3 prevents terminal differentiation of non-neurogenic astrocytes. (a) Schematic representation of the reactivation assay protocol. After the differentiation protocol, cultures were tripsinized and replated again in the presence of EGF and FGF. No matrigel was used to promote proliferation. **(b)** Immunocytochemistry images for S100β (red, upper panels), βIII-tubulin (red, middle panels) and O4 (red, lower panels) in *Tet3-Gfap*^{control} and *Tet3-Gfap*^{cre} cultures after 7 DIV in differentiation conditions. **(c)** Percentage of cells that are positive for S100β, βIII-tubulin and O4 in NSCs from both genotypes after 7 DIV of differentiation. **(d)** Number of neurospheres formed after detaching differentiated cells and replating again in proliferation conditions in *Tet3-Gfap*^{control} and *Tet3-Gfap*^{cre} cultures (left panel). Representative images of neurospheres formed in both genotypes after replating in proliferation conditions (right panels). All error bars show s.e.m. of at least 4 cultures per genotype. Number of samples used are indicated as coloured dots. Scale bar in d: 40 µm. P-values are indicated. **p-value<0.01; ***p-value<0.001.

2.3.3 TET3 regulates gene expression changes in the imprinted gene *Snrpn*

TET proteins have been found to play an important role in removal of DNA methylation at the imprinted regions during the resetting of genomic imprinting in the germline (Hackett et al., 2013, Piccolo et al., 2013, Yamaguchi et al., 2013). Moreover, 5hmC is shown to be enriched at enhancers and gene bodies of actively transcribing genes (Mellen et al., 2012, Sun et al., 2013) and a role for 5hmC in transcriptional priming has been hypothesized having essential roles in regulating gene expression and maintaining cellular identity (Costa et al., 2013). However, in adult NSCs, it is not established whether TET proteins are also involved in demethylation of DNA at the imprinted regions or whether they also regulate gene transcription. Therefore, to directly examine the function of TET3 and 5hmC on the regulation of genomic imprinting in neural progenitors an RNAseq expression analysis was performed in adult NSCs from control and *Tet3-Gfap*^{cre} neurospheres cultures. Based on changes in gene expression from the RNAseq data, a principal component analysis showed a clear segregation between *Tet3-Gfap*^{control} and *Tet3-Gfap*^{cre} groups (**Fig. 38a**). RNAseq confirmed a 70% downregulation of *Tet3* mRNA levels in *Tet3-Gfap*^{cre} compared to control cultures (LogFC in *Tet3-Gfap*^{cre} neurospheres cultures: -1.0074 with a FDR=3.97x10^{17}). At the basal level, *Tet3-Gfap*^{cre} NSCs exhibited differential expression of a large number of genes compared with control NSCs, with a similar number of genes downregulated (97 genes, **Table 1 Annex III**) than upregulated (96 genes, **Table 2 Annex III**) (**Fig. 38b,c**) supporting the hypothesis that TET3 might regulate NSCs function.

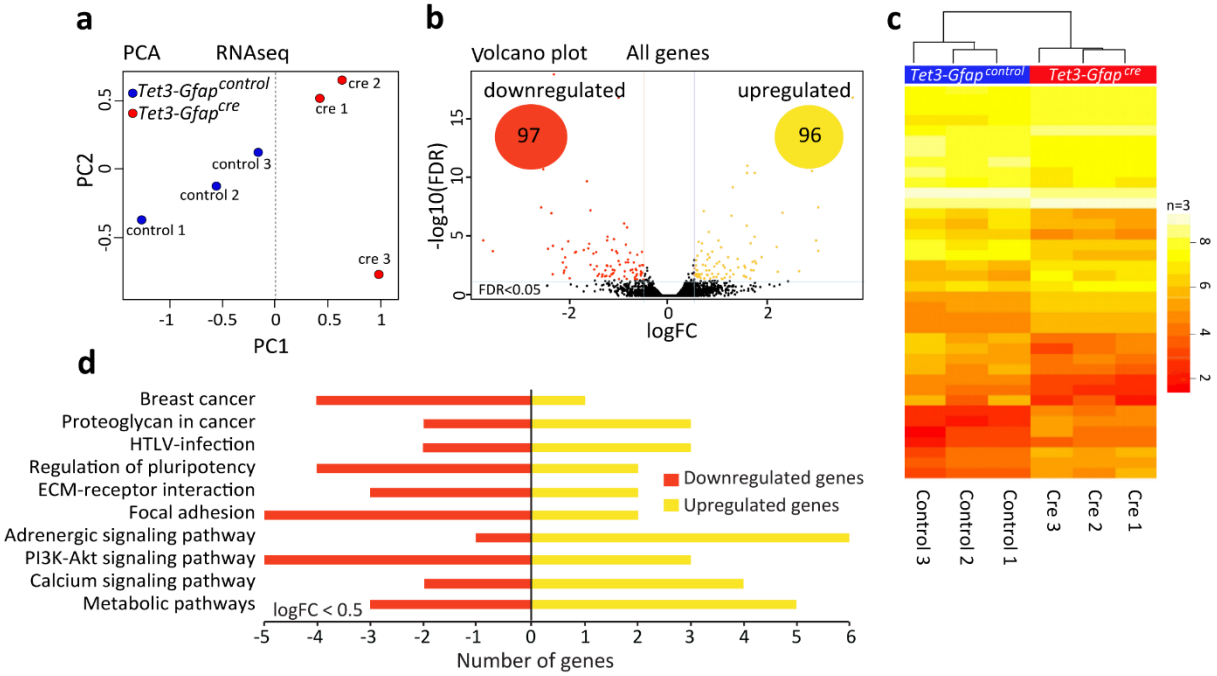

Figure 38. TET3 plays an important role in the regulation of gene expression. (a) Principal component analysis (PCA) of the transcriptome from RNAseq data showing segregation between *Tet3-Gfap*^{control} and *Tet3-Gfap*^{cre} NSCs. **(b)** Volcano plot for all genes differentially expressed by RNAseq. Vertical grey lines indicate logFC thresholds (logFC -0.5 and logFC 0.5). Horizontal grey lines represent FDR=0.05. Red dots represent upregulated genes while blue dots indicate downregulated genes (FDR<0.05). **(c)** Hierarchical clustering and heatmap of RNAseq data showing expression of the top 20% of more variable genes (FDR<1e-4) between *Tet3-Gfap*^{control} and *Tet3-Gfap*^{cre} NSCs. **(d)** Metabolic pathways in which more than 5 genes showed significant changes based on RNAseq data. Coloured bars represent the number of downregulated (red) and upregulated genes (yellow) in each metabolic pathway.

The resulted significantly expressed genes between both genotypes were then grouped according to the metabolic pathways in which they were implicated using the Enrichment Browser package (Geistlinger et al., 2016). As a result, we obtained a total of 10 KEGG (Kyoto Encyclopedia at Genes and Genomes) metabolic pathways in which at least 5 genes were altered in *Tet3-Gfap*^{cre} NSCS compared to controls. The altered pathways within TET3 deficient NSC included, among others, regulation of pluripotency of stem cells, cell adhesion pathways, calcium signalling or cancer (**Fig. 38d**), however in this thesis we focused on the function of TET3 on genomic imprinting. Thus we next analysed how imprinted genes were modified in *Tet3-Gfap*^{cre} compared to control cultures. Importantly, based on RNAseq data, from around 150 known imprinted genes, only three of them showed a significant change in mRNA expression based on RNAseq data. Concretely, *Cntn3* (contactin 3) was downregulated in *Tet3-Gfap*^{cre} NSCs (logFC= -1,137), whereas *Cobl* (cordon-bleu WH2 repeat) and *Snrpn* (small nuclear ribonucleoprotein-associated polypeptide N) showed increased levels of expression in TET3 deficient neurospheres compared to wild-type (**Fig. 39a**). To validate these results, a qPCR analysis was performed and this confirmed only the upregulation of *Snrpn* in *Tet3-Gfap*^{cre} NSCs (**Fig. 39b**). Notably, *Cobl* and *Cntn3* were expressed at a very low levels in NSCs, indicating that they

could not have a relevant role on NSCs. We also analysed by qPCR other imprinted genes such as *Gnas*, *p57*, *Peg3* or *H19* and confirmed that they were not modified in *Tet3* deficient neurospheres (**Fig. 39c**). Due to our interest in imprinting regulation, we next focused on the *Snrpn* gene regulation.

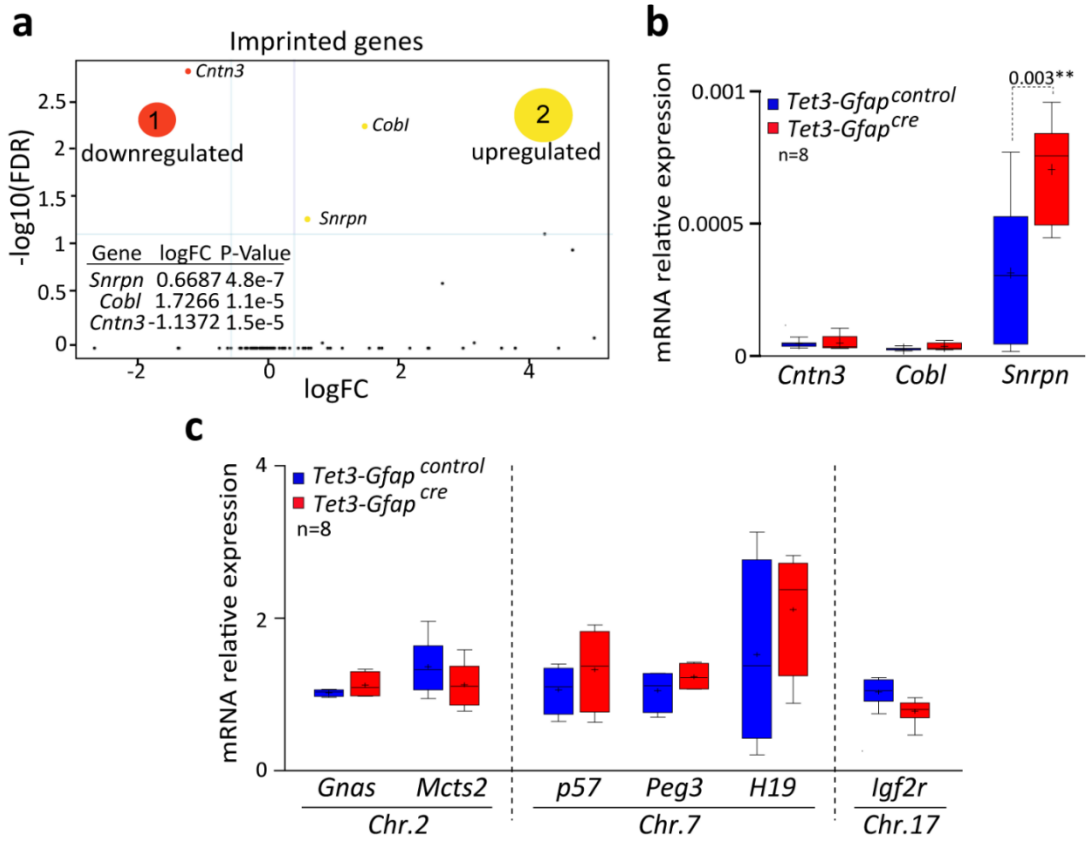

Figure 39. *Tet3* deficiency in NSCs causes an increase in the expression of the imprinted gene *Snrpn*. (a) Volcano plot for imprinted genes differentially expressed by RNAseq. Vertical grey lines indicate logFC thresholds (logFC -0.5 and logFC 0.5). Horizontal grey lines represent FDR=0.05. Red dots represent upregulated imprinted genes while blue dot indicates the downregulated imprinted gene (FDR<0.05). **(b)** Validation by qPCR for *Snrpn*, *Cntn3* and *Cobl* in *Tet3-Gfap*^{control} and *Tet3-Gfap*^{cre} cells. An increase in the expression of *Snrpn* was observed in *Tet3-Gfap*^{cre} cells relative to their control counterparts. **(c)** qPCR for some representative imprinted genes organized by chromosomes confirming no expression changes. *Gapdh* was used to normalize data. All error bars show s.e.m. of at least 8 cultures per genotype or tissue samples. P-values are indicated. *p-value<0.05, **p-value<0.01.

2.3.4 *Snrpn* downregulation reverts the phenotype in TET3 deficient NSCs

Analysis of *Snrpn* expression in NSCs revealed that the gene was significantly expressed both in proliferating and differentiating conditions with a pick of expression at the first steps of the induction of the differentiation into neural cell types (2 DIV) (**Fig. 40a**). Accordingly, although *Snrpn* was increased in *Tet3-Gfap*^{cre} compared to *Tet3-Gfap*^{control} proliferating NSCs, the maximum difference of *Snrpn* mRNA levels in both genotypes were observed after 2 DIV of differentiation (**Fig. 40a**).

Aiming to establish whether the augmented levels of *Snrpn* found in *Tet3* deficient NSCs were functionally responsible for their loss of stemness and enhanced astrocytic differentiation, we performed a *Snrpn* expression silencing experiment using a short hairpin RNA (shRNA) in NSCs. A lentivirus (Lv)-mediated shRNA was used to silence *Snrpn* (shSNRPN) expression in *Tet3-Gfap*^{cre} and in *Tet3-Gfap*^{control} neurospheres cultures. A shRNA scramble (shSCRAMBLE) was used as a control for infection. Downregulation of *Snrpn* was verified by qPCR in these cells (**Fig. 40b,c**) which resulted in the reversion of the self-renewal capacity of *Tet3* deficient cells to wild-type levels (**Fig. 40d,e**). Moreover, to determine whether this rescue in the self-renewal and expansion capacities in *Tet3-Gfap* deficient cultures could be due to an additional effect of *Snrpn* on proliferation, the size of the neurospheres formed was determined in transduced cells and no changes in mean diameter were observed in any condition (**Fig. 40f**). As a result, the bulk growth expansion rate after several passages was also rescued in *Tet3-Gfap*^{cre} neurospheres cultures infected with the shSNRPN (**Fig. 40g**), suggesting a functional role of *Snrpn* in the self-renewal capacity of adult NSCs.

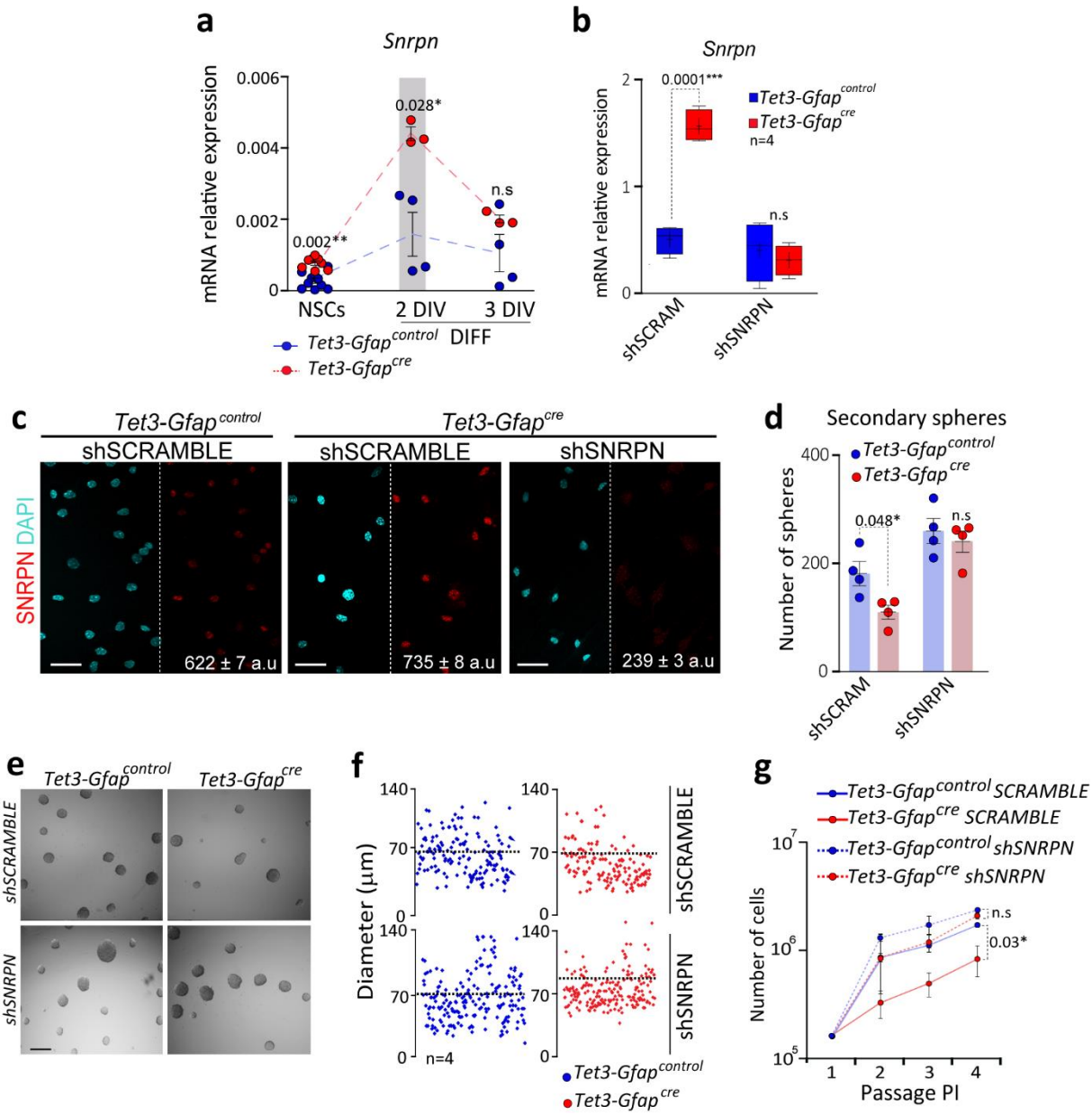

Figure 40. Downregulation of *Snrpn* in *Tet3-Gfap*^{cre} NSCs rescues the self-renewal defect. (a)qPCR of *Snrpn* in *Tet3-Gfap*^{control} and *Tet3-Gfap*^{cre} cultures in proliferation conditions (NSCs) and after 2 and 3 DIV of differentiation. Expression levels showed the largest differences at 2 DIV between *Tet3-Gfap*^{cre} and their controls (grey bar). **(b)** qPCR for *Snrpn* in *Tet3-Gfap*^{control} and *Tet3-Gfap*^{cre} NSCs that had been lentivirus infected with a shRNA for SNRPN (shSNRPN). A shRNA SCRAMBLE was used as a control of gene interference (shSCRAMBLE). A rescue in the upregulated expression of *Snrpn* was obtained in *Tet3-Gfap*^{cre} cells. **(c)** Immunocytochemistry images for SNRPN (red) in *Tet3-Gfap*^{control} and *Tet3-Gfap*^{cre} NSCs 7 days after the shRNA experiment. **(d)** Number of secondary spheres formed after shRNA experiment. A rescue in the neurosphere formation capacity in *Tet3-Gfap*^{cre} was observed after the interference of *Snrpn*. **(e)** Phase contrast images of neurospheres obtained after shRNA for SNRPN in *Tet3-Gfap*^{control} and *Tet3-Gfap*^{cre} NSCs. **(f)** Diameter of secondary spheres in shSCRAMBLE and shSNRPN conditions for both genotypes. Dashed lines represent the mean diameter for each condition. **(g)** Growth curve showing the total number of cells formed after 4 passages in *Tet3-Gfap*^{control} and *Tet3-Gfap*^{cre} neurospheres cultures that had been interfered with the shRNA. *Gapdh* was used to normalize qPCR data. All error bars show s.e.m. of at least 4 cultures per genotype and condition. Number of samples used are indicated as coloured dots. Scale bar in d: 150 µm. P-values are indicated. *p-value<0.05, **P-value<0.01.

Lentiviral delivery of the shSNRPN in *Tet3* deficient cells was also able to restore to wild-type levels the higher expression of *S100β* found in *Tet3-Gfap*^{cre} neurospheres after 2 and 7 DIV of differentiation (**Fig. 41a**). *Gfap* expression, also highly expressed in *Tet3-Gfap*^{cre} NSCs, was rescued to normal levels whereas no changes were observed in the neuronal gene *Tubb3* after interference of *Snrpn* in *Tet3-Gfap*^{cre} neurospheres (**Fig. 41b**). Consistently, the proportion of S100β positive cells in *Tet3-Gfap*^{cre} differentiated NSCs was rescued to the wild-type levels after lentiviral downregulation of *Snrpn* while no changes were observed in the proportion of βII-tubulin+ cells (**Fig. 41c,d**). These data suggest that TET3 can promote the neurogenic potential of multipotent stem cell-like astrocytes by repression of *Snrpn*, antagonizing their premature terminal differentiation. Thus, loss of *Tet3* in adult NSCs induces the upregulation of the *Snrpn* levels which causes the terminal differentiation and exhaustion of the stem cell pool.

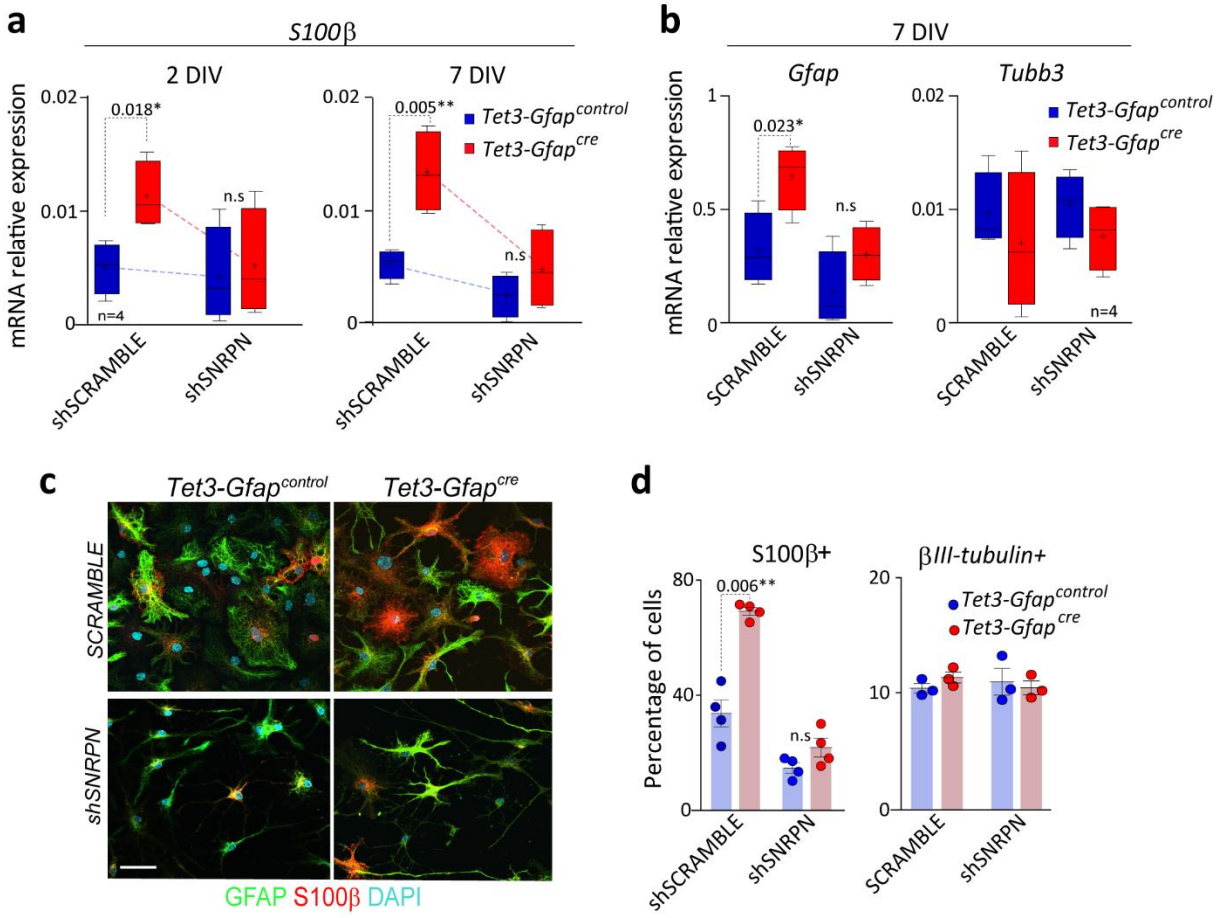

Figure 41. *Snrpn* interference rescues astrocytic premature differentiation in *Tet3-Gfap*^{cre} NSCs. (a) qPCR for the astrocytic differentiation marker *S100β* in interfered NSCs after 2 and 7 DIV of differentiation. A rescue in the expression of the gene was observed in *Tet3-Gfap*^{cre} after the shRNA for *Snrpn*. **(b)** qPCR for *Gfap* and *Tubb3* in shSCRAMBLE and shSNRPN conditions. A rescue in the expression of the *Gfap* gene was also observed in *Tet3-Gfap*^{cre} NSCs after *Snrpn* interference. **(c)** Immunocytochemistry images for S100β (red) and GFAP (green) in interfered NSCs of both genotypes after 7 DIV. DAPI was used to counterstain DNA. **(d)** Percentage of cells that are positive for S100β and βIII-tubulin in shRNA interfered *Tet3-Gfap*^{control} and *Tet3-Gfap*^{cre} NSCs after 7 DIV of differentiation. Downregulation of *Snrpn* rescues the premature differentiation of *Tet3-Gfap*^{cre} NSCs. *Gapdh* was used to normalize qPCR data. All error bars show s.e.m. of at least 3 cultures per genotype and condition. Number of samples used are indicated as coloured dots. Scale bar in c: 40 µm. P-values are indicated. *p-value<0.05, **p-value<0.01.

2.4 Genomic imprinting of *Snrpn* is maintained in TET3 deficient NSCs

Snrpn is located in the Prader-Willi syndrome imprinting gene cluster and is canonically expressed from the paternally inherited chromosome (Bervini and Herzog 2013). It has been previously shown the expected paternal expression of *Snrpn* in SVZ tissue and NSCs (Ferron et al., 2011), however the acquisition of biallelic expression of the gene could explain the higher expression of *Snrpn* in *Tet3-Gfap*^{cre} NSCs. To determine the imprinting status of *Snrpn* in *Tet3-Gfap*^{cre} NSCs, CRISPR was used to knockdown TET3 in NSCs derived from adult F1 mice hybrids offspring from *Mus musculus domesticus* (C57BL6/J) males and *Mus musculus castaneous* (CAST/EiJ) females (CxB NSCs), in which a single-nucleotide polymorphism (SNP) was identified at the *Snrpn* gene between the two subspecies (**Fig. 42a,b**). CxB hybrids NSCs were nucleofected with a CRISPR plasmid for *Tet3* containing a GFP reporter and GFP expressing NSCs were isolated by FACS (**Fig. 42b**). *Tet3* downregulation in CRISPR samples was verified (**Fig. 42c**). Due to the difficulty to isolate individual NSC, the analysis was performed with a heterogeneous population of CRISPR resulting cells. In order to study the heterogeneity level of each sample, CRISPR sample DNAs were sequenced and analysed (**Fig. 42d**). To precisely determine the spectrum and frequency of targeted mutations generated we used specific software called TIDE© (Tracking of Indels by Decomposition, Netherlands Cancer Institute) (https://tide.nki.nl/) (Brinkman et al., 2014) and we corroborated that at least 80% of the cells in each sample had nucleotide insertion or deletion altering the reading frame for the *Tet3* gene (**Fig. 42d,e**).

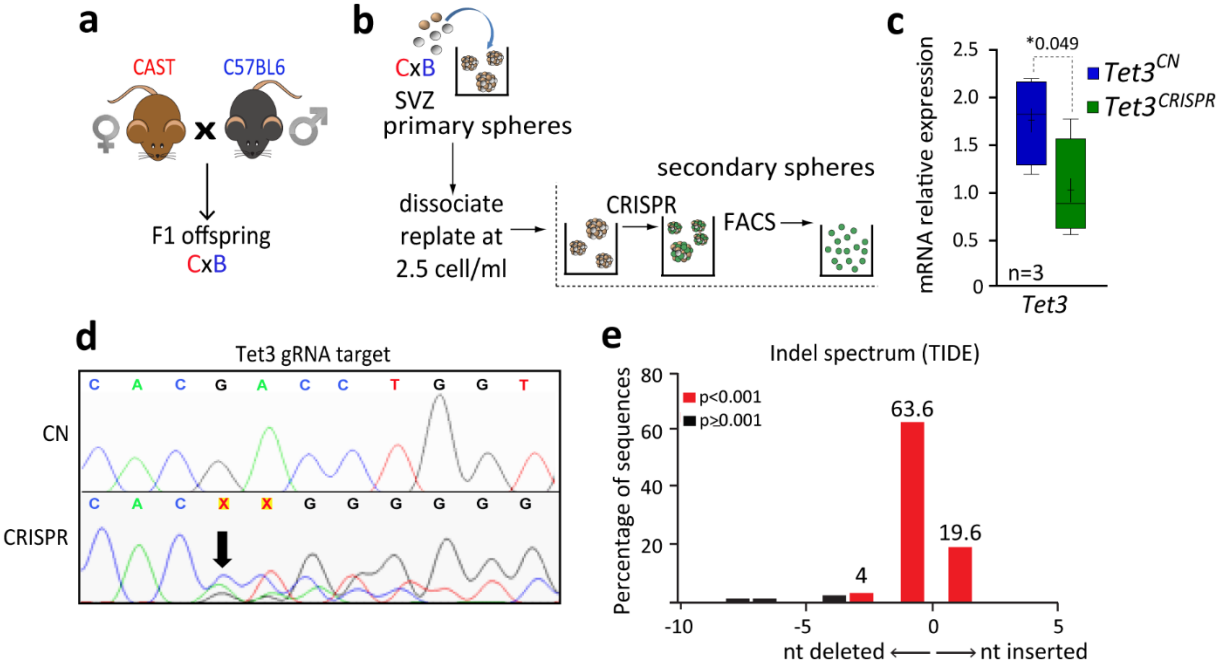

Figure 42. CRISPR/Cas9 strategy was used to generate deficient *Tet3* hybrids NSCs cultures. (a) Schematic of the generation of F1 hybrids mice. CAST females mice were crossed to C57BL6 male mice to generate CASTxBL6 (CxB) hybrids animals. **(b)** Schematic representing the CRISPR assay for *Tet3* and cell sorting in adult F1 hybrids NSCs. Secondary spheres were used for CRISPR experiments. GFP expression of the plasmid (green) was used for FACS. **(c)** qPCR for *Tet3* in CxB NSCs that had been assay for CRISPR. **(d)** Sequencing analysis of DNA fragments containing the *Tet3-gRNA* target site. The start of genome edition is indicated with an arrow. **(e)** Quantification by TIDE of the editing efficiency and simultaneously identification of the predominant types of insertions and deletions (indels) in the targeted pool of cells. Aberrant transcripts were produced. *Gapdh* was used to normalize data. All error bars show s.e.m. of at least 3 cultures per genotype and condition. P-values are indicated (*p-value<0.05).

As we mentioned before, we used CxB hybrids NSCs to identify SNPs between the two subspecies in some genes. Thus, direct sequencing of cDNA for *the gene of interest* in F1 CxB NSCs allowed us to analyse parental-specific expression of that gene. We first analysed the presence of the polymorphism in the *Snrpn* gene by sequencing cDNA of Cast and BL6 NSCs separately (**Fig. 43a**). This study confirmed the presence of a "T" in CAST and a "C" in C57BL6 NSCs at the gene (**Fig. 43a**). We next sequenced this SNP in CRISPR hybrids cells and found that they showed the expected paternally (C nucleotide) inherited imprinted expression of the gene (**Fig. 43a**). To quantify the percentage of expression of the maternal and paternal alleles for the *Snrpn* gene, we performed a pyrosequencing analysis on CRISPR samples (**Fig. 43b**). Consistently, we only observed expression from the *Snrpn* paternal allele and this was similar in CRISPR samples (**Fig. 43b**). To validate the data we also quantified the paternal and maternal allele expression of the *Dlk1* gene, known to be biallelically expressed in NSCs (Ferron et al., 2011). All these data confirmed that TET3 does not modify *Snrpn* genomic imprinting in adult NSCs. Therefore the elevated levels of the gene observed in *Tet3-Gfap*^{cre} neurospheres was not due to the acquisition of expression from the maternal allele, confirming its genomic imprinting in deficient NSCs.

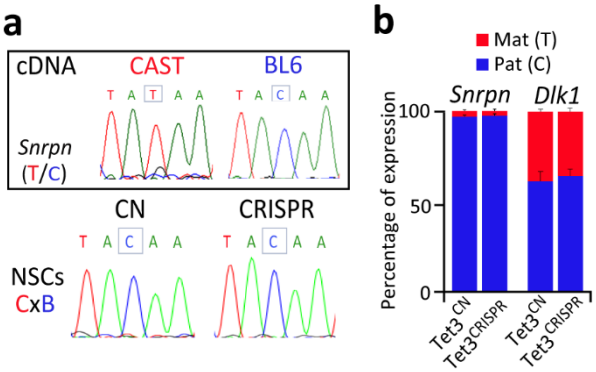

Figure 43. Genomic imprinting of *Snrpn* is maintained in *Tet3* deficient NSCs. (a) Genomic DNA sequence showing diagnostic strain-specific polymorphism (C/T) for detection of *Snrpn* imprinting using *Mus musculus domesticus* (BL6) and *Mus musculus castaneous* (CAST) mice (upper panel). Sequence analysis of RT-PCR products in CRISPR NSCs derived from reciprocal F1 hybrids (lower panel). **(b)** Allele-specific quantification of the relative levels of *Snrpn* in adult hybrids NSCs that have been depleted for *Tet3* using CRISPR. All error bars show s.e.m. of at least 3 cultures per genotype and condition.

2.5 TET3 dioxygenase is not implicated in the regulation of 5hmC levels in adult NSCs.

As we mentioned in the introduction TET3 can convert 5mC to 5hmC resulting in the removal of the methylated cytosine in somatic tissues, including the brain (Kriaucionis and Heintz 2009, Jin et al., 2010, Munzel et al., 2010, Szwagierczak et al., 2010, Szulwach et al., 2011). Thus, to investigate whether the effects of TET3 were mediated by modulating 5hmC levels, global distribution of 5hmC and 5mC in the adult brain, SVZ and NSCs was next determined by enzyme-linked immunosorbent assay (ELISA) (**Fig. 44a**). The levels of 5mC were found to be similar between tissues (**Fig. 44a**). Although lower than in whole brain, significant levels of 5hmC were found in neurospheres isolated from the SVZ of 2-months-old mice (**Fig. 44a**). In support to these data, immunocytochemistry for 5mC and 5hmC in neurospheres showed significant amounts of the two molecules in proliferating cells (**Fig. 44b**). Notably, the presence of the two molecules was exclusive (**Fig. 44b**, lower panels for detail).

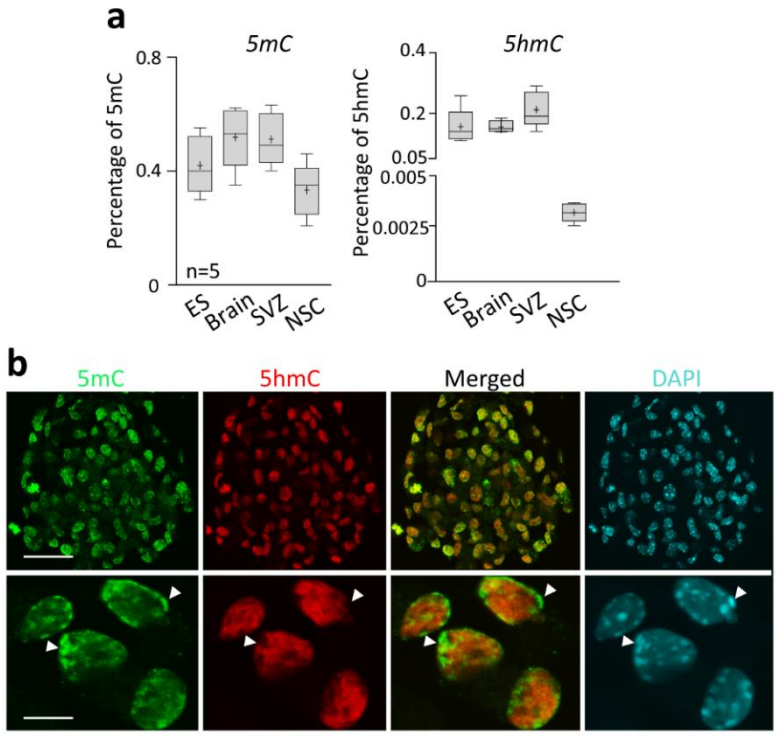

Figure 44. 5hmC and 5mC are abundant in SVZ-derived neurospheres. (a) Global quantification of the levels of 5mC and 5hmC determined by ELISA in ES, whole brain, SVZ and NSCs. **(b)** Immunocytochemistry for 5mC (green) and 5hmC (red) in neurospheres isolated and expanded *in vitro* from the adult SVZ. 5mC stainning is restricted to more condensed chromatin (arrowheads). 5hmC and 5mC are exclusive. DAPI was used to counterstain DNA. All error bars show s.e.m. of at least 5 samples. Scale bars in b, upper panels: 25 µm, lower panels: 7 µm.

Analysis of the distribution of 5hmC and 5mC by immunostaining in the adult SVZ *in vivo* showed variable intensities in different cellular populations (**Fig. 45b**). In particular, the SVZ showed high levels of 5hmC and low levels of 5mC in the GFAP+/SOX2+ stem cell population (**Fig. 45a,b**). In contrast, no 5hmC was found in the more differentiated cells such as the DCX+ neuroblast population (**Fig. 45b**). Thus, the presence of 5hmC in the adult stem cell population along with its apparent

exclusion from differentiated cells, suggested that formation of 5hmC may also participate in the function and/or maintenance of the undifferentiated state during the neurogenesis process in the adult neurogenic niches. Surprisingly, immunohistochemistry for 5hmC in the GFAP+/SOX2+ population within the *Tet3-Gfap*^{cre} SVZ revealed no significant changes in global 5hmC in *Tet3* deficient stem cells *in vivo* (**Fig. 45a**). Consistently, upon *Tet3* knockdown no changes in global 5mC or 5hmC, determined by ELISA, were observed in adult *Tet3-Gfap*^{control} and *Tet3-Gfap*^{cre} neurospheres cultures (**Fig. 45c**). These data suggest that TET3 is not implicated in the regulation of 5hmC/5mC global levels due to either specific effects in restricted targets or a catalytic-independent role in NSCs.

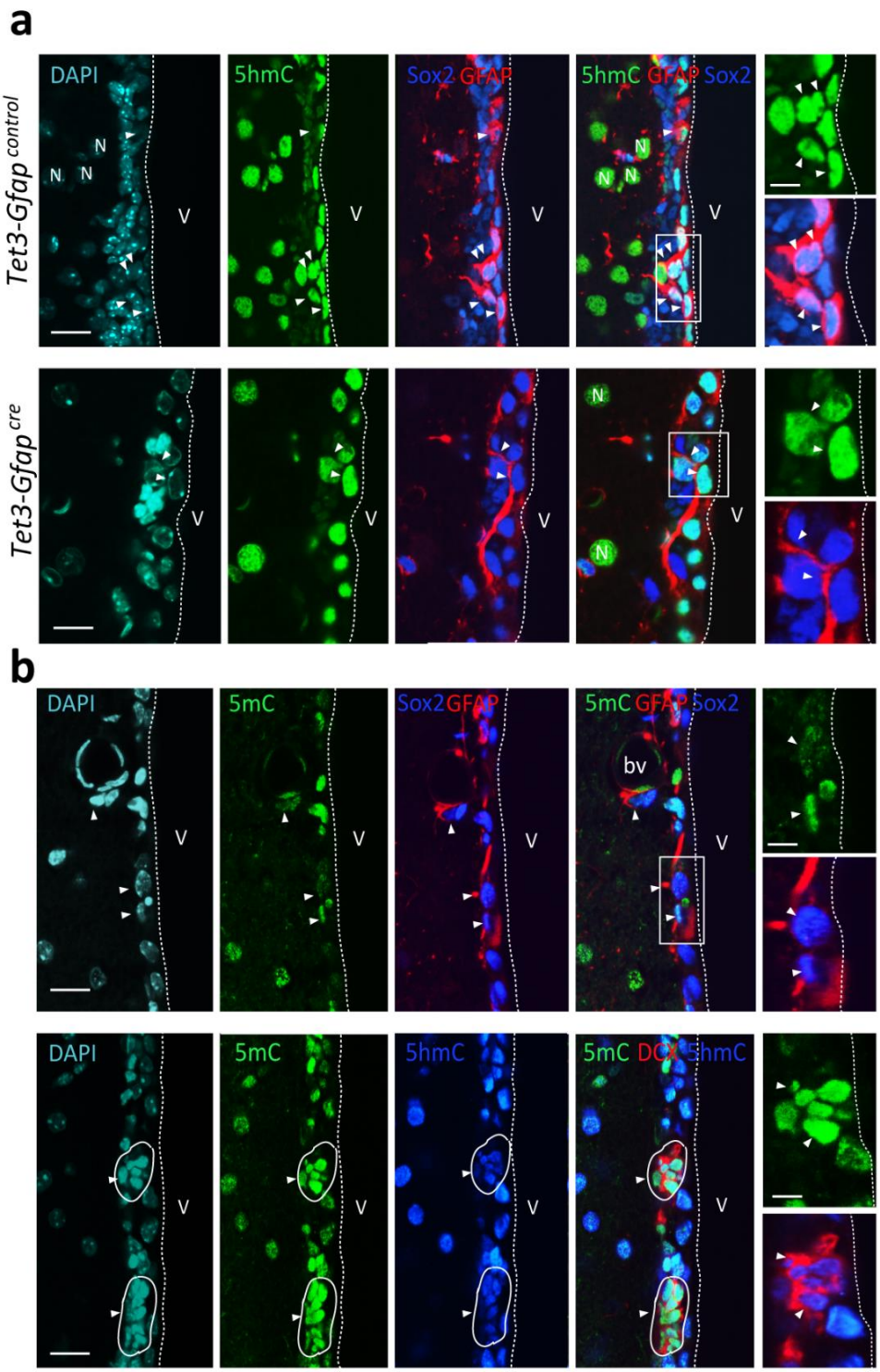
a
Tet3-Gfap control
Tet3-Gfap cre
DAPI
5hmC
Sox2 GFAP
5hmC GFAP Sox2
N
V
b
5mC
bv
5mC DCX 5hmC
c
5mC
5hmC
Percentage of 5mC
Percentage of 5hmC
Tet3-Gfap control
Tet3-Gfap cre
Brain
NSCs

Figure 45. 5hmC is abundant in the GFAP+ population within the adult SVZ. (a) Immunohystochemistry for 5hmC (green), GFAP (red) and SOX2 (blue) positive cells within the SVZ of *Tet3-Gfap*^{control} (upper panels) and *Tet3-Gfap*^{cre} (lower panels) adult mice. 5hmC is present in type B GFAP/SOX2+ cells close to the lateral ventricle wall. **(b)** Immunohistochemistry for 5mC (green) in GFAP (red) and SOX2 (blue) positive cells within the SVZ of wild-type adult mice (upper panel). Immunohistochemistry for 5mC (green), 5hmC (blue) and DCX (red) in the SVZ of wild-type mice (lower panel). Neuroblasts chains stained for DCX showed high levels of 5mC but low levels of 5hmC. **(c)** Global percentage of 5mC and 5hmC in *Tet3-Gfap*^{cre} and *Tet3-Gfap*^{control} NSCs and brain determined by ELISA. DAPI was used to counterstain DNA. All error bars show s.e.m. of at least 4 samples. Scale bars in a, b and c: 20 µm; inserts: 8 µm.

2.6 TET3 contributes to transcriptional repression of *Snrpn* in neural progenitors independently of 5hmC

As it has been previously reported, differentially methylated regions (DMRs) are genomic regions with different DNA methylation status across different biological samples and are regarded as possible functional regions involved in gene transcriptional regulation. The *Snrpn* DMR is maternally methylated at the 5´end and includes the *Snrpn* promoter and the entire intron (Miyazaki et al., 2009). Therefore, to define whether TET3-dependent modulation of 5hmC and 5mC might contribute to transcriptional fine-tuning of the *Snrpn* gene, a bisulfite sequencing analysis of *Snrpn* DMR (chr7: 60,003,561-60,005,296; Mouse GRCm38/mm10) (**Fig. 46a**) was performed in *Tet3-Gfap*^{cre} and *Tet3-Gfap*^{control} neurospheres cultures. Although bisulfite sequencing cannot distinguish between 5hmC and 5mC, it does distinguish both modified and unmodified cytosines (Huang et al., 2010, Jin et al., 2010), however we did not see a substantial conversion of 5hmC/5mC into 5C in the region analysed (**Fig. 46b**).

To find more information regarding the function of the 5hmC on the regulation of *Snrpn* expression, a hydroxymethylation immunoprecipitation (hMeDIP) using an antibody against 5hmC was developed in *Tet3-Gfap*^{control} and *Tet3-Gfap*^{cre} NSCs. Importantly, no differences were observed in the 5hmC enrichment at the *Snrpn* DMR in TET3 deficient samples (**Fig. 46c**), suggesting that catalytic activity of TET3 was not required to modulate *Snrpn* expression and thus terminal astrocytic identity of adult NSCs.

However, the remarkable increase of *Snrpn* gene levels in *Tet3* deficient NSCs, prompted us to explore the possibility that TET3 might have non-catalytic functions on NSCs to regulate transcription of this gene. Therefore, in order to first test the direct binding of TET3 to the *Snrpn* promoter, we performed chromatin immunoprecipitation (ChIP) assays using antibodies to TET3 in wild-type adult NSCs. We then analysed the association of TET3 to the *Snrpn* promoter by qPCR with primer pairs directed to regions containing part of the promoter (**Fig. 46d**). This ChIP analysis revealed specific TET3 binding enrichment to the promoter on a predicted region between positions -20 and +132 (Region 1, R1) and +271 and +434 (Region 2, R2). In contrast, we did not detect any specific amplification with

primers directed to a non-relevant distal region (-135 kb, Region 3, R3), which validated the specificity of the assay (**Fig. 46d**). Additionally, as a positive control we used a primer pair directed to the *Clcn6* promoter, previously described to bind to TET3 in mouse fetal neural progenitors (Jin et al., 2016) (**Fig 46d**). This data demonstrated that TET3 binding to the *Snrpn* promoter to contribute to transcriptional repression of the gene in adult neural progenitor independently of its catalytic function. Further studies in hybrids NSCs are needed to determine if TET3 binds and regulates expression of the active paternal allele.

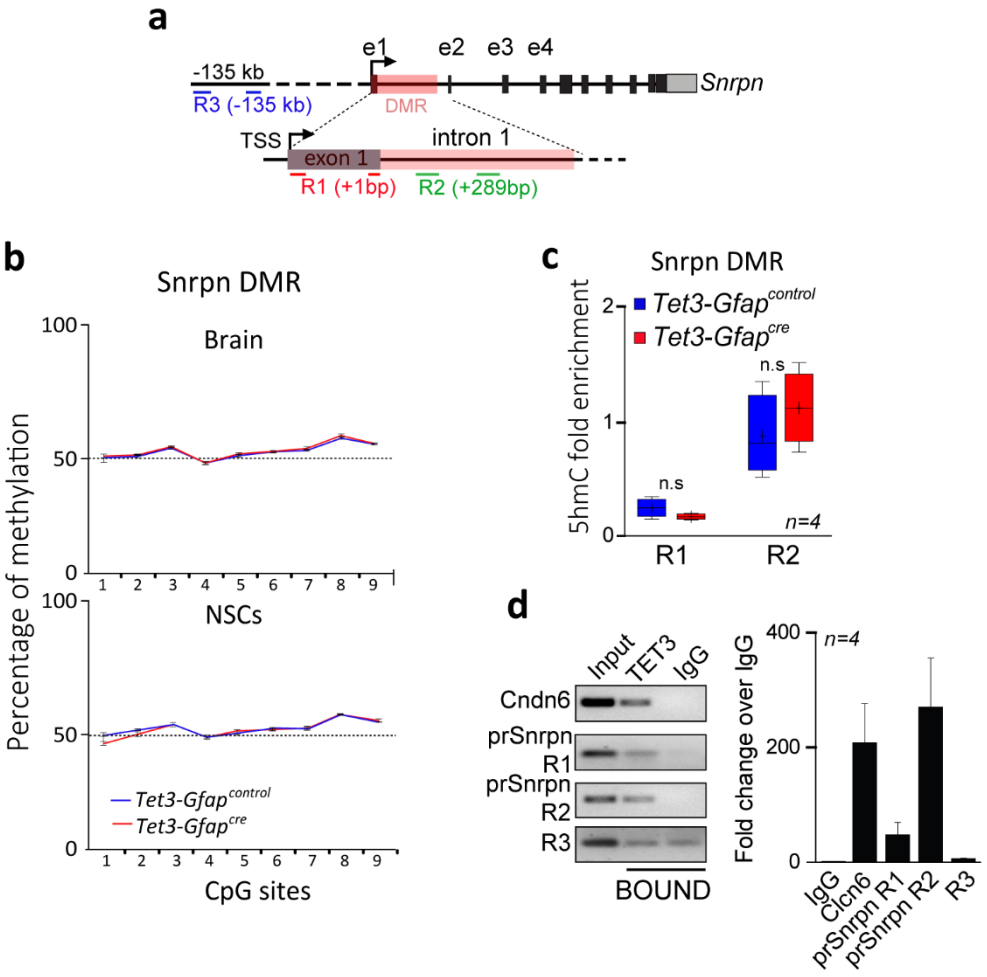

Figure 46. TET3 binds to *Snrpn* promoter and regulates its expression independently of methylation. (a) Schematic diagram showing the Snrpn gene. Snrpn DMR promoter and primers used are shown. Primers positions are numbered relative to the TSS. **(b)** Percentage of methylation determined by bisulfite sequencing and pyrosequencing at several CpG sites within the *Snrpn* DMR in *Tet3-Gfap*^{control} and *Tet3*-Gfap^{cre} NSCs and in whole brains. **(c)** Enrichment of 5hmC at the *Snrpn* DMR (R1 and R2) in NSCs and brains of both genotypes by hMeDIP. All error bars show s.e.m. of at least 3 cultures per genotype and condition. **(d)** qPCR for the chromatin immunoprecipitation (ChIP) in wild-type NSCs. Two regions (R1 and R2) of the *Snrpn* promoter are shown. *Clcn6* promoter was used as a control for TET3 binding. Values are shown as the fold increase over the IgG. All error bars show s.e.m. of at least 6 samples.

Annex III

Table 1 Annex III: Downregulated genes in *Tet3* deficient NSCs (RNAseq data; FDR<0.05).

Gene	FDR	Log2FC	Gene	FDR	Log2FC
Zic1	4,4807E-19	-2,2947	***Ppp4r4***	0,0036	-1,1644
Tet3	3,7751E-17	-1,0074	***Chl1***	0,0044	-2,0506
Elavl4	2,1173E-13	-2,2085	***Ralgds***	0,0048	-0,4408
Adora2b	3,2994E-11	-2,5047	***Calcrl***	0,0060	-0,6672
Gsap	3,2738E-10	-1,6370	***Gm5607***	0,0066	-1,492
Otx1	4,7820E-08	-2,5462	***Man1c1***	0,0068	-0,7335
Tnr	8,4616E-08	-1,5656	***Itga1***	0,0069	-1,126
Zic4	1,4557E-07	-2,3432	***Pde3a***	0,0075	-0,6533
Tspan14	1,0281E-06	-0,898	***Itga8***	0,0078	-1,2694
Qdpr	2,1805E-06	-0,8383	***Ephb1***	0,0078	-0,7687
Gria4	1,2940E-05	-1,2266	***Igsf11***	0,0078	-1,0867
Lrp4	2,0578E-05	-1,0992	***Shisa9***	0,0082	-2,0878
Adamts5	2,5755E-05	-1,235	***Igdcc4***	0,0085	-0,4373
Dmrta2	2,5755E-05	-3,6979	***Thrsp***	0,0094	-0,8841
Myof	3,1139E-05	-2,0089	***Shc4***	0,0095	-0,5611
Gpx7	4,9878E-05	-1,5921	***Klf15***	0,0121	-0,7217
Gas7	5,8524E-05	-0,8626	***Prokr1***	0,0128	-1,1093
Thy1	7,3953E-05	-2,3126	***Pcdhgb4***	0,0128	-2,0964
Fkbp10	0,0001	-1,6098	***Ptprd***	0,0129	-0,5390
Plcxd3	0,0001	-2,4104	***Cxxc5***	0,0154	-0,4770
Clmp	0,0001	-2,1266	***Vit***	0,0155	-1,3971
Cntn3	0,0002	-1,1372	***Hunk***	0,0155	-0,5664
Ebf1	0,0002	-1,6998	***Gm26737***	0,0160	-1,1320
Matn2	0,0002	-1,0555	***Mpped2***	0,0165	-0,6422
Parvb	0,0002	-3,5083	***Tmem144***	0,0165	-2,3168
Cacng5	0,0002	-1,8532	***Syt1***	0,0165	-1,1482
Gm15564	0,0002	-0,5422	***Olfml1***	0,0174	-1,3264
Jup	0,0002	-1,4526	***Fabp5***	0,0210	-0,5634
Fzd9	0,0003	-1,8741	***Kremen1***	0,0226	-0,4893
Mxra8	0,0003	-0,7777	***Pgm5***	0,0226	-1,424
Cacna1g	0,0003	-1,0333	***Gm6166***	0,0226	-0,6570
Chd3	0,0003	-1,5078	***Zic3***	0,0227	-1,2498
Ephb3	0,0004	-0,6353	***Wnt4***	0,0247	-1,2774
Scrg1	0,0007	-2,0705	***Ntng1***	0,0247	-1,1818
Il17rd	0,0010	-0,8200	***Kit***	0,0252	-0,8913
Syk	0,0013	-1,0076	***Pllp***	0,0258	-1,3368
Ccdc136	0,0017	-0,8165	***Lrrc8b***	0,0287	-0,382
Tubb4a	0,0017	-0,8645	***Gsx1***	0,0310	-0,6840
Camkk2	0,0017	-0,7046	***Nrk***	0,0360	-1,9797
Pcp4l1	0,0017	-2,1166	***Slc12a2***	0,0373	-0,4043
Efhd2	0,0026	-0,983	***Tns2***	0,0405	-0,8458
Gbx2	0,0027	-1,5649	***Slmo1***	0,0413	-0,9987
Aebp1	0,0028	-0,5372	***Foxg1***	0,0420	-0,6795
Slc9a3r1	0,0029	-0,5146	***Abcc12***	0,0430	-0,9997
Gcnt4	0,0030	-1,2420	***Stx3***	0,0440	-0,6382
Fam174b	0,0033	-0,5877	***Tnfaip8***	0,0460	-0,5118
Syne1	0,0034	-1,2308	***Rhbdf1***	0,0477	-0,4513
Eomes	0,0036	-1,4401	***Slc2a6***	0,0477	-0,6505

Table 2 Annex III: Upregulated genes in *Tet3* deficient NSCs (RNAseq data; FDR<0.05)

Gene	FDR	Log2FC	Gene	FDR	Log2FC
Pcdhb11	3,7751E-17	3,64952	***Tnfrsf12a***	0,0054	0,5042
Gm8396	1,6826E-11	1,55544	***Arhgap28***	0,0075	0,5465
Ppp2r2c	4,6304E-11	2,83939	***Sfrp1***	0,0078	0,7965
Tmem181b-ps	6,6494E-11	1,54655	***Smad3***	0,0078	0,5579
Mcam	6,6494E-11	1,70022	***Dpp10***	0,0078	1,6757
Thbd	1,0266E-09	1,26392	***Gdap1***	0,0079	1,2149
Dynlt1b	4,7820E-08	2,96314	***Lpo***	0,0081	0,7373
Ebf3	9,8096E-08	0,68708	***Hoxa5***	0,0092	2,5819
Fam78b	1,3172E-07	2,25242	***Pcdhga12***	0,0103	2,1580
Golga7b	2,3435E-07	1,23766	***Dynlt1-ps1***	0,0119	0,4915
Fbn2	1,5730E-06	1,54056	***Lmo4***	0,0144	0,4582
Egr4	5,2162E-06	0,78686	***Zcchc12***	0,0151	0,8541
Pde1b	1,2940E-05	1,69825	***Elmo1***	0,0153	0,5377
Syt13	2,6491E-05	0,97873	***Rundc3a***	0,0155	0,5482
Marc2	2,6491E-05	2,91989	***Adamts19***	0,0155	0,9732
Rftn2	3,4200E-05	0,58517	***Anxa2***	0,0157	1,1406
Pcdhgb2	4,5810E-05	0,65276	***Aldoc***	0,0160	0,5948
Scn7a	4,5810E-05	1,61770	***Abi2***	0,0160	0,3806
Gas6	8,9600E-05	2,13672	***Ptprt***	0,0160	0,6436
Hoxa4	9,8318E-05	1,03198	***Rab7b***	0,0166	1,2769
S100a16	0,0002	2,96224	***Mfap3l***	0,0179	0,5014
Dpysl4	0,0002	0,64086	***Ggct***	0,0183	0,7491
Brinp3	0,0002	0,85540	***Nptx2***	0,0197	0,7657
Itpkb	0,0004	0,77067	***Aldh1l2***	0,0211	0,5185
Atp2b2	0,0005	0,56131	***Atp1a3***	0,0225	0,5822
Rab26	0,0006	1,83631	***Nrap***	0,0225	1,4813
Plcl1	0,0006	1,17035	***Stk39***	0,0239	0,5507
Nrn1	0,0007	0,80126	***Adamts14***	0,0246	0,5588
Camk1g	0,0009	1,35944	***Pmaip1***	0,0257	0,6065
Akt3	0,0010	0,75788	***Rph3a***	0,0261	1,5133
Klf10	0,0011	0,53563	***Mxra7***	0,0280	1,2083
Agbl2	0,0011	0,49684	***Adcy2***	0,0280	0,9383
Ube2ql1	0,0014	1,70435	***Vwa5b1***	0,0284	1,5300
Tnfsf18	0,0016	0,99157	***Scml4***	0,0284	0,8831
Cobl	0,0016	1,65580	***Hbegf***	0,0285	0,5661
Kcnk2	0,0021	1,7265	***Lrrn2***	0,0305	0,3921
Snrpn	0,0022	0,9436	***Cobll1***	0,0310	0,3940
Plekhb1	0,0027	0,6687	***Pcdhac2***	0,0323	1,1039
Serpinb5	0,0031	0,5325	***Pfkp***	0,0349	0,6220
Rasal2	0,0031	1,0740	***Plxdc2***	0,0360	0,6973
Prkg2	0,0031	0,4782	***Il1rap***	0,0374	0,8139
Rftn1	0,0032	0,7218	***Cnpy1***	0,0382	1,6097
Anxa3	0,0033	1,4938	***Ptprn***	0,0397	1,0460
Tchh	0,0038	0,8950	***Sdc4***	0,0405	0,6973
Nr5a2	0,0045	1,3732	***Lama1***	0,0420	1,0597
Pcdhb8	0,0047	1,1024	***Slc41a2***	0,0433	0,4984
Asns	0,0047	1,5100	***Pmm1***	0,0476	0,4373

Discussion

The major findings of the present thesis are that: (1) adult NSCs can be efficiently reprogramed into iPSCs using only *Oct4* and *Klf4*, which causes the re-organization of their entire methylome consequently altering their transcriptome, including expression of imprinted genes; 2) the DNA dioxygenase TET3, present in adult NSCs, is downregulated during the reprogramming process to acquire a pluripotent state. TET3 has also an important role in the maintenance of a multipotent state in adult NSCs by preventing their premature differentiation into non-neurogenic astrocytes. Epigenetics events occurring in the NSC population, such as methylation and hydroxymethylation of DNA, are critical components to guarantee the success of these processes.

The acquisition of a pluripotent state in adult NSCs using exclusively Oct4 and Klf4 transcription factors implies significant changes in the epigenetic profile

Somatic cell reprogramming is a very useful tool to understand the mechanisms involved in the acquisition of a pluripotent state and gives information about the differentiation program attributed to the cell of origin. Since the discovery of the reprogramming process in 2006 by Takahashi and Yamanaka (Takahashi and Yamanaka 2006), researchers have reported the generation of iPSCs from different somatic tissues using the OSKM cocktail. However, only a few assays have reported a successful reprogramming with a reduced number of factors (Kim et al., 2008, Giorgetti et al., 2009, Kim et al., 2009b, Li et al., 2013). NSCs significantly express *c-myc*, *Sox2* and *Klf4* suggesting an intermediate state between differentiated and embryonic stem cells (Kim et al., 2008, Kim et al., 2009b). The presence of these three factors suggests the possibility to reprogram NSCs using only *Oct4* as exogenous factor. Indeed, the generation of iPSCs using *Oct4* was reported previously using 5-days-old mice NSCs (Kim et al., 2008, Kim et al., 2009b), however, using only *Oct4* to reprogram adult NSCs and we did not obtain any pluripotent colony probably due to the lower efficiency of the process in adult NSCs. Previous studies also reported that *Sox2* used in combination with *Oct4* did not give rise to iPSCs clones (Kim et al., 2008). In contrast, we demonstrate that true iPSCs can be obtained from NSCs derived from the adult SVZ using *Oct4* and *Klf4*. These iPSCs were able to form cells from the three germ layers and formed teratomas *in vivo* demonstrating their pluripotency capacity *in vitro*.

Analysis of previously described iPSCs revealed several retroviral integrations for all four factors (Wernig et al., 2007, Aoi et al., 2008). Thus, reprogramming of adult NSCs with only two factors has important implications as reducing the number of factors decreases the chance of retroviral insertional mutagenesis. *Oct4* and *Klf4* are sufficient to induce pluripotency in adult NSCs, which demonstrate their crucial role in the process of reprogramming and support the hypothesis that NSCs represent an intermediate state between differentiated and pluripotent cells. Moreover, *c-myc* has been related to tumorigenesis being this gene one of the most important oncogenes in mammals (Kuttler and Mai

2006). Thus, generation of iPSCs lacking *c-myc* obtained in this work, is also an important advantage for a safety potential clinical use of the iPSCs generated. Therefore, the induction of adult NSCs into iPSCs with a reduced number of factors is a powerful tool for the *in vitro* modelling of disease and mainly for the study of the particular properties of the NSCs of origin.

Our study also demonstrates that there exist partially reprogrammed cells, called pre-iPSCs that exhibit ESC-like morphology but retain retroviral genes expression and incomplete upregulation of pluripotency-associated genes, such as *Nanog*. These cells can be promoted to full pluripotent state applying defined conditions using inhibitors for MEK and GSK and in the presence of LIF (2i/LIF), as previously described (Silva et al., 2008). In response to 2i/LIF, pre-iPSCs reach rapidly a full pluripotent status with phenotypic and functional characteristic of ESCs. *Nanog* expression is critical for blocking the differentiation of pluripotent cells, and more importantly, for establishing the pluripotent ground state during somatic cell reprogramming (Suzuki et al., 2006, Wang et al., 2006, Saunders et al., 2013). Thus *Nanog* occupies a central position in the transcriptional network in the regulation of pluripotency being essential for the formation of iPSCs. In contrast, it has been also shown that *Nanog*, although important mediator of reprogramming, it is not required for establishing pluripotency in murine fibroblasts (Carter et al., 2014). Our data demonstrate that *Nanog* expression is absent in pre-iPSCs and that 2i/LIF treatment results in the activation of its expression which, in contrast to fibroblasts, is necessary to a fully establishment of pluripotency in adult NSCs. Therefore, successful reprogramming to pluripotency with divergent transcription factors and from different cells of origin suggests that there may be many distinct routes to acquire a pluripotent state.

So far, a variety of cell types have been reprogrammed into iPSCs including fibroblasts (Takahashi and Yamanaka 2006), neural progenitor cells (Kim et al., 2009c), hepatocytes and gastric epithelial cells (Aoi et al., 2008), B cells (Hanna et al., 2008), pancreatic β cells (Stadtfeld et al., 2008), melanocytes (Utikal et al., 2009) and keratinocytes (Aasen et al., 2008). Although these iPSCs exhibit a similarity with ESCs in their morphology, gene expression profile and pluripotency, new evidence showed substantial molecular and functional differences among iPSCs derived from distinctive cell types, including the tumorigenic potential or expression of different genes. This suggests an influence of the somatic origin on the properties of resultant iPSCs (Polo et al., 2010). For example, iPSCs derived from astrocytes possess more potential for neuronal differentiation compared to fibroblasts-iPSCs (Tian et al., 2011). Therefore, neural-derived iPSCs may retain a "*memory*" of the central nervous system, which confers additional potential (Nashun et al., 2015). Importantly, our results demonstrate that iPSCs obtained from adult NSCs are able to give rise to cells of the three germinal layers after differentiation demonstrating their pluripotency capability. Strikingly, these iPSCs have a higher

differentiation ability to form ectoderm compared to ESCs after differentiation (**Fig. 21**), but also expression of endodermal lineage determinants is induced, supporting the hypothesis of iPSCs having additional potential depending of the cell of origin.

Pluripotent stem cells maintain self-renewal and pluripotency because of a self-organizing network of transcription factors and intracellular pathways activated by extracellular signaling and epigenetic processes that maintain the chromatin in a plastic differentiation status. The determinants and the temporal order of epigenetic changes leading from a differentiated to a pluripotent cell during iPSC derivation are poorly understood. However, it is clear that to acquire pluripotency, cells must erase differentiation-specific epigenetic marks to achieve an ESC-like state implying important transcriptome changes (Hochedlinger and Jaenisch 2015). Genome-wide expression analysis using next generation sequencing in iPSCs and in the NSCs of origin, show that several markers are sequentially activated or repressed after the induction of reprogramming. Surprisingly, the majority of the most differentially expressed genes (FDR<2.5e-68) were upregulated genes in iPSC compare to NSCs. Moreover, a GSEA analysis identifies several sets of genes belonging to important biological pathways that are significantly upregulated (97 sets of genes) or downregulated (39 sets of genes) in iPSCs compared to NSCs confirming that the acquisition of a pluripotent state implies global transcriptome changes. More concretely and as expected, repression of the neural markers *Nestin* and *Olig2*, correlate with the activation of the pluripotency genes *Oct4*, *Nanog* and *Rex1* in iPSCs (**Fig. 23**).

Several studies have shown that changes in DNA methylation patterns are essential for successful nuclear reprogramming, exemplified by the necessity for loss of promoter methylation in pluripotency genes (Takahashi and Yamanaka 2006). In fact, methylation of CpG dinucleotides plays an important role in regulating gene transcription (Lee et al., 2014) thus if loss of DNA methylation is not achieved, cells will be only partially reprogrammed (Mikkelsen et al., 2008). Moreover, it has been described that DNA methylation is depending on the choice of reprogramming factors used (Planello et al., 2014). We demonstrate that the remodelling of the epigenetic profile during the reprogramming of NSCs into iPSCs with two factors is critical for pluripotency induction, as important changes in the methylation landscape of NSCs need to happen to obtain true pluripotent cells. Global DNA methylation changes were observed using MeDIP sequencing in iPSCs and comparing to the NSCs of origin. Importantly, methylome analysis in iPSCs showed global loss of methylation in the vast majority of differentially methylated regions (DMRs) analysed, correlating with the global induction of gene expression in iPSCs observed by RNAseq. Our work highlights the important role of DNA demethylation in the acquirement of a pluripotency state. *Nanog* expression has been related to the inhibition of global DNA methylation (Theunissen et al., 2011) suggesting its role in methylome re-establishment. When we analyse in detail the methylation profile in pluripotency-associated genes, we observe

hypomethylation, especially at the promoter levels, whereas an increase of methylation is exhibited in neural-associated genes in accordance with their repression.

Imprinted genes are a group of genes expressed monoalellicaly from either the maternally or the paternally inherited chromosomes. Approximately 150 imprinted genes have been described in mammals and are generally organized in clusters (Ferguson-Smith 2011). Studies of the generation of iPSCs from somatic cells *in vitro* represent a unique model system to study the role of these imprinted genes in the acquisition of a pluripotent state and can provide insights about the imprinting status in the cell of origin. In a genome-wide comparison of expression between identical mouse ESCs and iPSCs, no changes were observed in the vast majority of imprinted genes, demonstrating the similitude of both pluripotent cells (Stadtfeld et al., 2010). However, based on RNAseq data in iPSCs and NSCs, the analysis of expression of all known imprinted genes, show significant changes in around 50% of all imprinted genes analysed, suggesting a relevant importance of the imprinting regulation in NSCs behaviour and during the reprogramming process.

It is well described that DNA methylation is essential for establishment and maintenance of imprinting (Bartolomei and Ferguson-Smith 2011). Indeed, germline DMR are essential to establish monoallelic expression and secondary somatic DMRs play important roles in imprinting maintenance (Ferguson-Smith, 2011; Lozano-Ureña et al., 2017). More than 16 imprinted clusters are associated with maternal-specific methylation. For these loci, DNA methylation is found at promoters of protein-coding genes or non-coding RNA genes (Bartolomei and Ferguson-Smith 2011). In contrast, paternally methylated DMRs (there are only 4 described) are located in intergenic regions (Bartolomei and Ferguson-Smith 2011). Strikingly, our findings reveal that the majority of the DMRs at the imprinting clusters are hypomethylated. Indeed, more than 80% of the maternally methylated DMRs show hypomethylation. However, only 30% of paternally methylated DMRs are hypomethylated. These epigenetic changes at the maternally methylated DMRs correlate with changes in the expression levels of several genes within these clusters, whereas no significant changes were observed in the expression of genes at the paternally methylated clusters (**Fig. 47**). Consequently, our results suggest that, genomic imprinting might be finely regulated during development to acquire a specific somatic imprinting pattern in adult NSCs, essential for multipotency maintenance. However, changes in gene expression of imprinted genes do not answer if the imprinting status of these clusters is altered in iPSCs. Further experiments need to be done to determine the parental allele specific expression in the different clusters.

The methylation profile can be established, regulated and erased by both DNMTs and TETs family members (Bartolomei and Ferguson-Smith 2011, Pastor et al., 2013). However, we demonstrate

in our study that iPSCs contain less levels of methylation compared to NSCs indicating that the demethylation process is especially relevant in the acquisition of pluripotency. Active 5mC erasure in mammals is catalysed by TET enzymes and our data show that *Tet1* and *Tet2*, almost absent in NSCs, are highly upregulated in iPSC whereas *Tet3*, the most expressed member in NSCs, is profusely downregulated after reprogramming. Accordingly, reprogramming of *Tet3* knockdown NSCs into iPSCs shows a higher efficiency than wild-type NSCs, supporting the idea that TET3 has to be downregulated for a successful reprogramming (**Fig. 47**). Therefore, the global demethylation process observed in iPSCs could be mediated by TET1 and/or TET2, supported by previous published data that show that both are highly expressed in iPSCs and ESCs and can interact with NANOG to co-occupy genomic *loci* of genes associated with maintenance of pluripotency (Theunissen et al., 2011, Costa et al., 2013). This also suggests that TET3 might be implicated in the maintenance of adult NSCs identity and its expression defines a more committed state. Consistently with our result, it has been demonstrated that *Tet3* expression is undetectable in ESCs but increases rapidly during neuronal differentiation (Li et al., 2015) and some evidences also report the importance of TET3 in neural functions. Nevertheless, the role of TET3 in adult NSCs and in the neurogenesis process remains to be elucidated.

TET3 oxidase is a key epigenetic regulator of neural stemness maintenance in the adult SVZ

Previous studies have shown a role of TET3 in ESCs during the induction of neuronal differentiation (Hahn et al., 2013, Li et al., 2015). It has been also reported that TET3 regulates synaptic transmission and plasticity of neurons (Yu et al., 2015) and TET3 overexpression in mouse olfactory sensory neurons disrupts the axonal targeting of these cells (Colquitt et al., 2013). However the role of TET3 in adult tissues and more specifically in adult neurogenesis is still unknown. Our study is focused on determining the role of *Tet3* in the neural stem cell population within the adult SVZ. We have shown that loss of *Tet3* compromises the maintenance of the neural stem cells pool in this niche leading to reduced neurogenesis and affecting the differentiation capacity of neural progenitors both *in vivo* and *in vitro*. Although a role for another member of the TET dioxygenases, TET1 in regulating neural progenitor cell proliferation has been reported in the adult hippocampus (Zhang et al., 2013b), this work implicates for the first time TET3 in the maintenance of the stem cell pool in the adult SVZ and thus in the regulation of OB neurogenesis *in vivo*. Additionally, our work highlights a positive role of TET3 in the regulation of NSCs self-renewal by repressing the expression of the imprinting gene *Snrpn* independently of its catalytic function. However, it is still not know if TET3 is also required to maintain stemness identity in the dentate gyrus of the hippocampus as it happens in the SVZ.

The levels of expression of *Tet3* in NSCs are significantly higher than the other members of the family *Tet1* and *Tet2* being abundantly maintained postnatally and during differentiation of NSCs.

Moreover, protein distribution of TET3 within the SVZ shows specific staining in GFAP positive cells indicating a relevant role for this dioxygenase in adult NSCs behaviour. Analysing more in detail TET3 protein distribution in NSCs by immunohistochemistry shows nuclear distribution of the protein, although a light staining is also observed in the cytoplasm. In fact, it has been reported the particular presence of TET proteins, including TET3, in the mitochondria in the nervous system where they are thought to be regulating 5hmC levels (Dzitoyeva et al., 2012). It is well described that TET3 functions interacting with genomic DNA, cytoplasmic staining may be due to the presence of TET3 in the mitochondria in NSCs even though its role have not been addressed. Interestingly, when TET3 is absent in the GFAP+ population *in vivo*, by conditional deletion of the gene in this cells, a depletion of the adult NSCs pool is observed due to the terminal differentiation into non-neurogenic astrocytes. As a consequence of the continuous depletion of the neural stem cell pool in *Tet3* deficient mice, the process of neurogenesis to the olfactory bulb is impaired. Notably, we find an increased proportion of cells that are positive for S100β in 2-months-old *Tet3-Gfap*^{cre} SVZ which is largely absent from GFAP-expressing neurogenic astrocytes (Raponi et al., 2007). The analysis of NSCs *in vitro* identifies stem cells based on their self-renewal and differentiation capacities, being a quantitative read out of the number of stem cells *in vivo*. Indeed, we obtain a reduced number of primary neurospheres from *Tet3* deficient SVZ compared to their controls, in accordance with a more differentiated state of NSCs in the absence of the enzyme.

Differentiation of both mutant and wild-type NSCs into the three cell lineages of the CNS, astrocytes, oligodendrocytes and neurons *in vitro*, supports a premature differentiation of NSCs into S100β+ non-neurogenic astrocytes. Moreover, previous data from our laboratory reported the capacity of a low proportion of cells, after 7 days of differentiation, to detach, reactivate and form new neurospheres in the presence of mitogens (unpublished data). Remarkably, after 7 days of differentiation, the significant reduction of primary neurospheres obtained from *Tet3* deficient SVZ confirms the premature differentiation of NSCs in the niche. Thus, our findings demonstrate the role of TET3 in promoting stemness maintenance by preventing NSCs from a premature differentiation both *in vivo* and *in vitro* (**Fig. 47**).

Previous published data also suggest that TET3 deficiency causes an active apoptosis of neural progenitors derived from ESCs, which results in a reduction of neuronal production (Li et al., 2015). In contrast to these data, our study shows that *Tet3* deficiency does not modify the apoptosis or survival rates in adult NSCs, but we identify defects in the self-renewal capacity of primary and secondary *Tet3* deficient neurospheres *in vitro*. Interestingly, no changes in the proportion of the cell cycle phases are observed in the mutant cultures indicating that TET3 promotes self-renewal capacity without affecting the overall proliferation rate in adult NSCs.

Imprinted genes have been implicated in the maintenance and function of adult stem cells. For example, *Peg3* expression is restricted to stem cell/progenitors populations in the brain, gut, muscle and skin (Besson et al., 2011). The maternally expressed *H19* gene is also involved in the maintenance of adult haematopoietic stem cell (HCS) populations in the mouse (Venkatraman et al., 2013). Moreover, we have previously described that absence of *Dlk1* imprinting in mouse NSCs is crucial for postnatal neurogenesis (Ferron et al., 2011). These findings highlight the importance of specific contexts in imprinted gene regulation and underline the significance of gene dosage for imprinted genes in NSCs. There are some reports implicating TET functions in removal of DNA methylation imprint at the imprinted regions in the germline (Nakamura et al., 2012, Dawlaty et al., 2013, Hackett et al., 2013, Piccolo et al., 2013, Yamaguchi et al., 2013), however, it is not well established the particular role of TET3 in the regulation of expression of imprinted genes.

The RNAseq analysis comparing TET3 deficient NSCs with their controls demonstrate that TET3 is implicated in the transcriptional regulation of many genes in NSCs. Almost 200 genes are differentially expressed in *Tet3* deficient samples including some stem cells markers. Surprisingly, from around 150 imprinted genes tested in the RNAseq study of *Tet3* deficient NSCs, we only find an upregulation of the expression of the *Snrpn* (Small nuclear ribonucleoprotein-associated protein N) gene compared to controls. *Snrpn* belongs to the Prader-Willi syndrome imprinting gene and is canonically expressed from the paternally inherited chromosome (Bervini and Herzog 2013). This complex syndrome is caused by loss of expression of paternally inherited genes located in the *Snrpn* locus (Bervini and Herzog 2013). Clinically, the syndrome is characterized by severe neurodevelopmental effects including hyperphagia and onset obesity, short stature due to growth hormone deficiency, intellectual disability and behavioural problems (Butler 2011) suggesting the importance of *Snrpn* imprinting in neural function. *Snrpn* encodes the RNA-associated SmN (survival motor neurons) protein implicated in pre-mRNA edition, contributing to tissue-specific alternative splicing (Li et al., 2016). It is well established that *Snrpn* is highly expressed in brain and its expression is increased markedly during postnatal brain development (Li et al., 2016). Moreover, lower levels of SmN have been implicated in spinal muscular atrophy, affecting predominantly spinal motor neurons probably due to neural trafficking defects (Prescott et al., 2014). All previous data together indicate the important role of *Snrpn* gene in neural regulation.

Our data suggest that although TET3 is not involved in the global regulation of the genomic imprinting process in adult NSCs, does play a role in the regulation of very specific imprinted regions in adult NSCs. Concretely a relevant function of TET3 on the regulation of the imprinted gene *Snrpn* is confirmed using shRNA interference experiments for the gene in deficient NSCs. This experiments show a clear rescue of the terminally differentiated phenotype observed in Tet3-Gfapcre NSCs

demonstrating that loss of TET3 causes the upregulation of the *Snrpn* levels driving the NSCs population to the terminal differentiation and exhaustion of the stem cell pool in the SVZ. Importantly, the upregulation of *Snrpn* after TET3 removal is not due to alterations of the imprinted status of the gene as allele-specific expression for *Snrpn* in adult NSCs show the expected paternally expression of the gene.

TET enzymes are able to convert 5mC into 5hmC, which constitutes about 40% of modified cytosine in the brain (Kriaucionis and Heintz 2009, Munzel et al., 2010, Szwagierczak et al., 2010, Szulwach et al., 2011). It has been previously involved the 5hmC modification in stemness maintenance, for example it has been shown the importance of this modification in self-renewal and pluripotency in ESCs (Koh et al., 2011) as well as in the hematopoietic stem cell maintenance (Ko et al., 2010). Although 5hmC intermediate is especially relevant in the brain its role in NSCs has not been elucidated. Our data show significant amounts of the two molecules, 5mC and 5hmC, in proliferating cells where both marks are exclusive. 5mC is enriched in more condensed chromatin accordingly to its role in the prevention of expression (Schilling and Rehli 2007) and is present in the neuroblast population, whereas 5hmC mark is present in the most relaxed chromatin indicating, as previously described the role of 5mC oxidation in transcription elongation (Wu and Zhang 2017). In contrast, 5hmC is found in GFAP-expressing cells within the SVZ and in mature neurons in the striatal parenchyma. Thus, the presence of 5hmC in the adult stem cell population along with its apparent exclusion from differentiated cells suggests that formation of 5hmC may also participate in the function and/or maintenance of the undifferentiated state during the neurogenesis process. On the other hand, we see that 5mC mark is especially abundant in more committed progenitors which might be related to the silencing of stemness-associated genes.

However, quantification of the global levels of 5mC/5hmC in *Tet3* deficient NSCs shows no differences between mutant and controls. Consistently, immunohistochemistry analysis of 5hmC in the SVZ of *Tet3* deficient mice also reveals no significant changes in global 5hmC after *Tet3* deletion in vivo. These data suggest that TET3 is not regulating global levels of 5hmC in adult NSCs. This finding is in accordance with previous published data in which TET3 was involved in the regulation of synaptic plasticity through the regulation of specific genes such as the modulation of surface GluR1 levels without affecting global levels of 5hmC (Yu et al., 2015). In addition, it has been reported that the upregulation of *Tet3* during neural development together with the increase of 5hmC levels affects specific genes rather that the genome globally (Hahn et al., 2013). This indicates that TET3 can modulate particular genes depending on cell and genomic context. Other members of TET family have been also implicated in the regulation of 5hmC at particular genes without affecting global 5hmC levels such as TET1 deficiency in oocytes that does not affect the genome-wide demethylation in primordial

germ cells, but leads to defective DNA demethylation of a subset of meiotic genes (Yamaguchi et al., 2013).

TET proteins might play a partially redundant role in DNA methylation. Therefore one explanation for the results observed in *Tet3* deficient NSCs, is that TET1 or TET2 could be compensating changes in global methylation after TET3 removal. However, TET1 which is absent in NSCs, is not a plausible candidate for it. TET2 although lower than TET3 is still present so it could be implicated on regulating the levels of 5hmC in NSCs. Our data indicate that *Tet2* does not change after *Tet3* removal. However, our expression data suggest that *Tet2* is probably the enzyme implicated in the regulation of 5hmC in NSCs, but additional studies are needed to address this point.

As it has been previously mentioned, the catalytic effects of TET3 can be restricted to specific targets without affecting the 5hmC global levels (Hahn et al., 2013, Yu et al., 2015). Moreover, recently published data show an increase of 5hmC on the *Snrpn* transcribed allele suggesting that 5hmC is positively associated with transcription at these *loci* (Hernandez Mora et al., 2017). However our results from the hidroxyMeDIP assay of the *Snrpn* DMR in *Tet3* deficient NSCs and their controls show no differences in 5hmC levels between both genotypes indicating that TET3 does not regulate *Snrpn* expression by controlling their gene-specific 5hmC levels. This implies that the phenotype observed in the absence of TET3 may result from catalytic-independent functions of TET3 protein. Some examples have been recently published demonstrating catalytic-activity-independent functions of TET family members (Wu and Zhang 2017). Concretely, TET3 has been implicated in the stabilization of thyroid hormones nuclear receptors promoting their binding of targets genes and transcriptional activation where TET3 catalytic domain is not implicated (Guan et al., 2017) and experiments in *Xenopus laevis* show that TET3 catalytic dead mutant can rescue the developmental defects caused by TET3 knockdown (Xu et al., 2012). Indeed, our data demonstrate that TET3 binds to the *Snrpn* promoter to contribute to transcriptional repression of the gene in adult neural progenitor probably by a catalytic-independent activity mechanism (**Fig. 47**). We cannot discard that catalytic-activity-dependent and –independent functions might coordinate to reinforce the functional outcome.

Finally, three TET3 isoforms have been described in mammals, TET3o, TET3s and TET3FL (Jin et al., 2016). TET3o lacks an N-terminal CXXC domain and participate in oxidation of the paternal pronuclear DNA in zygotes (Gu et al., 2011) being absent in NSCs. TET3FL is the full-length isoform containing an N-terminal CXXC domain whereas TET3s, the shortest isoforms, lacks this domain. Our data reveal that TET3s is the most expressed isoform in the brain and the SVZ, however, in NSCs the expression of TET3FL is significantly higher than in brain or SVZ, suggesting a relevant role of the longest isoform in NSCs. Interestingly, the CXXC domain in TET3FL has functional implications. It has

been described that, despite all isoforms present the catalytic domain and are functionally active, TET3FL has the lowest oxidative capacity (Jin et al., 2016). Moreover, in the same work, the authors observe that TET3FL CXXC domain bound more strongly to the oligonucleotide containing 5caC than normal cytosine and they propose that binding of the CXXC domain to 5caC restricts its genome-wide 5mC oxidation capacity. They also suggest that binding of TET3FL near the TSS of unmethylated CpG islands have a housekeeping function to prevent methylation of critical CpG sites near the transcription start site by the cooperation between the DNA binding domain and the catalytic domain. In addition, their gene ontology analysis in NPCs suggest that TET3FL preferentially targets genes functioning in lysosome pathways, base excision repair and mRNA processing, including members of the *Snrpn* family such as *Snrpa* and *Snrp40*. These implication of TET3FL in the regulation of mRNA processing genes together with our data showing that this isoform is especially present in NSCs where TET3 downregulation do not affect 5hmC global levels, suggest that TET3FL may play a principal role in regulating *Snrpn* expression in adult NSCs. However, further experiments are needed to elucidate the particular contribution of each isoform in the neurogenesis process.

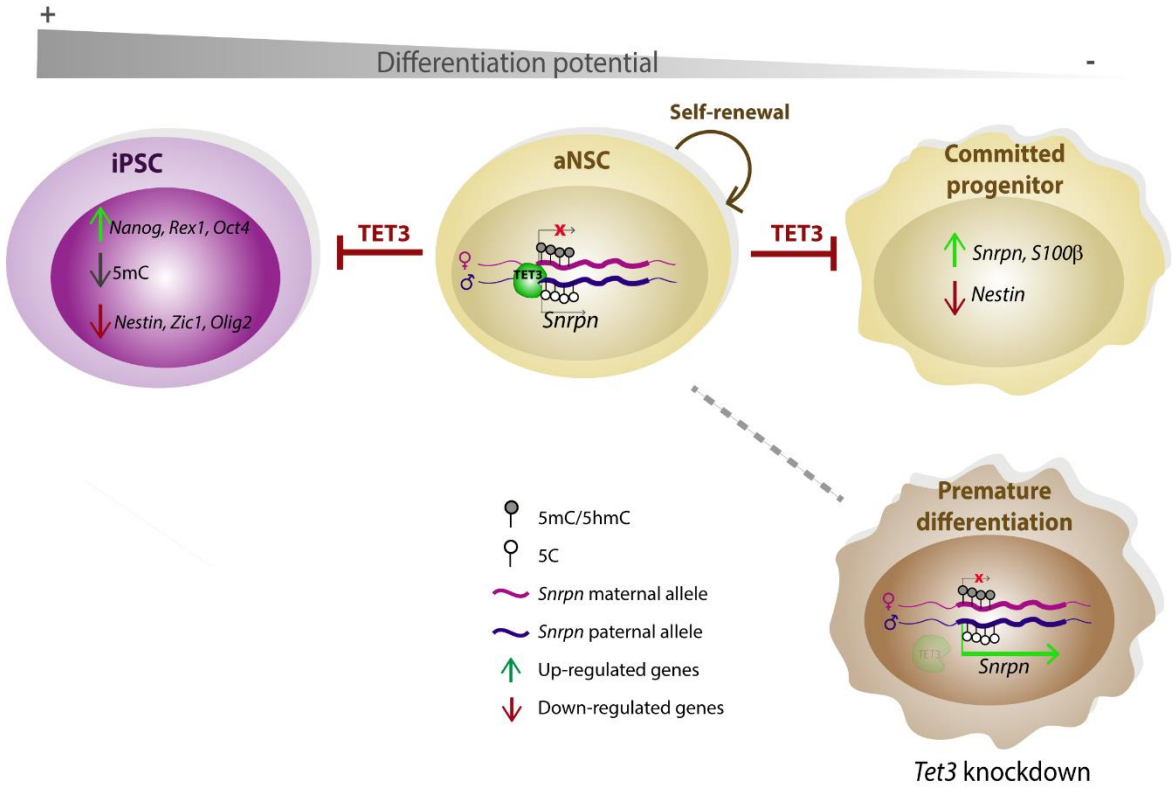

Figure 47. TET3 prevents terminal differentiation of adult NSCs by a non-catalytic action on the imprinted gene *Snrpn*. TET3 directly promotes neurogenic potential and self-renewal capacity of the multipotent stem cell-like astrocytes. It binds to the Snrpn promoter to contribute to transcriptional repression of the imprinted gene independently of its catalytic function. Loss of TET3 in the adult NSCs causes the upregulation of Snrpn levels which induces the cell to a premature differentiation state. Adult NSCs are successfully reprogrammed into iPSCs using only Oct4 and Klf4 factors. Tet3 downregulation is essential for the acquisition of a pluripotent state characterized by the expression of pluripotency genes and the downregulation of neural genes. Acquisition of pluripotency in NSCs implies a re-establishment of the methylation landscape in the genome to modulate the new gene expression profile.

Conclusions

1. Adult SVZ NSCs successfully reprogram into iPSCs with ESCs-like features using exclusively *Oct4* and *Klf4* transcription factors, indicating that NSCs are in an epigenetic intermediate state between differentiated and pluripotent cells.

2. NSCs-derived iPSCs have higher differentiation ability to form ectoderm than ESCs, suggesting that they may retain a memory of the central nervous system. Endodermal lineage determinants are also induced, thus iPSCs may have additional potential depending of the cell of origin.

3. The acquisition of a pluripotent state in adult NSCs implies significant changes in the expression of imprinted genes. More than half of the paternally and maternally expressed genes present originally in NSCs, are altered in iPSCs, indicating that regulation of genomic imprinting is crucial in this process.

4. Changes in the expression levels of imprinted genes correlate with modifications of the DNA methylation pattern at imprinted clusters. The majority of imprinted DMRs are substantially hypomethylated. Strikingly DNA methylation changes mainly occur in maternally methylated DMRs correlating with changes in the expression levels of several genes within these clusters.

5. The TET3 hydroxylase is highly expressed in adult NSCs preventing their reprogramming into iPSCs. Therefore, TET3 is not the enzyme that catalyses the demethylation process observed in imprinting clusters.

6. TET3, highly expressed in the GFAP population within the SVZ, promotes NSC maintenance by avoiding their premature differentiation into non-neurogenic astrocytes *in vivo* and *in vitro*.

7. TET3 deficiency in GFAP+ NSCs results in the reduction of the number of newborn neurons reaching the olfactory bulb.

8. Monoallelic upregulation of the imprinted gene *Snrpn* is responsible for the premature differentiation into terminally differentiated astrocytes in TET3 deficient NSCs.

9. TET3 binds to *Snrpn* promoter to contribute to transcriptional repression of the imprinted gene in neural progenitors independently of its catalytic function.

Bibliography

Aasen T., Raya A., Barrero M. J., Garreta E., Consiglio A., Gonzalez F., Vassena R., Bilic J., Pekarik V., Tiscornia G., Edel M., Boue S. and Izpisua Belmonte J. C. (2008). "Efficient and rapid generation of induced pluripotent stem cells from human keratinocytes". *Nat Biotechnol* 26: 1276-1284.

Abad M., Mosteiro L., Pantoja C., Canamero M., Rayon T., Ors I., Grana O., Megias D., Dominguez O., Martinez D., Manzanares M., Ortega S. and Serrano M. (2013). "Reprogramming in vivo produces teratomas and iPS cells with totipotency features". *Nature* 502: 340-345.

Alvarez C. V., Garcia-Lavandeira M., Garcia-Rendueles M. E., Diaz-Rodriguez E., Garcia-Rendueles A. R., Perez-Romero S., Vila T. V., Rodrigues J. S., Lear P. V. and Bravo S. B. (2012). "Defining stem cell types: understanding the therapeutic potential of ESCs, ASCs, and iPS cells". *J Mol Endocrinol* 49: R89-111.

Aoi T., Yae K., Nakagawa M., Ichisaka T., Okita K., Takahashi K., Chiba T. and Yamanaka S. (2008). "Generation of pluripotent stem cells from adult mouse liver and stomach cells". *Science* 321: 699-702.

Apostolou E. and Hochedlinger K. (2013). "Chromatin dynamics during cellular reprogramming". *Nature* 502: 462-471.

Apple D. M., Solano-Fonseca R. and Kokovay E. (2017). "Neurogenesis in the aging brain". *Biochem Pharmacol* 141: 77-85.

Arai F., Hirao A., Ohmura M., Sato H., Matsuoka S., Takubo K., Ito K., Koh G. Y. and Suda T. (2004). "Tie2/angiopoietin-1 signaling regulates hematopoietic stem cell quiescence in the bone marrow niche". *Cell* 118: 149-161.

Ballas N., Grunseich C., Lu D. D., Speh J. C. and Mandel G. (2005). "REST and its corepressors mediate plasticity of neuronal gene chromatin throughout neurogenesis". *Cell* 121: 645-657.

Barker N., van Es J. H., Kuipers J., Kujala P., van den Born M., Cozijnsen M., Haegebarth A., Korving J., Begthel H., Peters P. J. and Clevers H. (2007). "Identification of stem cells in small intestine and colon by marker gene Lgr5". *Nature* 449: 1003-1007.

Barlow D. P. and Bartolomei M. S. (2014). "Genomic imprinting in mammals". *Cold Spring Harb Perspect Biol* 6.

Bartolomei M. S. and Ferguson-Smith A. C. (2011). "Mammalian genomic imprinting". *Cold Spring Harb Perspect Biol* 3.

Belenguer G., Domingo-Muelas A., Ferron S. R., Morante-Redolat J. M. and Farinas I. (2016). "Isolation, culture and analysis of adult subependymal neural stem cells". *Differentiation* 91: 28-41.

Ben-Porath I., Thomson M. W., Carey V. J., Ge R., Bell G. W., Regev A. and Weinberg R. A. (2008). "An embryonic stem cell-like gene expression signature in poorly differentiated aggressive human tumors". *Nat Genet* 40: 499-507.

Bernemann C., Greber B., Ko K., Sterneckert J., Han D. W., Arauzo-Bravo M. J. and Scholer H. R. (2011). "Distinct developmental ground states of epiblast stem cell lines determine different pluripotency features". *Stem Cells* 29: 1496-1503.

Bervini S. and Herzog H. (2013). "Mouse models of Prader-Willi Syndrome: a systematic review". *Front Neuroendocrinol* 34: 107-119.

Besson V., Smeriglio P., Wegener A., Relaix F., Nait Oumesmar B., Sassoon D. A. and Marazzi G. (2011). "PW1 gene/paternally expressed gene 3 (PW1/Peg3) identifies multiple adult stem and progenitor cell populations". *Proc Natl Acad Sci U S A* 108: 11470-11475.

Bird A. (2002). "DNA methylation patterns and epigenetic memory". *Genes Dev* 16: 6-21.

Bird A. (2007). "Perceptions of epigenetics". *Nature* 447: 396-398.

Bird A. P. (1986). "CpG-rich islands and the function of DNA methylation". *Nature* 321: 209-213.

Biteau B., Hochmuth C. E. and Jasper H. (2011). "Maintaining tissue homeostasis: dynamic control of somatic stem cell activity". *Cell Stem Cell* 9: 402-411.

Bjornsson C. S., Apostolopoulou M., Tian Y. and Temple S. (2015). "It takes a village: constructing the neurogenic niche". *Dev Cell* 32: 435-446.

Blanpain C. and Fuchs E. (2009). "Epidermal homeostasis: a balancing act of stem cells in the skin". *Nat Rev Mol Cell Biol* 10: 207-217.

Bond A. M., Ming G. L. and Song H. (2015). "Adult Mammalian Neural Stem Cells and Neurogenesis: Five Decades Later". *Cell Stem Cell* 17: 385-395.

Boumahdi S., Driessens G., Lapouge G., Rorive S., Nassar D., Le Mercier M., Delatte B., Caauwe A., Lenglez S., Nkusi E., Brohee S., Salmon I., Dubois C., del Marmol V., Fuks F., Beck B. and Blanpain C. (2014). "SOX2 controls tumour initiation and cancer stem-cell functions in squamous-cell carcinoma". *Nature* 511: 246-250.

Brinkman E. K., Chen T., Amendola M. and van Steensel B. (2014). "Easy quantitative assessment of genome editing by sequence trace decomposition". *Nucleic Acids Res* 42: e168.

Brons I. G., Smithers L. E., Trotter M. W., Rugg-Gunn P., Sun B., Chuva de Sousa Lopes S. M., Howlett S. K., Clarkson A., Ahrlund-Richter L., Pedersen R. A. and Vallier L. (2007). "Derivation of pluripotent epiblast stem cells from mammalian embryos". *Nature* 448: 191-195.

Butler M. G. (2011). "Prader-Willi Syndrome: Obesity due to Genomic Imprinting". *Curr Genomics* 12: 204-215.

Calatayud C., Carola G., Consiglio A. and Raya A. (2017). "Modeling the genetic complexity of Parkinson's disease by targeted genome edition in iPS cells". *Curr Opin Genet Dev* 46: 123-131.

Carter A. C., Davis-Dusenbery B. N., Koszka K., Ichida J. K. and Eggan K. (2014). "Nanog-independent reprogramming to iPSCs with canonical factors". *Stem Cell Reports* 2: 119-126.

Cleaton M. A., Edwards C. A. and Ferguson-Smith A. C. (2014). "Phenotypic outcomes of imprinted gene models in mice: elucidation of pre- and postnatal functions of imprinted genes". *Annu Rev Genomics Hum Genet* 15: 93-126.

Coan P. M., Burton G. J. and Ferguson-Smith A. C. (2005). "Imprinted genes in the placenta--a review". *Placenta* 26 Suppl A: S10-20.

Codega P., Silva-Vargas V., Paul A., Maldonado-Soto A. R., Deleo A. M., Pastrana E. and Doetsch F. (2014). "Prospective identification and purification of quiescent adult neural stem cells from their in vivo niche". *Neuron* 82: 545-559.

Colquitt B. M., Allen W. E., Barnea G. and Lomvardas S. (2013). "Alteration of genic 5-hydroxymethylcytosine patterning in olfactory neurons correlates with changes in gene expression and cell identity". *Proc Natl Acad Sci U S A* 110: 14682-14687.

Costa Y., Ding J., Theunissen T. W., Faiola F., Hore T. A., Shliaha P. V., Fidalgo M., Saunders A., Lawrence M., Dietmann S., Das S., Levasseur D. N., Li Z., Xu M., Reik W., Silva J. C. and Wang J. (2013). "NANOG-dependent function of TET1 and TET2 in establishment of pluripotency". *Nature* 495: 370-374.

Chaker Z., Codega P. and Doetsch F. (2016). "A mosaic world: puzzles revealed by adult neural stem cell heterogeneity". *Wiley Interdiscip Rev Dev Biol* 5: 640-658.

Chamberlain S. J., Chen P. F., Ng K. Y., Bourgois-Rocha F., Lemtiri-Chlieh F., Levine E. S. and Lalande M. (2010). "Induced pluripotent stem cell models of the genomic imprinting disorders Angelman and Prader-Willi syndromes". *Proc Natl Acad Sci U S A* 107: 17668-17673.

Chambers I. and Smith A. (2004). "Self-renewal of teratocarcinoma and embryonic stem cells". *Oncogene* 23: 7150-7160.

da Rocha S. T. and Ferguson-Smith A. C. (2004). "Genomic imprinting". *Curr Biol* 14: R646-649.

Dawlaty M. M., Breiling A., Le T., Raddatz G., Barrasa M. I., Cheng A. W., Gao Q., Powell B. E., Li Z., Xu M., Faull K. F., Lyko F. and Jaenisch R. (2013). "Combined deficiency of Tet1 and Tet2 causes epigenetic abnormalities but is compatible with postnatal development". *Dev Cell* 24: 310-323.

Daynac M., Morizur L., Kortulewski T., Gauthier L. R., Ruat M., Mouthon M. A. and Boussin F. D. (2015). "Cell Sorting of Neural Stem and Progenitor Cells from the Adult Mouse Subventricular Zone and Live-imaging of their Cell Cycle Dynamics". *J Vis Exp*.

Delgado A. C., Ferron S. R., Vicente D., Porlan E., Perez-Villalba A., Trujillo C. M., D'Ocon P. and Farinas I. (2014). "Endothelial NT-3 delivered by vasculature and CSF promotes quiescence of subependymal neural stem cells through nitric oxide induction". *Neuron* 83: 572-585.

Doege C. A., Inoue K., Yamashita T., Rhee D. B., Travis S., Fujita R., Guarnieri P., Bhagat G., Vanti W. B., Shih A., Levine R. L., Nik S., Chen E. I. and Abeliovich A. (2012). "Early-stage epigenetic modification during somatic cell reprogramming by Parp1 and Tet2". *Nature* 488: 652-655.

Doetsch F. (2003). "The glial identity of neural stem cells". *Nat Neurosci* 6: 1127-1134.

Doetsch F., Garcia-Verdugo J. M. and Alvarez-Buylla A. (1997). "Cellular composition and three-dimensional organization of the subventricular germinal zone in the adult mammalian brain". *J Neurosci* 17: 5046-5061.

Doetsch F., Garcia-Verdugo J. M. and Alvarez-Buylla A. (1999). "Regeneration of a germinal layer in the adult mammalian brain". *Proc Natl Acad Sci U S A* 96: 11619-11624.

Dzitoyeva S., Chen H. and Manev H. (2012). "Effect of aging on 5-hydroxymethylcytosine in brain mitochondria". *Neurobiol Aging* 33: 2881-2891.

Edwards C. A. and Ferguson-Smith A. C. (2007). "Mechanisms regulating imprinted genes in clusters". *Curr Opin Cell Biol* 19: 281-289.

Elhamamsy A. R. (2017). "Role of DNA methylation in imprinting disorders: an updated review". *J Assist Reprod Genet* 34: 549-562.

Eminli S., Utikal J., Arnold K., Jaenisch R. and Hochedlinger K. (2008). "Reprogramming of neural progenitor cells into induced pluripotent stem cells in the absence of exogenous Sox2 expression". *Stem Cells* 26: 2467-2474.

Evans M. J. and Kaufman M. H. (1981). "Establishment in culture of pluripotential cells from mouse embryos". *Nature* 292: 154-156.

Faigle R. and Song H. (2013). "Signaling mechanisms regulating adult neural stem cells and neurogenesis". *Biochim Biophys Acta* 1830: 2435-2448.

Fan G., Beard C., Chen R. Z., Csankovszki G., Sun Y., Siniaia M., Biniszkiewicz D., Bates B., Lee P. P., Kuhn R., Trumpp A., Poon C., Wilson C. B. and Jaenisch R. (2001). "DNA hypomethylation perturbs the function and survival of CNS neurons in postnatal animals". *J Neurosci* 21: 788-797.

Feng B., Ng J. H., Heng J. C. and Ng H. H. (2009). "Molecules that promote or enhance reprogramming of somatic cells to induced pluripotent stem cells". *Cell Stem Cell* 4: 301-312.

Feng J., Zhou Y., Campbell S. L., Le T., Li E., Sweatt J. D., Silva A. J. and Fan G. (2010). "Dnmt1 and Dnmt3a maintain DNA methylation and regulate synaptic function in adult forebrain neurons". *Nat Neurosci* 13: 423-430.

Ferguson-Smith A. C. (2011). "Genomic imprinting: the emergence of an epigenetic paradigm". *Nat Rev Genet* 12: 565-575.

Ferron S. R., Andreu-Agullo C., Mira H., Sanchez P., Marques-Torrejon M. A. and Farinas I. (2007). "A combined ex/in vivo assay to detect effects of exogenously added factors in neural stem cells". *Nat Protoc* 2: 849-859.

Ferron S. R., Charalambous M., Radford E., McEwen K., Wildner H., Hind E., Morante-Redolat J. M., Laborda J., Guillemot F., Bauer S. R., Farinas I. and Ferguson-Smith A. C. (2011). "Postnatal loss of Dlk1 imprinting in stem cells and niche astrocytes regulates neurogenesis". *Nature* 475: 381-385.

Ferron S. R., Radford E. J., Domingo-Muelas A., Kleine I., Ramme A., Gray D., Sandovici I., Constancia M., Ward A., Menheniott T. R. and Ferguson-Smith A. C. (2015). "Differential genomic imprinting regulates paracrine and autocrine roles of IGF2 in mouse adult neurogenesis". *Nat Commun* 6: 8265.

Finch B. W. and Ephrussi B. (1967). "RETENTION OF MULTIPLE DEVELOPMENTAL POTENTIALITIES BY CELLS OF A MOUSE TESTICULAR TERATOCARCINOMA DURING PROLONGED CULTURE in vitro AND THEIR EXTINCTION UPON HYBRIDIZATION WITH CELLS OF PERMANENT LINES". *Proc Natl Acad Sci U S A* 57: 615-621.

Foret M. R., Sandstrom R. S., Rhodes C. T., Wang Y., Berger M. S. and Lin C. H. (2014). "Molecular targets of chromatin repressive mark H3K9me3 in primate progenitor cells within adult neurogenic niches". *Front Genet* 5: 252.

Foti S. B., Chou A., Moll A. D. and Roskams A. J. (2013). "HDAC inhibitors dysregulate neural stem cell activity in the postnatal mouse brain". *Int J Dev Neurosci* 31: 434-447.

Fuchs E., Tumbar T. and Guasch G. (2004). "Socializing with the neighbors: stem cells and their niche". *Cell* 116: 769-778.

Gage F. H., Kempermann G., Palmer T. D., Peterson D. A. and Ray J. (1998). "Multipotent progenitor cells in the adult dentate gyrus". *J Neurobiol* 36: 249-266.

Garcia A. D., Doan N. B., Imura T., Bush T. G. and Sofroniew M. V. (2004). "GFAP-expressing progenitors are the principal source of constitutive neurogenesis in adult mouse forebrain". *Nat Neurosci* 7: 1233-1241.

Geistlinger L., Csaba G. and Zimmer R. (2016). "Bioconductor's EnrichmentBrowser: seamless navigation through combined results of set- & network-based enrichment analysis". *BMC Bioinformatics* 17: 45.

Gilbert P. M., Havenstrite K. L., Magnusson K. E., Sacco A., Leonardi N. A., Kraft P., Nguyen N. K., Thrun S., Lutolf M. P. and Blau H. M. (2010). "Substrate elasticity regulates skeletal muscle stem cell self-renewal in culture". *Science* 329: 1078-1081.

Giorgetti A., Montserrat N., Aasen T., Gonzalez F., Rodriguez-Piza I., Vassena R., Raya A., Boue S., Barrero M. J., Corbella B. A., Torrabadella M., Veiga A. and Izpisua Belmonte J. C. (2009). "Generation of induced pluripotent stem cells from human cord blood using OCT4 and SOX2". *Cell Stem Cell* 5: 353-357.

Goll M. G. and Bestor T. H. (2005). "Eukaryotic cytosine methyltransferases". *Annu Rev Biochem* 74: 481-514.

Goodell M. A., Nguyen H. and Shroyer N. (2015). "Somatic stem cell heterogeneity: diversity in the blood, skin and intestinal stem cell compartments". *Nat Rev Mol Cell Biol* 16: 299-309.

Goto K., Numata M., Komura J. I., Ono T., Bestor T. H. and Kondo H. (1994). "Expression of DNA methyltransferase gene in mature and immature neurons as well as proliferating cells in mice". *Differentiation* 56: 39-44.

Gritti A., Frolichsthal-Schoeller P., Galli R., Parati E. A., Cova L., Pagano S. F., Bjornson C. R. and Vescovi A. L. (1999). "Epidermal and fibroblast growth factors behave as mitogenic regulators for a single multipotent stem cell-like population from the subventricular region of the adult mouse forebrain". *J Neurosci* 19: 3287-3297.

Gu T. P., Guo F., Yang H., Wu H. P., Xu G. F., Liu W., Xie Z. G., Shi L., He X., Jin S. G., Iqbal K., Shi Y. G., Deng Z., Szabo P. E., Pfeifer G. P., Li J. and Xu G. L. (2011). "The role of Tet3 DNA dioxygenase in epigenetic reprogramming by oocytes". *Nature* 477: 606-610.

Guan W., Guyot R., Samarut J., Flamant F., Wong J. and Gauthier K. C. (2017). "Methylcytosine dioxygenase TET3 interacts with thyroid hormone nuclear receptors and stabilizes their association to chromatin". *Proc Natl Acad Sci U S A* 114: 8229-8234.

Gurdon J. B. (1962). "The developmental capacity of nuclei taken from intestinal epithelium cells of feeding tadpoles". *J Embryol Exp Morphol* 10: 622-640.

Hackett J. A., Sengupta R., Zylicz J. J., Murakami K., Lee C., Down T. A. and Surani M. A. (2013). "Germline DNA demethylation dynamics and imprint erasure through 5-hydroxymethylcytosine". *Science* 339: 448-452.

Hahn M. A., Qiu R., Wu X., Li A. X., Zhang H., Wang J., Jui J., Jin S. G., Jiang Y., Pfeifer G. P. and Lu Q. (2013). "Dynamics of 5-hydroxymethylcytosine and chromatin marks in Mammalian neurogenesis". *Cell Rep* 3: 291-300.

Hanna J., Markoulaki S., Schorderet P., Carey B. W., Beard C., Wernig M., Creyghton M. P., Steine E. J., Cassady J. P., Foreman R., Lengner C. J., Dausman J. A. and Jaenisch R. (2008). "Direct reprogramming of terminally differentiated mature B lymphocytes to pluripotency". *Cell* 133: 250-264.

Hayashi K. and Surani M. A. (2009). "Self-renewing epiblast stem cells exhibit continual delineation of germ cells with epigenetic reprogramming in vitro". *Development* 136: 3549-3556.

He S., Nakada D. and Morrison S. J. (2009). "Mechanisms of stem cell self-renewal". *Annu Rev Cell Dev Biol* 25: 377-406.

He Y. F., Li B. Z., Li Z., Liu P., Wang Y., Tang Q., Ding J., Jia Y., Chen Z., Li L., Sun Y., Li X., Dai Q., Song C. X., Zhang K., He C. and Xu G. L. (2011). "Tet-mediated formation of 5-carboxylcytosine and its excision by TDG in mammalian DNA". *Science* 333: 1303-1307.

Hernandez Mora J. R., Sanchez-Delgado M., Petazzi P., Moran S., Esteller M., Iglesias-Platas I. and Monk D. (2017). "Profiling of oxBS-450K 5-hydroxymethylcytosine in human placenta and brain reveals enrichment at imprinted loci". *Epigenetics*: 0.

Hester M. E., Song S., Miranda C. J., Eagle A., Schwartz P. H. and Kaspar B. K. (2009). "Two factor reprogramming of human neural stem cells into pluripotency". *PLoS One* 4: e7044.

Hirai H., Karian P. and Kikyo N. (2011). "Regulation of embryonic stem cell self-renewal and pluripotency by leukaemia inhibitory factor". *Biochem J* 438: 11-23.

Hirasawa R. and Feil R. (2010). "Genomic imprinting and human disease". *Essays Biochem* 48: 187-200.

Hochedlinger K. and Jaenisch R. (2015). "Induced Pluripotency and Epigenetic Reprogramming". *Cold Spring Harb Perspect Biol* 7.

Hochedlinger K., Yamada Y., Beard C. and Jaenisch R. (2005). "Ectopic expression of Oct-4 blocks progenitor-cell differentiation and causes dysplasia in epithelial tissues". *Cell* 121: 465-477.

Hooper M., Hardy K., Handyside A., Hunter S. and Monk M. (1987). "HPRT-deficient (Lesch-Nyhan) mouse embryos derived from germline colonization by cultured cells". *Nature* 326: 292-295.

Hopfl G., Gassmann M. and Desbaillets I. (2004). "Differentiating embryonic stem cells into embryoid bodies". *Methods Mol Biol* 254: 79-98.

Hotta A. and Ellis J. (2008). "Retroviral vector silencing during iPS cell induction: an epigenetic beacon that signals distinct pluripotent states". *J Cell Biochem* 105: 940-948.

Hsieh J. and Gage F. H. (2004). "Epigenetic control of neural stem cell fate". *Curr Opin Genet Dev* 14: 461-469.

Huang Y., Pastor W. A., Shen Y., Tahiliani M., Liu D. R. and Rao A. (2010). "The behaviour of 5-hydroxymethylcytosine in bisulfite sequencing". *PLoS One* 5: e8888.

Hutnick L. K., Golshani P., Namihira M., Xue Z., Matynia A., Yang X. W., Silva A. J., Schweizer F. E. and Fan G. (2009). "DNA hypomethylation restricted to the murine forebrain induces cortical degeneration and impairs postnatal neuronal maturation". *Hum Mol Genet* 18: 2875-2888.

Iqbal K., Jin S. G., Pfeifer G. P. and Szabo P. E. (2011). "Reprogramming of the paternal genome upon fertilization involves genome-wide oxidation of 5-methylcytosine". *Proc Natl Acad Sci U S A* 108: 3642-3647.

Ito S., D'Alessio A. C., Taranova O. V., Hong K., Sowers L. C. and Zhang Y. (2010). "Role of Tet proteins in 5mC to 5hmC conversion, ES-cell self-renewal and inner cell mass specification". *Nature* 466: 1129-1133.

Ito S., Shen L., Dai Q., Wu S. C., Collins L. B., Swenberg J. A., He C. and Zhang Y. (2011). "Tet proteins can convert 5-methylcytosine to 5-formylcytosine and 5-carboxylcytosine". *Science* 333: 1300-1303.

Iyer L. M., Tahiliani M., Rao A. and Aravind L. (2009). "Prediction of novel families of enzymes involved in oxidative and other complex modifications of bases in nucleic acids". *Cell Cycle* 8: 1698-1710.

Jaenisch R. and Bird A. (2003). "Epigenetic regulation of gene expression: how the genome integrates intrinsic and environmental signals". *Nat Genet* 33 Suppl: 245-254.

Jawerka M., Colak D., Dimou L., Spiller C., Lagger S., Montgomery R. L., Olson E. N., Wurst W., Gottlicher M. and Gotz M. (2010). "The specific role of histone deacetylase 2 in adult neurogenesis". *Neuron Glia Biol* 6: 93-107.

Jelinic P. and Shaw P. (2007). "Loss of imprinting and cancer". *J Pathol* 211: 261-268.

Jensen J. B. and Parmar M. (2006). "Strengths and limitations of the neurosphere culture system". *Mol Neurobiol* 34: 153-161.

Jin S. G., Kadam S. and Pfeifer G. P. (2010). "Examination of the specificity of DNA methylation profiling techniques towards 5-methylcytosine and 5-hydroxymethylcytosine". *Nucleic Acids Res* 38: e125.

Jin S. G., Zhang Z. M., Dunwell T. L., Harter M. R., Wu X., Johnson J., Li Z., Liu J., Szabo P. E., Lu Q., Xu G. L., Song J. and Pfeifer G. P. (2016). "Tet3 Reads 5-Carboxylcytosine through Its CXXC Domain and Is a Potential Guardian against Neurodegeneration". *Cell Rep* 14: 493-505.

Johnson W. B., Ruppe M. D., Rockenstein E. M., Price J., Sarthy V. P., Verderber L. C. and Mucke L. (1995). "Indicator expression directed by regulatory sequences of the glial fibrillary acidic protein (GFAP) gene: in vivo comparison of distinct GFAP-lacZ transgenes". *Glia* 13: 174-184.

Kaas G. A., Zhong C., Eason D. E., Ross D. L., Vachhani R. V., Ming G. L., King J. R., Song H. and Sweatt J. D. (2013). "TET1 controls CNS 5-methylcytosine hydroxylation, active DNA demethylation, gene transcription, and memory formation". *Neuron* 79: 1086-1093.

Kar S., Parbin S., Deb M., Shilpi A., Sengupta D., Rath S. K., Rakshit M., Patra A. and Patra S. K. (2014). "Epigenetic choreography of stem cells: the DNA demethylation episode of development". *Cell Mol Life Sci* 71: 1017-1032.

Kempermann G., Song H. and Gage F. H. (2015). "Neurogenesis in the Adult Hippocampus". *Cold Spring Harb Perspect Biol* 7: a018812.

Kim J. B., Greber B., Arauzo-Bravo M. J., Meyer J., Park K. I., Zaehres H. and Scholer H. R. (2009a). "Direct reprogramming of human neural stem cells by OCT4". *Nature* 461: 649-643.

Kim J. B., Sebastiano V., Wu G., Arauzo-Bravo M. J., Sasse P., Gentile L., Ko K., Ruau D., Ehrich M., van den Boom D., Meyer J., Hubner K., Bernemann C., Ortmeier C., Zenke M., Fleischmann B. K., Zaehres H. and Scholer H. R. (2009b). "Oct4-induced pluripotency in adult neural stem cells". *Cell* 136: 411-419.

Kim J. B., Zaehres H., Arauzo-Bravo M. J. and Scholer H. R. (2009c). "Generation of induced pluripotent stem cells from neural stem cells". *Nat Protoc* 4: 1464-1470.

Kim J. B., Zaehres H., Wu G., Gentile L., Ko K., Sebastiano V., Arauzo-Bravo M. J., Ruau D., Han D. W., Zenke M. and Scholer H. R. (2008). "Pluripotent stem cells induced from adult neural stem cells by reprogramming with two factors". *Nature* 454: 646-650.

Kim K., Zhao R., Doi A., Ng K., Unternaehrer J., Cahan P., Huo H., Loh Y. H., Aryee M. J., Lensch M. W., Li H., Collins J. J., Feinberg A. P. and Daley G. Q. (2011). "Donor cell type can influence the epigenome and differentiation potential of human induced pluripotent stem cells". *Nat Biotechnol* 29: 1117-1119.

Kim M. J., Choi H. W., Jang H. J., Chung H. M., Arauzo-Bravo M. J., Scholer H. R. and Do J. T. (2013). "Conversion of genomic imprinting by reprogramming and redifferentiation". *J Cell Sci* 126: 2516-2524.

Kleinsmith L. J. and Pierce G. B., Jr. (1964). "Multipotentiality of Single Embryonal Carcinoma Cells". *Cancer Res* 24: 1544-1551.

Ko M., Huang Y., Jankowska A. M., Pape U. J., Tahiliani M., Bandukwala H. S., An J., Lamperti E. D., Koh K. P., Ganetzky R., Liu X. S., Aravind L., Agarwal S., Maciejewski J. P. and Rao A. (2010). "Impaired hydroxylation of 5-methylcytosine in myeloid cancers with mutant TET2". *Nature* 468: 839-843.

Koh K. P., Yabuuchi A., Rao S., Huang Y., Cunniff K., Nardone J., Laiho A., Tahiliani M., Sommer C. A., Mostoslavsky G., Lahesmaa R., Orkin S. H., Rodig S. J., Daley G. Q. and Rao A. (2011). "Tet1 and Tet2 regulate 5-hydroxymethylcytosine production and cell lineage specification in mouse embryonic stem cells". *Cell Stem Cell* 8: 200-213.

Kohli R. M. and Zhang Y. (2013). "TET enzymes, TDG and the dynamics of DNA demethylation". *Nature* 502: 472-479.

Kokovay E., Wang Y., Kusek G., Wurster R., Lederman P., Lowry N., Shen Q. and Temple S. (2012). "VCAM1 is essential to maintain the structure of the SVZ niche and acts as an environmental sensor to regulate SVZ lineage progression". *Cell Stem Cell* 11: 220-230.

Kouzarides T. (2007). "Chromatin modifications and their function". *Cell* 128: 693-705.

Kriaucionis S. and Heintz N. (2009). "The nuclear DNA base 5-hydroxymethylcytosine is present in Purkinje neurons and the brain". *Science* 324: 929-930.

Krishnakumar R. and Blelloch R. H. (2013). "Epigenetics of cellular reprogramming". *Curr Opin Genet Dev* 23: 548-555.

Kuang S., Kuroda K., Le Grand F. and Rudnicki M. A. (2007). "Asymmetric self-renewal and commitment of satellite stem cells in muscle". *Cell* 129: 999-1010.

Kuhn H. G., Eisch A. J., Spalding K. and Peterson D. A. (2016). "Detection and Phenotypic Characterization of Adult Neurogenesis". *Cold Spring Harb Perspect Biol* 8: a025981.

Kuttler F. and Mai S. (2006). "c-Myc, Genomic Instability and Disease". *Genome Dyn* 1: 171-190.

Lapidot T. and Kollet O. (2002). "The essential roles of the chemokine SDF-1 and its receptor CXCR4 in human stem cell homing and repopulation of transplanted immune-deficient NOD/SCID and NOD/SCID/B2m(null) mice". *Leukemia* 16: 1992-2003.

Lee H. J., Hore T. A. and Reik W. (2014). "Reprogramming the methylome: erasing memory and creating diversity". *Cell Stem Cell* 14: 710-719.

Lee H. K., Lee D. S. and Park J. C. (2015). "Nuclear factor I-C regulates E-cadherin via control of KLF4 in breast cancer". *BMC Cancer* 15: 113.

Li B., Carey M. and Workman J. L. (2007). "The role of chromatin during transcription". *Cell* 128: 707-719.

Li H., Zhao P., Xu Q., Shan S., Hu C., Qiu Z. and Xu X. (2016). "The autism-related gene SNRPN regulates cortical and spine development via controlling nuclear receptor Nr4a1". *Sci Rep* 6: 29878.

Li L. and Xie T. (2005). "Stem cell niche: structure and function". *Annu Rev Cell Dev Biol* 21: 605-631.

Li Q., Fan Y., Sun X. and Yu Y. (2013). "Generation of induced pluripotent stem cells from human amniotic fluid cells by reprogramming with two factors in feeder-free conditions". *J Reprod Dev* 59: 72-77.

Li T., Yang D., Li J., Tang Y., Yang J. and Le W. (2015). "Critical role of Tet3 in neural progenitor cell maintenance and terminal differentiation". *Mol Neurobiol* 51: 142-154.

Li X., Barkho B. Z., Luo Y., Smrt R. D., Santistevan N. J., Liu C., Kuwabara T., Gage F. H. and Zhao X. (2008). "Epigenetic regulation of the stem cell mitogen Fgf-2 by Mbd1 in adult neural stem/progenitor cells". *J Biol Chem* 283: 27644-27652.

Liang G. and Zhang Y. (2013). "Genetic and epigenetic variations in iPSCs: potential causes and implications for application". *Cell Stem Cell* 13: 149-159.

Lim D. A. and Alvarez-Buylla A. (2016). "The Adult Ventricular-Subventricular Zone (V-SVZ) and Olfactory Bulb (OB) Neurogenesis". *Cold Spring Harb Perspect Biol* 8.

Lin S. P., Youngson N., Takada S., Seitz H., Reik W., Paulsen M., Cavaille J. and Ferguson-Smith A. C. (2003). "Asymmetric regulation of imprinting on the maternal and paternal chromosomes at the Dlk1-Gtl2 imprinted cluster on mouse chromosome 12". *Nat Genet* 35: 97-102.

Lozano-Ureña A., Montalbán-Loro R., Ferguson-Smith AC. and Ferrón SR. (2017). "Genomic imprinting and the regulation of postnatal neurogenesis". *Brain Plasticity* 3: 89-98.

Liu L., Mao S. Q., Ray C., Zhang Y., Bell F. T., Ng S. F., Xu G. L. and Li X. (2015). "Differential regulation of genomic imprinting by TET proteins in embryonic stem cells". *Stem Cell Res* 15: 435-443.

Lu X. and Zhao T. (2013). "Clinical therapy using iPSCs: hopes and challenges". *Genomics Proteomics Bioinformatics* 11: 294-298.

Luger K. and Richmond T. J. (1998). "DNA binding within the nucleosome core". *Curr Opin Struct Biol* 8: 33-40.

Lunyak V. V., Burgess R., Prefontaine G. G., Nelson C., Sze S. H., Chenoweth J., Schwartz P., Pevzner P. A., Glass C., Mandel G. and Rosenfeld M. G. (2002). "Corepressor-dependent silencing of chromosomal regions encoding neuronal genes". *Science* 298: 1747-1752.

Lyssiotis C. A., Walker J., Wu C., Kondo T., Schultz P. G. and Wu X. (2007). "Inhibition of histone deacetylase activity induces developmental plasticity in oligodendrocyte precursor cells". *Proc Natl Acad Sci U S A* 104: 14982-14987.

Llorens-Bobadilla E. and Martin-Villalba A. (2017). "Adult NSC diversity and plasticity: the role of the niche". *Curr Opin Neurobiol* 42: 68-74.

Llorens-Bobadilla E., Zhao S., Baser A., Saiz-Castro G., Zwadlo K. and Martin-Villalba A. (2015). "Single-Cell Transcriptomics Reveals a Population of Dormant Neural Stem Cells that Become Activated upon Brain Injury". *Cell Stem Cell* 17: 329-340.

Malatesta P., Hartfuss E. and Gotz M. (2000). "Isolation of radial glial cells by fluorescent-activated cell sorting reveals a neuronal lineage". *Development* 127: 5253-5263.

Marmorstein R. and Trievel R. C. (2009). "Histone modifying enzymes: structures, mechanisms, and specificities". *Biochim Biophys Acta* 1789: 58-68.

Masui S., Nakatake Y., Toyooka Y., Shimosato D., Yagi R., Takahashi K., Okochi H., Okuda A., Matoba R., Sharov A. A., Ko M. S. and Niwa H. (2007). "Pluripotency governed by Sox2 via regulation of Oct3/4 expression in mouse embryonic stem cells". *Nat Cell Biol* 9: 625-635.

Mellen M., Ayata P., Dewell S., Kriaucionis S. and Heintz N. (2012). "MeCP2 binds to 5hmC enriched within active genes and accessible chromatin in the nervous system". *Cell* 151: 1417-1430.

Menn B., Garcia-Verdugo J. M., Yaschine C., Gonzalez-Perez O., Rowitch D. and Alvarez-Buylla A. (2006). "Origin of oligodendrocytes in the subventricular zone of the adult brain". *J Neurosci* 26: 7907-7918.

Merkle F. T., Tramontin A. D., Garcia-Verdugo J. M. and Alvarez-Buylla A. (2004). "Radial glia give rise to adult neural stem cells in the subventricular zone". *Proc Natl Acad Sci U S A* 101: 17528-17532.

Mich J. K., Signer R. A., Nakada D., Pineda A., Burgess R. J., Vue T. Y., Johnson J. E. and Morrison S. J. (2014). "Prospective identification of functionally distinct stem cells and neurosphere-initiating cells in adult mouse forebrain". *Elife* 3: e02669.

Mikkelsen T. S., Hanna J., Zhang X., Ku M., Wernig M., Schorderet P., Bernstein B. E., Jaenisch R., Lander E. S. and Meissner A. (2008). "Dissecting direct reprogramming through integrative genomic analysis". *Nature* 454: 49-55.

Ming G. L. and Song H. (2011). "Adult neurogenesis in the mammalian brain: significant answers and significant questions". *Neuron* 70: 687-702.

Mirzadeh Z., Merkle F. T., Soriano-Navarro M., Garcia-Verdugo J. M. and Alvarez-Buylla A. (2008). "Neural stem cells confer unique pinwheel architecture to the ventricular surface in neurogenic regions of the adult brain". *Cell Stem Cell* 3: 265-278.

Miura T., Katakura Y., Yamamoto K., Uehara N., Tsuchiya T., Kim E. H. and Shirahata S. (2001). "Neural stem cells lose telomerase activity upon differentiating into astrocytes". *Cytotechnology* 36: 137-144.

Miyazaki K., Mapendano C. K., Fuchigami T., Kondo S., Ohta T., Kinoshita A., Tsukamoto K., Yoshiura K., Niikawa N. and Kishino T. (2009). "Developmentally dynamic changes of DNA methylation in the mouse Snurf/Snrpn gene". *Gene* 432: 97-101.

Montagner S., Leoni C., Emming S., Della Chiara G., Balestrieri C., Barozzi I., Piccolo V., Togher S., Ko M., Rao A., Natoli G. and Monticelli S. (2017). "TET2 Regulates Mast Cell Differentiation and Proliferation through Catalytic and Non-catalytic Activities". *Cell Rep* 20: 1744.

Montalban-Loro R., Domingo-Muelas A., Bizy A. and Ferron S. R. (2015). "Epigenetic regulation of stemness maintenance in the neurogenic niches". *World J Stem Cells* 7: 700-710.

Morita S., Kojima T. and Kitamura T. (2000). "Plat-E: an efficient and stable system for transient packaging of retroviruses". *Gene Ther* 7: 1063-1066.

Morrens J., Van Den Broeck W. and Kempermann G. (2012). "Glial cells in adult neurogenesis". *Glia* 60: 159-174.

Morrison S. J. and Kimble J. (2006). "Asymmetric and symmetric stem-cell divisions in development and cancer". *Nature* 441: 1068-1074.

Morshead C. M., Reynolds B. A., Craig C. G., McBurney M. W., Staines W. A., Morassutti D., Weiss S. and van der Kooy D. (1994). "Neural stem cells in the adult mammalian forebrain: a relatively quiescent subpopulation of subependymal cells". *Neuron* 13: 1071-1082.

Munzel M., Globisch D., Bruckl T., Wagner M., Welzmiller V., Michalakis S., Muller M., Biel M. and Carell T. (2010). "Quantification of the sixth DNA base hydroxymethylcytosine in the brain". *Angew Chem Int Ed Engl* 49: 5375-5377.

Nakamura T., Liu Y. J., Nakashima H., Umehara H., Inoue K., Matoba S., Tachibana M., Ogura A., Shinkai Y. and Nakano T. (2012). "PGC7 binds histone H3K9me2 to protect against conversion of 5mC to 5hmC in early embryos". *Nature* 486: 415-419.

Nashun B., Hill P. W. and Hajkova P. (2015). "Reprogramming of cell fate: epigenetic memory and the erasure of memories past". *EMBO J* 34: 1296-1308.

Nichols J. and Smith A. (2009). "Naive and primed pluripotent states". *Cell Stem Cell* 4: 487-492.

Noctor S. C., Flint A. C., Weissman T. A., Dammerman R. S. and Kriegstein A. R. (2001). "Neurons derived from radial glial cells establish radial units in neocortex". *Nature* 409: 714-720.

Olins D. E. and Olins A. L. (2003). "Chromatin history: our view from the bridge". *Nat Rev Mol Cell Biol* 4: 809-814.

Paddison P. J., Caudy A. A., Bernstein E., Hannon G. J. and Conklin D. S. (2002). "Short hairpin RNAs (shRNAs) induce sequence-specific silencing in mammalian cells". *Genes Dev* 16: 948-958.

Papp B. and Plath K. (2013). "Epigenetics of reprogramming to induced pluripotency". *Cell* 152: 1324-1343.

Park D. H., Hong S. J., Salinas R. D., Liu S. J., Sun S. W., Sgualdino J., Testa G., Matzuk M. M., Iwamori N. and Lim D. A. (2014). "Activation of neuronal gene expression by the JMJD3 demethylase is required for postnatal and adult brain neurogenesis". *Cell Rep* 8: 1290-1299.

Park I. H., Lerou P. H., Zhao R., Huo H. and Daley G. Q. (2008a). "Generation of human-induced pluripotent stem cells". *Nat Protoc* 3: 1180-1186.

Park I. H., Zhao R., West J. A., Yabuuchi A., Huo H., Ince T. A., Lerou P. H., Lensch M. W. and Daley G. Q. (2008b). "Reprogramming of human somatic cells to pluripotency with defined factors". *Nature* 451: 141-146.

Pastor W. A., Aravind L. and Rao A. (2013). "TETonic shift: biological roles of TET proteins in DNA demethylation and transcription". *Nat Rev Mol Cell Biol* 14: 341-356.

Pastrana E., Cheng L. C. and Doetsch F. (2009). "Simultaneous prospective purification of adult subventricular zone neural stem cells and their progeny". *Proc Natl Acad Sci U S A* 106: 6387-6392.

Pastrana E., Silva-Vargas V. and Doetsch F. (2011). "Eyes wide open: a critical review of sphere-formation as an assay for stem cells". *Cell Stem Cell* 8: 486-498.

Pera M. F. and Tam P. P. (2010). "Extrinsic regulation of pluripotent stem cells". *Nature* 465: 713-720.

Perera A., Eisen D., Wagner M., Laube S. K., Kunzel A. F., Koch S., Steinbacher J., Schulze E., Splith V., Mittermeier N., Muller M., Biel M., Carell T. and Michalakis S. (2015). "TET3 is recruited by REST for context-specific hydroxymethylation and induction of gene expression". *Cell Rep* 11: 283-294.

Perez J. D., Rubinstein N. D. and Dulac C. (2016). "New Perspectives on Genomic Imprinting, an Essential and Multifaceted Mode of Epigenetic Control in the Developing and Adult Brain". *Annu Rev Neurosci* 39: 347-384.

Pesce M., Gross M. K. and Scholer H. R. (1998). "In line with our ancestors: Oct-4 and the mammalian germ". *Bioessays* 20: 722-732.

Piccolo F. M., Bagci H., Brown K. E., Landeira D., Soza-Ried J., Feytout A., Mooijman D., Hajkova P., Leitch H. G., Tada T., Kriaucionis S., Dawlaty M. M., Jaenisch R., Merkenschlager M. and Fisher A. G.

(2013). "Different roles for Tet1 and Tet2 proteins in reprogramming-mediated erasure of imprints induced by EGC fusion". *Mol Cell* 49: 1023-1033.

Planello A. C., Ji J., Sharma V., Singhania R., Mbabaali F., Muller F., Alfaro J. A., Bock C., De Carvalho D. D. and Batada N. N. (2014). "Aberrant DNA methylation reprogramming during induced pluripotent stem cell generation is dependent on the choice of reprogramming factors". *Cell Regen (Lond)* 3: 4.

Polo J. M., Liu S., Figueroa M. E., Kulalert W., Eminli S., Tan K. Y., Apostolou E., Stadtfeld M., Li Y., Shioda T., Natesan S., Wagers A. J., Melnick A., Evans T. and Hochedlinger K. (2010). "Cell type of origin influences the molecular and functional properties of mouse induced pluripotent stem cells". *Nat Biotechnol* 28: 848-855.

Porlan E., Marti-Prado B., Morante-Redolat J. M., Consiglio A., Delgado A. C., Kypta R., Lopez-Otin C., Kirstein M. and Farinas I. (2014). "MT5-MMP regulates adult neural stem cell functional quiescence through the cleavage of N-cadherin". *Nat Cell Biol* 16: 629-638.

Porlan E., Perez-Villalba A., Delgado A. C. and Ferron S. R. (2013). "Paracrine regulation of neural stem cells in the subependymal zone". *Arch Biochem Biophys* 534: 11-19.

Potten C. S. and Loeffler M. (1990). "Stem cells: attributes, cycles, spirals, pitfalls and uncertainties. Lessons for and from the crypt". *Development* 110: 1001-1020.

Prescott A. R., Bales A., James J., Trinkle-Mulcahy L. and Sleeman J. E. (2014). "Time-resolved quantitative proteomics implicates the core snRNP protein SmB together with SMN in neural trafficking". *J Cell Sci* 127: 812-827.

Prokhorova T. A., Harkness L. M., Frandsen U., Ditzel N., Schroder H. D., Burns J. S. and Kassem M. (2009). "Teratoma formation by human embryonic stem cells is site dependent and enhanced by the presence of Matrigel". *Stem Cells Dev* 18: 47-54.

Przyborski S. A. (2005). "Differentiation of human embryonic stem cells after transplantation in immune-deficient mice". *Stem Cells* 23: 1242-1250.

Ramirez-Castillejo C., Sanchez-Sanchez F., Andreu-Agullo C., Ferron S. R., Aroca-Aguilar J. D., Sanchez P., Mira H., Escribano J. and Farinas I. (2006). "Pigment epithelium-derived factor is a niche signal for neural stem cell renewal". *Nat Neurosci* 9: 331-339.

Raponi E., Agenes F., Delphin C., Assard N., Baudier J., Legraverend C. and Deloulme J. C. (2007). "S100B expression defines a state in which GFAP-expressing cells lose their neural stem cell potential and acquire a more mature developmental stage". *Glia* 55: 165-177.

Reynolds B. A. and Rietze R. L. (2005). "Neural stem cells and neurospheres--re-evaluating the relationship". *Nat Methods* 2: 333-336.

Reynolds B. A. and Weiss S. (1992). "Generation of neurons and astrocytes from isolated cells of the adult mammalian central nervous system". *Science* 255: 1707-1710.

Ribeiro Xavier A. L., Kress B. T., Goldman S. A., Lacerda de Menezes J. R. and Nedergaard M. (2015). "A Distinct Population of Microglia Supports Adult Neurogenesis in the Subventricular Zone". *J Neurosci* 35: 11848-11861.

Rraklli V., Sodersten E., Nyman U., Hagey D. W. and Holmberg J. (2016). "Elevated levels of ZAC1 disrupt neurogenesis and promote rapid in vivo reprogramming". *Stem Cell Res* 16: 1-9.

Sanchez-Danes A., Richaud-Patin Y., Carballo-Carbajal I., Jimenez-Delgado S., Caig C., Mora S., Di Guglielmo C., Ezquerra M., Patel B., Giralt A., Canals J. M., Memo M., Alberch J., Lopez-Barneo J., Vila M., Cuervo A. M., Tolosa E., Consiglio A. and Raya A. (2012). "Disease-specific phenotypes in dopamine neurons from human iPS-based models of genetic and sporadic Parkinson's disease". *EMBO Mol Med* 4: 380-395.

Santos F., Peat J., Burgess H., Rada C., Reik W. and Dean W. (2013). "Active demethylation in mouse zygotes involves cytosine deamination and base excision repair". *Epigenetics Chromatin* 6: 39.

Saunders A., Faiola F. and Wang J. (2013). "Concise review: pursuing self-renewal and pluripotency with the stem cell factor Nanog". *Stem Cells* 31: 1227-1236.

Schilling E. and Rehli M. (2007). "Global, comparative analysis of tissue-specific promoter CpG methylation". *Genomics* 90: 314-323.

Schofield R. (1978). "The relationship between the spleen colony-forming cell and the haemopoietic stem cell". *Blood Cells* 4: 7-25.

Siebzehnrubl F. A., Buslei R., Eyupoglu I. Y., Seufert S., Hahnen E. and Blumcke I. (2007). "Histone deacetylase inhibitors increase neuronal differentiation in adult forebrain precursor cells". *Exp Brain Res* 176: 672-678.

Sikorska M., Sandhu J. K., Deb-Rinker P., Jezierski A., Leblanc J., Charlebois C., Ribecco-Lutkiewicz M., Bani-Yaghoub M. and Walker P. R. (2008). "Epigenetic modifications of SOX2 enhancers, SRR1 and SRR2, correlate with in vitro neural differentiation". *J Neurosci Res* 86: 1680-1693.

Silva-Vargas V., Crouch E. E. and Doetsch F. (2013). "Adult neural stem cells and their niche: a dynamic duo during homeostasis, regeneration, and aging". *Curr Opin Neurobiol* 23: 935-942.

Silva J., Barrandon O., Nichols J., Kawaguchi J., Theunissen T. W. and Smith A. (2008). "Promotion of reprogramming to ground state pluripotency by signal inhibition". *PLoS Biol* 6: e253.

Smallwood S. A. and Kelsey G. (2012). "De novo DNA methylation: a germ cell perspective". *Trends Genet* 28: 33-42.

Smith A. G., Heath J. K., Donaldson D. D., Wong G. G., Moreau J., Stahl M. and Rogers D. (1988). "Inhibition of pluripotential embryonic stem cell differentiation by purified polypeptides". *Nature* 336: 688-690.

Smrt R. D., Eaves-Egenes J., Barkho B. Z., Santistevan N. J., Zhao C., Aimone J. B., Gage F. H. and Zhao X. (2007). "Mecp2 deficiency leads to delayed maturation and altered gene expression in hippocampal neurons". *Neurobiol Dis* 27: 77-89.

Soen Y., Mori A., Palmer T. D. and Brown P. O. (2006). "Exploring the regulation of human neural precursor cell differentiation using arrays of signaling microenvironments". *Mol Syst Biol* 2: 37.

Spelke D. P., Ortmann D., Khademhosseini A., Ferreira L. and Karp J. M. (2011). "Methods for embryoid body formation: the microwell approach". *Methods Mol Biol* 690: 151-162.

Sridharan R., Tchieu J., Mason M. J., Yachechko R., Kuoy E., Horvath S., Zhou Q. and Plath K. (2009). "Role of the murine reprogramming factors in the induction of pluripotency". *Cell* 136: 364-377.

Stadtfeld M., Apostolou E., Akutsu H., Fukuda A., Follett P., Natesan S., Kono T., Shioda T. and Hochedlinger K. (2010). "Aberrant silencing of imprinted genes on chromosome 12qF1 in mouse induced pluripotent stem cells". *Nature* 465: 175-181.

Stadtfeld M., Brennand K. and Hochedlinger K. (2008). "Reprogramming of pancreatic beta cells into induced pluripotent stem cells". *Curr Biol* 18: 890-894.

Stadtfeld M. and Hochedlinger K. (2010). "Induced pluripotency: history, mechanisms, and applications". *Genes Dev* 24: 2239-2263.

Strahl B. D. and Allis C. D. (2000). "The language of covalent histone modifications". *Nature* 403: 41-45.

Strogantsev R., Krueger F., Yamazawa K., Shi H., Gould P., Goldman-Roberts M., McEwen K., Sun B., Pedersen R. and Ferguson-Smith A. C. (2015). "Allele-specific binding of ZFP57 in the epigenetic regulation of imprinted and non-imprinted monoallelic expression". *Genome Biol* 16: 112.

Suh H., Consiglio A., Ray J., Sawai T., D'Amour K. A. and Gage F. H. (2007). "In vivo fate analysis reveals the multipotent and self-renewal capacities of Sox2+ neural stem cells in the adult hippocampus". *Cell Stem Cell* 1: 515-528.

Sun Z., Terragni J., Borgaro J. G., Liu Y., Yu L., Guan S., Wang H., Sun D., Cheng X., Zhu Z., Pradhan S. and Zheng Y. (2013). "High-resolution enzymatic mapping of genomic 5-hydroxymethylcytosine in mouse embryonic stem cells". *Cell Rep* 3: 567-576.

Surani M. A., Hayashi K. and Hajkova P. (2007). "Genetic and epigenetic regulators of pluripotency". *Cell* 128: 747-762.

Sutcliffe J. S., Nakao M., Christian S., Orstavik K. H., Tommerup N., Ledbetter D. H. and Beaudet A. L. (1994). "Deletions of a differentially methylated CpG island at the SNRPN gene define a putative imprinting control region". *Nat Genet* 8: 52-58.

Suzuki A., Raya A., Kawakami Y., Morita M., Matsui T., Nakashima K., Gage F. H., Rodriguez-Esteban C. and Izpisua Belmonte J. C. (2006). "Nanog binds to Smad1 and blocks bone morphogenetic protein-induced differentiation of embryonic stem cells". *Proc Natl Acad Sci U S A* 103: 10294-10299.

Szulwach K. E., Li X., Li Y., Song C. X., Wu H., Dai Q., Irier H., Upadhyay A. K., Gearing M., Levey A. I., Vasanthakumar A., Godley L. A., Chang Q., Cheng X., He C. and Jin P. (2011). "5-hmC-mediated epigenetic dynamics during postnatal neurodevelopment and aging". *Nat Neurosci* 14: 1607-1616.

Szwagierczak A., Bultmann S., Schmidt C. S., Spada F. and Leonhardt H. (2010). "Sensitive enzymatic quantification of 5-hydroxymethylcytosine in genomic DNA". *Nucleic Acids Res* 38: e181.

Tahiliani M., Koh K. P., Shen Y., Pastor W. A., Bandukwala H., Brudno Y., Agarwal S., Iyer L. M., Liu D. R., Aravind L. and Rao A. (2009). "Conversion of 5-methylcytosine to 5-hydroxymethylcytosine in mammalian DNA by MLL partner TET1". *Science* 324: 930-935.

Taiwo O., Wilson G. A., Morris T., Seisenberger S., Reik W., Pearce D., Beck S. and Butcher L. M. (2012). "Methylome analysis using MeDIP-seq with low DNA concentrations". *Nat Protoc* 7: 617-636.

Takahashi K. and Yamanaka S. (2006). "Induction of pluripotent stem cells from mouse embryonic and adult fibroblast cultures by defined factors". *Cell* 126: 663-676.

Takahashi N., Gray D., Strogantsev R., Noon A., Delahaye C., Skarnes W. C., Tate P. H. and Ferguson-Smith A. C. (2015). "ZFP57 and the Targeted Maintenance of Postfertilization Genomic Imprints". *Cold Spring Harb Symp Quant Biol* 80: 177-187.

Tavazoie M., Van der Veken L., Silva-Vargas V., Louissaint M., Colonna L., Zaidi B., Garcia-Verdugo J. M. and Doetsch F. (2008). "A specialized vascular niche for adult neural stem cells". *Cell Stem Cell* 3: 279-288.

Tesar P. J., Chenoweth J. G., Brook F. A., Davies T. J., Evans E. P., Mack D. L., Gardner R. L. and McKay R. D. (2007). "New cell lines from mouse epiblast share defining features with human embryonic stem cells". *Nature* 448: 196-199.

Tessarz P. and Kouzarides T. (2014). "Histone core modifications regulating nucleosome structure and dynamics". *Nat Rev Mol Cell Biol* 15: 703-708.

Theunissen T. W., van Oosten A. L., Castelo-Branco G., Hall J., Smith A. and Silva J. C. (2011). "Nanog overcomes reprogramming barriers and induces pluripotency in minimal conditions". *Curr Biol* 21: 65-71.

Thorvaldsen J. L., Duran K. L. and Bartolomei M. S. (1998). "Deletion of the H19 differentially methylated domain results in loss of imprinted expression of H19 and Igf2". *Genes Dev* 12: 3693-3702.

Tian C., Wang Y., Sun L., Ma K. and Zheng J. C. (2011). "Reprogrammed mouse astrocytes retain a "memory" of tissue origin and possess more tendencies for neuronal differentiation than reprogrammed mouse embryonic fibroblasts". *Protein Cell* 2: 128-140.

Till J. E. and Mc C. E. (1961). "A direct measurement of the radiation sensitivity of normal mouse bone marrow cells". *Radiat Res* 14: 213-222.

Tobin S. C. and Kim K. (2012). "Generating pluripotent stem cells: differential epigenetic changes during cellular reprogramming". *FEBS Lett* 586: 2874-2881.

Tramontin A. D., Garcia-Verdugo J. M., Lim D. A. and Alvarez-Buylla A. (2003). "Postnatal development of radial glia and the ventricular zone (VZ): a continuum of the neural stem cell compartment". *Cereb Cortex* 13: 580-587.

Tropberger P. and Schneider R. (2013). "Scratching the (lateral) surface of chromatin regulation by histone modifications". *Nat Struct Mol Biol* 20: 657-661.

Tumbar T., Guasch G., Greco V., Blanpain C., Lowry W. E., Rendl M. and Fuchs E. (2004). "Defining the epithelial stem cell niche in skin". *Science* 303: 359-363.

Utikal J., Maherali N., Kulalert W. and Hochedlinger K. (2009). "Sox2 is dispensable for the reprogramming of melanocytes and melanoma cells into induced pluripotent stem cells". *J Cell Sci* 122: 3502-3510.

Venkatraman A., He X. C., Thorvaldsen J. L., Sugimura R., Perry J. M., Tao F., Zhao M., Christenson M. K., Sanchez R., Yu J. Y., Peng L., Haug J. S., Paulson A., Li H., Zhong X. B., Clemens T. L., Bartolomei M. S. and Li L. (2013). "Maternal imprinting at the H19-Igf2 locus maintains adult haematopoietic stem cell quiescence". *Nature* 500: 345-349.

Vierbuchen T., Ostermeier A., Pang Z. P., Kokubu Y., Sudhof T. C. and Wernig M. (2010). "Direct conversion of fibroblasts to functional neurons by defined factors". *Nature* 463: 1035-1041.

Vila-Cejudo M., Ibanez E. and Santalo J. (2017). "Derivation of Stem Cell Lines from Mouse Preimplantation Embryos". *J Vis Exp*.

Waddington C. H. (1957). The strategy of the genes; a discussion of some aspects of theoretical biology. London,, Allen & Unwin.

Wagers A. J. (2012). "The stem cell niche in regenerative medicine". *Cell Stem Cell* 10: 362-369.

Wang J., Rao S., Chu J., Shen X., Levasseur D. N., Theunissen T. W. and Orkin S. H. (2006). "A protein interaction network for pluripotency of embryonic stem cells". *Nature* 444: 364-368.

Weismann A., Parker W. N. and Rōnníeldt H. (1893). The germ-plasm: a theory of heredity. New York,, C. Scribner's sons.

Weissman I. L. (2000). "Stem cells: units of development, units of regeneration, and units in evolution". *Cell* 100: 157-168.

Wernig M., Meissner A., Cassady J. P. and Jaenisch R. (2008). "c-Myc is dispensable for direct reprogramming of mouse fibroblasts". *Cell Stem Cell* 2: 10-12.

Wernig M., Meissner A., Foreman R., Brambrink T., Ku M., Hochedlinger K., Bernstein B. E. and Jaenisch R. (2007). "In vitro reprogramming of fibroblasts into a pluripotent ES-cell-like state". *Nature* 448: 318-324.

Wilkinson L. S., Davies W. and Isles A. R. (2007). "Genomic imprinting effects on brain development and function". *Nat Rev Neurosci* 8: 832-843.

Williams R. L., Hilton D. J., Pease S., Willson T. A., Stewart C. L., Gearing D. P., Wagner E. F., Metcalf D., Nicola N. A. and Gough N. M. (1988). "Myeloid leukaemia inhibitory factor maintains the developmental potential of embryonic stem cells". *Nature* 336: 684-687.

Williamson C. M., Turner M. D., Ball S. T., Nottingham W. T., Glenister P., Fray M., Tymowska-Lalanne Z., Plagge A., Powles-Glover N., Kelsey G., Maconochie M. and Peters J. (2006). "Identification of an imprinting control region affecting the expression of all transcripts in the Gnas cluster". *Nat Genet* 38: 350-355.

Wu H., Coskun V., Tao J., Xie W., Ge W., Yoshikawa K., Li E., Zhang Y. and Sun Y. E. (2010). "Dnmt3a-dependent nonpromoter DNA methylation facilitates transcription of neurogenic genes". *Science* 329: 444-448.

Wu X. and Zhang Y. (2017). "TET-mediated active DNA demethylation: mechanism, function and beyond". *Nat Rev Genet* 18: 517-534.

Xu L., Tang X., Wang Y., Xu H. and Fan X. (2015). "Radial glia, the keystone of the development of the hippocampal dentate gyrus". *Mol Neurobiol* 51: 131-141.

Xu Y., Xu C., Kato A., Tempel W., Abreu J. G., Bian C., Hu Y., Hu D., Zhao B., Cerovina T., Diao J., Wu F., He H. H., Cui Q., Clark E., Ma C., Barbara A., Veenstra G. J., Xu G., Kaiser U. B., Liu X. S., Sugrue S. P., He X., Min J., Kato Y. and Shi Y. G. (2012). "Tet3 CXXC domain and dioxygenase activity cooperatively regulate key genes for Xenopus eye and neural development". *Cell* 151: 1200-1213.

Yamaguchi S., Shen L., Liu Y., Sendler D. and Zhang Y. (2013). "Role of Tet1 in erasure of genomic imprinting". *Nature* 504: 460-464.

Yao B., Christian K. M., He C., Jin P., Ming G. L. and Song H. (2016). "Epigenetic mechanisms in neurogenesis". *Nat Rev Neurosci* 17: 537-549.

Ying Q. L., Stavridis M., Griffiths D., Li M. and Smith A. (2003). "Conversion of embryonic stem cells into neuroectodermal precursors in adherent monoculture". *Nat Biotechnol* 21: 183-186.

Ying Q. L., Wray J., Nichols J., Batlle-Morera L., Doble B., Woodgett J., Cohen P. and Smith A. (2008). "The ground state of embryonic stem cell self-renewal". *Nature* 453: 519-523.

Yu H., Su Y., Shin J., Zhong C., Guo J. U., Weng Y. L., Gao F., Geschwind D. H., Coppola G., Ming G. L. and Song H. (2015). "Tet3 regulates synaptic transmission and homeostatic plasticity via DNA oxidation and repair". *Nat Neurosci* 18: 836-843.

Yu J., Vodyanik M. A., Smuga-Otto K., Antosiewicz-Bourget J., Frane J. L., Tian S., Nie J., Jonsdottir G. A., Ruotti V., Stewart R., Slukvin, II and Thomson J. A. (2007). "Induced pluripotent stem cell lines derived from human somatic cells". *Science* 318: 1917-1920.

Zhang J., Dublin P., Griemsmann S., Klein A., Brehm R., Bedner P., Fleischmann B. K., Steinhauser C. and Theis M. (2013a). "Germ-line recombination activity of the widely used hGFAP-Cre and nestin-Cre transgenes". *PLoS One* 8: e82818.

Zhang J., Niu C., Ye L., Huang H., He X., Tong W. G., Ross J., Haug J., Johnson T., Feng J. Q., Harris S., Wiedemann L. M., Mishina Y. and Li L. (2003). "Identification of the haematopoietic stem cell niche and control of the niche size". *Nature* 425: 836-841.

Zhang R. R., Cui Q. Y., Murai K., Lim Y. C., Smith Z. D., Jin S., Ye P., Rosa L., Lee Y. K., Wu H. P., Liu W., Xu Z. M., Yang L., Ding Y. Q., Tang F., Meissner A., Ding C., Shi Y. and Xu G. L. (2013b). "Tet1 regulates adult hippocampal neurogenesis and cognition". *Cell Stem Cell* 13: 237-245.

Zhang W., Xia W., Wang Q., Towers A. J., Chen J., Gao R., Zhang Y., Yen C. A., Lee A. Y., Li Y., Zhou C., Liu K., Zhang J., Gu T. P., Chen X., Chang Z., Leung D., Gao S., Jiang Y. H. and Xie W. (2016). "Isoform Switch of TET1 Regulates DNA Demethylation and Mouse Development". *Mol Cell* 64: 1062-1073.

Zhao C., Deng W. and Gage F. H. (2008). "Mechanisms and functional implications of adult neurogenesis". *Cell* 132: 645-660.

Resumen

INTRODUCCIÓN

1. Células madre, unidades de desarrollo y regeneración.

Las células madre (SC, del inglés *Stem Cell*) son células no especializadas con la habilidad de autorrenovarse (dar lugar a células idénticas) y capaces de diferenciarse (adquisición de una identidad celular concreta) en uno o más tipos celulares especializados. De acuerdo con su potencial de diferenciación, las células madre se pueden clasificar en totipotentes, aquellas encontradas en el cigoto y capaces de dar lugar a todos los tejidos embrionarios y extraembrionarios, las células pluripotentes, localizadas en la masa celular interna del blastocisto con capacidad de diferenciarse en células de las tres capas embrionarias, y las multipotentes, situadas en los tejidos embrionarios y adultos y con capacidad de dar lugar a tipos celulares de un determinado linaje. Además, en base a su origen, podemos encontrar: células madre fisiológicas, donde quedarían englobadas las anteriores, células pluripotentes generadas por ingeniería genética (iPSCs, del inglés *Induced Pluripotent Stem Cells*) o las células madre cancerosas (CSC, del inglés *Cancer Stem Cell*).

Células madre embrionarias y pluripotencia

Las células madre embrionarias de ratón (ESCs, del inglés *Embryonic Stem Cells*) se obtienen de la masa celular interna del blastocisto y pueden ser expandidas *in vitro* en presencia de LIF (del inglés, *Leukaemia Inhibitor Factor*), además de diferenciadas en cualquiera de las tres capas embrionarias, mesodermo, endodermo y ectodermo. Esta pluripotencia puede ser testada mediante su capacidad de generar cuerpos embrioides (EB, del inglés *Embryoid body*) *in vitro* y teratomas *in vivo*. Las células del epiblasto (EpiSC, del inglés *Epiblast Stem Cells*) son células pluripotentes generadas en el embrión tras la implantación, aunque su potencialidad está algo más restringida que el de las ESCs.

Células pluripotentes inducidas y reprogramación

En el año 2006, Takahasi y Yamanaka consiguieron, mediante la introducción de cuatro factores exógenos (*Oct4*, *Klf4*, *Sox2* y *c-myc*), la conversión por primera vez de una célula madre diferenciada en una célula pluripotente inducida con características que mimetizaban a las ESCs, proceso conocido como *reprogramación celular*, el cual supuso un gran avance para la comunidad investigadora. Desde entonces, las iPSCs han sido obtenidas a partir de múltiples tejidos y son un modelo de estudio incomparable para el desarrollo temprano así como una prometedora herramienta en terapia celular. La forma más habitual de generar iPSCs requiere el uso de retrovirus como vectores para la introducción de los factores exógenos, que deben ser silenciados en las fases finales del proceso para conseguir una verdadera pluripotencia. Sin embargo, el uso de estos retrovirus, así como la relación de los factores exógenos con procesos cancerosos, hacen de estas células impropias para su uso en

terapia celular aunque se están desarrollando prometedoras tecnologías alternativas mediante el uso de proteínas recombinantes.

Células madre adultas: reservorios de precursores multipotentes

Las células madre adultas (ASC, del inglés *Adult Stem Cells*) tienen la capacidad de dividirse y generar células diferenciadas funcionales, fundamentales en la homeostasis y reparación tisular. Hasta la fecha, han sido identificadas y caracterizadas células madre en múltiples tejidos adultos, incluyendo el sistema nervioso. En condiciones de homeostasis, las ASCs tienen la capacidad de dar lugar a progenitores de rápida amplificación (TAP, del inglés *Transit Amplifying Cells*) para acabar diferenciándose en células funcionales específicas del tejido en particular. Estas ASC se encuentran en regiones concretas bien organizadas denominadas "*microambientes o nichos*" en los que los factores extrínsecos están finamente regulados para mantener a las células madre. De entre estos factores destacan los secretados por la vasculatura, los contactos célula-célula, las moléculas de señalización, etc. Las propiedades de las células madre adultas las convierten en candidatos plausibles en medicina regenerativa por lo que la comprensión de su regulación son requerimientos cruciales para su uso en terapia. En la actualidad, estas ASC están mejor posicionadas para su uso en terapia que las iPSC debido a que se encuentran de forma natural en el organismo y pueden ser moduladas *in vitro*. Además hay diversos tejidos accesibles para el uso de estas células como el cordón umbilical o la médula ósea.

2. Células madre neurales y neurogénesis adulta

La neurogénesis es el proceso de generar nuevas neuronas a partir de células madre neurales (NSC, del inglés *Neural Stem Cells*) que tienen la habilidad de dividirse, autorrenovarse y generar células diferenciadas durante toda la edad adulta. Las NSCs derivan de la glia radial embrionaria, reteniendo su carácter astrocitario y quedando localizadas en el adulto en dos regiones concretas, la zona subventricular (SVZ, del inglés *Subventricular Zone*) y la zona subgranular del giro dentado del hipocampo (SGZ, del inglés *Subgranular Zone*).

La zona subventricular y la neurogénesis al bulbo olfatorio

La SVZ es el nicho neurogénico más activo en ratones. En él residen las NSCs (células tipo B) que tienen la capacidad de autorrenovarse y diferenciarse en astrocitos, oligodendrocitos y neuronas. Estas células tipo B contactan con el ventrículo por un pequeño proceso apical rodeado de células ependimarias formando una típica organización en forma de roseta. Por su parte basal, estas células están en contacto con la vasculatura de la que reciben importantes señales. Una vez activadas, las células madre dan lugar a las células tipo C o TAPs que producen, a su vez, neuroblastos capaces de migrar hacia el bulbo olfatorio (OB, del inglés *Olfactory Bulb*) por la ruta de migración rostral (RMS, del

inglés *Rostral Migratory Stream*) donde finamente se integran y se diferencian en interneuronas. De forma importante en este proceso, el nicho neurogénico de la SVZ está finamente regulado por señales extrínsecas que garantizan el proceso durante toda la vida adulta. Debido a su arquitectura especial, las células reciben señales tanto del líquido cerebroespinal como de los vasos sanguíneos. Además, tanto los contactos célula-célula como las señales que reciben de su propia progenie promueven su quiescencia.

Las NSCs muestran características astrocitarias como son la expresión de GFAP o GLAST, aunque no se dispone de un marcar único que permita su distinción. Además, está bien establecida la coexistencia de dos estados diferentes, las NSCs quiescentes (qNSCs) y las NSCs activadas (aNSCs). Estas células, así como las distintas poblaciones de la SVZ pueden ser estudiadas mediante combinación de diferentes marcadores.

Células madre in vitro: el ensayo de neurosferas

Las células madre neurales pueden ser cultivadas *in vitro* en presencia de los mitógenos FGF (del inglés *Fibroblast Growth Factor*) y EGF (del inglés *Epidermal Growth factor*) y en condiciones no adherentes, donde su capacidad de autorrenovación puede ser estudiada. Para ello, tras la disección y disociación del tejido, las células son cultivadas, y una pequeña proporción es capaz de crecer formando agregados clonales conocidos como "*neurosferas*". Además, en condiciones adherentes, estás células son capaces de diferenciarse dando lugar a células del tejido neural: astrocitos, oligodendrocitos y neuronas. A pesar de las evidentes ventajas, el uso de neurosferas tiene unas ciertas limitaciones. Primero, la heterogeneidad de la neuroesfera donde las NSCs conviven con su progenie incluyendo células diferenciadas. Además, los progenitores TAP también son capaces de formar esferas aunque de forma más limitada. Por otra parte, la estimulación mitogénica provoca que tenga lugar una selección de las aNSCs mientras que las qNSC no son capaces de formar esferas. Recientemente, los avances conseguidos en el aislamiento de las distintas poblaciones de la SVZ mediante FACS (del inglés *Fluorescence Activated Cell Sorting*) permiten el estudio detallado de las mismas incluyendo a las qNSCs. Sumado a todo esto, la variabilidad experimental introducida en los cultivos entre diferentes laboratorios hace difícil en ocasiones el comparar o reproducir entre experimentos. Por todo esto, a pesar de que el ensayo de neurosferas en una herramienta útil para evaluar la capacidad de autorrenovación y la diferenciación de estas células, la complementación con los ensayos *in vivo* es todavía indispensable.

Reprogramación de NSCs

Las NSCs expresan de manera endógena los factores de reprogramación *Sox2*, *Klf4* y *c-myc*. Debido a esto, la reprogramación de estas células es posible utilizando únicamente dos (*Klf4* y *Oct4*) o un factor (*Oct4*), aunque con mucha menos eficiencia, lo que indica que estas células se encuentran en un estado intermedio entre el diferenciado y el pluripotente. En muchas ocasiones, la pluripotencia no es adquirida completamente hasta que en el medio no son aplicadas condiciones controladas y particulares. Esas condiciones incluyen el uso de inhibidores de rutas de señalización implicadas en diferenciación (MEK y GSK) así como el LIF (2i/LIF) permitiendo la generación de células verdaderamente pluripotentes.

3. Regulación epigenética de los nichos neurogénicos adultos

La epigenética es definida como el estudio de los cambios del genoma heredables que no implican cambios en la secuencia del ADN. Estas modificaciones son capaces de modular la expresión génica y entre ellas destacan la metilación del ADN y las modificaciones de histonas.

Metilación del ADN

La metilación del ADN supone la adición de un grupo metilo a la citosina y suelen tener lugar en regiones del ADN ricas en dinucleótidos CpG conocidas como “islas CpG”, siendo las ADN metiltransferasas (DNMTs) las implicadas en el establecimiento de este patrón de metilación. Por regla general, la presencia de metilaciones está relacionada con una inhibición de la transcripción, siendo un proceso esencial en el desarrollo neural, además de que la unión de diversos factores implicados en neurogénesis está regulada por la presencia de esta modificación. Por ejemplo, se ha descrito que el ADN está hipometilado en los progenitores neurales y la metilación es adquirida progresivamente durante la diferenciación neuronal.

La metilación es una marca reversible que puede ser eliminada de forma pasiva, por replicación del ADN, o de forma activa mediada por las enzimas TET (del inglés *Ten-Eleven Translocation proteins*) que son capaces de convertir la 5-metilcitosina (5mC) en 5-hidroximetilcitosina (5hmC), 5-formilcitosina (5fC) y 5- carboxilcitosina (5caC). Estos derivados pueden ser posteriormente eliminados a través de la ruta de escisión de bases (BER, del inglés *Base Excision Repair*) o por dilución pasiva. Se han descrito tres miembros de la familia: TET1, TET2 y TET3, y su actividad puede ser diferente dependiendo del momento y contexto celular. Además, recientemente se han establecido diferentes funciones para estas proteínas independientes de su actividad catalítica. La 5hmC es especialmente relevante en el cerebro, habiendo sido asociada al proceso de diferenciación. Particularmente, la metilación del ADN parece jugar un papel fundamental en el proceso de neurogénesis, además de que

enzimas como TET1 han sido implicadas en la regulación de la proliferación de los progenitores neurales en el hipocampo.

Modificaciones de histonas

El ADN es empaquetado alrededor de octámeros de histonas formando los nucleosomas. Estas histonas dejan al descubierto su residuo N-terminal para ser susceptible de modificación, provocando cambios en la estructura tridimensional de la cromatina reprimiendo o activando la transcripción. Entre las modificaciones de histonas destacan la acetilación y la metilación. La acetilación, catalizada por la histona acetiltransferasa, potencia la unión de factores de transcripción a la cromatina. Por otra parte, la metilación de las histonas, catalizada por la histona metiltransferasa, está asociada tanto con represión como con activación. Ambas modificaciones juegan papeles importantes en el proceso de neurogénesis habiendo, por ejemplo, marcas como la tri-metilación de la histona H3 en su lisina 9 ($H3K9me^3$) están asociadas con el mantenimiento del estado indiferenciado.

Impronta genómica y su papel en la neurogénesis adulta

En los mamíferos, a pesar de que la mayoría de genes son bialélicamente expresados o reprimidos, hay un pequeño porcentaje de genes, denominados "*genes imprintados*" que son expresados monoalélicamente dependiendo de su origen parental. Estos genes están generalmente organizados en grupos y regulados por regiones diferencialmente metiladas (DMR, del inglés *Differentially Methylated Region*) entre los dos cromosomas parentales. Estos patrones de metilación son establecidos en la línea germinal y mantenidos en la edad adulta aunque este estado de impronta puede ser regulado de una manera tejido-específica. Los genes imprintados están implicados en una gran diversidad de procesos siendo las funciones neurológicas de las más importantes.

4. Cambios epigenéticos durante el proceso de reprogramación

El proceso de reprogramación celular implica cambios necesarios en el estado de la cromatina en las células reprogramadas. Se trata de un proceso ineficiente indicando que los factores de transcripción necesitan superar barreras epigenéticas que ha sido gradualmente impuestas durante la diferenciación. Los factores de reprogramación interaccionan con modificadores de histonas, así como enzimas implicadas en la regulación de la metilación de ADN, para que el proceso culmine en el estado pluripotente. Se ha descrito que las iPSCs tienen unos menores niveles de metilación que las células diferenciadas de origen, además de que la pérdida de metilación en los genes de pluripotencia es fundamental para su expresión. En concreto, la capacidad de reprogramar NSCs mediante el uso de *Oct4* como único factor sugiere que el epigenoma de estas células es más fácil de reprogramar. Sin

embargo, los mecanismos epigenéticos concretos implicados en el proceso de reprogramación permanecen por ser dilucidados.

OBJETIVOS

El descubrimiento de las células madre neurales (NSCs) en el sistema nervioso central (CNS) implicó la existencia potencial de reparación endógena y el uso de terapias celulares en el cerebro adulto. Aunque estas aplicaciones potenciales se preveen como consecuencias a largo plazo, determinar los reguladores que trabajan coordinadamente para proveer de un número óptimo de NSCs y de sus subtipos celulares, es crucial para su futuro uso en terapia celular. Los cambios epigenéticos implicados en el mantenimiento de las células madre neurales adultas no han sido ampliamente dilucidados, por lo tanto el objetivo principal de este trabajo es la identificación de la firma epigenética (incluyendo la impronta genómica) que pueda controlar el comportamiento de estas células en condiciones fisiológicas.

Los objetivos específicos de esta Tesis son:

1. Reprogramación celular de NSCs adultas a un estado pluripotente con un número mínimo de factores exógenos.

2. Identificación de los cambios epigenéticos que ocurren en NSCs adultas durante la adquisición del estado pluripotente incluyendo la regulación de la impronta genómica y la metilación del ADN.

3. Estudio del papel de la dioxigenasa TET3 en la regulación del mantenimiento de las NSCs y la neurogénesis en la SVZ adulta.

MATERIAL Y MÉTODOS

1. Animales de experimentación

Los animales utilizados durante esta tesis así como los procedimientos experimentales fueron aprobados por el comité de ética de la Universidad de Valencia. En el caso del uso de técnicas invasivas, los animales fueron anestesiados previamente.

Cepas: todos los experimentos fueron realizados con ratones de 2-4 meses de edad. Las cepas utilizadas a lo largo de este trabajo han sido: C57BL6 (cepa salvaje), CAST/EiJ (cepa salvaje utilizada para la generación de animales híbridos), *Tet3*$^{loxP/loxP}$ (cepa utilizada para generar animales deficientes en TET3 en células GFAP positivas), *GFAPcre* (cepa transgénica en la que la *cre-recombinasa* se expresa

bajo el promotor de la GFAP, utilizada para cruzar con los animales *Tet3*$^{loxP/loxP}$), *Tet3-GFAPcre* (cepa resultante del cruce entre la *Tet3*$^{loxP/loxP}$ y la *GFAPcre* en la que el gen *Tet3* es específicamente eliminado en las células GFAP+) y la cepa *NU/J* (cepa inmunodeprimida utilizada para el ensayo de formación de teratomas).

2. Estudio de la citoarquitectura de la SVZ

Administración de BrdU: el análogo de timidina 2-Bromo-deoxiuridina (BrdU) es incorporado al ADN en la fase S del ciclo celular en el momento de su administración. Tres semanas después, los progenitores de rápida amplificación en la SVZ diluyen la marca mientras que las NSCs de lenta división (LRC, del inglés *Label Retaining Cells*) la retienen así como las nuevas neuronas generadas en el bulbo olfatorio que incorporan el nucleótido justo antes de diferenciarse e integrarse en el OB. Para ello, los animales fueron inyectados cada 2h durante 12 horas y sacrificados 3 semanas después para su análisis por inmunohistoquímica.

Técnicas histológicas: Para la fijación del tejido, los animales fueron sacrificados por perfusión con paraformaldehido (PFA) al 4% en 0.1M PBS y los cerebros fueron seccionados utilizando un vibratomo (Leica® VT1000S). Para el estudio de las estructuras en forma de roseta de las paredes del ventrículo, el tejido fue diseccionado, tras dislocación cervical del ratón, y post-fijado en PFA durante una noche.

Inmunohistoquímica: en este tesis se incluyen técnicas inmunofluorescentes y de detección de peroxidasa. Las muestras de tejido fueron lavadas con PBS para su posterior incubación con los anticuerpos primarios específicos para cada caso. Específicamente, para las incubaciones con los anticuerpos de BrdU, 5mC y 5hmC se llevó a cabo un paso previo de apertura de cromatina con HCl 2N. Además, en el caso de la detección de la peroxidasa, la peroxidasa endógena fue previamente neutralizada con peróxido de hidrógeno al 3%. Tras la incubación con los anticuerpos primarios durante toda la noche y varios lavados con PBS, las muestras fueron incubadas con los anticuerpos secundarios específicos durante 1h, los núcleos fueron teñidos con DAPI y las muestras montadas sobre portaobjetos con FluorSave™ (Millipore). Para la detección de la β-galactosidasa, la muestras fueron incubadas en solución de lavado A (2 mM $MgCl_2$, 5 mM EGTA and 0.1 M PO_4, pH 7.4) y solución de lavado B (2 mM $MgCl_2$, 0.01% sodium deoxycholate (Sigma), 0.02% Nonidet P-40 (Sigma) y 0.1 M PO_4 pH 7.4) antes de la incubación con la solución de marcaje (0.1 M PO_4 pH 7.4, 2 mM $MgCl_2$, 0.01% sodium deoxycholate, 0.02% Nonidet P-40, 5 mM $K_3Fe(CN)_6$, 5 mM $K_4Fe(CN)_6$ and 1 mg/ml X-Gal).

Contaje de las poblaciones celulares de la SVZ: Las muestras previamente teñidas fueron fotografiadas en un microscopio confocal (FluoView FV10i, Olympus). Las distintas poblaciones

celulares fueron contadas a mano y relativizadas al número total de DAPI. Para las LRC, las células fueron contadas en un microscopio fluorescente (Nikon Eclipse Ni) aplicando el principio de Cavalieri.

3. Cultivo de células madre neurales adultas.

Disección de la SVZ y disociación del tejido: animales de 2-4 meses de edad fueron sacrificados por dislocación cervical y la SVZ fue finamente diseccionada. La muestra de tejido fue incubada en una solución de papaína (Worthington Biochemical Corporation), disgregada, sembrada en medio completo (conteniendo FGF y EFG) e incubada a 37º y 5% de CO_2 para permitir el desarrollo de neurosferas. El número de neurosferas primarias fue manualmente contado siendo considerado una estimación del número de células formadoras de esferas en la SVZ.

Subcultivo y expansión: las neurosferas primarias fueron disgregadas con la ayuda de Acutasa® (Sigma), contadas en el contador automático Adam (NanoEnTek®) y sembradas a una determinada densidad (10.000 cells/cm^2) en medio completo. Tras 5-7 días de incubación a 37º y 5% de CO_2 las nuevas esferas estaban preparadas para un nuevo pase. El número de células obtenidas tras cada pase se utilizó para la representación de la curva de crecimiento.

Ensayo de formación de neurosferas: la capacidad de autorrenovación puede ser evaluada *in vitro*. Para ello, tras la disociación de las esferas, las células fueron sembradas a baja densidad (5 cel/µl) y, tras 5 días de incubación, se contó el número de nuevas esferas obtenidas, que fueron también fotografiadas para la medición de su diámetro.

Determinación de la capacidad de proliferación: células en cultivo fueron tratadas con 2µM de BrdU durante 5 min para su posterior análisis por inmunocitoquímica. Además, se llevó a cabo un ensayo de ciclo celular mediante citometría de flujo (FACSVerse, BD) utilizando un kit comercial (BD Cycletest™ Plus DNA Kit) para el marcaje de las distintas fases.

Ensayos de diferenciación y reactivación: para evaluar la capacidad de las células de dar lugar a neuronas, astrocitos y oligodendrocitos, estas fueron disgregadas y sembradas sobre sustrato adherente (Matrigel®, BD) con medio conteniendo FGF. Tras dos días, el FGF fue sustituido por FBS al 2% incubando las células cinco días más para ser analizadas por inmunocitoquímica. Para los ensayos de reactivación, tras 7 días de diferenciación, las células fueron levantadas con tripsina/EDTA (Gibco) y sembradas en medio completo. El número de neurosferas obtenidas fue contabilizado.

4. Silenciamiento mediante shRNA

Para la regulación a la baja del gen *Snrpn* se utilizó un shRNA específico (Mission®, Sigma) que fue introducido mediante infección con lentivirus. Para la generación de las partículas víricas, células

HEK293T fueron transfectadas con lipofectamina (Invitrogen) con los plásmidos específicos, incluyendo el shRNA para *Snrpn* (shSNRPN) y un shRNA vacío (shSCRAMBLE) como control. Aproximadamente 30h tras la transfección de las 293T procedimos a la infección de las NSCs en cultivo. Las NSCs disociadas fueron incubadas con el sobrenadante viral suplementado con polibreno (Sigma) durante 4-6 horas. Posteriormente, se sembraron en medio apropiado para cada experimento y fueron adecuadamente analizadas.

5. Edición genética de NSCs mediante CRISPR-Cas9

El plásmido para el CRISPR utilizado fue cedido por el laboratorio de la Dra. Myriam Hemberger (Babraham Institute, Cambridge). La técnica CRISPR/Cas9 fue utilizada para regular a la baja la expresión de *Tet3* en NSCs obtenidas de animales híbridos generados mediante el cruce de hembras CAST/EiJ con machos C57BL6 (CxB), cepas en las que se han identificado polimorfismos (SNPs) en el gen de *Snrpn*. Las NSCs fueron nucleofectadas (Nucleofector™, Amaxa) para la introducción del ADN exógeno siguiendo las instrucciones del fabricante. Las células nucleofectas fueron incubadas 2 días para después ser separadas y aisladas por citometría de flujo (MoFlo® XDP, Beckman Coulter) en base a la expresión fluorescente del plásmido que contenía un reportero con la proteína fluorescente verde.

6. Análisis inmunocitoquímico

Para el análisis de proliferación, cultivos de neuroesferas fueron adheridas en cubreobjetos tratados con matrigel durante 20 min y posteriormente fijadas con 2% PFA antes de proceder al marcaje. Para el análisis de células en diferenciación, estas fueron fijadas a 2, 3 y 7 días. Tras varios lavados y bloqueo de las uniones inespecíficas, las muestras fueron incubadas con los anticuerpos primarios y secundarios específicos, tal y como se ha explicado anteriormente. Para la detección de la BrdU, un pre-tratamiento con HCl a 2N fue requerido. Finalmente las muestras fueron montadas para su posterior análisis.

7. Criopreservación celular

Las células utilizadas a lo largo de este trabajo fueron conservadas en 10% de Dimetilsulfóxido (DMSO) a -80ºC o en N_2 líquido para almacenamientos más prolongados

8. Reprogramación de NSCs

Para la reprogramación celular únicamente se usaron *Oct4* y *Klf4* como factores exógenos, debido a la expresión endógena de *c-myc* y *Sox2* de las NSCs, que fueron introducidos mediante el uso de retrovirus. Para su producción, células Plat-E empaquetadoras fueron transfectadas con los plásmidos específicos pMXs-Oct4, pMXs-*Klf4* y Cherry. Al día siguiente el medio fue sustituido por

medio completo de NSCs para dos días después proceder a la infección de las esferas, siendo incubadas con la mezcla del sobrenadante viral durante una noche. Cinco días después, las esferas fueron disgregadas y sembradas sobre células SNL, previamente mitomizadas (Mitomycin C, Sigma) para evitar su crecimiento, en medio de reprogramación con LIF. Tras la aparición de las pre-iPSCs, el medio fue sustituido por medio 2i/LIF para permitir la completa reprogramación.

La pluripotencia de las células fue testada de diversas maneras. Por una parte se utilizó el marcaje con fosfatasa alcalina, marcador específico de pluripotencia. También se llevó a cabo el ensayo de formación de cuerpos embrioides (EBs) mediante el protocolo de las gotas colgantes, con el que se obtuvieron organoides donde se pudieron identificar las tres capas embrionarias mediante inmunocitoquímica. Además, para descartar posibles alteraciones en el número de cromosomas, se analizó el cariotipo celular deteniendo a las células en metafase con colchicina (KarioMAX® Colcemid, Gibco) y tiñendo los cromosomas mediante tinción de Leishman (Sigma). Tanto las iPSC como los EBs fueron analizados por inmunocitoquímica tal y como se ha descrito anteriormente. Finalmente, para testar la capacidad pluripotente *in vivo* se llevó a cabo el ensayo de formación de teratomas en el que ratones inmunodeprimidos fueron inoculados subcutáneamente con una suspensión de iPSCs para comprobar su capacidad de dar lugar a este tipo de tumores. Estos fueron extraídos, fijados con PFA 4%, embebidos en parafina y seccionados mediante micrótomo (Leica) para ser después teñidos con hematoxilina/eosina.

9. Análisis de la expresión génica

Extracción de ARN, síntesis de ADN complementario (ADNc) y PCR a tiempo real (qPCR): Las muestras de ARN fueron obtenidas con un kit (RNeasy Mini Kit, Qiagen) siguiendo las instrucciones del fabricante. Tras ello, se llevó a cabo la síntesis de ADNc (RevertAid H Minus First Strand cDNA Synthesis Kit, Thermo Fisher) y se procedió al análisis de la expresión mediante qPCR utilizando sondas específicas de tipo TaqMan™ o cebadores, dependiendo del ensayo. El gen *Gapdh* fue utilizado como normalizador.

ARNseq: El análisis transcriptómico fue llevado a cabo por el *Servei Central de Suport a la Investigació Experimental* de la Universidad de Valencia. El análisis de los datos fue realizado externamente por EpiDisease S.L.

10. Inmunodetección de proteínas por *western-blot*

Para la extracción de proteína, las células fueron lisadas con tampón RIPA e inhibidores de proteasas (Complete®, Roche) para seguidamente ser desnaturalizadas y resueltas en gel de poliacrilamida en condiciones desnaturalizantes (SDS-PAGE). Finalmente, estas proteínas fueron

transferidas a membranas usando el sistema automatizado Trans-Blot Turbo transfer device (Bio-Rad). Tras esto, se procedió a la inmunodetección de las mismas. Tras el bloqueo de las uniones inespecíficas, las membranas fueron incubadas con los anticuerpos primarios específicos, para después lavar e incubar con los anticuerpos secundarios marcados con peroxidasa. Para el revelado se utilizó Lightning® Plus-ECL (Perkin Elmer) y la señal fue procesada con el sistema Alliance Mini HD9 (UVITEC).

11. Análisis de la metilación del DNA

Determinación de los niveles globales de 5hmC y 5mC por ELISA: el ADN fue adherido al fondo del pocillo mediante una solución específica (Reacti-Bind DNA Coating Solution, Thermo Fisher). Tras esto, las uniones inespecíficas fueron bloqueadas antes de proceder a la incubación con los anticuerpos primarios 5mC/5hmC, continuando con la incubación con los anticuerpos secundarios conjugados con peroxidasa. Las muestras fueron incubadas con la solución de revelado (TMB-ELISA Substrate Solution, Thermo Fisher) para medir finalmente su absorbancia a 450nm.

MeDIP-seq: en este experimento, las librerías y la secuenciación final fueron realizadas por el SCSIE. Para la inmunoprecipitación, el ADN fue incubado con el anticuerpo anti-5mC tras el bloqueo de uniones inespecíficas durante 2h. Tras esto, bolas magnéticas específicas (Dynabeads®) fueron añadidas e incubadas durante toda la noche. Seguidamente, mediante el uso de un imán, la fracción unida fue separada del sobrenadante. Finalmente, esta fracción unida fue tratada con proteinasa K y purificada.

Estudio del enriquecimiento en 5mC y 5hmC en el DMR de Snrpn: para la cuantificación de los niveles de 5mC, el ADN fue convertido bisulfíticamente mediante un kit (EZ DNA Methylation-Gold™ kit, Zymo) y amplificado por PCR previamente a su secuenciación mediante pirosecuenciación utilizando el sistema PiroMark® (Qiagen). Para evaluar los niveles de 5hmC en la misma región, se procedió a inmunoprecipitar el ADN de la misma forma que anteriormente (MeDIP-seq) usando el anticuerpo específico anti-5hmC. Tras la purificación, el ADN fue amplificado por qPCR para calcular el enriquecimiento. La fracción no unida fue usada como control.

12. Análisis de la impronta genómica

Para el estudio del estado de imprinting en NSCs, se obtuvo cDNA de muestras de NSCs híbridas (CxB) en las que se han identificado SNPs específicos para cada cepa. El cDNA fue amplificado por PCR con cebadores específicos y secuenciado posteriormente mediante pirosecuenciación para calcular el porcentaje de expresión de cada alelo.

RESULTADOS

1. El estado epigenético de las NSCs cambia significativamente durante la reprogramación

Las NSCs adquieren el estado pluripotente similar a las ESC solo con el uso de Oct4 y Klf4

Inicialmente, analizamos los niveles de expresión de los cuatro "factores de Yamanaka" (OSKM) observando que las NSCs expresaban significativamente *Sox2*, *Klf4* y *c-myc* mientras que *Oct4* estaba ausente. Por ello, desarrollamos un protocolo de reprogramación para inducir la pluripotencia de las iPSC utilizando únicamente dos factores, *Oct4* y *Klf4* (2F), o un factor, *Oct4* (1F). 30-40 días después de la infección, en la condición 2F aparecieron agregados celulares de apariencia pluripotente mientras que no lo hicieron en la condición 1F. Estos agregados habían adquirido características pluripotentes aunque carecían de algunas importantes como la expresión de Nanog. Estas fueron denominadas pre-iPSCs. Tras esto aplicamos condiciones de cultivo definidas incluyendo los inhibidores MEK y GSK3 junto con LIF, observando la adquisición de un estado pluripotente completo (silenciamiento de los genes retrovirales, adquisición de genes de pluripotencia y silenciamiento de genes neurales) después de 10-20 días. Tras esto, las iPSCs obtenidas fueron exhaustivamente caracterizadas.

El número de cromosomas es mantenido tras la reprogramación.

Para comprobar que las líneas de iPSC obtenidas no portaban aberraciones cromosómicas llevamos a cabo el estudio de su cariotipo. Comprobamos que la mayoría de ellas mantenían un número normal en torno a 40 mientras que un pequeño porcentaje portaban duplicaciones cromosómicas de forma que fueron descartados del estudio.

Las iPSCs generadas con 2F pueden ser diferenciadas *in vitro* e *in vivo* en las tres capas embrionarias.

Con el propósito de testar la capacidad de diferenciación de estas células *in vitro* e *in vivo* se llevaron a cabo sendos experimentos de formación de cuerpos embrioides (EBs) y teratomas, respectivamente. En el primero de casos, tras la obtención de los EBs, fue comprobado por ICC y qPCR las presencia de las tres capas germinales mientras que, con el mismo resultado, los teratomas fueron analizados mediante tinción con hematoxilina/eosina.

La expresión de los genes imprintados cambia durante la generación de iPSC de NSCs.

La mayoría de los genes imprintados tienen una función relevante en el cerebro además de que la impronta puede ser selectivamente eliminada en determinados contextos celulares. Con el propósito de estudiar los cambios en expresión génica ocurridos durante el proceso de

reprogramación, con un enfoque especial en los genes imprintados, llevamos a cabo un ARNseq. El resultado mostró un gran número de genes diferencialmente expresados, con un total de 6062 con menor expresión y 5301 con un incremento de su expresión. En cuanto a los genes imprintados, de un total de 126 genes analizados, observamos cambios en 47 de ellos, indicado que la adquisición del estado pluripotente requiere cambios importantes en el transcriptoma y que la impronta genómica es crucial en este proceso. Para evaluar los cambios en el metiloma ocurridos durante el proceso de reprogramación y la posible firma epigenética característica de las NSCs, llevamos a cabo un ensayo de análisis de metilación mediante MeDIP-seq. Los resultados mostraron primero que los cambios de expresión ocurridos en los genes de pluripotencia y neurales descritos anteriormente estaban asociados con menor y mayores niveles de metilación respectivamente, sobre todo a nivel del promotor.

La metilación de los DMR en las regiones de control de imprinting son modificados durante la reprogramación.

Como ya se ha mencionado anteriormente, los genes imprintados se encuentran agrupados en clústeres, bajo el control de regiones de control de imprinting (ICR, del inglés *Imprinting Control Region*) que son DMRs que controlan la expresión de los genes imprintados del clúster. Encontramos dos tipos de DMR: los que establecen el patrón de metilación en la línea germinal (gDMR) o los que son diferencialmente metilados tras la fecundación (sDMR). Debido a los efectos de los DMR en la expresión de los genes imprintados, nos centramos en el estudio de la metilación de diferentes clústeres encontrando que, de 32 analizados, aparecían diferencias en 22 de ellos, y de los cuales el 86% mostraba una reducción de los niveles de metilación siendo más frecuentes en los metilados maternos. Además, estos cambios en metilación estaban asociados, en muchos casos, con cambios en la expresión en múltiples genes del clúster, indicando su posible relación.

TET3 previene la reprogramación de las NSCs en iPSCs.

En mamíferos, la eliminación activa de 5mC es catalizada por las enzimas TET, habiendo sido también implicadas en imprinting. Tras la cuantificación de los niveles de estas enzimas en el proceso de reprogramación, observamos que la expresión de *Tet1* y *Tet2* aumentaba considerablemente en las iPSCs comparadas con las NSCs mientras que *Tet3* era profundamente regulado a la baja. Para clarificar el posible papel de TET3 en el mantenimiento del fenotipo neural, generamos iPSCs a partir de NSCs deficientes en TET3 (el modelo animal es explicado en el capítulo siguiente) observando el aumento de la eficiencia de la reprogramación cuando TET3 estaba ausente, sugiriendo su posible papel en el mantenimiento de la identidad neural, que fue analizado posteriormente.

2. TET3 juega un papel importante en la regulación de las NSCs de la SVZ

Las hidroxilasas de la familia TET son especialmente abundantes en el cerebro, pudiendo convertir 5mC en 5hmC y, desde su descubrimiento en 2009, han sido implicadas en una variedad de procesos biológicos, aunque su papel en las NSCs permanecía por dilucidar. Inicialmente, nuestros datos de qPCR mostraron bajos niveles de *Tet1* y *Tet2* y elevados para *Tet3* en las NSCs adultas. Además, estos niveles de *Tet3* eran mantenidos postnatalmente y en células en diferenciación. Comprobamos que de las tres isoformas descritas para TET3, la *Tet3s* era la mayoritaria aunque niveles sustanciales de la *Tet3FL* podían detectarse. Tras esto, determinamos la distribución celular de la enzima mediante IHC/ICC observando que era expresada específicamente en células GFAP+ *in vivo* y en SOX2+ *in vitro*, siendo mantenida en diferenciación.

Tet3 promueve el estado de célula madre en la SVZ adulta

Para estudiar de manera específica el papel de TET3 en la SVZ adulta, generamos un modelo de ratón condicional en el que el gen *Tet3* estaba delecionado en las células GFAP+, mediante el cruce de la cepa $Tet3^{loxP/loxP}$ con la *GFAPcre* (los animales deficientes en TET3 son denominados como $Tet3\text{-}Gfap^{cre}$ mientras que sus respectivos controles son $Tet3\text{-}Gfap^{control}$). Tras verificar la especificidad de la recombinación, así como la bajada de *Tet3* en estas células, llevamos a cabo los experimentos *in vivo* e *in vitro*.

- Experimentos *in vivo*: mediante la técnica de marcaje con BrdU, con la que podemos marcar células de lenta división, observamos que los animales deficientes en *Tet3* poseían un menor número de células LCR-GFAP+, identificadas como NSCs, que incluso eran menos proliferativas. Además, observamos que en los mutantes el número de astrocitos no neurogénicos (S100β+) estaba también elevado, así como una reducción en el número de NSCs contactando con el ventrículo. Esta disminución del *pool* de NSCs estaba provocando también defectos en neurogénesis en el OB, postulando que TET3 podría estar implicada en evitar la diferenciación terminal de las NSCs.

- Experimentos *in vitro*: mediante en ensayo de neurosferas evaluamos las capacidades de autorrenovación, proliferación y diferenciación *in vitro*. Como esperábamos, las NSCs aisladas de animales mutantes para *Tet3* daban lugar a un menor número de esferas primarias y secundarias comparado con los controles, no viéndose alterados el diámetro ni el ciclo celular de las mismas, lo que indica que *Tet3* podría estar implicada en el proceso de autorrenovación de las NSCs sin afectar a su proliferación. Tras esto, sometimos a las células a un protocolo de diferenciación observando el mismo fenotipo de diferenciación temprana a astrocitos no-neurogénicos que habíamos observado *in vivo*. Consecuentemente, tras el ensayo de reactivación, corroboramos que una menor proporción de

células formadoras de esferas era mantenida tras 7DIV en diferenciación. Para dilucidar si TET3 podía estar implicada en la regulación de la impronta genómica en las NSCs adultas, llevamos a cabo un RNAseq donde comprobamos que multitud de genes estaban siendo alterados tras la deficiencia en *Tet3*. Sin embargo, dentro de los genes imprintados, únicamente *Snrpn* mostraba un incremento significativo de su expresión en los mutantes. Para saber si *Snrpn* podía estar contribuyendo al fenotipo observado, hicimos un experimento de silenciamiento del gen mediante shRNA en las NSCs mutantes comprobando que tanto el fenotipo en autorrenovación como en diferenciación eran rescatados a niveles normales, antagonizando, por tanto, su diferenciación prematura.

La impronta genómica de Snrpn se mantiene en NSCs deficientes en TET3

Snrpn pertenece al grupo de genes causantes de la enfermedad de Prader-Willi, caracterizada por múltiples afecciones neurológicas. En nuestro caso, la perdida de impronta en el gen podría explicar el fenotipo de sobreexpresión. Para evaluarlo, llevamos a cabo un experimento de regulación a la baja de *Tet3* mediante CRISPR en NSCs híbridas para poder estudiar la expresión específica de cada alelo. Tras cuantificar el porcentaje de expresión de cada alelo por pirosecuenciación, comprobamos que la impronta materna estaba mantenida en los mutantes.

TET3 no está implicada en la regulación de los niveles globales de 5hmC en las NSCs adultas

Como ya sabemos, las enzimas TET son capaces de convertir la 5mC en 5hmC. Para conocer si TET3 podía estar implicada en el mantenimiento de los niveles globales de 5hmC, llevamos a cabo su cuantificación por ELISA. Los resultados mostraron que, aunque menores que en cerebro y SVZ, los niveles de 5hmC eran significativos en NSCs. Los estudios mediante IHC, mostraron que ambas marcas tenían un patrón excluyente. Mientras las NSCs GFAP+/SOX2+ eran ricas en 5hmC, los neuroblastos mostraban un enriquecimiento en 5mC, asociado, probablemente a su fenotipo más restringido. Sin embargo, estos niveles globales de 5hmC y 5mC no se veían afectados en los mutantes, por lo que TET3 no parecía estar implicada en su regulación.

TET3 contribuye a la represión transcripcional de Snrpn en los progenitores neurales independientemente a la 5hmC

Tal y como se ha explicado anteriormente, las regiones DMRs están implicadas en la regulación del estado de la impronta genómica. Para conocer en detalle si TET3 podría estar alterando el estado de metilación de esta región, analizamos sus niveles de 5mC por conversión bisulfítica y posterior pirosecuenciación, mientras que cambios en los niveles de 5hmC fueron evaluados por hMeDIP y posterior qPCR. Los resultados mostraron que tanto los niveles de 5mC como los de 5hmC estaban

siendo mantenidos en las NSCs mutantes para *Tet3*, lo que sugiere que TET3 no está regulando los niveles de expresión de *Snrpn* a través de cambios en los niveles de 5mC/5hmC en la región DMR.

Para explorar si TET3 podía estar ejerciendo funciones no catalíticas en las NSCs a nivel de *Snrpn*, llevamos a cabo una inmunoprecipitación de cromatina (ChIP) utilizando anticuerpos anti TET3 en NSCs salvajes. El análisis reveló el enriquecimiento específico de TET3 a la región promotora del gen *Snrpn*. Estos datos demuestran que TET3 se une al promotor de *Snrpn* para contribuir a la represión transcripcional del gen en los progenitores neurales independientemente de su función catalítica.

CONCLUSIONES

1. Las NSCS adultas se reprograman exitosamente en iPSCs usando exclusivamente *Oct4* y *Klf4* como factores exogenos, lo que indica que las NSCs se encuentran en un estado epigenético intermedio entre el estado diferenciado y el pluripotente.

2. Las iPSCs derivadas de las NSCs poseen una mayor capacidad de formar ectodermo que las ESC, sugiriendo que podrían estar reteniendo memoria del Sistema Nervioso Central. Marcadores del linaje endodérmico son también inducidos por lo que las iPSCs podrían tener un potencial adicional que dependería de su célula de origen.

3. La adquisición de un estado pluripotente en las NSCs implica cambios significativos en la expresión de los genes imprintados, tanto maternos como paternos. Más de la mitad de los genes imprintados originariamente expresados en las NSCs muestran alteración en las iPSCs, indicando que la regulación de la impronta genómica es crucial en este proceso.

4. Los cambios en los niveles de expresión de los genes imprintados correlacionan con modificaciones en el patrón de metilación del ADN en los clústeres imprintados. La mayoría de los DMRs de genes imprintados son importantemente hipometilados. Sorprendentemente, los cambios en la metilación del ADN principalmente ocurren en los DMR maternos relacionándose con cambios en los niveles de expresión de varios genes de estos clústeres.

5. La dioxigenasa TET3 está altamente expresada en las NSCs adultas y previene su reprogramación a iPSCs. Por consiguiente, TET3 no es la enzima encargada del proceso de demetilación observado en los clústeres de genes imprintados.

6. TET3 está altamente expresada en la población de células GFAP en la SVZ, promoviendo el mantenimiento de las NSCs y evitando su diferenciación prematura a astrocitos no neurogénicos.

7. La deficiencia de TET3 en las NSCs GFAP+ provoca una reducción del número de nuevas neuronas alcanzando el bulbo olfatorio.

8. El incremento monoalélico de la expresión de *Snrpn* es responsable de la diferenciación prematura de las NSCs deficientes en TET3 a astrocitos terminalmente diferenciados.

9. TET3 interacciona con el promotor de *Snrpn* reprimiendo la expresión de dicho gen imprintado de una forma independiente a su actividad catalítica.

Publications

PUBLICATIONS DERIVED FROM THIS THESIS

Montalbán-Loro R, Lozano-Ureña A, Ito M, Strogantsev R, Reik W, Ferguson-Smith AC and Ferrón SR. TET3 prevents terminal differentiation of adult NSCs by a non-catalytic action on the imprinted gene *Snrpn*. Submitted to *Cell Stem Cell.*

Montalbán-Loro R, Lozano-Ureña A, Barberá E, Lleches A, Ferrón SR. Genomic imprinting profile is lost during the acquisition of a pluripotent state in adult neural stem cells. In preparation for *Cell Research*.

Lozano-Ureña A, Montalbán-Loro R, Ferguson-Smith AC and Ferrón SR (2017). Genomic imprinting and the regulation of postnatal neurogenesis. *Brain plasticity-special issue "Molecular mechanism and neurogenesis"*; pp. 1-10.

Montalbán-Loro R, Domingo-Muelas A, Bizy A, Ferrón SR (2015). Epigenetic regulation of stemness maintenance in the neurogenic niches. *World J Stem Cells*; 7(4): 700-710.

OTHER PUBLICATIONS

Montalbán-Loro R, Lassi G, Charalambous, Horner A, Saksida L, Bussey T, Tucci V, Ferguson-Smith A, Ferrón SR. Dlk1 dosage regulates hippocampal neurogenesis and cognition. Under review in *Nature Neuroscience*.

Montalbán-Loro R, Lozano-Ureña A, Domino-Muelas A, Charalambous M, Menheniott TR and Ferrón SR. Choroid plexus epithelial cells induce self-renewal and differentiation of adult neural stem cells. Under review in *Stem Cell International*.